Modulus-Based Construction Specification for Compaction of Earthwork and Unbound Aggregate: Appendices

DRAFT FINAL REPORT

Prepared for

National Cooperative Highway Research Program
NCHRP Project 10-84

Transportation Research Board
of
The National Academies

Submitted by:

The University of Texas at El Paso
Center for Transportation Infrastructure Systems
500 West University Avenue
El Paso, TX 79968-0516

August 2014

Appendix A

PROPOSED MODULUS-BASED SPECIFICATION

This appendix contains a preliminary specification and two test procedures entitled:

- Standard Specification for Modulus-Based Quality Management of Earthwork and Unbound Aggregates, and
- Estimating Compaction Quality of Embankment and Unbound Aggregate Layers with Portable Falling Weight Devices
- Estimating Compaction Quality of Embankment and Unbound Aggregate Layers with Portable Seismic Property Analyzer (PSPA)

Since different SHAs' requirements and practices are quite diverse, the values and guidelines provided are our best effort to provide a set of consensus values and procedures.

The specifications are maintained as general as possible so that different SHAs can customize them to their requirements. Comments are incorporated to explain our thought process and means of adopting the specification to local practices.

STANDARD SPECIFICATION FOR MODULUS-BASED QUALITY MANAGEMENT OF EARTHWORK AND UNBOUND AGGREGATES

AASHTO Designation M XXX

1. SCOPE[1]

This specification covers the quality management of compacted geomaterials with modulus-based methods. This specification pertains to construction of embankments and pavement layers such as prepared subgrade, subbase and base without stabilizing agents.

2. REFERENCED DOCUMENTS

AASHTO Standards:

- M 57, Materials for Embankments and Subgrades
- M 147, Materials for Aggregate and Soil-Aggregate Subbase, Base, and Surface Courses
- T 2, Sampling of Aggregates
- T 11, Materials Finer Than 75-µm (No. 200) Sieve in Mineral Aggregates by Washing
- T 27, Sieve Analysis of Fine and Coarse Aggregates
- T 99, Moisture-Density Relations of Soils Using a 2.5-kg (5.5-lb) Rammer and a 305-mm (12-in.) Drop
- T 180, Moisture-Density Relations of Soils Using a 4.54-kg (10-lb) Rammer and a 457-mm (18-in.) Drop
- T 217, Determination of Moisture in Soils by Means of a Calcium Carbide Gas Pressure Moisture Tester
- T 265, Laboratory Determination of Moisture Content of Soils
- T 310, In-Place Density and Moisture Content of Soil and Soil-Aggregate by Nuclear Methods

3. DEFINITIONS

3.1. Lift: Lift is a unit of material within a layer that is placed for compaction.

3.2. Layer: Layer is the total thickness for each material type and may be comprised of one or more lifts.

3.3. Optimum Moisture Content[2]: The optimum moisture content is determined by the Standard Proctor Density Method (AASHTO T 99) or Modified Proctor Density Method (AASHTO T 180).

3.4. Maximum Dry Density[2]: Maximum dry density is determined by the AASHTO T 99 or AASHTO T 180.

---

[1] The goal of the project was to migrate from density-based acceptance to modulus- based acceptance. Changes in the type and gradation of the materials and moisture content at compaction have significant impact on the modulus of the compacted geomaterials. As reflected in the accompanied report, a reasonably rigid process control will ensure a uniform and high quality final product.

[2] This is the practice carried out as part of this study. The SHAs are encouraged to modify their local practices.

4. MATERIALS[3]

4.1. Unless waived or altered by the Engineer, materials shall conform to the requirements of the relevant specifications listed in Table 4.1.

Table 4.1 Material Specifications

Material	Specification[3]
Embankment	AASHTO M 57
Subgrade	AASHTO M 57
Subbase	AASHTO M 147
Base	AASHTO M 147

4.2. The Contractor shall produce, deliver, and stockpile materials at the designated sites as directed by the Engineer that conforms to the requirements in Table 4.1.

4.3. The Contractor shall be responsible for maintaining a gradation process control program in accordance with random sampling procedures in AASHTO T 2[3].

4.4. A change in material source without permission of the engineer is prohibited.

4.5. The Contractor shall assume full responsibility for the production and placement of acceptable materials.

5. PLACING MATERIALS

5.1. Each lift of material should conform to Section 4 requirements.

5.2. Limit lift thickness by the capability of the equipment to uniformly blend and compact the entire lift.

5.3. Place adequate material in uniform lifts, parallel to the profile grade, over the full width of the roadway.

5.4. At the time of depositing the materials on the road, the roadbed shall be so compact that no rutting or displacement will occur.

5.5. Water shall be added or removed during mixing operations in the quantity necessary to yield proper compaction.

5.6. Uniformly blend the entire thickness of each lift before testing moisture content.

5.7. At the time of spreading the material, the material shall be so uniformly mixed that it meets specified gradation requirements.

5.8. The material for each lift shall be spread and compacted with adequate moisture content to the required cross section before placing the succeeding lift.

5.9. The surface of each lift shall be maintained until the next lift is placed.

6. CONTRACTOR QUALITY CONTROL

6.1 The Contractor shall develop a Quality Control Program which addresses all elements affecting the quality of the compacted geomaterials including but not limited to the following items:

- Material Uniformity as defined in Section 6.3
- Moisture Content at Compaction as defined in Section 6.4
- Minimum Density at Compaction as defined in Section 6.5

6.2. The Quality Control Plan shall indicate appropriate action that shall be taken when the process is out of control.

[3] SHAs can replace the AASHTO specifications and/or test methods with their own specifications and methods.

6.2.1. At the discretion of the Engineer, a proofing test section may be required for equipment calibration, establishment of compaction process, and demonstration of the feasibility of the Quality Control Program prior to initiation of the construction.

6.3. Material Uniformity[4]

6.3.1. Aggregate gradation compliance will be documented in accordance with Table 6.1. The Contractor shall correct the unacceptable material. Upon completion of any corrective work, whether by blending, mixing, adding and/or replacing material, the corrected material will be sampled and tested for compliance.

Table 6.1 Material Control Requirements

Material	Percent Difference from Target Gradation[5]			
	Sieve 1 in. (25.0 mm)	Sieve No. 4 (4.75 mm)	Sieve No. 40 (425 µm)	Sieve No. 200 (75 µm)
Embankment (if applicable)	10%	10%	10%	10%
Subgrade	10%	10%	10%	10%
Subbase	5%	8%	5%	3%
Base	5%	8%	5%	3%

6.3.2. The gradation of the material is determined as per AASHTO T 27 and/or T 11 or other method specified by the Engineer.

6.4. Moisture Content at Compaction[5]

6.4.1. The moisture content of the material at the time of compaction shall not be outside the permissible ranges in Table 6.2.

6.4.2. Compliance with moisture content will be documented before compaction as per AASHTO T 217 or other method specified by the Engineer.

6.4.3. Samples for moisture content testing will be taken randomly prior to compaction, in accordance with random sampling procedures contained in AASHTO T 2 or other method specified by the Engineer.

6.4.4. The Contractor shall rework the material that does not meet the specification to achieve the specified moisture content.

Table 6.2 Moisture Content Requirements

Optimum Moisture Content (OMC)	Moisture Content	
	Min.	Max.
<10%	OMC-2%	OMC + 2%
≥10%	0.8 OMC	1.2 OMC

6.5. Minimum Density[4]

6.5.1. The full thickness of each lift shall be compacted to not less than the percent of maximum density as reflected in Table 6.3.

[4] SHAs can replace the test methods and values with their own test methods and values.

[5] This item is extremely critical to the successful implementation of modulus-based specification. SHAs may consider tightening the requirements, if feasible.

6.5.2. Compliance with moisture content will be documented before quality acceptance as per AASHTO T 217 or other method specified by the Engineer.

6.5.3. Samples for density testing will be taken randomly prior to compaction, in accordance with random sampling procedures contained in AASHTO T 2 or other method specified by the Engineer.

6.5.4. The Contractor shall rework the material that does not meet the specification to achieve the specified dry density.

6.5.5. The density requirements can be waived by the Engineer, if the lift is compacted with instrumented rollers as per intelligent compaction concept.

Table 6.3 Relative Density Requirements for Compaction

Material	Min. Required Relative Density
Embankment	85% of Maximum Dry Density
Subgrade	90% of Maximum Dry Density
Subbase	95% of Maximum Dry Density
Base	95% of Maximum Dry Density

7. ENGINEER QUALITY ACCEPTANCE (QA)

7.1. The acceptance of the compacted lift is based on achieving adequate moisture-adjusted modulus when tested as per AASHTO T E1E[6] or other method specified by the Engineer.

7.2. The moisture content of the material at the time of modulus-based testing shall be measured as per AASHTO T 310 or other method specified by the Engineer.

7.3. Modulus measurements should be carried out in a timely manner and before the moisture content of the compacted layer falls below 1% (2% for materials with OMC >10%) of the moisture content measured at the time of compaction under Item 7.4[7].

7.4. The measured modulus shall be adjusted for the moisture content at the time of testing as specified in AASHTO T E1E or other method specified by the Engineer.

7.5. The Contractor shall rework the material that does not meet the specification to achieve the specified modulus. Upon completion of any corrective work, the corrected material shall be sampled and tested for acceptance.

7.6. Unless altered by the Engineer, compliance shall be documented in accordance with the minimum frequency of testing for modulus and moisture content reflected in Table 7.1[8]. This frequency can be reduced as justified by the use of continuous compaction control during the contractor's process control. Modulus/moisture content testing will be carried out randomly in accordance with random sampling procedures contained in AASHTO T 2.

Table 7.1 Minimum Schedule of Modulus-based Tests

Material	Maximum Lot Size[7]	No. of Sublots[7]	No. of Tests per Sublot[9]
Embankment	4000 yd^2 (3400 m^2)	2	5
Subgrade	3000 yd^2 (2500 m^2)	2	5
Subbase	2400 yd^2 (2000 m^2)	2	5
Base	2000 yd^2 (1700 m^2)	2	5

[6] Light Weight Deflectometer

[7] Since modulus of a compacted layer increase significantly with time, this item is added to ensure that the acceptance is done in a timely manner.

[8] SHAs can replace the values in Table 7.1 with their own values.

[9] This value is derived from the variability analyses of the devices in this project

7.7. Unless altered by the Engineer, moisture-adjusted modulus shall be evaluated for acceptance on a lot basis using the method of estimating percentage of material within specification limits (PWL)[10].

7.8. Unless altered by the Engineer, the lower specification tolerance limit for moisture-adjusted modulus shall be 0.8[11] times the target modulus specified in AASHTO T E1E. Unless altered by the Engineer, the Contractor shall target production quality to achieve 90 PWL or higher.

7.9. Unless altered by the Engineer, the lot shall be acceptable if the PWL of the lot equals or exceeds 50[12].

[10] SHAs may replace this method with other methods they currently use.
[11] This value is derived from the preliminary variability analyses of the devices in the report. SHAs can replace this value with their own value.
[12] This value seems to be common among most specifications. SHAs can replace this value with their own value.

Standard Test Method for

ESTIMATING MODULUS OF EMBANKMENT AND UNBOUND AGGREGATE LAYERS WITH PORTABLE FALLING WEIGHT DEVICES

AASHTO Designation: T E1E

1. SCOPE

1.1. This test method describes the procedure for determining the in-place modulus of compacted geomaterials used in embankments, subgrade, subbase or base layers (without stabilizing agents) and establishing the target modulus for comparison with the measured values. The modulus is measured with a device that conforms to ASTM E 2835 or E 2583.

2. REFERENCED DOCUMENTS

ASTM Standards:

- E 2835, Standard Test Method for Measuring Deflections using a Portable Impulse Plate Load Test Device.
- E 2583, Standard Test Method for Measuring Deflections with a Light Weight Deflectometer (LWD).

3. SIGNIFICANCE

3.1. The test method described is useful as a rapid, nondestructive technique for the in-place determination of modulus of compacted geomaterials.

3.2. The test method is used for quality acceptance/quality control testing of compacted geomaterials for construction.

3.3. Test result may be affected by the gradation of the material, sample consistency, moisture content, density and the surface texture of the material being tested.

4. INTERFERENCES

4.1. The device is sensitive to the moduli of the underlying layers. As such, appropriate adjustments should be made in assigning target modulus.

4.2. Oversize rocks, surficial cracks, uneven or rough surface texture or scaled surface may affect the measurements with the LWD. Consideration should be given to these matters during testing.

4.3. Moisture contents at the time of compaction and at the time of testing significantly affect the measured modulus with the device. The measured modulus should be appropriately adjusted as discussed in Section 9.

5. APPARATUS

5.1. While exact details of construction of the device may vary, the system shall conform to either the ASTM E 2835 or ASTM E 2583. This test method is a type of plate bearing test with the following attributes:

5.1.1. The load is a force pulse [typically 1000 lb (4.5 kN) to 2000 lb (9 kN)] generated by a falling mass dropped onto a spring or buffer assembly that transmits the load pulse to a plate [typically 6 in. (150 mm) to 12 in. (300 mm) in diameter] resting on the material under test.

5.1.2. The mass is raised to a preset height [typically 12 in. (300 mm) to 18 in. (450 mm)] and then dropped to deliver the desired force pulse.

5.1.3. The resulting deflection is measured using suitable instrumentation (typically a geophone or accelerometer). The resulting force is measured with a suitable instrumentation (typically a load cell) or estimated (typically based on potential energy). Multiple drops (typically six) from the same preset drop height may be performed at the same test location.

5.1.4. The peak deflection and load (if applicable) resulting from each drop at each location are recorded for further analysis.

5.2. Even though the operation of the devices that conform to ASTM E 2835 and ASTM E 2583 is similar, their measured parameters are different.

5.2.1. A device that conforms to ASTM E 2835 reports the movement of the loading plate as deflection, and typically is not equipped with a load cell. As such, the applied load is estimated based on the drop height, the drop mass and spring buffer stiffness.

5.2.2. A device that conforms to ASTM E 2583 reports the movement of the surface of the compacted layer as deflection, and is equipped with a load cell to measure the applied load.

5.2.3. The differences between the deflections measured by the two devices can be significant and their results and interpretation of their results cannot be used interchangeably.

6. SAFETY PRECAUTIONS

6.1. Effective user instruction together with routine safety procedures are a recommended part of the operation and transport of this device.

6.2. Keep back straight and lift with leg muscles when elevating, dropping, and catching the mass.

6.3. Make sure that hands are not positioned beneath the elevated mass.

6.4. Secure load mass into the lower locked position prior to and during transportation between test locations.

7. CALIBRATION

7.1. Calibration of the device will be in accordance with the ASTM E 2835 or E 2583.

8. PROCEDURE

8.1. Operation of the device will be in accordance with the ASTM E 2835 or E 2583. The steps to be taken are as follows:

8.1.1. Position load plate on properly prepared test site.

8.1.2. Perform six falling mass drops. Use the first three drops for seating and the next three drops for analysis.

8.1.3. Use the following procedure for each drop:

8.1.3.1. Raise falling mass to preset drop height and snap into the release mechanism.

8.1.3.2. Adjust guide rod to vertical.

8.1.3.3. Release falling mass and allow it to fall freely.

8.1.3.4. Catch the falling mass after rebound as recommended by the manufacturer.

8.1.3.5. Raise and snap load mass into the release mechanism after rebound.

8.1.3.6. Record resulting peak deflections and applied loads (if applicable).

8.1.4. Record supporting information such as location, material type, and other identification information as needed.

8.2. Measure the moisture content of the material at the time of testing as per AASHTO T 310, or other method specified by the Engineer at the same time that the modulus-based measurements are made.

9. CALCULATION OF LWD EFFECTIVE AND ADJUSTED MODULUS

9.1. Obtain the peak deflection, d_{eff}, as per ASTM E 2835 or E 2583

9.2. Obtain the peak load, F, as per ASTM E 2835 or E 2583

9.3. Estimate the Poisson's ratio of the geomaterial, ν (see Appendix I for recommended values)[13].

9.4. Estimate the shape factor, f, based on the soil type and plate rigidity (see Appendix II for recommended values).

9.5. Calculate the effective modulus of the geomaterial, E_{eff}, from:

$$E_{eff} = [(1 - \nu^2)\, F / (\pi.a.d_{eff})]\, f \tag{9.1}$$

where a = radius of load plate, d_{eff} = peak deflection on top the compacted layer, ν = Poisson's ratio of the geomaterials, f = plate rigidity factor.

9.6. Estimate the adjusted modulus, E_{adj}, from:

$$E_{adj} = E_{eff} * K_{adj} \tag{9.2}$$

where K_{adj} is calculated as discussed in Section 10.

9.7. Alternatively, the measured deflection, d_{eff}, in Item 9.1 can be converted to adjusted deflection, d_{adj}, from:

$$d_{adj} = d_{eff} / K_{adj} \tag{9.3}$$

10. ESTABLISHING ADJUSTMENT FACTOR, K_{adj}

10.1. Obtain, K_{adj}, from Equation 10.1.

$$K_{adj} = K_{lab\text{-}field}\, K_{moist} \tag{10.1}$$

where $K_{lab\text{-}field}$ is an adjustment factor that accounts for differences in lab and field moduli at the same moisture content and density, and K_{moist} is an adjustment factor for differences in the compaction and testing moisture contents.

10.2. Estimate $K_{lab\text{-}field}$ from the following relationship:

$$K_{lab\text{-}field} = (F_{env})^{\lambda} \tag{10.2}$$

where λ = - 0.36[14] and F_{env}[15] is calculated from Equation 10.3

$$\log F_{env} = \left[(-0.40535) + \frac{1.20693}{1+e^{\left[0.68184+1.33194\times\left(\frac{S-S_{opt}}{100}\right)\right]}}\right] \tag{10.3}$$

where S_{opt} = degree of saturation at optimum moisture content and S = degree of saturation at compaction moisture content.

10.3. Estimate K_{moist} in the following manner.

$$K_{moist} = e^{\eta(\omega C - \omega T)}\ \textbf{16} \tag{10.4}$$

---

[13] Changes in Poisson's ratio will affect the acceptance rate. As such, the Poisson's ratio to be used for calculating the target modulus and/or to estimate the LWD modulus should be specified and not altered during the project.

[14] Please see the report for the rationale in selecting this value.

[15] This relationship is essentially the relationship proposed by Cary and Zapata (2010) simplified by replacing *wPI* with zero. As reflected in the report, that relationship is so far the most appropriate.

where: η[17] = 0.18 for fine-grained soils and 1.19 for unbound aggregates;
ω_T = moisture content at time of testing (in percent);
ω_C = moisture content at time of compaction (in percent);

11. ESTABLISHING TARGET MODULUS/DEFLECTION[18]

11.1. The target modulus/deflection shall be set in a way that is compatible with the algorithm used during the structural design of the pavement.

11.2. The following steps shall be used to set the target values:

11.2.1. Determine the resilient modulus parameters of the layer under test and the underlying layer(s). In the order of preference, these values should be obtained from one of the options below.

11.2.1.1. Option 1 — Measure the resilient modulus of the geomaterial over the range of stress states in accordance with AASHTO T 307 on specimens prepared from the stockpile. Prepare specimens at their corresponding optimum moisture contents (OMC) and maximum dry densities (MDD). Obtain regression parameters k'_1 through k'_3 that best describes the following relationship for each material.

$$MR_{opt} = k'_1 P_a \left[\frac{\theta}{P_a} + 1\right]^{k'_2} \left[\frac{\tau_{oct}}{P_a} + 1\right]^{k'_3} \quad (11.1)$$

where θ = bulk stress, τ_{oct} = octahedral shear stress, P_a = Atmospheric pressure, and $k'_{1,2,3}$ = Regression constants.

11.2.1.2. Option 2 — Estimate k_1 through k_3 related to Equation 11.2 for the optimum moisture content and maximum dry density from a catalog of materials tested locally, often in conjunction with the implementation of the mechanistic-empirical design algorithms and convert them to k'_1 through k'_3 according to the process discussed in Section 11.2.2.

$$MR_{opt} = k_1 P_a \left[\frac{\theta}{P_a}\right]^{k_2} \left[\frac{\tau_{oct}}{P_a} + 1\right]^{k_3} \quad (11.2)$$

11.2.1.3. Option 3 — Estimate regression parameters k_1 through k_3 related to Equation 11.2 for the optimum moisture content and maximum dry density from relationships established in the literature. The relationships developed from the Federal Highway Administration (FHWA) Long Term Pavement Performance (LTPP) program are shown in Appendix III.

---

[16] This relationship is described in the report.

[17] This relationship seems reasonable based on our Phase II and Phase III study. However, the number of soils used is limited. The SHAs are encouraged to calibrate this equation to fit their common soils.

[18] Establishing the target modulus or deflection in the field using a test section is also an option. MnDOT has developed an excellent set of guidelines for this purpose.

11.2.2. Convert the regression parameters k_1 through k_3 from Equation 11.2 determined in Section 11.2.1.2 or 11.2.1.3 to k'_1 through k'_3 for Equation 11.1, using the following relationships:[19]

$$k'_1 = k_1 \, e^{(-1.32\, k2)} \quad (11.3)$$

$$k'_2 = 1.88\, k_2 \quad (11.4)$$

$$k'_3 = k_3 \quad (11.5)$$

11.2.3. Determine, the target modulus, E_{target}, or target deflection, d_{target}, using one of the options below (Option 1 is preferred).

11.2.3.1. Option 1 - Estimate target deflection, d_{target}, of the pavement system through the following steps:

11.2.3.1.1. Model the pavement section up to the layer to be tested in a nonlinear structural pavement algorithm that uses Equation 11.1[20]. Input the corresponding k'_1, k'_2 and k'_3

11.2.3.1.2. Model the LWD load on top of the layer to be tested by inputting the diameter and nominal load of the device to be used in the field

11.2.3.1.3. The surface deflection at the center of the load is considered as the target deflection, d_{target}.

Note 1: Target LWD modulus, E_{target}, of the pavement system can be estimated using Equation 9.1 once d_{target} is established.

Note 2: Make sure that the Poisson's ratio and other parameters in Equation 9.1 are identical to those selected for the device during measurements.

11.2.3.2. Option 2 - Estimate target LWD modulus, E_{target}, of a one-layer uniform compacted geomaterial using Equation 11.1 with the following values of θ and τ_{oct}[21]

$$\theta = \sigma_0 \, [(0.001D^2 - 0.012D - 0.169) \ln k'_2 + (0.04D + 0.2)] \quad (11.6)$$

$$\tau = \sigma_0 \exp [(-0.01D - 1.47) + k'_2 \, (-0.006D^2 + 0.066D - 1.269)] \quad (11.7)$$

where D = plate diameter (in.) and σ_0 = surface stress (psi) from LWD.

Note 1: Target LWD deflection, d_{target}, of the pavement system can be estimated using Equation 9.1 once E_{target} is established.

Note 2: Make sure that the Poisson's ratio and other parameters in Equation 9.1 are identical to those selected for the device during measurements.

11.2.3.3. Option 3 - Estimate target LWD modulus, E_{target}, of two-layer systems using an artificial neural network prediction model[22] by inputting regression

[19] Please see the report for the derivation of these relationships
[20] Such an algorithm can be downloaded from https://ctis.utep.edu/
[21] Please see the report for the derivation of these relationships
[22] Such an algorithm can be downloaded from https://ctis.utep.edu/

parameters (k'_1, k'_2, and k'_3) and Poisson's ratios of top and underlying layers, load magnitude of LWD, and top layer thickness

Note 1: Target LWD deflection, d_{target}, of the pavement system can be estimated using Equation 9.1 once E_{target} is established.

Note 2: Make sure that the Poisson's ratio and other parameters in Equation 9.1 are identical to those selected for the device during measurements.

Appendix I – Typical Poisson's Ratio Values for Unbound Granular and Subgrade Materials (from MEPDG)

Material Description	Poisson's Ratio	
	Range	Typical
Clay (Saturated)	0.4 – 0.5	0.45
Clay (Unsaturated)	0.1 – 0.3	0.20
Sandy Clay	0.2 – 0.3	0.25
Silt	0.3 – 0.35	0.32
Dense Sand	0.2 – 0.4	0.30
Coarse-grained Sand	0.15	0.15
Fine-grained Sand	0.25	0.25
Bedrock	0.1 – 0.4	0.25

Appendix II – Recommended Shape Factors for LWD Modulus Estimation (from Terzaghi and Peck, 1967; and Fang, 1991)

Soil Type	Plate Type	Shape Factor, C
Clay (elastic material)	Rigid	$\pi/2$
Cohesionless Sand	Rigid	8/3
Material with intermediate characteristics	Rigid	$\pi/2$ to 2
Clay (elastic material)	Flexible	2
Cohesionless Sand	Flexible	8/3

Appendix III – Estimating Resilient Modulus Constitutive Model Coefficients (as per FHWA-LTPP)

Crushed Stone Base Materials:

$$k_1 = 0.7632 + 0.008(P_{3/8}) + 0.0088(LL) - 0.00371(w_{opt}) - 0.0001(\gamma_{opt}) \quad \text{(III.1)}$$

$$k_2 = 2.2159 - 0.0016\,(P_{3/8}) + 0.0008\,(LL) - 0.038(w_{opt}) - 0.006(\gamma_{opt}) + 0.00000024(\gamma^2_{opt} / P_{\#40}) \quad \text{(III.2)}$$

$$k_3 = -1.1720 - 0.0082(LL) - 0.0014(w_{opt}) + 0.0005\,(\gamma_{opt}) \quad \text{(III.3)}$$

Embankments, Soil – Aggregate Mixture, Coarse-Grained:

$$k_1 = -0.5856 + 0.0130(P_{3/8}) - 0.0174(P_{\#4}) + 0.0027(P_{\#200}) + 0.0149(PI) + 0.0000016(\gamma_{opt}) - 0.0426(w_s) + 1.6456[\gamma_s / \gamma_{opt}] + 0.3932[w_s / w_{opt}] - 0.00000082[\gamma^2_{opt} / P_{\#40}] \quad \text{(III.4)}$$

$$k_2 = 0.7833 - 0.0060\,(P_{\#200}) - 0.0081(PI) + 0.0001(\gamma_{opt}) - 0.1483[w_s / w_{opt}] + 0.000000027[\gamma^2_{opt} / P_{\#40}] \quad \text{(III.5)}$$

$$k_3 = -0.1906 - 0.0026(P_{\#200}) + 0.00000081[\gamma^2_{opt} / P_{\#40}] \quad \text{(III.6)}$$

Embankments, Soil – Aggregate, Fine-Grained:

$$k_1 = -0.7668 + 0.0051(P_{\#4}) + 0.0128\,(P_{\#200}) + 0.0030(LL) - 0.051(w_{opt}) + 1.179[\gamma_s / \gamma_{opt}] \quad \text{(III.7)}$$

$$k_2 = 0.4951 - 0.0141(P_{\#4}) - 0.0061(P_{\#200}) + 1.3941[\gamma_s / \gamma_{opt}] \quad \text{(III.8)}$$

$$k_3 = 0.9303 + 0.293(P_{3/8}) + 0.0036(LL) - 3.8903[\gamma_s / \gamma_{opt}] \quad \text{(III.9)}$$

Fine-Grained Clay Soil

$$k_1 = 1.3577 + 0.0106(Clay) - 0.0437(w_s) \quad \text{(III.10)}$$

$$k_2 = 0.5193 - 0.0073(P_{\#4}) + 0.0095(P_{\#40}) - 0.0027(P_{\#200}) - 0.0030(LL) - 0.0049(w_{opt}) \quad \text{(III.11)}$$

$$k_3 = 1.4258 - 0.0288(P_{\#4}) + 0.0303(P_{\#40}) - 0.0521(P_{\#200}) + 0.025(Silt) + 0.0535(LL) - 0.0672(w_{opt}) - 0.0026(\gamma_{opt}) + 0.0025(\gamma_s) - 0.6055\,[w_s / w_{opt}] \quad \text{(III.12)}$$

where:

LL = Liquid Limit
PI = Plasticity index of soil
w_s = Water content of the test specimen (%)
γ_s = Dry density of the test specimen
w_{opt} = Optimum water content (%)
γ_{opt} = Maximum dry unit weight of soil
$P_{3/8}$ = Percentage passing sieve #3/8 sieve
$P_{\#4}$= Percentage passing #4 sieve
$P_{\#40}$= Percentage passing #40 sieve
$P_{\#200}$ = Percent passing #200 sieve
$Clay$ = Percentage of clay (%)
$Silt$ = Percentage of silt (%)

Standard Test Method for

ESTIMATING MODULUS OF EMBANKMENT AND UNBOUND AGGREGATE LAYERS WITH PORTABLE SEISMIC PROPERTY ANALYZER (PSPA)

AASHTO Designation: T E3E

1. SCOPE

1.1. This test method describes the procedure for determining the in-place modulus of compacted geomaterials used in embankments and pavement layers (e.g., prepared subgrade, subbase and base without stabilizing agents), and establishing the target modulus for comparison with the measured values. The modulus will be determined with a device comparable to a Portable Seismic Property Analyzer (PSPA) device.

2. REFERENCED DOCUMENTS

ASTM Standards: Currently there is no ASTM standard for this device.

3. SIGNIFICANCE

3.1. The test method described is useful as a rapid, nondestructive technique for the in-place determination of modulus of underlying compacted geomaterials.

3.2. The test method is used for quality acceptance/quality control testing of compacted geomaterials for construction.

3.3. Test result may be affected by the gradation of the material, sample consistency, moisture content, density and the surface texture of the material being tested.

4. INTERFERENCES

4.1. Moisture contents at the time of compaction and at the time of testing significantly affect the measured modulus with the device. The measured modulus should be appropriately adjusted as discussed in Section 9.

4.2. The device reports the unconfined low-strain, high-strain rate modulus of the material that should be adjusted for pavement design purposes.

5. APPARATUS

5.1. PSPA is a single and nondestructive method that directly measures the modulus of the layer based on the following assumptions.

5.1.1. The operating principle of the PSPA is based on generating and detecting stress waves in a medium.

5.1.2. The device consists of two transducers (accelerometers) and a source packaged into a hand-portable system, which can perform high frequency seismic tests.

5.1.3. The device is operated from a computer connected to the hand-carried transducer unit through a cable that carries operational commands to the PSPA and returns the measured signals to the computer.

5.1.4. The Ultrasonic Surface Wave (USW) interpretation method is used to determine the modulus of the material.

6. SAFETY PROCAUTIONS

6.1. Effective user instruction together with routine safety procedures are a recommended part of the operation and transport of this device.

7. CALIBRATION

7.1. No calibration is required for this device.

8. PROCEDURE

8.1. Operation of the device and the steps to be taken are as follows:

8.1.1. Adjust the PSPA sensor spacing at 4 in. (100 mm) [when the underlying layer thickness is less than 6 in. (150 mm)] and 6 in. (150 mm) [when the compacted layer thickness is greater than 6 in. (150 mm)].

8.1.2. Initiate testing sequence through the computer to activated source and record the responses of the receivers.

8.2. Measure the moisture content of the material at the time of testing as per AASHTO T 310, or other method specified by the Engineer at the same time that the modulus-based measurements are made.

9. CALCULATION OF EFFECTIVE AND ADJUSTED PSPA MODULUS

9.1. The following relationships are used to estimate the modulus

9.1.1. The device measures the shear velocity, V_s, of the layer.

9.1.2. Estimate the shear modulus, G, from Equations 9.1:

$$G = (\gamma / g) V_s^2 \quad (9.1)$$

where γ = total unit weight of the material and g = acceleration of gravity.

9.1.3. Estimate the PSPA seismic modulus, E_{PSPA}, from Equations 9.3:

$$E_{PSPA} = 2 (1+\upsilon) G \quad (9.2)$$

where υ = Poisson's ratio.

9.1.4. Estimate the adjusted modulus, E_{adj}, from:

$$E_{adj} = E_{PSPA} * K_{adj} \quad (9.3)$$

where K_{adj} is calculated as discussed in Section 10.

10. ESTABLISHING ADJUSTMENT FACTOR, K_{adj}

10.1. Obtain, K_{adj}, from Equation 10.1.

$$K_{adj} = K_{lab\text{-}field} K_{moist} \quad (10.1)$$

where $K_{lab\text{-}field}$ is an adjustment factor that accounts for differences in lab and field moduli at the same moisture content and density, and K_{moist} is an adjustment factor for differences in the compaction and testing moisture contents.

10.2. Estimate $K_{lab\text{-}field}$ from the following relationship:

$$K_{lab\text{-}field} = (F_{env})^{\lambda} \quad (10.2)$$

where λ = - 0.36[23] and F_{env}[24] is calculated from Equation 10.3

[23] Please see the report for the rationale in selecting this value.

$$\log F_{env} = \left[(-0.40535) + \frac{1.20693}{1+e^{\left[0.68184+1.33194\times\left(\frac{S-S_{opt}}{100}\right)\right]}}\right] \quad (10.3)$$

where S_{opt} = degree of saturation at optimum moisture content and S = degree of saturation at compaction moisture content.

10.3. Estimate K_{moist} in the following manner.

$$K_{moist} = e^{\eta(\omega C - \omega T)} \quad (10.4)$$

[25]

where: η[26] = 0.18 for fine-grained soils and 1.19 for unbound aggregates,
ω_T = moisture content at time of testing (in percent), and
ω_C = moisture content at time of compaction (in percent).

11. ESTABLISHING PSPA TARGET MODULUS

11.1. The target modulus, $E_{T\text{-}PSPA}$, is directly determined from laboratory Free-Free Resonant Column (FFRC) test (conforming to ASTM C 215) results using the following equation:

$$E_{T\text{-}PSPA} = E_{FFRC\text{-}Lab} / [(1+\upsilon).(1-2\upsilon)/(1-\upsilon)] \quad (11.1)$$

where $E_{FFRC\text{-}Lab}$ = measured modulus with the FFRC device on the laboratory specimen and υ = Poisson's ratio of the material.

[24] This relationship is essentially the relationship proposed by Cary and Zapata (2010) simplified by replacing *wPI* with zero. As reflected in the report, that relationship is so far the most appropriate.
[25] This relationship is described in the report.

Appendix B

TOOLS FOR QUALITY ACCEPTANCE

BRIAUD COMPACTION DEVICE (BCD)

Description of Technology

The BCD estimates the modulus of the soil below by measuring the bending of a plate resting on the ground surface. The BCD works by applying a small load to a thin plate in contact with the compacted soil of interest, and recording the resulting stains. A large strain indicates a weaker soil while a small strain indicates a stiffer soil.


Hardware

The BCD consists of the following components: a plate, a load cell, a tube, a handle, and a display. A stainless steel plate in contact with the surface of the soil is 2 mm thick and 150 mm in diameter to fit the requirements of depth of influence in the field. This plate is instrumented with eight strain gauges placed on top of the plate close to the rod. Above the plate is the load cell, which detects the force applied by the person leaning on the BCD.

Data Analysis

The load recorded by the load cell and the resulting deflections of the thin plate calculated from the readings of the radial and axial strain gauges mounted on the thin plate are used to estimate the BCD modulus. The proprietary software within the device uses correlations established by numerical simulation determined from field and laboratory tests to estimate a low strain modulus. The strain level associated with the BCD is on the order of 10^{-3} in./in. A modulus compaction curve in the lab has to be first developed to establish a target modulus from that curve.

Advantages

The BCD can be used both in the lab to obtain the target modulus and in the field to verify that the target modulus has been achieved.

Limitations

The device is effective in soils with moduli ranging from 5 MPa to 150 MPa. For soft soils, the BCD plate simply penetrates in the soil without bending. For stiff soils, the bending of the plate is not adequate for precise measurements of the strains.

Training Requirements

Training for operation of BCD takes less than one day.

Costs

Not available at this time.

Speed
Actual testing will take 5 seconds.

Ease of Use
The equipment is easy to use with very limited training. It can be carried and operated by one person.

Accuracy and Precision
The repeatability of the method is around 4%.

Case Histories
Briaud et al. (2006) describe the theory and the experiments that have been performed to validate the BCD. The validation was based on a comparison to a simple plate test and numerical simulations of the BCD test.

Weidinger and Ge (2009) evaluated the BCD for soil compaction control. That study indicated that the BCD modulus could be compared to other tests such as the ultrasonic pulse velocity test. However, they noted that due to the limitation of the BCD's influence depth, it would be difficult to effectively assess the soil modulus beyond several inches below the ground surface. In that regard, the value of the BCD might be somewhat limited when compared to other QA/QC methods which assess soil characteristics to greater depths.

CLEGG IMPACT HAMMER (ASTM STANDARD D 5874)

Description of Technology

The basic principle behind the Clegg Impact Soil Tester is to obtain a measurement of the deceleration of a free falling mass or hammer from a set height onto the soil. The impact of the hammer produces an electrical pulse, which is converted and displayed on the Control Unit.

Hardware

The Clegg Hammer consists of a compaction hammer operating within a vertical guide tube and an electronic display. The hammer is raised in the guide to a predetermined drop height. An accelerometer built into the hammer measures the peak deceleration of the hammer when it impacts the soil surface.

Data Analysis

The electronic display registers the deceleration in units of Impact Value (IV). The IV is related to soil strength and correlated with the California Bearing Ratio (CBR) values. A target impact value needs to be established in the laboratory.

Advantages

The device can be transported and operated by one person. It is also a nondestructive test and results could be correlated with California Bearing Ratio values.

Limitations

One of the limitations for the Clegg Impact Tester is its inability to track changes in density and moisture content. There is a possibility of boundary effects when calibrating the device using Proctor molds. Another important limitation is that different hammers of different weights report different CIV values.

Training Requirements

Minimal training is required.

Costs

The basic system costs around $3000, but the complete system can cost up to $20,000.

Speed
Each test can be completed in less than 1 minute. The impact value is displayed directly and instantaneously upon competition of the test.

Ease of Use
The equipment is easy to use with very limited training. It can be carried and operated by one person.

Accuracy and Precision
The coefficient of variation is 4% for conditions of high uniformity and 20% for highly variable conditions.

Case Histories
Mathur and Coghlan (1987) provided a review of applications and operation of the Clegg Impact Tester. They reported positive correlation between the California Bearing Ratio (CBR) and the Clegg Impact Value (CIV), but they indicated that the correlation might vary for different materials. Their tests showed that the depth to which an underlying material would influence the CIV is at least 12 in. No correlation was found between the CIV and the Benkelman Beam deflections, but good correlation was found with the Falling Weight Deflectometer readings.

Garrick and Scholer (1985) investigated the potential use of the Clegg impact tester. They showed that the CIV accurately predicted pavement performance. In many cases, they could convert CIV to an equivalent California bearing ratio value.

Pidwervesky (1997) results showed that the Clegg Hammer had deficiencies when compared with the other devices. They did not observe any correlation or trend against which quality control parameters could be confidently set.

Al-Amoudi et al. (2002) assessed the efficacy of the Clegg impact hammer for estimating the strength of compacted soils by conducting a comparative study between the California-bearing ratio (CBR) and CIH tests. Their results indicated that the Clegg impact values correlated relatively well with the CBR values from laboratory and field tests.

Peterson and Wiser (2003) compared field CIVs with traditional measurements for the New York State Electric and Gas Corporation. They concluded that the Clegg Hammer accurately identified the target 90% relative compaction for 84% of the measurements obtained.

Fairbrother et al. (2010) compiled correlations published by Gulen and McDaniel (1990), Al-Amoudi et al. (2002), Pidwerbesky (1997), Mathur and Coghlan (1987), and Clegg (1978). They also tested subgrade soil samples from forest roads located throughout the East Cape region of New Zealand. Their analysis indicated a relatively strong correlation between the CIV and CBR for forest subgrade soils. Clayey and excessively wet soils had a significant negative impact on their correlation. They indicated that, while their CIV to CBR correlation was not highly accurate, the simplicity and efficiency of the CIH made it an effective tool to promote a greater understanding of subgrade bearing strength.

Farrag (2005) implemented a modified CIH as an alternative to the Nuclear Density Gauge in soil compaction control. The hammer was redesigned for ease of transport and mobility. They indicated that the modification improved the precision and accuracy of measured CIVs.

DYNAMIC CONE PENETROMETER (ASTM STANDARD D6951)

Description of Technology

The Dynamic Cone Penetrometer (DCP) test involves driving a cone shaped probe into the soil using a dynamic load and measuring the advancement of the device for each applied blow or interval of blows. The depth of penetration is a directly impacted by the drop height of the weight, cone size, and cone shape. Also, the resistance to penetration is dependent on the strength of the material. The strength, in turn, is dependent on density, moisture, and material type of the layer evaluated.

Hardware

The DCP consists of a 0.62 in. (15.8 mm) diameter steel rod with a standard cone shaped tip, a 17.6-lb (8-kg) hammer that is dropped by a fixed height of 22.6 in (575 mm), a coupler assembly, and a handle. The cone tip has a diameter of 0.79 in (20 mm) with an angle of 60 degrees to reduce side friction. The entire device is made of stainless steel to protect it from corrosion. However, the cone tip is made of hardened tool steel or a similar material to resist wear and tear.

Data Analysis

The data recorded include the number of blows and the depth of penetration. The rate of penetration is defined as the depth of penetration per blow, and is often referred to as the penetration index or the DCP ratio. The penetration rate is determined as the slope of the curve relating the number of blows to the depth of penetration. The penetration rate can be converted to the CBR, resilient modulus, unconfined compressive strength, and shear strengths using empirical relationships.

Advantages

The DCP requires minimum maintenance, is very portable, and provides continuous measurements of the in-situ strength of pavement section and the underlying subgrade layers. The DCP is able to penetrate into underlying layers and locate zones of weakness within the pavement structure with minimal disturbance. The results are layer specific with no influence on the results by the underlying layers and therefore no composite modulus values.

Limitations

High variability exists particularly in the case of large, well-graded granular materials. The use of DCP for materials with a maximum aggregate size of larger than 1 to 2 in. is questionable. Some of the existing strength relationships are only applicable to certain material types and conditions.

Training Requirements

Training for operation of DCP takes less than 1day.

Costs

The initial cost of the equipment is less than $3,000 for the manual device. The automated device costs around $40,000.

Speed
Each test point takes about 5 minutes.

Ease of Use
The equipment is easy to use with proper training. One person can operate the automated version. However, it is recommended that two person operate the manual DCP.

Accuracy and Precision
Different DCPs exhibit many similarities in their mechanics of operation although there are some differences in their design and mode of operation, which lead to variations in the measured results. For a depth of penetration of 6 in., an error of estimate of less than 20% is reported.

Case Histories
Amini (2003) provided detail documentation of the history and applications of the DCP. References listed included De Beer and van der Merwe (1991); Meier and Baladi (1988); Newcomb et al. (1994); Newcomb et al. (1995); Parker et el. (1998); Truebe and Evans (1995); Tumay (1994); Burnham and Johnson (1993) and White, et al. (2002). They also document the list of investigators that have used the DCP from Allersma (1988); Bester and Hallat (1977); Bukoski and Selig (1981); Chen et al. (1999); Chen et al. (2001); and Chan and Armitage (1997). Finally, they summarized the relationships of DCP penetration rate with CBR, resilient modulus and strength.

Chen et al. (2001) indicated that the DCP was useful for determining the layer thickness, and could be a useful tool when the FWD backcalculated moduli were not accurate.

Siekmeier et al. (1999) used DCP on several projects in Minnesota. They correlated the strength as estimated with the DCP with the elastic deformation modulus, measured using the PFWD and SSG.

Rahim and George (2002) investigated the viability of using the automated dynamic cone Penetrometer for subgrade characterization through correlation between DCP index and laboratory resilient modulus. Twelve as-built subgrade sections, reflecting a range of typical Mississippi subgrade materials, were selected and tested with the DCP. Their developed models seemed to provide useful predictions of resilient modulus.

Abu-Farsakh et al. (2005) presented the results of a comprehensive testing program that was conducted to evaluate the potential use of the DCP in the quality control/quality assurance procedure during the construction of pavement layers and embankments. They successfully correlated the DCP penetration index with the FWD moduli and CBR values.

Thompson (2009) examined correlations among the responses of five devices, including the DCP. His analyses of the data revealed statistically significant correlations among the DCP penetration index and moduli from other NDT devices.

Swenson et al. (2006) studied the effects of moisture and density on modulus and strength of four subgrade soils in Minnesota. Their results revealed that both moisture and density had measurable effects on the modulus and strength of all four soils. The DCP was effective in quantifying the uniformity of compacted soil volumes, and through empirical formulae, the apparent modulus.

Davich et al. (2006) studied the dynamic cone penetrometer (DCP) and light weight deflectometer (LWD) on the laboratory prepared specimens. They found that the MnDOT DCP specification accurately assessed the compaction quality with some suggestions for improvement.

Von Quintus et al. (2009) evaluated the DCP because of its current use in QA operations in selected agencies. The DCP was successful in locating areas with anomalies at an acceptable rate. They also found that the DCP results were more dependent on aggregate sizes than other NDT devices.

GEOGAUGE (ASTM STANDARD D6758)

Description of Technology

Geogauge is a hand-portable gauge that provides a means of estimating lift stiffness and soil modulus for compaction process control. The Geogauge measures the impedance at the surface of an unbound layer by imposing a known stress to the surface of a layer and measuring the resulting surface velocity as a function of time at 25 steady state frequencies between 100 and 196 Hz.

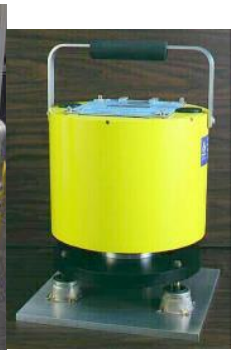

Hardware

The Geogauge consists of an external case housing an electro-mechanical shaker, upper and lower velocity sensors, a power supply, and a control and display unit. A rigid foot with annular ring is fixed at the base of the case. The Geogauge weighs about 10 kg (22 lbs), is 280 mm (11 in.) in diameter and 254 mm (10 in.) tall. Its annular ring that contacts the soil has an outside diameter of 114 mm (4.50 in.), an inside diameter of 89 mm (3.50 in.) with a thickness of 13 mm (0.5 in.).

Data Analysis

The Geogauge modulus is estimated from the Boussinesq theory from the average of 25 stiffness values obtained at 25 different frequencies that can be converted to soil elastic modulus using a direct relationship.

Advantages

The Geogauge is a hand-portable instrument that provides a simple, rapid means of measuring in-place load bearing characteristics of compacted materials. It can be used to develop modulus growth curves as material is being compacted by the rollers.

Limitations

The Geogauge modulus does not represent the stress levels that occur under truck loadings. The modulus has to be adjusted to account for the design loads. The moduli of the underlying materials can influence the results when trying to test relatively thin unbound layers. Intimate contact between the Geogauge and soil is difficult to achieve in practice without preparation.

Training Requirements

Training for operation of Geogauge takes less than 1day.

Costs

The cost is close to $6,000.

Speed

The Geogauge measures the in-place stiffness of compacted soil at the rate of about one test in less than 2 minutes.

Ease of Use
The equipment is easy to use with proper training.

Accuracy and Precision
As reported by the manufacturer, the coefficient of variation is less than 10%. The bias of a Geogauge measurement, relative to the value of the moving mass, is less than 1%. The precision of a Geogauge measurement on fine grained soils is reported as less than 2% and on coarse grained soils and crushed aggregate less than 5%. Von Quintus et al. (2009) reported a typical coefficient of variation of 15% for repeated tests. They reported a material-dependent standard deviation for repeatability measurements varying from 0.3 to 3.5 ksi.

Case Histories
Lenke et al. (2001) evaluated the Geogauge for the New Mexico State Transportation Department. The Geogauge was found to measure soil stiffness consistent with mechanical strength of soils. However, because of the dynamic nature of the measurement obtained via the Geogauge, specific control of moisture was recommended.

Nazzal (2003) and Abu-Farsakh et al. (2004) evaluated the potential use of the Geogauge in measuring the in situ moduli of subgrades, compacted soils, and base layers in Louisiana. They reported good empirical correlations among the Geogauge modulus and the measurements with standard tests, indicating that the Geogauge device could be a promising tool in evaluating the moduli of pavement layers. Their results indicated that the influence depth of the Geogauge ranged from 190 mm to 200 mm (7.5 in. to 8.0 in).

Gudishala (2004) developed models to estimate the modulus of base or subgrade soils from in situ tests with the Geogauge. Two types of cohesive soils and three types of granular soils commonly used in Louisiana were considered. Their statistical models correlated the resilient modulus to the in-situ Geogauge results and basic soil properties.

Baus and Li (2006) investigated the feasibility of relaxing South Carolina Department of Transportation (SCDOT) gradation specifications and layer thickness restrictions. Seven granular base materials used by the SCDOT were included in a laboratory plate load tests and measurements with the Geogauge. They recommended the Geogauge as an alternative tool for pavement material quality assurance and construction control.

Alshibli et al. (2005) assessed the potential use of the Geogauge as quality control/quality assurance devices for testing subgrades, base courses, and compacted soil layers. The study showed that the Geogauge can be used to calculate the modulus/stiffness characteristics of compacted layers.

Problems with the field use of the Geogauge have been reported in several studies, including Simmons (2000); Miller and Mallick (2003); and Ellis and Bloomquist (2003). Many of the problems centered on the seating of the Geogauge at the soil-foot interface. They reported that the recommended 60% contact area between the Geogauge ring and soil was difficult to achieve in practice. Site preparation with leveling sand, as recommended by the manufacturer, was shown to significantly alter the measurements depending on the thickness of sand used (Simmons, 2000). Simmons (2000) and Miller and Mallick (2003) showed concerns with the malfunction of the Geogauge due to vibrations from passing vehicles, compaction equipment, or trains.

Von Quintus et al. (2009) indicated that the Geogauge provided a reasonable estimate of the laboratory measured values with the exception of the fine-grained, clay soils. Von Quintus et al. (2010), as part of a study for Wisconsin DOT, used the Geogauge to evaluate the effectiveness of the intelligent compaction technology. The Geogauge was calibrated to the project materials and conditions in order to improve its accuracy.

LIGHT WEIGHT DEFLECTOMETER (ASTM STANDARD E2583)

Description of Technology

The Light Weight Deflectometer (LWD) is a portable Falling Weight Deflectometer (PFWD) that has been developed as an alternative in-situ testing device to the plate load test. Generally, the LWD consists of a loading device that produces a defined load pulse, a loading plate, one center displacement sensor (and up to two optional additional sensors) to measure the center deflection or a deflection bowl. Similar to FWD, the LWD determines the stiffness of pavement system by measuring the material's response under the impact of a load with a known magnitude and dropped from a known height.

Hardware

LWD consists of a geophone or an accelerometer and a falling mass that impacts a loading plate. It weighs about 25 kg (60 lb) and typically has a 10 kg (22 lb) falling weight that impacts a spring to produce a load pulse of 15-20 milliseconds. Typical load range is from 1-15 kN (1500 lbs to 2700 lbs). The loading plate diameter can be switched between 300 mm (11.8 in.) and100 mm (3.9 in.).

Data Analysis

Automated data analysis software is available in most devices. The software associated with the equipment is used to determine the soil modulus. Normally the center deflection of the loading plate is used to estimate the LWD elastic stiffness modulus. The modulus of a layered media is calculated using the Boussinesq elastic half space assuming a uniform Poisson's ratio and constant loading.

Advantages

The LWD provides a more representative picture of a pavement's ability to handle traffic loads than density measurements. The LWD can be a direct verification of the soil values used during pavement design, with no lab work so inspector stays on-site.

Limitations
Poor correlation between compaction level and LWD moduli has been reported (Steinert et al., 2005). The LWD has high variability in measured modulus reported for the same material tested with different LWD devices. Different LWD devices report different moduli for the same geomaterial layers. This could be attributed to the different methods used to determine deflections in different devices (Steinert et al., 2005 and White et al., 2007).

Training Requirements
Training for operation of LWD and its software takes 1 to 2 days.

Costs
$10,000 to $15,000

Speed
Actual testing will take about 2 minutes.

Ease of Use
The equipment is easy to use with proper training. The tester can be operated by one operator, but normally two is used.

Accuracy and Precision
The typical ideal precision for deflection sensors is ± 2µm. The equipment bias for the load cell and deflection sensors are ± 2%. Fleming et al. (2000) suggested a typical ±20% scatter when comparing devices with small differences in plate seating, even at nominally the same location. Alshibli (2005) reported wide scatter and poor repeatability of measurements (coefficient of variation ranged from 1.2% to 46.3%), especially when testing weak subgrade layers. Nazzal (2003) reported coefficients of variation ranging from 2.1 to 28% for modulus values.

Case Histories
According to Von Quintus et al. (2009) provided the following assessment of the LWD:

- Technology was unable to consistently identify those areas with anomalies.
- The moduli could be influenced by the underlying layers, resulting in lower or higher and more variable moduli.
- The normalized dispersion was found to be high, relative to the other NDT devices.
- Any error in thickness of the layer being tested can result in large errors and more variability that could lead to wrong decisions being made by the contractor and agency about the construction operation.

The key features of eight commonly used LWD devices as summarized by Vennapusa and White (2009) are presented in Table B.1. They found that the LWD moduli are affected by the size of loading plate, plate contact stresses, type and location of deflection sensor; plate rigidity, loading rate, and buffer stiffness.

Livneh et al. (2001) presented two case studies during construction of two major interchanges in Israel. LWD testing was found to be useful in identifying local spots with poor performance. LDW device for measuring the mechanical properties of the formation of flexible pavements was also examined and found to be a cost-effective testing device for quality control and assurance during subgrade and capping-layer compaction.

Steinert et al. (2005) investigated the effectiveness of the LWD for evaluating the support capacity of pavements during the spring thaw and the adequacy of subgrade and base compaction during construction. Comparisons were made with the traditional FWD as well as other portable measuring

devices. The LWD was able to follow seasonal stiffness variations and compared well with FWD-derived moduli on both asphalt and gravel surfaces. A technique was recommended for using a LWD for compaction quality control for aggregate base and subbase courses.

Table B.1 - Comparison of Different LWD Devices (Vennapusa and White 2009)

Device	Plate Diameter (mm)	Plate Thickness (mm)	Falling Weight (kg)	Maximum Applied Force (kN)	Load Cell	Total Load Pulse (ms)	Type of Buffers	Deflection Transducer		
								Type	Location	Measuring Range (mm)
Zorn	100, 150, 200, 300	124, 45, 28, 20	10, 15	7	No	18±2	Steel Spring	Acceler-ometer	Plate	0.2-30 (±0.02)
Keros	150, 200, 300	20	10, 15, 20	15	Yes	15-30	Rubber (Conical shape)	Velocity	Ground	0-2.2 (±0.002)
Dynatest 3031	100, 150, 200, 300	20	10, 15, 20	15	Yes	15-30	Rubber (Flat)	Velocity	Ground	0-2.2 (±0.002)
Prima	100, 200, 300	20	10, 20	15	Yes	15-20	Rubber (Conical shape)	Velocity	Ground	0-2.2 (±0.002)
Loadman	110, 132, 200, 300	-	10	18	Yes	25-30	Rubber	Acceler-ometer	Plate	-
ELE	300	-	10		Yes			Velocity	Plate	-
TFT	200, 300	-	10	8.5	Yes	15-25	Rubber	Velocity	Ground	-
CSM	200, 300	-	10	8.8	Yes	15-20	Urethane	Velocity	Plate	-

Alshibli et al. (2005) assessed the potential use of the LWD as quality control/quality assurance devices for testing subgrades, base courses, and compacted soil layers. A comprehensive laboratory experimental program was conducted on compacted layers of silty clay, clayey silt, cement-treated clay, sand, gravel, recycled asphalt pavement, and limestone aggregates. That study showed that the LWD could be used to calculate the stiffness characteristics of compacted layers and the initial moduli of cement-treated clays. Good statistical correlations were obtained between the LWD modulus and both the initial and reloading elastic moduli obtained from the Plate Load tests. The R^2 values were 0.84 and 0.90 for initial and reloading, respectively.

Fleming et al. (2007) provided a general overview and evaluation of the LWD for construction quality control or material investigation for earthworks and road construction. They concluded that the device was a useful and versatile field quality control and pavement investigation tool if an understanding of the device issues was considered by the data users.

Petersen et al. (2007) investigated the use of the LWD to measure in-situ soil stiffness and the feasibility of developing a stiffness-based specification for embankment soil compaction quality control for the Kansas Department of Transportation (KDOT). They found that the equivalent predicted moduli from laboratory resilient modulus tests did not correlate with the in-situ stiffness moduli. In addition, their testing showed that the in-situ modulus of fine grained soils has a high degree of spatial variability preventing the development of a quality control procedure.

Mohammad et al. (2010) evaluated the potential use of foamed asphalt treated RAP as a base course material in lieu of a crushed lime stone base for continuously reinforced concrete pavement using the LWD as one of the NDT devices. The LWD moduli compared well with the results of the FWD and Dynaflect, all showing a higher stiffness for the foamed asphalt treated RAP compared to crushed lime base. The authors mentioned that devices such as the LWD are more convenient and more promising than the traditional FWD and Dynaflect because of their light-weight and portability.

Horak et al. (2008), Livenh and Goldberg (2001), Fleming et al. (2000), Fleming (2001), Nazzal (2003), and Rahimzadeh (2004) showed different levels of correlation between the FWD and LWD moduli. All studies agreed that although there were correlations and trend between the two devices they tend to vary depending on the material type and pavement structure.

George et al. (2009) worked on establishing correlations among the LWD moduli with those from traditional approaches on lateritic soils in India. They reported that their regression models could predict CBR values based on the LWD moduli of subgrade at field density and moisture contents.

Thompson (2009) analyzed the LWD data and other relevant test results from 41 project-sites on treated and untreated base, subbase, and subgrade layers, representing 15 different material types in Iowa, Louisiana, Utah, and Wyoming. They found significant correlations among the LWD measurements and the stiffness properties of the materials tested. Comparable correlation was obtained between the LWD and other NDT devices such as the FWD, in studies by Nazzal et al. (2004 and 2007). In that study, the LWD device reliably measured the in-situ moduli of pavement layers and subgrades from different projects.

Mooney and Miller (2008), Chaddock and Brown (1995), Fleming et al (2000 and 2007), Frost (2000) and Hoffman et al. (2004) studied the LWD tests based on their in situ stress and strain responses. The LWD depth of influence was reported as 0.9 - 1.5 the plate diameter.

Hoffmann et al. (2003) studied the accuracy of the stiffness estimates from the LWD. Their objective was to propose an alternative method to interpret the LWD data. Using the frequency response functions of a single degree of freedom system analog, the static stiffness from LWD measurements were extracted. Test results show good agreement between the estimates based on the modified analysis and true beam stiffness. They proposed the implementation of their alternative data interpretation method for quality assurance field measurements.

PORTABLE SEISMIC PROPERTY ANALYZER

Description of Technology

The Portable Seismic Property Analyzer (PSPA) uses the Spectral-Analysis-of-Surface-Waves (SASW) method which is based upon measuring surface waves propagating in layered elastic media. The SASW test is a non-intrusive seismic test method that relies on the measurement of Rayleigh type surface waves. The key point in the SASW method is the measurement of the dispersive nature of the surface waves, which are used to determine the shear wave velocity of the pavement, the base, and the subgrade. The generation and detection of surface waves are controlled by an impact source and two receivers (or accelerometers) placed on the pavement surface. The two vibration transducers are located at known distances from the source. Typically, one of the distances is kept equal to two times the shorter distance.

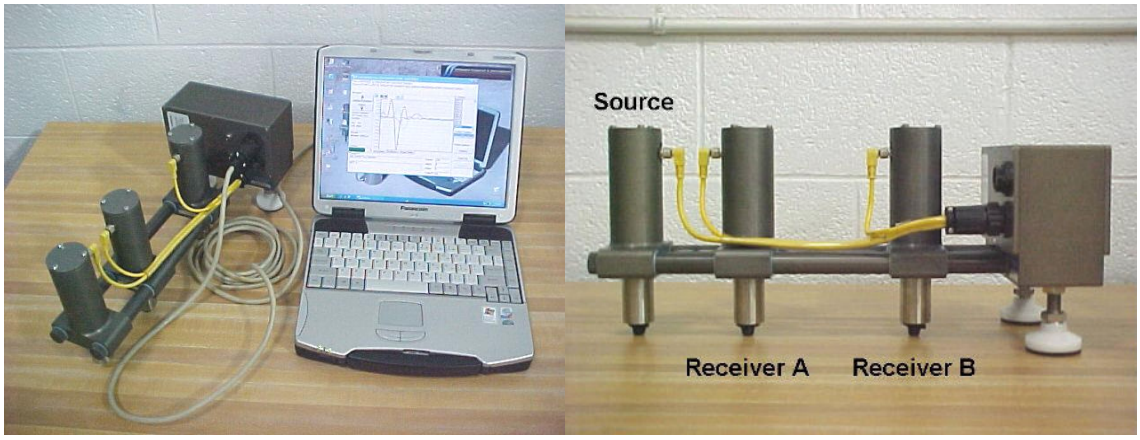

Hardware

Automated hardware, such as Portable Seismic Property Analyzer (PSPA), is available.

Data Analysis

Automated data analysis software is available in devices such as PSPA. Data analysis is conducted on site by the software. The method provides qualitative variation of modulus with depth.

Advantages

The major advantage of seismic methods is that similar results are anticipated from the field and laboratory tests as long as the material is tested under comparable conditions. This unique feature of seismic methods in material characterization is particularly significant in QA operations.

Limitations

One of the limitations of using seismic technology for QA application is that the seismic modulus does not represent the stress levels that occur under truck loadings. The seismic moduli have to be adjusted to account for the design loading frequency and strain.

Training Requirements

Training for operation of PSPA or similar devices takes about two days and training for data interpretation takes another three to four days.

Costs

$20,000 to $30,000.

Speed
Actual testing will take about 15 seconds. Considering point-to-point movement during testing, 200 to 400 points per day can be tested.

Ease of Use
The equipment is easy to use with proper training. It can be carried and operated by one person.

Accuracy and Precision
The repeatability of the method is better than 15% on average.

Case Histories
Nazarian et al. (2002 and 2004) developed several field protocols and test equipment that combine the results from laboratory and field tests with those used for quality control during construction based on seismic technology. The study focused on repeatability, reproducibility of the methods, means of relating the measured parameters to the design moduli, and relating the parameters to performance of the pavement.

Rathje et al. (2006) studied and evaluated non-nuclear devices such as the PSPA as potential replacements for the nuclear gauge for soil compaction control. The specific application was for the quality control of compaction of earth embankments and mechanically stabilized earth (MSE) wall backfill. The researchers present the strengths such as the ability to measure the elastic modulus of a pavement system. They also remarked this device requires extensive operators training and categorized this device as one of the most expensive considered for their study.

Von Quintus et al. (2009) considered the PSPA favorably because it provided a measure of the layer modulus and could be used to test both thin and thick layers during and shortly after placement. The PSPA was the device that had the highest success rate in identifying areas with different physical conditions or anomalies.

Abdallah et al. (2002) described a methodology for combining the laboratory and field seismic technology to determine design modulus. Several case studies were used to illustrate the concept. That concept was also presented in Ke et al. (2000). The relationship between the resilient modulus and seismic modulus was further documented in Williams et al. (2002) and Nazarian et al. (2003).

Gucunski and Maher (2002) examined the applicability of the seismic technology in pavement structural evaluation, detection of defects and distresses, and other uses relevant for pavement evaluation and condition monitoring. They concluded that this technology is a well-designed automated data collection and analysis system for seismic testing of pavements.

Guo et al. (2006) documented the successful use of seismic techniques for mechanistic design procedures.

Jersey and Edwards (2009) evaluated the use of the PSPA and other tools on eleven soil test beds that were constructed at the U.S. Army Engineer Research and Development Center. They indicated that the tools were simple to use and generally obtained repeatable results, but additional information regarding the true nature of the modulus measured by these tools was required to implement their use in new mechanistic design methods. Joh et al. (2006) and Sawangsuriya et al. (2006) also presented case histories based on the field and laboratory seismic testing.

Mallick et al. (2005, 2006) presented the use of seismic technology in Maine for evaluating stiffness of subsurface pavement reclaimed layers for thin surfaced HMA pavements. The process was reported as effective especially in predicting moduli that can be used effectively in mechanistic empirical design of pavement structures.

Seismic wave-based testing has been reported to have considerable potential since it bridges the disconnect between lab and field parameter measurements (Nazarian et al. 2002, Ryden et al. 2006, Åhnberg 2008, Hillbrich et al. 2007).

Toohey et al. (2010) presented seismic testing protocols and results which indicated their effectiveness as a combined quality management technique. Schuettpelz et al. (2010) used seismic technology to determine resilient modulus of base course materials with correction factors.

Celaya et al. (2010) presented a case study that showed the potential of an approach that integrates design, laboratory and field quality management processes based on seismic technology.

ELECTRICAL DENSITY GAUGE (EDG) (ASTM STANDARD D7698)

Description of Technology

The Electrical Density Gauge (EDG) is a non-nuclear alternative for determining the moisture and density of compacted soils used in road beds and foundations. The EDG is a portable, battery-powered instrument capable of being used anywhere without the concerns and regulations associated with nuclear safety.

Hardware

The hardware consists of four tapered 6 inch spikes, hammer, soil sensor and cables, template, temperature probe, battery charger, and hard case.

Data Analysis

The EDG employs an electronic system for measuring the electrical dielectric properties of soils at a high radio frequency, and a computer for the necessary mathematic computations that are involved in the determination of dry density, percent moisture content, and percent compaction. Four electrical measurements are made in a cross pattern and automatically examined for outliers, and the best are averaged to provide values representing the electrical characteristics of that spot. In addition, a probe inserted into the soil measures its temperature. A proprietary correction algorithm is used to assure accurate results over the range of expected field temperatures.

Advantages

The system is user-friendly and does not require a highly-trained or licensed technician.

Limitations

Tedious and highly material-dependent calibration process, difficulties in placing the spikes into coarse-grained materials, and lack of the sensitivity of the results are considered as the disadvantages of this device.

Training Requirements

It does not require a highly-trained or licensed technician.

Costs

$8,000 - $15,000

Speed

Results can be obtained within less than a minute after the spikes are placed. Total test time typically 10 to 20 minutes.

Ease of Use
The device is easy to setup and use. However, the four spikes increase the likelihood of disrupting the soil if hitting a rock.

Accuracy and Precision
As reported by the manufacturer, the device is designed to monitor percent moisture to within ±2% accuracy and ±3% for density.

Case Histories
Bennert and Maher (2008) evaluated the EDG on recycled concrete aggregates in a dense-graded base course. The unit was used on five separate field trials and compared against the NJDOT's nuclear density gauge. The EDG results did not correlate well with those from the NDG.

Rathje et al. (2006) performed a field study to assess rapid methods for density control of MSE walls and embankments. They used the EDG at three construction sites in Austin, Texas. These sites encompassed CH, CL, and sandy clay (CH) soils. The EDG did not provide accurate measurements of either water content or dry unit weight. In addition, the EDG could not be field calibrated.

Von Quintus et al. (2009) reported that the EDG consistently provided coefficients of variation of measurements of less than 1%. They recommended that this device and technology be evaluated in more detail and that studies be initiated to improve its accuracy.

MOISTURE + DENSITY INDICATOR (M+DI) (ASTM STANDARD D6780)

Description of Technology

The Moisture+Density Indicator (M+DI) uses Time Domain Reflectometry (TDR) to measure the travel time of an electromagnetic step pulse produced by the TDR pulse generator through four soil spikes in the ground.

Hardware

The apparatus consist of four spike probes that are encased in a probe head that is connected by a coaxial cable lead by a pulse generator. The generator is attached to a PDA with proprietary software.

Data Analysis

The voltage signal is analyzed to determine apparent dielectric constant and bulk electrical conductivity of the soil. A set of equations is used to relate these two properties to water content and density which are displayed on the screen. Two field testing methods can be used: a) One-Step Method and b) Two-Step Method. The One-Step method consists of measuring the bulk electrical conductivity in addition to the dielectric constant of the soil in-place with one measurement. The Two-Step method consists of measuring the dielectric constant of the soil in-place (Step One) and the soil in a compaction mold (Step Two) with the M+D Indicator.

Advantages

The equipment requires no certified operators or safety training. It also requires no instrument calibration.

Limitations

The M+DI apparatus is time consuming to set up. The proper installation of the four spikes has been reported as a concern, especially in coarse materials. The device requires prior calibration of the device for each specific soil using laboratory compaction molds. In addition, highly organic or highly plastic soils at higher water contents may attenuate the M+DI response signal.

Training Requirements

Training requirements is necessary to follow the one and two step methods discussed in data analysis.

Costs

Stats at $6,000

Speed

Time to perform field tests is less than 20 minutes.

Ease of Use
The entire process of the M+DI requires several steps as summarized in the data analysis.

Accuracy and Precision
As reported by the developers, water content accuracy compared to oven-dry measurement is 1% and for dry density measurements 3%

Case Histories
Siddiqui and Drnevich (1995) and Yu and Drnevich (2004) presented efforts to extend the application of TDR to measure the gravimetric water content and the dry density of soils for geotechnical engineering applications such as compacted fills and embankments.

Yu and Drnevich (2004) reported that M+DI testing is limited to soils that have 30% or less, by weight, retained on the No. 4 sieve, and a maximum particle size of 0.75-in. They also mentioned that there might also be problems obtaining accurate measurements in high plasticity clays because of the attenuation of the electromagnetic wave.

Yu and Drnevich (2004) and Chen et al. (2006) applied M+DI to the compaction control of chemically modified soils. They observed that the estimation of the dielectric constant using travel time analysis was challenging because the chemically modified soils could be highly conductive, which caused significant energy attenuation.

Khalid et al. (2005) concluded that the dry unit weights reported by the M+DI did not agree favorably with the dry unit weights measured with the nuclear gauge or rubber balloon. In the CH soil, dry unit weights measured with the M+DI device were 10 to 20% greater than those from the nuclear gauge and rubber balloon, while in the CL soil the dry unit weights measured with the M+DI device were about 10% less. In the sandy clay, all dry unit weight measurements by the M+DI were within 10% of the nuclear gauge readings. The M+DI measurements of water content in the CH soil were all smaller than the water contents measured by the nuclear gauge and oven drying.

Bennert and Maher (2008) reported that the M+DI readings did not compare well with the nuclear density gauge readings. This was mainly attributed to the TDR's soil constant calibration procedure. The dry densities recorded by the M+DI were typically less than those from the nuclear gauges. The differences were up to 13% in the dry density measurements.

SOIL DENSITY GAUGE (SDG)

Description of Technology

The SDG builds on the technology of the Pavement Quality Indicator (PQI). The SDG uses electrical impedance spectroscopy (EIS) for determining the in-place density, and moisture content of unbound pavement materials. The SDG generates and monitors radio frequency range electromagnetic field using a transmitter and receiver.

Hardware

SDG is a self-contained unit. It is designed for use on a standard 12" (300 mm) layer of soil during or after compaction. The sensing area is an 11 in. diameter base that allows measurement on fine and coarse material types. The unit weighs about 12.8 lb (5.8 kg). The unit is also equipped with a GPS unit.

Data Analysis

SDG is able to make measurements of soil density and moisture content using advanced electrical impedance spectroscopy (EIS). With proper calibration, the measurement can be converted to wet density, dry density and moisture content.

Advantages

The SDG is designed to eliminate unit licensing and certification associated with nuclear materials usage.

Limitations

This device is new and limited research has been performed using this device.

Training Requirements

Minimal training is required

Costs

The cost of the device is $10,000.

Speed
The entire measurement takes less than five minute.

Ease of Use
The SDG is easy to operate.

Accuracy and Precision
This unit is new and limited research has been performed using this device. However, •the device is designed to monitor soil density, percent compaction and percent moisture to within ±2% accuracy.

Case Histories
Sawangsuriya et al. (2008) presented preliminary results at one highway construction site in Bangkok, Thailand. The SDG among other density devices were used on three types of pavement materials: a) sand embankment, b) soil-aggregate subbase, and c) crushed rock base. The device showed good potential for future use in the pavement and subgrade property evaluation during construction phase.

Gamache et al. (2008a, 2008b) reported good agreement between the SDG and oven dry moisture contents with a priori calibration in the laboratory on samples representative of the major USCS classifications.

Pluta and Hewitt (2009) reported that the accuracy of SDG could be improved by accounting for the specific surface area of the material being tested. Wet densities differed by 19% when compared to the Nuclear Density Gauge's wet densities. Unpublished data from Texas Transportation Institute confirms such bias in the results.

SPEEDY MOISTURE TESTER (ASTM STANDARD D4944)

Description of Technology

Speedy moisture tester (a.k.a. speedy calcium carbide moisture tester) is a portable system for measuring moisture content of soils typically used for roads and foundations.

Hardware

The system consists of a rugged plastic case containing a low-pressure vessel fitted with a pressure gauge and an electronic scale and ancillaries.

Data Analysis

Moisture measurements are made by mixing a weighed sample of the material with a calcium carbide reagent in the sealed pressure vessel. The reagent reacts chemically with water in the sample, producing acetylene gas that in turn increases the pressure within the vessel. The pressure increase in the vessel is proportional to the amount of water in the sample, and thereby the moisture content can be read directly from the calibrated pressure gauge.

Advantages

The main advantage is the rapid production of results.

Limitations

Some highly plastic clay soils or other soils not friable enough to break up may not produce representative results because some of the water may be trapped inside soil clods or clumps which cannot come in contact with the reagent. The calcium carbide reagent used with the Speedy tester is a hazardous product that must be handled with care by the user and with consideration for the environment. Some soils may contain compounds or chemicals that will react unpredictably with the reagent and give erroneous results.

Training Requirements

Training for operation takes one day.

Costs

$ 2000.

Speed

It takes less than 5 minutes to obtain results.

Ease of Use
The equipment is easy to use with proper training.

Accuracy and Precision
The accuracy of within 0.5% on most materials is reported by the manufacturer. When compared with oven test results, Speedy readings may be low if the material under investigation contains volatile components other than water as these may evaporate with the water at elevated temperatures.

Case Histories
Partridge et al. (1999) used several devices such as the Speedy moisture tester on waste foundry sand (WFS) being placed on a highway embankment. One conclusion was that the Speedy moisture meter was preferred for the measurement of moisture contents in the field.

Dai and Kremer (2006) and Oman (2004) compared the results from the Speedy Moisture Meter and traditional oven burner methods. They reported a strong relationship between the moisture contents from the two methods.

Alleman et al. (1996) assessed several devices such as the Speedy Moisture Meter. Their results show that water contents measured using the Speedy Moisture Meter were overestimated by 1.25%. However, once calibrated it was considered reliable. They recommended using the Speedy Moisture Meter to check the water content of coal combustion by-product before placement as a means of quality control in the field.

George (2001) presented a field trial initiated to investigate various methods to alleviate the shrinkage cracking problem in cement stabilized layers. The results from the Speedy Moisture Meter were comparable to the results of sand cone and the nuclear density gauge.

ROADBED WATER CONTENT METER (DOT600)

Description of Technology

The DOT600 estimates the volumetric and gravimetric moisture content in samples of geomaterials based on the dielectric permittivity of the material surrounding the devices' probe rods.

Hardware

The device consists of a 3 inch diameter sample chamber which is retrofitted with a waveguide with interlaced circuit traces that form a capacitor. The waveguide floats on precision springs. The accompanied electronic hardware generates and measures a scaled oscillation resonant frequency. Magnetic linear sensors measure sample mass and volume to allow for the determination of gravimetric moisture content.

Data Analysis

The weight volume and resonant period of the capacitor are used to estimate the volumetric water content. As water content of the sample increases, the oscillation frequency of the circuit decreases, and this frequency is related to water content through empirical calibration. The water content measurement uses a calibration derived by the DOT600 manufacturer using soils with a range of textures. The calibration coefficients are selected using material type. The water content response is linear so a one-point calibration will work.

Advantages

This tool allows operators to monitor roadbed volumetric and gravimetric water content. In addition, the system is completely portable.

Limitations

The accuracy of the reported moisture contents are sensitive to the type of soil tested. Coarser materials cannot be tested. The response can be affected by soil salinity.

Training Requirements

Minimal training required.

Costs

Not available.

Speed
DOT600 makes one measurement in approximately 90 seconds.

Ease of Use
The equipment is easy to use.

Accuracy and Precision

As per manufacturer, repeated measurements on the sandy loam soil over the water content range from air dry to about 70% saturation showed deviations from independent measurements of less than ±1.5% volumetric water content. Overall accuracy of ±2% VWC is recommended. The DOT600 resolution is reported as 1% volumetric water content and its precision is 0.75% volumetric water content.

Case Histories
Researchers of MnDOT studied the accuracy and effectiveness of the DOT600 for measuring soil moisture content. They compared DOT600 measurements to those taken using the standard Proctor laboratory test for 270 soil specimens from 62 different soil samples (MnDOT Innovation Update, February 2012). Results indicated that the optimum moisture contents based on the DOT600's measurement of electrical properties were consistent with the measurements determined by the standard Proctor test. Additionally, they concluded that where the optimum gravimetric moisture value determined by the Proctor test varied considerably between soil types, the DOT600's optimum period appeared far less variable (Hansen and Neiber, 2013). Researchers recommended the DOT600 as a possible alternative to the nuclear density gauge or the sand cone and Proctor tests. However, they suggest making the device rugged enough for regular field use before it is considered as an alternative.

INITIAL EVALUATION OF TECHNOLOGIES

Von Quintus et al. (2009) conducted a utility analysis to objectively evaluate NDT technologies. The same process is followed in this study first. The factors considered in this study to evaluate modulus-based NDT devices consist of the following:

- ***Applicability to goals of this project.*** The most important attribute of a given device is its applicability to the goals of this project that is to develop a specification that relates field quality management to the structural pavement design. To that end, the following parameters are important:
  - ***Ability to harmonize pavement design parameters and field measurements.*** Ideally the selected device should provide a stiffness or modulus that can be related to the design modulus. The design modulus can be obtained through laboratory testing or can be estimated through empirical correlations with index properties of soils. Empirical correlations may be practical but are less desirable since they lend themselves to site- or material-specific calibration.
  - ***Ability to make layer specific measurements.*** Since quality acceptance should be layer specific, direct measurement of the layer modulus is desirable. However, a device that requires the estimation of the modulus from stiffness of the pavement system can also be used effectively with proper considerations.
- ***Suitability of device.*** Another important attribute of a given device is its suitability for field measurements. To that end, the following parameters are important:
  - ***Ability to detect construction defects:*** To ensure the durability of a compacted geomaterial during construction, the measurements should be sensitive to the construction defects (such as segregation and under-compaction). This parameter was not studied in this project. However, Von Quintus et al. (2009) evaluated the sensitivity of different devices to intentionally-placed defects during construction. The rates of success of different devices in locating those defects as reported by Von Quintus et al. are shown in Table B.2. The moisture-density devices could detect 36% of the defects.

    Table B.2 - Percent Defects Identified with Different Methods (from Von Quintus et al. 2009)

Device	PSPA	Geogauge	DCP	LWD
Success Rate, %	86	77	64	64

  - ***Repeatability, precision and sensitivity of device.*** The repeatability, which is defined as the variation in a measured parameter when the measurements are made at a given point without removing a device, is an indication of the stability of the hardware and robustness of the software. The precision in this study is defined as the variability in the measured parameter when the device is moved over a small area. The sensitivity is defined as the relative differences in the values when a construction parameter (e.g., moisture content) changes. A lack of sensitivity may provide a false sense of precision in the results. A comparison of Tables B.2 and 2.4.1 demonstrated that sensitivity and precision are both important.
- ***Practicality of device.*** No matter how well the device fulfills the requirements above, a number of practical issues should also be considered. These items include the following:
  - ***Applicability of device to different types of compacted geomaterials.*** The goal of the project is to recommend one device for all types of compacted geomaterials. Devices that can function on only a certain type of geomaterial were excluded from consideration because of the additional costs of acquiring and training the staff.
  - ***Availability of commercial equipment.*** The equipment should be commercially available with proper and prompt repair and calibration services. Therefore, equipment with a distributed sales

and repair network is preferred. The availability of ASTM or AASHTO standards is also desirable.

- ***Equipment reliability and ruggedness.*** The reliability of a device in terms of breakdown and frequency of the repair is of utmost importance. In addition, as much as possible the equipment should be self-contained and rugged.
- ***User friendliness.*** The user-friendliness is defined as the amount of site preparation required before a test can be performed, and the ease of use and the intuitiveness of the software associated with a device. Based on this definition, a user-friendly device may not necessary mean that the device can be used effectively without proper training and experience.
- ***Expertise needed for data collection and interpretation.*** Most devices require some judgment by the technicians about the quality of data collected. However, different devices require different levels of expertise to set appropriate parameters for the devices. The easier and more straightforward these tasks are, the more appropriate the selected device will be.
- ***Initial and Operational Costs.*** The initial cost is the cost of acquiring the device and training the operator. The operational cost includes the number of persons needed to conduct the test, and the speed of data collection and analysis. The initial and the operational costs should be balanced.

The relative weights for the major criteria established in consultation with several DOT representatives are provided in Table B.3. Table B.4 contains the ranking definitions of the parameters indicated above for different devices.

The rankings of the four devices included in Table B.5 can be found in Table B.6. The PSPA is most appropriate in terms of applicability to the goals of this study since it makes layer-specific and direct measurement of the modulus. The DCP and LWD rank the highest in terms of practicality. Based on this analysis, all four devices were further evaluated as discussed in the next section.

The field of measuring moisture and density with non-nuclear devices is evolving quite rapidly. A comprehensive evaluation of these devices is difficult since they have not been used as extensively as the modulus-based devices. Berney et al (2011) conducted a comprehensive evaluation of many of these devices.

Table B.7 contains the criteria used to evaluate the moisture devices. Table B.8 contains a quantification of these parameters while Table B.9 contains the best effort in ranking the devices. The SDG, Campbell Scientific DOT 600 and Speedy Moisture Tester seem to be viable options.

Zapata et al. (2009) contains an excellent review of the suction measurement technologies. The advantages and disadvantages of a number of suction devices are summarized in Table B.10. Even though it is desirable to measure the suction (as opposed to moisture content), none of these devices are currently ready for in situ measurements during QC/QA activities. In addition, based on the survey, highway agencies are not eager to move toward measuring suction directly.

Table B.3 - Weight Factors for Main Criteria Considered for Evaluation of Modulus Devices

Criterion	Weight
Applicability to the goals of this project	40%
Suitability of device	35%
Practicality of the device	25%

Table B.4 - Weight Factors for Parameters Considered in Evaluation of Modulus Devices

Parameter		Weight Factor	Description of Ranking
Applicability to goals of this project	Ability to harmonize pavement design parameters and field measurements	50%	Empirical = 1 Semi-empirical = 3 Rigorous = 5
	Ability to make layer specific measurements	50%	System Response = 1 Property can be backcalculated =3 Direct measurement = 5
Suitability of device	Ability to detect construction defects	50%	Low = 1 Moderate = 3 High = 5
	Repeatability, precision and sensitivity of device	50%	Low = 1 Moderate = 3 High = 5
Practicality of device	Applicability of the device to different types of compacted geomaterials	17%	Only works on soft geomaterials = 1 Works on most geomaterials =3 Works on all geomaterials = 5
	Availability of commercial equipment	17%	Being developed = 1 Prototypes are available = 3 Off the shelf = 5
	Equipment reliability and ruggedness	17%	Not field worthy = 1 Field worthy = 3 Ruggedized = 5
	User-friendliness	17%	Tedious to use = 1 Moderately easy to use = 3 Easy to use = 5
	Expertise needed for data collection and interpretation	17%	Advanced = 1 Several days of training needed = 3 Less than 1 day of training = 5
	Initial and Operational Costs	17%	High = 1 Moderate = 3 Low = 5

Table B.5 - Comparison of Tools for Measuring Modulus

Device	DCP	Geogauge	LWD	PSPA
Parameter Reported	Penetration Rate	Modulus	Deflection/ Modulus	Modulus
ASTM Standard	D-6951	D-6758	E-2583	None
Expertise needed for data collection and interpretation	Minimal	Moderate	Moderate	Moderate but more than other devices
User-friendliness	Easy	Easy	Easy	Easy
Speed	10 minutes	2 minutes	2 minutes	30 seconds
Initial Costs	$3,000	$6,000	$15,000	$20,000

Table B.6 - Ranking of Parameters Considered in Evaluation of Modulus Measuring Devices

Device		DCP	Geogauge	LWD	PSPA
Applicability to the goals of this project	Ability to harmonize pavement design parameters and field measurements	1	3	3	3
	Ability to make layer specific measurements	5	3	3	3
Suitability of device	Ability to detect construction defects	1	3	3	3
	Repeatability, precision and sensitivity of device	1	3	3	3
Practicality of the device	Applicability of the device to different types of compacted geomaterials	3	3	5	3
	Availability of commercial equipment	5	5	5	5
	Equipment reliability and ruggedness	5	5	5	5
	User-friendliness	5	3	3	3
	Expertise needed for data collection and interpretation	5	3	5	3
	Initial and Operational Costs	1	5	3	3
Overall ranking with 5 being ideal device		**3.2**	**3.6**	**3.8**	**3.4**

Table B.7 - Description of Ranking and Weight Factors for Parameters Considered in Evaluation of Moisture-Density Devices

Parameter		Weight Factor	Description of Ranking
Suitability of device	Ability to detect construction defects	50%	Low = 1 Moderate = 3 High = 5
	Repeatability, Precision and Sensitivity of device	50%	Low = 1 Moderate = 3 High = 5
Practicality of device	Applicability of the device to different types of compacted geomaterials	17%	Only works on soft geomaterials = 1 Works on most geomaterials =3 Works on all geomaterials = 5
	Availability of commercial equipment	17%	Being developed = 1 Prototypes are available = 3 Off the shelf = 5
	Equipment reliability and ruggedness	17%	Not field worthy = 1 Field worthy = 3 Ruggedized = 5
	User-friendliness	17%	Tedious to use = 1 Moderately easy to use = 3 Easy to use = 5
	Expertise needed for data collection and interpretation	17%	Advanced = 1 Several days of training needed = 3 Less than 1 day of training = 5
	Initial and Operational Costs	17%	High = 1 Moderate = 3 Low = 5

Table B.8 - Comparison of Tools for Measuring Moisture Density

Device	Soil Density Gauge	Speedy Moisture Tester	DOT 600
Parameter Reported	Density and Moisture Content	Moisture Content	Moisture Content
ASTM Standard	None	D 4944	None
Expertise needed for data collection and interpretation	Moderate	Minimal	Minimal
User-friendliness	Easy	Easy	Easy
Speed	1 minute	5 minutes	3 minute
Initial and Operational Costs	$10,000	$2,000	NA

Table B.9 - Ranking of Parameters Considered in Evaluation of Moisture-Density Devices

Device		Soil Density Gauge	Speedy Moisture Tester	DOT 600
Suitability of Device	Ability to detect construction defects	1	3	2
	Repeatability, Precision and Sensitivity of device	2	4	3
Practicality of Device	Applicability of the device to different types of compacted geomaterials	3	1	1
	Availability of commercial equipment	5	5	3
	Equipment reliability and ruggedness	5	5	3
	User-friendliness	5	5	5
	Expertise needed for data collection and interpretation	5	5	5
	Initial and Operational Costs	3	5	--
Overall ranking with 5 being ideal device		**3.60**	**4.10**	**3.10**

Table B.10 - Advantages and Disadvantages of Suction Devices

Device	Description	Advantages	Disadvantages
Standard Tensiometer	Measures matric suction ranging from 0 to 90 kPa	Can be used for low suction levels.	Require daily maintenance; range in suction is limited by air-entry value of ceramic.
Thermister Psychrometers	Measures total suction ranging from 100 to 10,000 kPa	Simple to use; accurate at high suction ranges.	Poor sensitivity in low suction range; frequent re-calibration is required.
Transistor Psychrometers	Measures total suction ranging from 100 to 18,000 kPa	Relatively good accuracy as compared to other psychrometers in low suction ranges.	Accuracy is user-dependent; highly affected by temperature changes.
Thermocouple Psychrometers	Measures total suction ranging from 300 to 7,500 kPa	can be used in the field if temperature gradients are minimized; relatively fast equilibration time, data can be collected continuously using a data logger.	Affected by temperature fluctuations and gradients; sensitivity deteriorates with time.
Thermal Conductivity Sensors	Measures matric suction ranging from 0 to 1000+ kPa	Continuous monitoring of matric suction with a data logger.	High failure rate; long-term problems associated with drift and deterioration with time.

REFERENCES

- Abdallah, I., Meshkani, A., Yuan, D., and Nazarian, S., (2002), "Modulus Values Using Seismic Moduli SMART (User Manual)," Research Report 1780-4, Center for Highway Materials Research, UTEP, El Paso, TX.
- Abu-Farsakh, M., Alshibli K., Nazzal M., and Mohammad L., (2004), "Evaluation of in-situ stiffness modulus of subgrades and base layers using the Geogauge device," International Journal of Pavements, volume 3, No. 1-2, pp. 89-101.
- Abu-Farsakh, M. Y., Nazzal, M. D., Alshibli, K., Seyman, E., (2005), "Application of DCP in Pavement Construction Control," Submitted to 84th Transportation Research Board Annual Meeting, January 9-13, 2005, Washington, DC.
- Åhnberg, H., Holmen, M., (2008), "Laboratory Determination of Small-Strain Moduli in Stabilized Soils," Swedish Geotechnical Institute, Sweden.
- Al-Amoudi, O. S. B., Asi, M. I., Al-Abdul Wahhab, H. I., Khan, Z. A., (2002), "Clegg Hammer-California Bearing Ratio," Journal of Materials in Civil Engineering, Volume 14, Issue 6, pp. 512–523.
- Alshibli, K. A., Abu-Farsakh, M., and Seyman, E., (2005), "Laboratory Evaluation of the Geogauge and Light Falling Weight Deflectometer As Construction Control Tools," Journal of Materials in Civil Engineering, Vol. 17, No. 5, pp. 560–569.
- Alleman, J.E., Fox, P.J., and De Battista, D.J., (1996), "Performance Evaluation of Highway Embankment Constructed Using Coal Ash," final report for Indiana Department of Transportation, Joint Transportation Research Program. Paper 163. http://docs.lib.purdue.edu/jtrp/163.
- Allersma, H. G. B., (1988), "Optical Analysis of Stress and Strain around the Trip of a Penetrating Probe," Proc. First International Symposium on Penetration Testing, Orlando, FL., pp. 615–620.
- Amini, F., (2003), "Potential Applications of the Static and Dynamic Cone Penetrometers in MDOT Pavement Design and Construction," In cooperation with the Mississippi Department of Transportation and the U.S. Department of Transportation Federal Highway Administration, September 2003.
- Baus, R. L., Li, T., (2006), "Investigation of Graded Aggregate Base (GAB) Courses," Submitted to the South Carolina Department of Transportation and The Federal Highway Administration.
- Bennert, T., and Maher, A., (2008), "The Use of Recycled Concrete Aggregate in a Dense Graded Aggregate Base Course," Final Report FHWA-NJ-2008-002, Dept. of Civil & Environmental Engineering, Center for Advanced Infrastructure & Transportation (CAIT), Rutgers, The State University, Piscataway, NJ 08854-8014.
- Berney, I.V., Ernest, S., and Wahl, R.E. (2011), "Device Comparison for Determining Field Soil Moisture Content," US Army Corps of Engineers, Report No. ERDC/GSL-TR-08-3, Washington, D.C.
- Bester, M. D., and Hallat, L., (1977), "Dynamic Cone Penetrometer," University of Pretoria, Pretoria.
- Briaud, J. L., Li, Y., Rhee, K., (2006), "BCD: A Soil Modulus Device for Compaction Control", Journal of Geotechnical and Geoenvironmental Engineering, Vol.132, No. 1, January 2006, pp.108–115.
- Bukoski, R. F., and Selig, E. T., (1981), "Cone Penetration Testing and Experience, Geotechnical Eng. Division at the ASCE National Convention," St. Louis, MO., pp. 228–236.
- Burnham, T. R., and Johnson, D., (1993), "In Situ Foundation Characterization Using the Dynamic Cone Penetrometer," Final Report, Minnesota Department of Transportation, Maplewood, MN.

- Cary, C. E., and Zapata, C. E., (2010), "Enhanced Model for Resilient Response of Soils Resulting from Seasonal Changes as Implemented in Mechanistic-Empirical Pavement Design Guide," Transportation Research Record: Journal of the Transportation Research Board, 2170, 36-44.
- Celaya, M., Nazarian, S., and Yuan, D., (2010), "Implementation of Quality Management of Base Materials with Seismic Methods: Case Study in Texas," 89th Annual Transportation Research Board Meeting in Washington, DC.
- Chaddock, B., Brown, A. J., (1995), "Road Foundation Assessment," Proc. of the 4th Int. Symp., Unbound Aggregates in Roads (UNBAR4), Nottingham University, pp 200–208.
- Chan, F. W. K., and Armitage, R. J., (1997), "Evaluation of Flexible Pavements in the Middle East," Proc. the 8th International Conference on Asphalt Pavements, August, pp. 459–469.
- Chen, J., Hossain, M., and LaTorella, T. M., (1999), "Use of Falling Weight Deflectometer and Dynamic Cone Penetrometer in Pavement Evaluation," Transportation Research. Record 1655, Transportation Research Board, pp. 145–151.
- Chen, D. H., Wang, J. N., and Bilyeu, J., (2001), "Application of Dynamic Cone Penetrometer in Evaluation of Base and Subgrade Layers," Transportation Research Record 1764.
- Chen, R. P., Daita, R. K., Drnevich, V. P., and Kim, D. H. (2006), "Laboratory TDR monitoring of physico-chemical process in lime kiln dust stabilized clayey soil," Chinese J. Geotech. Eng., 28(2), 249–255.
- Clegg, B., (1978), "An Impact Soil Test for Low Cost Roads" Presented 2nd Conference of the Road Engineering Association of Asia & Australia, Manila.
- Dai, S. and Kremer, C., (2006), "Improvement and Validation of MnDOT DCP Specifications for Aggregate Base Materials and Select Granular," for Minnesota Department of Transportation Office of Materials and Road Research, 1400 Gervais Avenue, Maplewood, Minnesota 55109.
- Davich, P., Camargo, F., Larsen, B., Roberson, R., and Siekmeier, J., (2006), "Validation of DCP and LWD Moisture Specifications for Granular Materials," MN/RC-2006-20, Minnesota Department of Transportation, St. Paul, MN.
- De Beer, M., and Van der Merwe, C. J., (1991), "Use of the Dynamic Cone Penetrometer (DCP) in the Design of Road Structures," Minnesota Department of Transportation, St. Paul, MN.
- Ellis, R., and Bloomquist, D. (2003), "Development of Compaction Quality Control Guidelines that Account for Variability in Pavement Embankments in Florida," University of Florida Department of Civil and Coastal Engineering.
- Fairbrother, S., McGregor, R., Aleksandrov, I., (2010), "Development of a Correlation Equation between Clegg Impact Values and California Bearing Ratio for In-Field Strength Assessment of Forest Road Subgrades."
- Fang, H., (1991), "Foundation Engineering Handbook," 2nd ed., Van Nostrand Reinhold, New York, pp. 170–171.
- Farrag, K., (2005), "Modification of the Clegg Hammer as an Alternative to Nuclear Density Gauge to Determine Soil Compaction," U.S. Environmental Protection Agency.
- Fleming, P. R., Frost, M. W., and Rogers, C. D. F., (2000), "A Comparison of Devices for Measuring Stiffness in Situ," In Unbound Aggregates in Road Construction, editor Andrew R Dawson, Balkema, pp. 193–200.
- Fleming, P. R., (2001), "Field Measurement of Stiffness Modulus for Pavement Foundations," Transportation Research Record 1755, Submitted to the 2001 Annual Meeting of the Transportation Research Board for presentation and publication, Washington, DC.
- Fleming, P. R., Frost, M. W., Lambert, J. P., (2007), "A Review of the Lightweight Deflectometer (LWD) for Routine In situ Assessment of Pavement Material Stiffness," Transportation Research Record 2004, Soil Mechanics, pp. 80–87, ISSN 0361-1981.
- Fleming, P. R., Frost, M. W., and Lambert, J. P., (2007), "Review of Lightweight Deflectometer for Routine in Situ Assessment of Pavement Material Stiffness," Transportation Research Record:

Journal of the Transportation Research Board, No. 2004, Transportation Research Board of the National Academies, Washington, DC., pp. 80–87.
- Frost, M. W., (2000), "The Performance of Pavement Foundations during Construction," Ph.D. thesis, Loughborough University.
- Gamache, R. W., Kianirad, E., Pluta, S., Jersey, S. R., Alshawabkeh, A. N., (2008a), "A Rapid Field Soil Characterization System for Construction Control," Submitted for presentation at the 2009 TRB Annual Meeting and Publication in the Transportation Research Record: Journal of the Transportation Research Board.
- Gamache, R.W., Kianirad, E. Pluta, S., and Spinelli, D., (2008b), "Minimally Invasive Technologies for Measurement Of Water in Pavement Systems," ISAP2008 Minimally Invasive Technologies for Measurement.
- Garrick, N. W., Scholer, C. F., (1985), "Rapid Determination of Base Course Strength using the Clegg Impact Tester," Transportation Research Record No. 1022, pp. 115–119.
- George, K.P., (2001),"Soil Stabilization trial," FHWA/MS-DOT-RD-01-133, Interim Report, University of Mississippi, Department of Civil Engineering, University, MS 38677.
- George, V., Rao, N. C., and Shivashankar, R., (2009), "PFWD, DCP and CBR Correlations for Evaluation of Lateritic Subgrades," International Journal of Pavement Engineering, pp.189–199.
- Glossary of Highway Quality Assurance Terms, (2005), Transportation Research Circular E-C074, Washington, DC, Transportation Research Board.
- Gucunski, N., and Maher, A., (2002), "Evaluation of Seismic Pavement Analyzer for Pavement Condition Monitoring," Final report, FHWA-NJ-2002-012, Federal Highway Administration, U.S. Department of Transportation, Washington, DC.
- Gudishala, R., (2004), "Development of Resilient Modulus Prediction Models for Base and Subgrade Pavement Layers from In Situ Devices Test Results," Department of Civil end Environmental Engineering, Louisiana State University and Agricultural and Mechanical College.
- Gulen, S., McDaniel, R. S., (1990), "Use of Clegg Hammer for Compaction Control," Indiana Department of Transportation, 17pp.
- Guo, R., Prozzi, J., and Ling, J., (2006), "Material Characterizations with Seismic Technology," ASCE Conference Proceeding Paper, Proceedings of Sessions of GeoShanghai, pp. 55–62.
- Hansen, B. J. and Neiber, J. L., (2013), "Performance-Based Measurement of Optimum Moisture Content for Soil Compaction," Research Report No. MN/RC 2013-28, Sponsored by Minnesota Department of Transportation, University of Minnesota, St. Paul, MN.
- Highways Agency, (2009), "Design Guidance for Road Pavement Foundations," Interim Advice Note 73, Highways Agency, London.
- Hoffmann, O., Guzina, B., and Drescher, A., (2003), "Enhancements and Verification Tests for Portable Deflectometers," MN/RC-2003-10, Minnesota Department of Transportation, St. Paul.
- Hoffman, O., Guzina, B. B., Drescher, A., (2004), "Stiffness Estimates Using Portable Deflectometers," Transportation Research Record 186, 59–66.
- Horak, E., Maina, D., Guiamba, D., Nartman, A., (2008), "Correlation Study with the Light Weight Deflectometer in South Africa," Proceedings of the 27th Southern African Transport Conference (SATC 2008), Pretoria, South Africa.
- Hilbrich, S. L., and Scullion, T., (2007), "Rapid Alternative for Laboratory Determination of Resilient Modulus Input Values on Stabilized Materials for AASHTO Mechanistic-Empirical Design Guide," Transportation Research Record: Journal of the Transportation Research Board, 2026, 63-69.
- http://www.campbellsci.com/roadbed-water-content
- Jersey, S. R., and Edwards, L., (2009), "Stiffness-Based Assessment of Pavement Foundation Materials Using Portable Tools," Journal of the Transportation Research Board, No. 2116, Transportation Research Board of the National Academies, Washington, D.C., pp. 26–34.

- Joh, S.-H., Kang, T.-H., Kwon, S. A., and Won, M. C., (2006), "Accelerated Stiffness Profiling of Aggregate Bases and Subgrades for Quality Assessment of Field Compaction," Journal of the Transportation Research Board, No. 1975, Transportation Research Board of the National Academies, Washington, DC., pp. 63–72.
- Ke, L., Nazarian, S., Abdallah, I., and Yuan, D., (2000), "A Sensitivity Study of Parameters Involved in Design with Seismic Moduli," Research Report 1780-2, Center for Highway Materials Research, the University of Texas at El Paso.
- Khalid, F., Vetter, D., Hill, B., Esposito, R., (2005), "Evaluation of Soil Compaction Measuring Devices," Distribution & Pipeline Technology Division, Gas Technology Institute, 1700 South Mount Prospect Road, Des Plaines, IL 60018.
- Lenke, L. R., McKeen, R. G., Grush, M., (2001), "Evaluation of a Mechanical Stiffness Gauge for Compaction Control of Granular Media," ATR Institute University of New Mexico, 1001 University Blvd., SE, Suite 103 Albuquerque, NM 87106.
- Livneh, M., and Goldberg, Y., (2001), "Quality Assessment During Road Formation and Foundation Construction: Use of Falling-Weight Deflectometer and Light Drop Weight," In Transportation Research Record: Journal of Transportation Research Board, No. 1755, Transportation Research Board of the National Academies, Washington, DC., pp. 69–77.
- Mallick, R. B., Das, A., and Nazarian, S., (2005), "Fast Nondestructive Field Test Method to Determine Stiffness of Subsurface Layer in Thin Surface Hot Mix Asphalt Pavement," Journal of the Transportation Research Board, No. 1905, Transportation Research, Washington, DC. pp. 82–89.
- Mallick, R. B., Bradley, J. E., and Nazarian, S., (2006), "In-Place Determination of Stiffness of Subsurface Reclaimed Layers in Thin Surface Hot-Mix Asphalt Pavements," Transportation Research Record, Journal of the Transportation Research Board, No. 1949, Washington, D.C., 2006, pp. 11–19.
- Mathur, T. S., Coghlan, G. T., (1987), "The Use of the Clegg Impact Tester in Managing and Designing Aggregate-Surfaced Roads," Transportation Research Record Volume 1, No. 1106, pp. 232–236.
- Meier, R. W., and Baladi, G. Y., (1988), "Cone Index Based Estimates of Soil Strength: Theory and User's Guide for Computer Code CIBESS," Technical Report No. SL-88-11, Waterways Experiment Station, Vicksburg, MS.
- Miller, H., and Mallick, R. (2003), "Field Evaluation of a New Compaction Monitoring Device," prepared for the New England Transportation Consortium.
- Mohammad, L. N., Abu-Farsakh, M. Y., Zhong, W., and Abadie, C., (2010), "Louisiana Experience with Foamed Recycled Asphalt Pavement Base Materials," Committee on Characteristics of Nonbituminous Components of Bituminous Paving Mixtures.
- Mooney, M. A., and Miller, P. K., (2008), "Analysis of Lightweight Deflectometer Test Based On In Situ Stress and Strain Response," Journal of Geotechnical and Geoenvironmental Engineering, ASCE.
- Nazarian, S., Yuan, D., and Arellano, M., (2002), "Quality Management of Base and Subgrade Materials with Seismic Methods," Transportation Research Record, No. 1786, Washington, DC., pp. 3–10.
- Nazarian, S., Williams, R., and Yuan, D., (2003), "A Simple Method for Determining Modulus of Base and Subgrade Materials," ASTM STP 1437, ASTM, West Conshohocken, PA, pp. 152–164.
- Nazarian, S., Yuan, D., Tandon, V., and Arellano, M., (2004), "Quality Management of Flexible Pavement Layers with Seismic Method," Research Report 1735-3, Center for Transportation Infrastructure Systems, University of Texas at El Paso.
- Nazzal, M. D., (2003), "Field Evaluation of In-situ Test Technology for QC/QA During Construction of Pavement Layers and Embankments," Master's Thesis, Louisiana State University, Baton Rouge.

- Nazzal, M. D., Abu-Farsakh, M. Y., Alshibli, K. A., and Mohammad, L., (2004), "Evaluating the Potential Use of a Portable LFWD for Characterizing Pavement Layers and Subgrades," ASCE, Proceedings of GeoTrans.
- Nazzal, M. D., Abu-Farsakh, M. Y., Alshibli, K., and Mohammad, L. (2007), "Evaluating the Light Falling Weight Deflectometer Device for in Situ Measurement of Elastic Modulus of Pavement Layers," Transportation Research Record: Journal of the Transportation Research Board, No. 2016, Transportation Research Board of the National Academies, Washington, DC., pp. 13–22.
- Newcomb, D. E., Van-Deusen, D. A., and Burnham, T. R., (1994), "Characterization of Subgrade Soils at the Minnesota Road Research Project," Report No. MN/RD-94/19, Minnesota Department of Transportation, St. Paul, MN.
- Newcomb, D. E., Chabourn, B. A., Van-Deusen, D. A., and Burnham, T. R., (1995), "Initial Characterization of Subgrade Soils and Granular Base Materials at the Minnesota Road Research Project," Report No. MN/RC-96/19, Minnesota Department of Transportation, St. Paul, MN.
- Oman, M., (2004), "Advancement of Grading & Base Material Testing," final report Minnesota Department of Transportation, Office of Materials, 1400 Gervais Avenue, MS 645, Maplewood, MN 55109.
- Parker, F., Hammons, M., and Hall, J., (1998), "Development of an Automated Dynamic Cone Penetrometer for Evaluating Soils and Pavement Materials," Final Report, Project No. FLDOT-ADCP-WPI #0510751, Florida Department of Transportation, Gainesville, FL.
- Partridge, B.K., Fox, P.J., Alleman, J.E., and Mast, D.G., (1999), "Field Demonstration of Highway Embankment Construction Using Waste Foundry Sand," Transportation Research Record 1670 Paper No. 99-0612.
- Peterson, A., and Wiser, D., (2003), "What Measures Backfill Compaction Best?," Gas Utility Manager Magazine, January, http://www.gasindustries.com/articles/jan03b.htm.
- Petersen, J. S., Romanoschi, S. A., and Hossain, M., (2007), "Development of Stiffness-based Specifications for In-situ Embankment Compaction Quality Control," K-TRAN: KSU-04-6, Kansas Department of Transportation, Topeka.
- Pidwerbesky, B., (1997), "Evaluation of Non-Destructive In-Situ Tests for Unbound Granular Pavements," IPENZ Transactions, Vol. 24, No.1.
- Pluta, S. E. and Hewitt, J. W., (2009), "Non-Destructive Impedance Spectroscopy Measurement for Soil Characteristics," Characterization, Modeling, and Performance of Geomaterials: Selected Papers From the 2009 GeoHunan International Conference (GSP 189) pp. 144–149.
- Rahim, A. M., George, K. P., (2002), "Automated Dynamic Cone Penetrometer for Subgrade Resilient Modulus Characterization," Transportation Research Record 1806, Paper No. 02-2039.
- Rahimzadeh, B., Jones, M., and Thom, N., (2004), "Performance Testing of Unbound Materials Within the Pavement Foundation," 6th International Symposium on Pavement Unbound-UNBAR, Nottingham.
- Rathje, E. M., Wright, S. G., Stokoe II, K. H., Adams, A., Tobin, R., Salem, M., (2006), "Evaluation of Non-Nuclear Methods for Compaction Control," FHWA/TX-06/0-4835. FHWA, U.S. Department of Transportation.
- Ryden, N., Ekdahl, U., and Lindh, P., (2006), "Quality Control of Cement Stabilized Soils using Non-Destructive Seismic Tests," Advanced Testing of Fresh Cementitious Materials, Lecture 34, August 3–4, 2006, Stuttgart, Germany.
- Sawangsuriya, A., Bosscher, P. J., Edil, T. B., (2006), "Application of Soil Stiffness Gauge in Assessing Small-Strain Stiffness of Sand with Different Fabrics and Densities," Geotechnical Testing Journal, Vol. 29, No. 3, 2006, pp. 1–10.
- Sawangsuriya , A., Wacharanon, V and Wachiraporn, S., (2008), "Innovative Tools for Highway Construction Quality Control," http://www.transtechsys.com/pdf/DOH%20article-english%20version.pdf.

- Schuettpelz, C. C., Fratta, D., Edil, T. B., (2010), "Mechanistic Corrections for Determining the Resilient Modulus of Base Course Materials Based on Elastic Wave Measurements," Journal of Geotechnical and Geo-environmental Engineering, Vol. 136, No. 8.
- Siddiqui, S. I., and Drnevich, V. P., (1995), "Use of time domain reflectometry for the determination of water content and density of soil," FHWA/IN/JHRP-95/9, Purdue Univ., West Lafayette, Ind.
- Siekmeier, J. A., Young, D., Beberg, D., (1999), "Comparison of the Dynamic Cone Penetrometer with Other Tests During Subgrade and Granular Base Characterization in Minnesota," Nondestructive Testing of Pavements and Backcalculation of Moduli: Third Volume, ASTM STP 1375, S. D. Tayabji and E. O. Lukanen, Eds., American Society for Testing and Materials, West Conshohocken, PA.
- Simmons, C., (2000), "Letter of Finding: Memorandum to the Missouri Department of Transportation Research, Development and Technology Division," July 25.
- Steinert, B. C., Humphrey, D. N., and Kestler, M. A., (2005), "Portable Falling Weight Deflectometer Study," NETCR52, New England Transportation Consortium, Storrs, CT.
- Swenson, J., Guzina, B., Labuz, J., Drescher, A., (2006), "Moisture Effects on PVD and DCP Measurements."
- Terzaghi, K., and Peck, R. B., (1967), "Soil Mechanics in Engineering Practice," 2nd ed., John Wiley & Sons, Inc., NewYork, pp. 281–283.
- Thompson, W., (2009), "Correlating Responses of Portable Responses of Portable Field Instruments Used for Testing Aggregate And Soil Pavement Layers," Master Thesis, Department of Civil and Environmental Engineering, Brigham Young University.
- Toohey N. M., Mooney, M.A., Ryden, N., (2010), "Quality Management of stabilized soil construction using lab and field seismic testing," SAGEEP 2010, Keystone, Colorado.
- Truebe, M. A., and Evans, G. L., (1995), "Lowell Test Road: Helping Improve Road Surfacing Design," Proc. 6th Int. Conf. on Low-Volume Roads, Minneapolis, Minnesota, Vol. 2, June.
- Tumay, M. T., (1994), "Implementation of Louisiana Electric Cone Penetrometer System (LECOPS) For Design of Transportation Facilities Executive Summary," Louisiana Transportation Research Center, Baton Rouge, LA.
- Vennapusa, P., White, D. J. (2009) "Comparison of Light Weight Deflectometer Measurements for Pavement Foundation Materials," Geotechnical Testing Journal, Volume 32, Issue 3, ASTM.
- Von Quintus, H. L., Minchin, Jr., R.E, Nazarian, S., Maser, K.R., and Prowell, B., (2009), "NDT Technology for Quality Assurance of HMA Pavement Construction," NCHRP Report 626, Transportation Research Board, Washington, D.C.
- Von Quintus, H. L., Rao, C., Titi, H., Bhattacharya, B., English, R., (2010), "Evaluation of Intelligent Compaction Technology for Densification of Roadway Subgrades and Structural Layers," Draft Final Report WHRP Project ID 0092-08-07, Submitted to Wisconsin Highway Research Program.
- Weidinger, D.M., and Ge, L., (2009), "Laboratory Evaluation of the Briaud Compaction Device," J. Geotech. and Geoenvir. Engrg. Volume 135, Issue 10, pp. 1543-1546.
- White, D. J., Bergeson, K. L., and Jahren, C. T., (2002), "Embankment Quality: Phase III," Final Report, Iowa Department of Transportation.
- White, D., Thompson, M., and Vennapusa, P., (2007), "Field Validation of Intelligent Compaction Monitoring Technology for Unbound Materials," Report No. 2007-10, Minnesota Department of Transportation, Saint Paul, MN, USA.
- Williams, R. R., Nazarian, S., Yuan, D., (2002), "Methods of Data Analysis for correlating Resilient Modulus and Seismic Modulus Test Results," Journal of Materials in Engineering, American Society of Civil Engineers, New York, NY.

- Yu, X., and Drnevich, V. P., (2004), "Time Domain Reflectometry for Compaction Control of Stabilized Soils," Journal of the Transportation Research Board, Vol. 1868, Transportation Research Board of the National Academies, Washington, D.C., pp. 14–22.

Appendix C

ONLINE HIGHWAY AGENCIES' SURVEY FOR NCHRP 10-84 PROJECT

NCHRP Project 10-84, FY 2010
Modulus-Based Construction Specification for Compaction of Earthwork and Unbound Aggregate

Earthwork and unbound aggregates are a significant portion of the construction of highway pavements and structures and play an important role in their performance. However, measurement of the dry unit weight and moisture content of earthwork and unbound aggregates for construction control, while relatively straightforward and practical, does not provide as direct a connection between design and construction as there could be if mechanical properties such as moduli and strengths were used. For example, both the 1993 AASHTO Pavement Design Guide and the new Mechanistic-Empirical Pavement Design Guide (MEPDG) require the resilient moduli of base layers and subgrade as major input for pavement structural design.

Several test methods and devices are available to determine the stiffness or modulus of earthwork and unbound aggregates in the field. However, there is a reluctance to accept field measurements of stiffness or modulus as a criterion for control and acceptance of compaction due to concerns about how such measurements relate to the long-term performance of compacted earthwork and unbound aggregates. Therefore, a prospective modulus-based construction specification must provide criteria or limits related to long-term performance of the earthwork or unbound aggregate as well as to compaction at the time of construction.

The modulus (and, correspondingly, the performance) of earthwork and unbound aggregate is strongly influenced by the seasonal variation of their moisture content. This variation depends on material composition, degree of compaction, and available free moisture, which is primarily controlled by the local climatic environment and the distance from the ground water table. In developing a modulus-based construction specification for compaction of earthwork and unbound aggregate that will provide a direct link with design parameters, all three factors should be examined on the basis of the principles of unsaturated soil mechanics with respect to highway engineering and construction. More information about the project is available at http://144.171.11.40/cmsfeed/TRBNetProjectDisplay.asp?ProjectID=2908

The NCHRP 10-84 team (University of Texas at El Paso, Louisiana Transportation Research Center and University of Texas at Arlington) has prepared the following short survey as part of this project. Your responses will be used to develop the Phase II and Phase III work plan in a manner that the final outcomes are implementable and practical. Thank you very much in advance for your time and input. Please feel free to contact Dr. Anand Puppala at anand@uta.edu or (817) 272-5821, should you have any questions about the survey.

Continue to survey >>

NCHRP Project 10-84, FY 2010
Modulus-Based Construction Specification for Compaction of Earthwork and Unbound Aggregate

Name:
Agency:
Email:
Phone:

1. Please provide feedback in terms of your current quality control/quality assurance specifications for compaction of subgrade/unbound materials?

   Our current specification considers the following parameters:

   A. ☐ Density using ○ Nuclear Density Gauge or ○ other method
   If other, specify

   B. ☐ Moisture Content using ○ Nuclear Density Gauge or ○ other method
   If other, specify

   C. ☐ Other Parameters
   Specify

2. What method and criteria does your agency use for acceptance?

   ○ Percent within limit
   ○ Percent defective
   ○ Average absolute deviation
   ○ Fixed value
   ○ Other method, specify

3. Is your agency using or considering the use of a mechanistic-empirical pavement design process?

- ◯ Yes, we
  - ◯ already use or
  - ◯ will use
  - ◯ AASHTO MEPDG or
  - ◯ Others, specify _____
- ◯ No, we use
  - ◯ AASHTO 1993/1998 or
  - ◯ Others, specify _____

4. Please specify whether your agency uses the moduli of different layers in the following activities?

A. Pavement Design ◯ Yes ◯ No

B. Pavement Rehab Design ◯ Yes ◯ No

5. How does your agency determine the moduli of subgrade/unbound materials?

A. ◯ Laboratory Triaxial (Resilient Modulus) Test as per
- ◯ AASHTO T307 or
- ◯ NCHRP 10-28
- ◯ Older Protocols AASHTO T-292, T-294
- ◯ Other protocols, specify _____

B. ◯ Other Laboratory Tests, specify _____

C. ◯ Field Tests, specify method _____

D. ◯ Use presumptive values (established moduli for various soil types)

E. ◯ Other approaches including Mr- CBR and other types of correlations, specify _____

6. Does your agency consider the stress-sensitivity of the moduli of subgrade/unbound materials in your pavement analyses and design?

   A. ◯ Yes, by using laboratory resilient modulus test results

   B. ◯ Yes, by using presumptive values

   C. ◯ Yes, other approach, specify

   D. ◯ No

7. Does your agency use unsaturated soil mechanics concepts in the determination of moduli of subgrade/unbound materials?

   A. ◯ Yes, based on laboratory suction measurements

   B. ◯ Yes, indirect from approached such as MEPDG

   C. ◯ Yes, other approach, specify

   D. ◯ No

8. Does your agency account for moisture variations in subsoils for design?

   ◯ Yes
   The process we use consists of
   (Please specify the procedures developed or in development that you follow)

   ◯ No

9. Please provide us feedback in terms of implementing modulus-based quality control/quality assurance specifications of subgrade/unbound materials? (please answer all questions).

   A. ◯ We have implemented such specifications in our day-to-day operation or on trial basis.

   ◯ We have not implemented such specifications in our day-to-day operation or on trial basis.

   B. ◯ We have developed such specifications.

   ◯ We have not developed such specifications.

   If your agency has, could you please let us know when?

   C. ◯ We have conducted in-house research on implementing such specifications.

   ◯ We have not conducted in-house research on implementing such specifications.

   If your agency has, could you please let us know when?

   D. ◯ We have funded research projects on implementing such specifications.

   ◯ We have not funded research projects on implementing such specifications.

   If your agency has, could you please let us know when

   and with which University/firm

   E. ◯ We are interested in such specifications at this time.

   ◯ We are not interested in such specifications at this time.

10. If your agency is interested in modulus-based specifications, could you please help us to formulate the best approach to develop a practical specification that your agency can benefit the most?

A. ☐ Institutional limitations (e.g., lack of funds, equipment, personnel) that the research team should be aware of, please specify

B. ☐ Technical issues that you would like to see addressed in this project

C. ☐ Issues in term of practical implementation that you would like to share with the research team

D. ☐ The following other issues, please specify

11. How likely will it be that your agency would implement a modulus-based specification, if it contains the following items:

A. ☐ Resilient modulus laboratory test as per AASHTO specifications on subgrade materials

○ Likely ○ Likely on major projects ○ Unlikely

B. ☐ Resilient modulus laboratory test as per AASHTO specifications on unbound (i.e., base) materials

○ Likely ○ Likely on major projects ○ Unlikely

C. ☐ Resilient modulus estimation from correlation with in-situ tests

○ Likely ○ Likely on major projects ○ Unlikely

D. ☐ Laboratory soil suction measurements on subgrade or unbour als

○ Likely ○ Likely on major projects ○ Unlikely

Install
Cancel
Properties

E. ☐ Incorporating pilot test sections (control strips) on subgrade a se) materials during construction

12. If your agency is not currently interested in a modulus-based specification, could you please help us to understand the reasons?

A. ☐ Institutional reasons, please specify

B. ☐ Concerns on technical validity of the process based on (mark all that applies)

○ in-house research ○ externally-funded research ○ research by other agencies

Please specify your top technical concerns

C. ☐ Concerns on practicality of the process, please specify top practical concerns

D. ☐ The following other reasons, please specify

13. Please specify your agency's perception about the use of the following devices in the field for compaction quality control?

A. Intelligent Compaction	○ Good	○ Needs improvement	○ No experience
B. Falling Weight Deflectometer	○ Good	○ Needs improvement	○ No experience
C. Dynamic Cone Penetrometer	○ Good	○ Needs improvement	○ No experience
D. Lightweight or Portable FWD	○ Good	○ Needs improvement	○ No experience
E. Geogauge	○ Good	○ Needs improvement	○ No experience
F. Portable Seismic Property Analyzer	○ Good	○ Needs improvement	○ No experience
G. Other	○ Good	○ Needs improvement	○ No experience

Specify Other:

14. What improvements are desirable for each specific device?

A. Intelligent Compaction		☐ No experience
B. FWD		☐ No experience
C. DCP		☐ No experience
D. LWD		☐ No experience
E. Geogauge		☐ No experience
F. PSPA		☐ No experience
G. Other, specify		

15. What type of preparation does your agency recommend prior to use of each specific device in the field?

A. Intelligent Compaction		☐ No experience
B. FWD		☐ No experience
C. DCP		☐ No experience
D. LWD		☐ No experience
E. Geogauge		☐ No experience
F. PSPA		☐ No experience
G. Other, specify		

16. In the analysis of data to obtain subgrade/unbound base moduli from these devices does your agency include the following variables?

A. Underlying layers in the pavement foundation

○ Yes ○ No ○ Do not know

B. Material Type

○ Yes ○ No ○ Do not know

C. Stress Dependency of Material

○ Yes ○ No ○ Do not know

D. Moisture Effect on Material

○ Yes ○ No ○ Do not know

E. Subgrade suction (tensile stress due to moisture films)

○ Yes ○ No ○ Do not know

Please provide other parameters you may include in the analysis:

17. Does your agency use predetermined device-specific target modulus for field measurement to achieve proper compaction?

- ◯ Yes with lab based modulus measurements
- ◯ Yes, with certain specific value
- ◯ No

18. Does your agency consider the pavement structure in setting field target modulus?

- ◯ Yes with lab based modulus measurements
- ◯ No

19. Please specify your agency's perception about the use of the following devices in the field for moisture measurement as part of compaction quality control?

A. Nuclear Density Gauge
◯ Good ◯ Needs improvement ◯ No experience

B. Electrical Density Gauge
◯ Good ◯ Needs improvement ◯ No experience

C. Soil Quality Indicator
◯ Good ◯ Needs improvement ◯ No experience

D. Purdue M+DI TDR Device
◯ Good ◯ Needs improvement ◯ No experience

E. Other
◯ Good ◯ Needs improvement ◯ No experience

Specify other

20. What improvements are desirable for each specific device?

A. Nuclear Density Gauge		☐ No experience
B. Electrical Density Gauge		☐ No experience
C. Soil Quality Indicator		☐ No experience
D. Purdue M+DI TDR Device		☐ No experience
E. Other, specify		

21. What type of preparation does your agency recommend prior to use of each specific device in the field?

A. Nuclear Density Gauge		☐ No experience
B. Electrical Density Gauge		☐ No experience
C. Soil Quality Indicator		☐ No experience
D. Purdue M+DI TDR Device		☐ No experience
E. Other, specify		

22. Does your agency include soil suction measurement while performing field compaction assessment studies?

- ◯ Yes please specify the field method
- ◯ No

Submit

C.1 Summary of Highway Agencies' Survey

Table C.1 - Target Pavement Foundation Surface Modulus Values (Highways Agency, 2009)

Long-Term In-Service Modulus (MPa)			Class I	Class II	Class III	Class IV
			≥50	≥100	≥200	≥400
Target Mean Modulus (MPa)	Unbound		40	80	…	…
	Bound	Fast Curing	50	100	300	600
		Slow Curing	40	80	150	300
Target Minimum Modulus (MPa)	Unbound		25	50	…	…
	Bound	Fast Curing	25	50	150	300
		Slow Curing	25	50	75	150

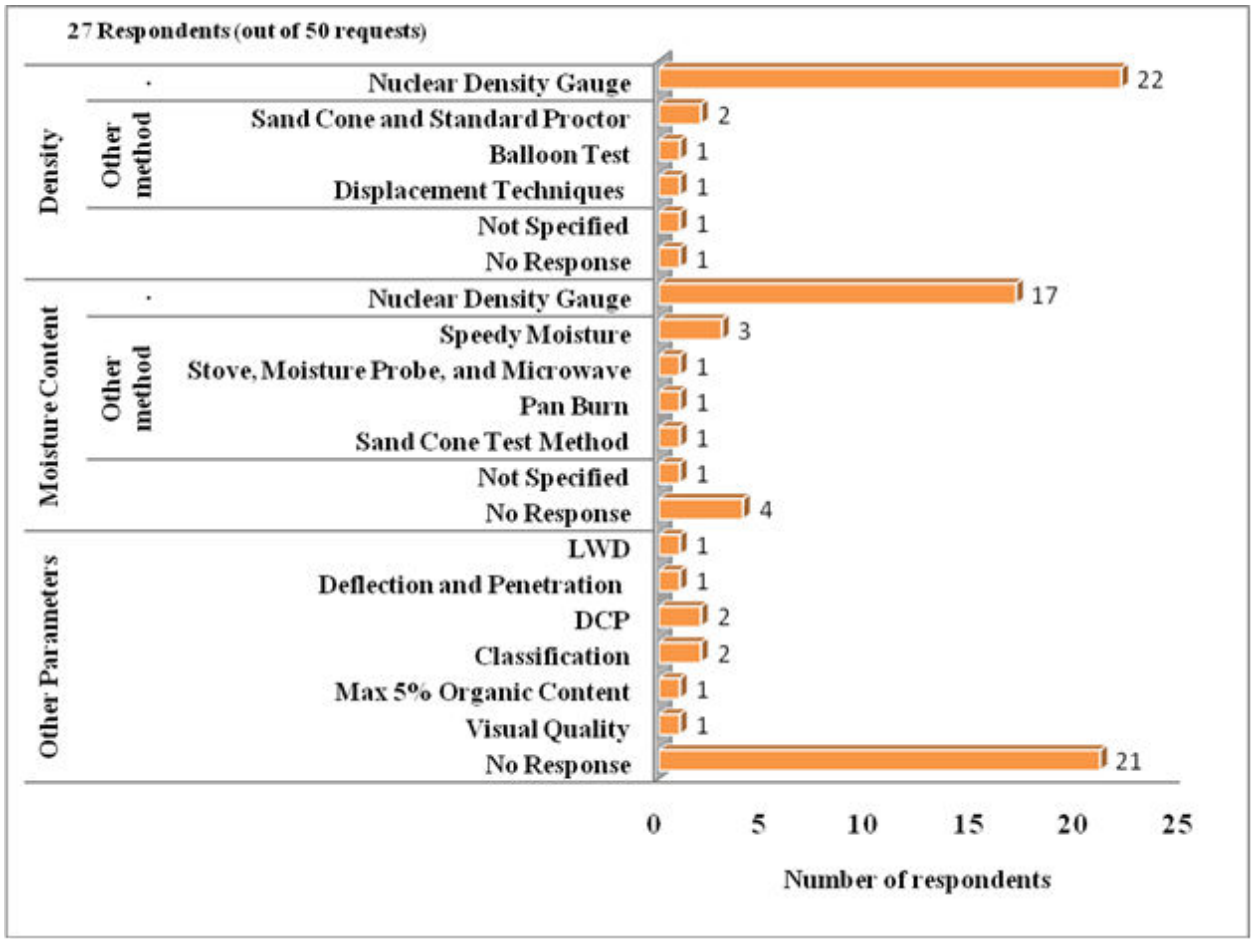

Figure C.1 - Details on Methods Currently Used in Quality Control/Quality Assurance

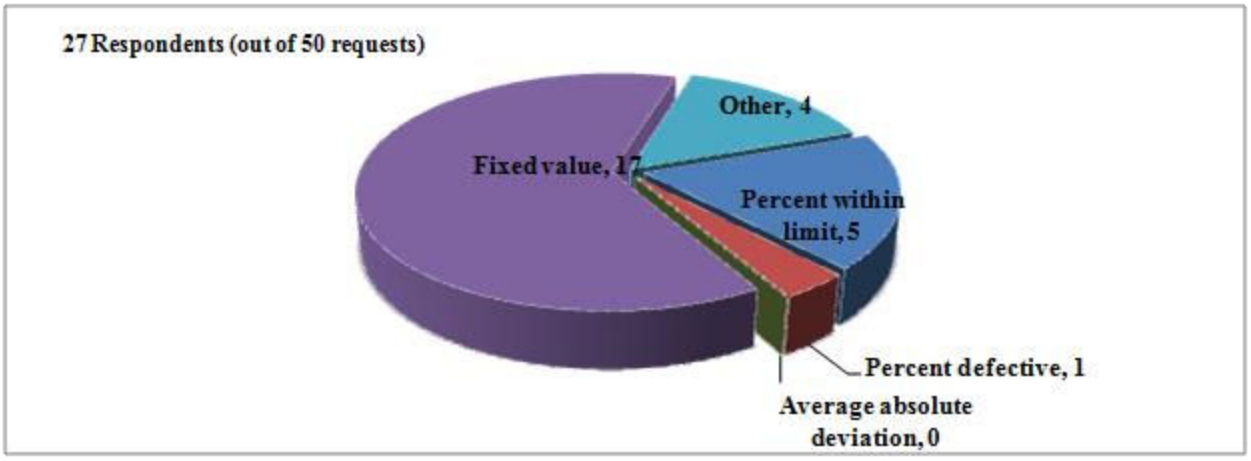

Figure C.2 - Responses on Methods and Criteria Used for Acceptance

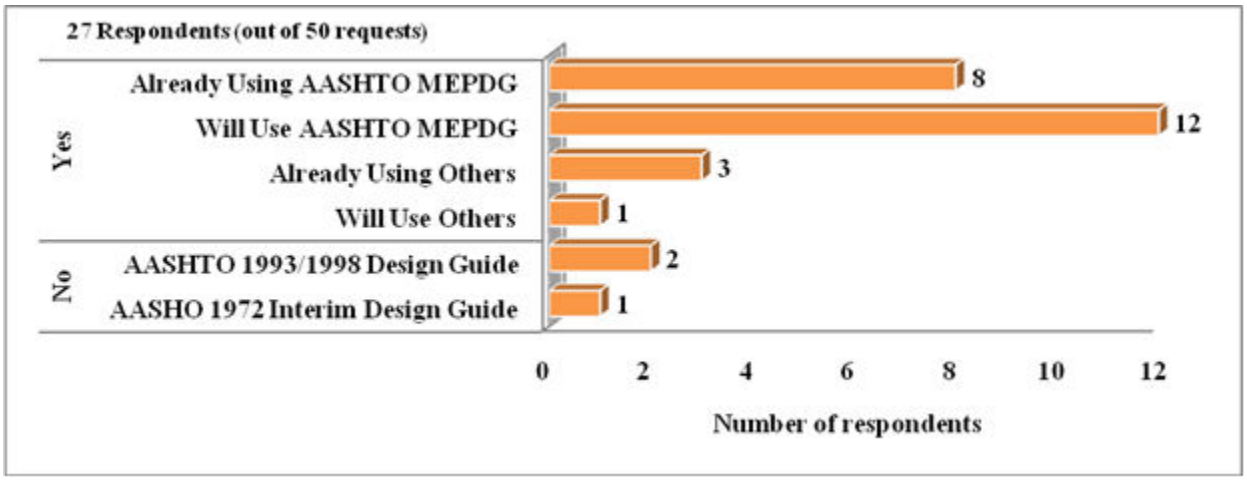

Figure C.3 - Responses on Use of Mechanistic Pavement Design Guide

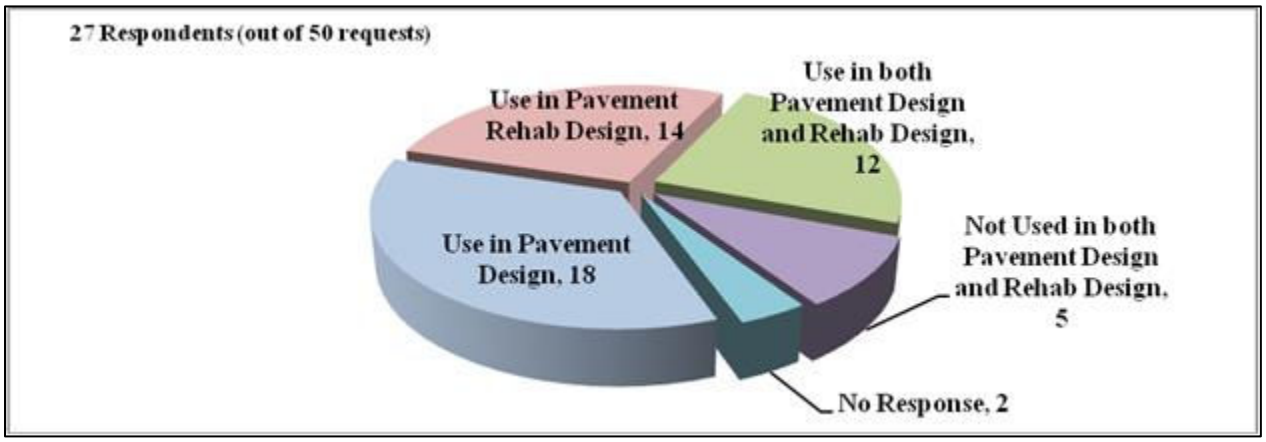

Figure C.4 - Number of Respondents Using Moduli of Different Layers in Design

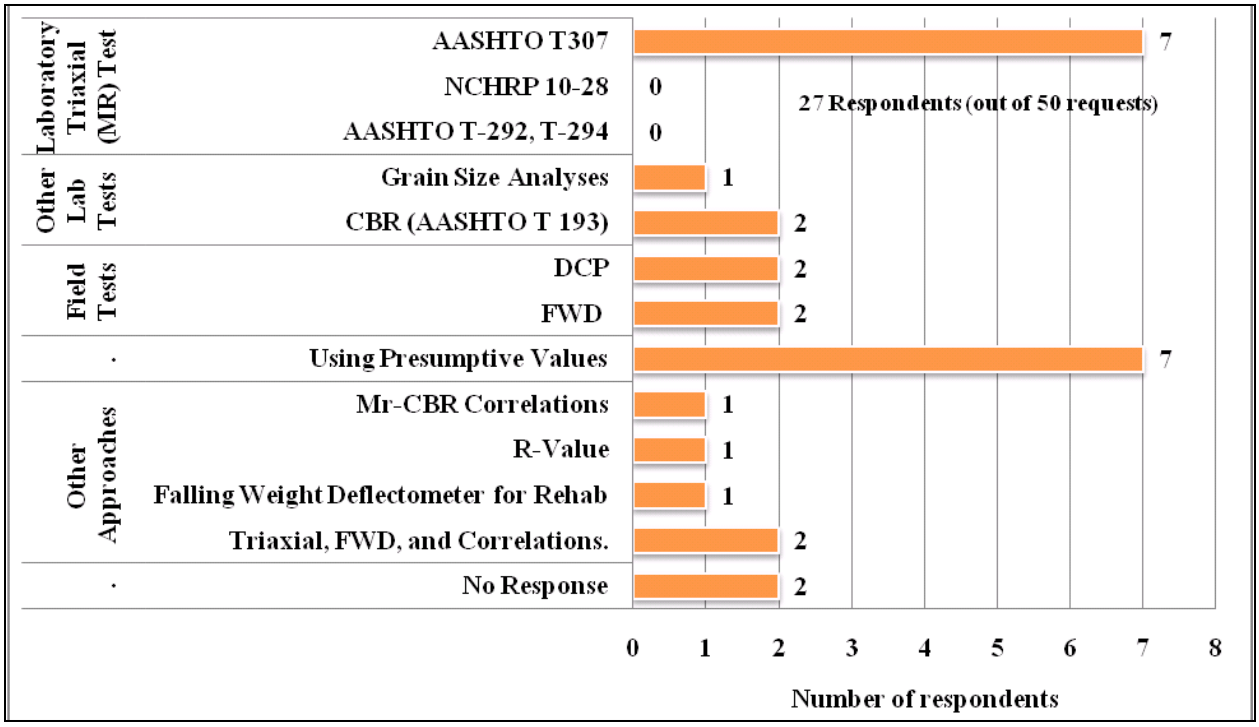

Figure C.5 - Responses Related to the Ways to Determine the Moduli of Subgrade/Unbound Materials

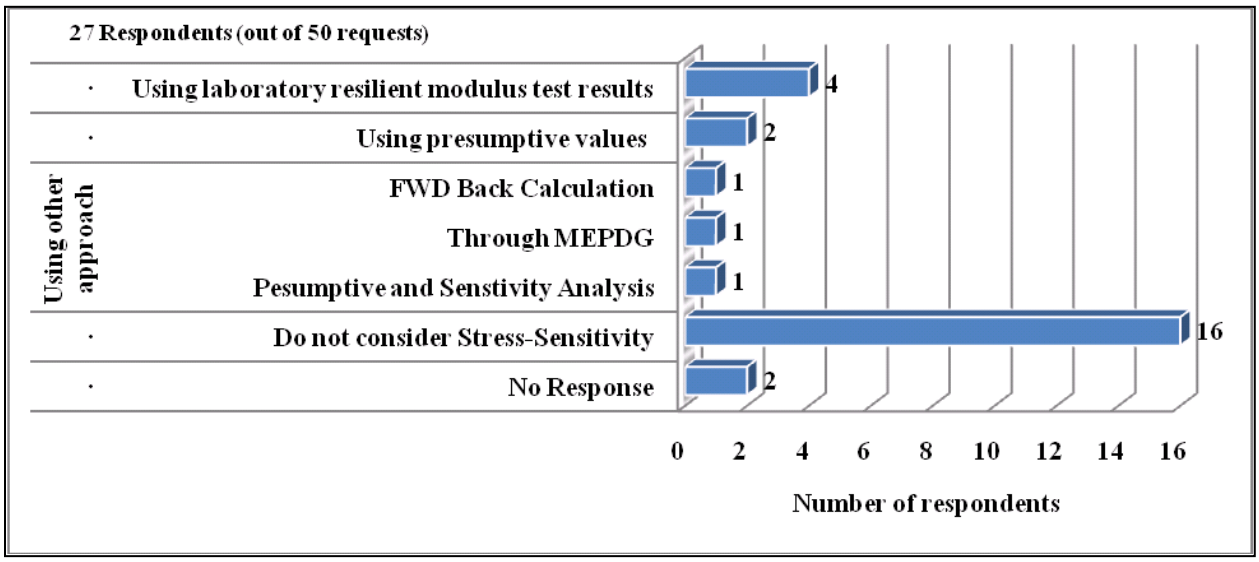

Figure C.6 - Agencies that Consider Stress-Sensitivity of Moduli of Subgrade/Unbound Materials in Pavement Analyses and Design

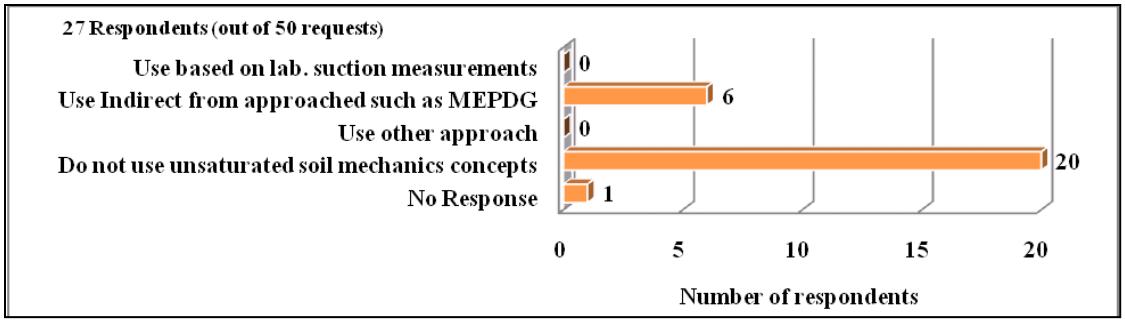

Figure C.7 - Responses on the Usage of Unsaturated Soil Mechanics Concepts in the Determination of Moduli of State/Unbound Materials

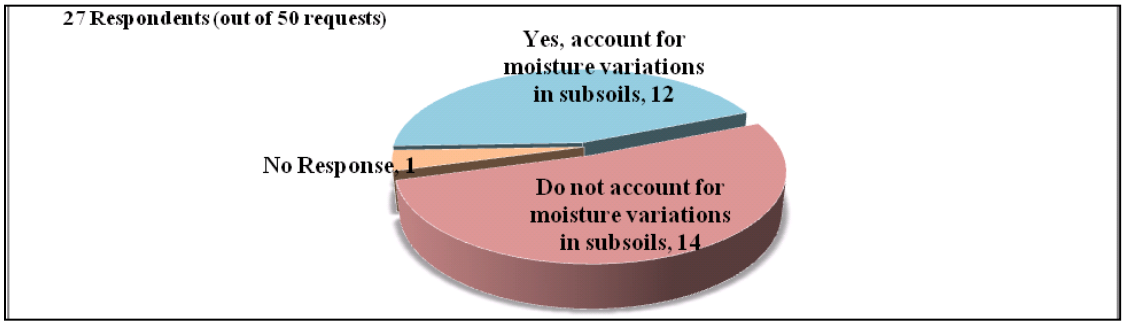

Figure C.8 - Responses on Accounting for Moisture Content Variation in Subsoils in Design

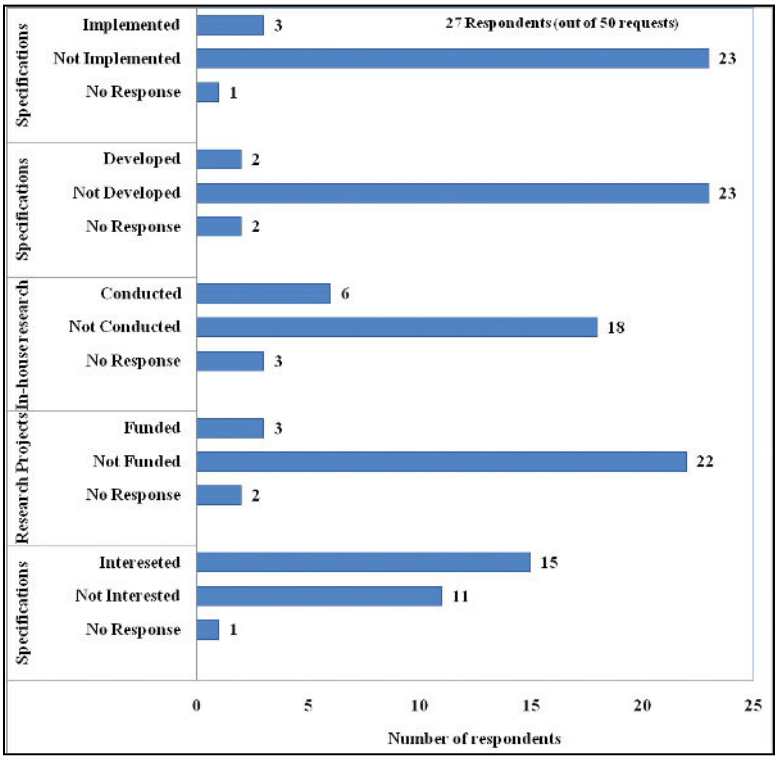

Figure C.9 - Responses Regarding Implementation of Modulus-Based Quality Control/Quality Assurance Specifications of Subgrade/Unbound Materials

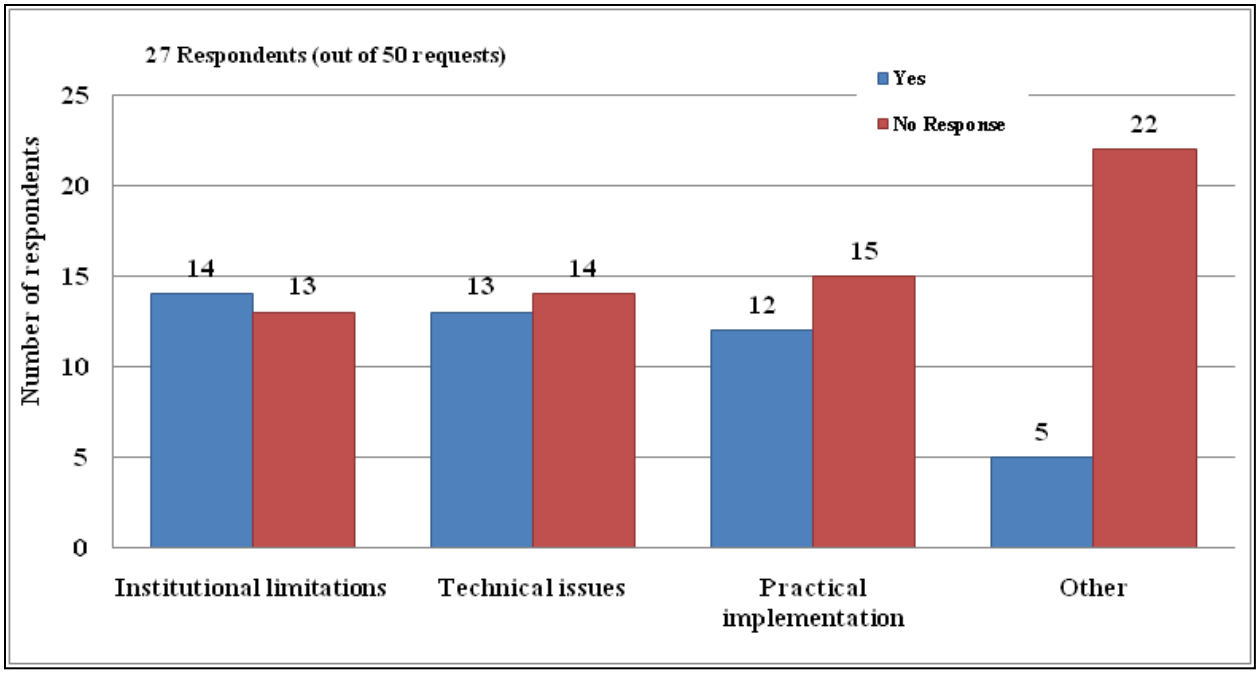

Figure C.10 - Responses on Issues for the Best Approach to Develop a Practical Specification

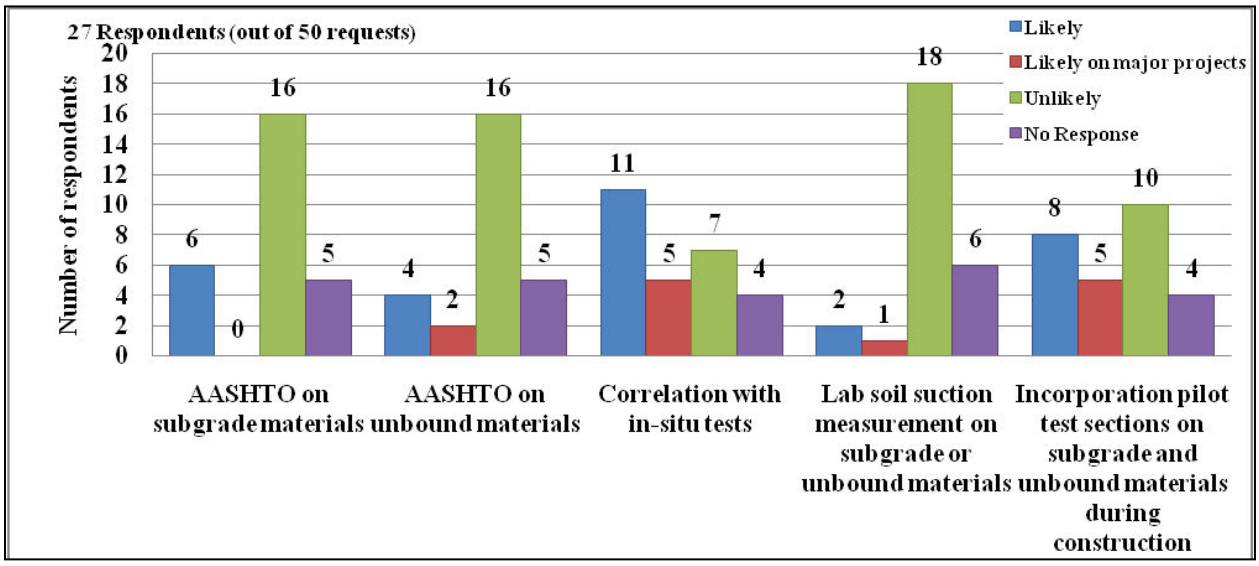

Figure C.11 - Implementation of Modulus-Based Specification

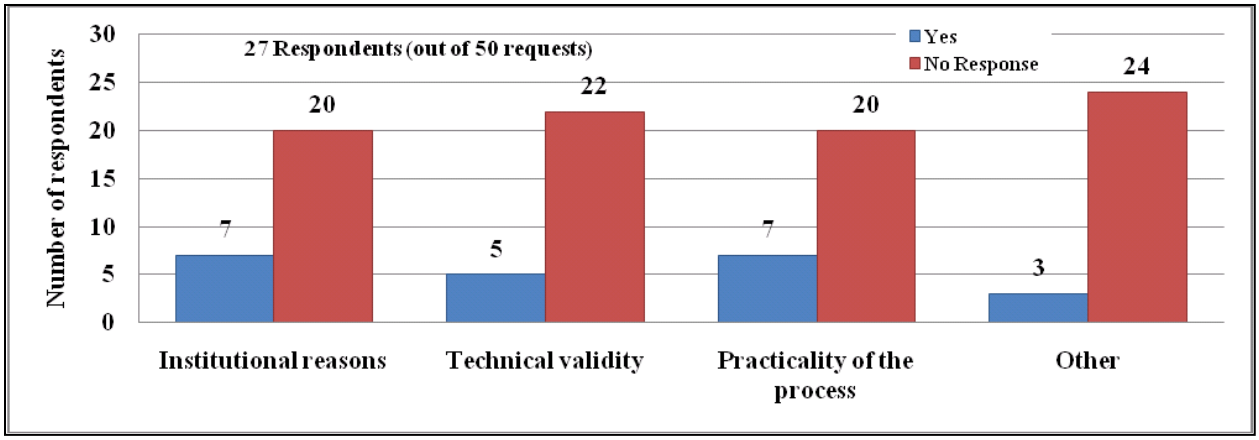

Figure C.12 - Reasons for Not Being Interested in Modulus-Based Specification

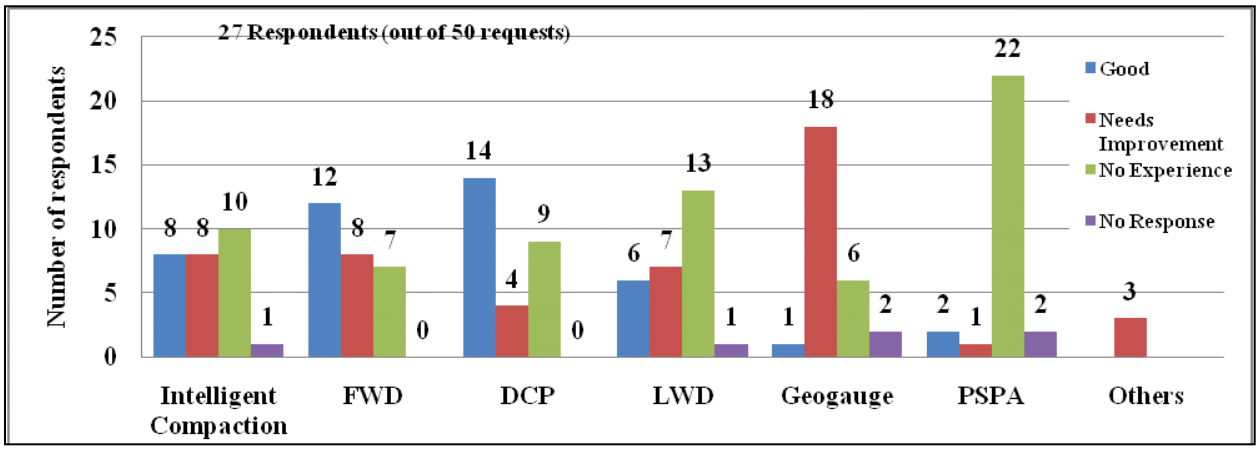

Figure C.13 – Reaction of DOTs to Field Devices for Compaction Quality Control

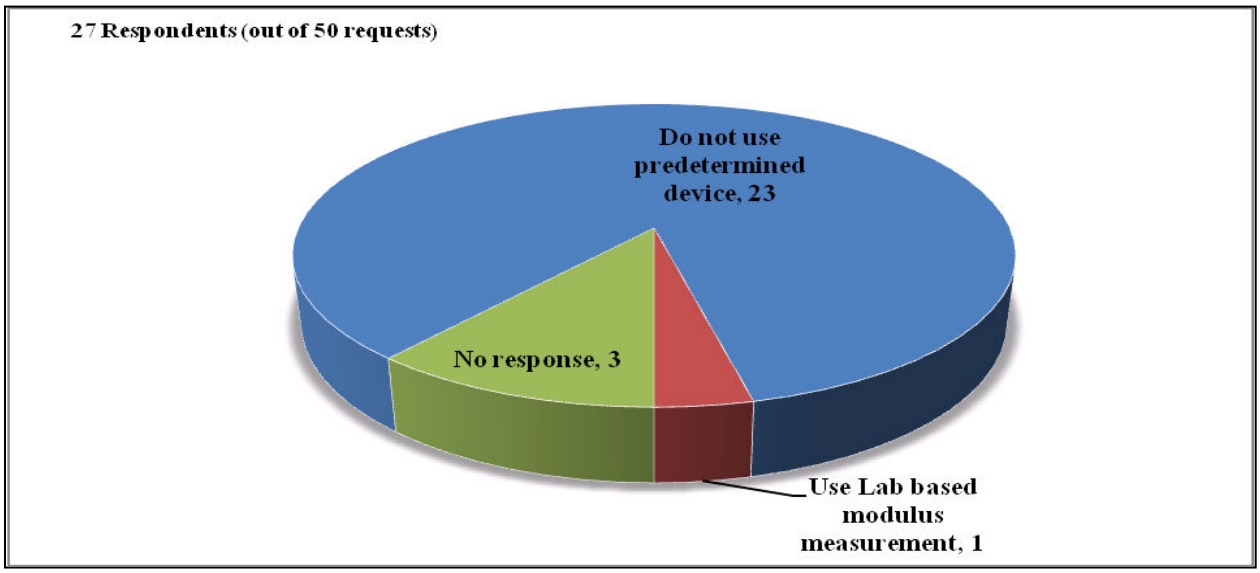

Figure C.14 - Responses Related to the Use of Predetermined Device-Specific Target Modulus

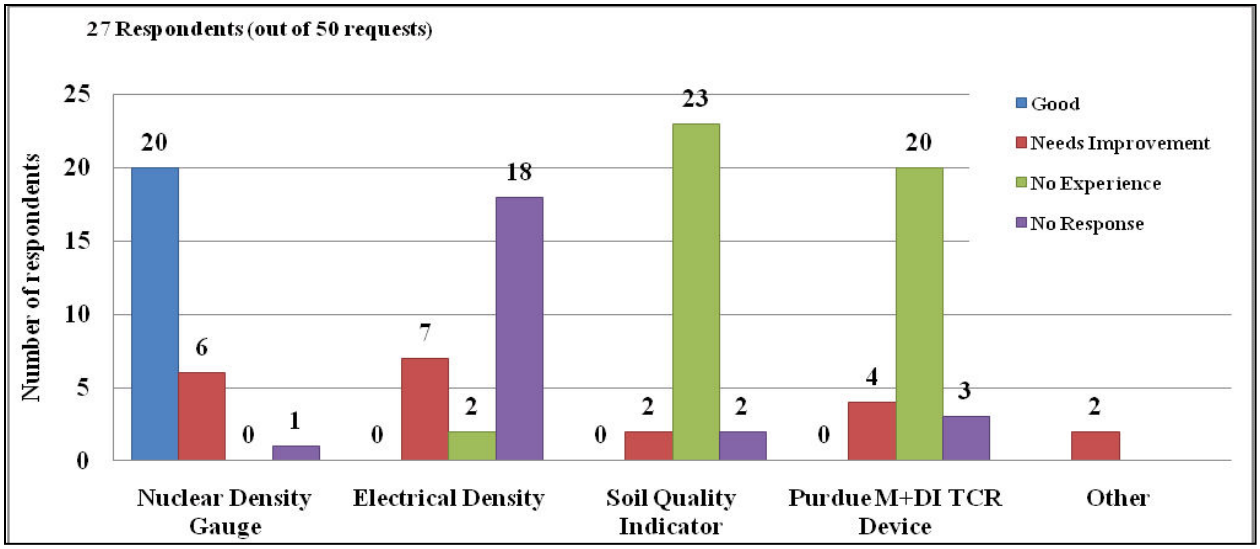

Figure C.15 - Perception of DOTs about Field Devices for Moisture Measurement

Appendix D

PROCESS FOR CONVERTING NONLINEAR PARAMETERS FROM MEPDG MODEL TO OOI'S MODEL

As demonstrated in the report, the modified MEPDG model (Equation D.1) is more appropriate for estimating the responses of the modulus-based devices. However, most highway agencies use the MEPDG constitutive model (Equation D.2) to estimate the nonlinear parameters (k_1, k_2, k_3 in Equation D.2) of unbound pavement layers.

$$MR = k'_1 P_a \left[\frac{\theta}{P_a} + 1\right]^{k'_2} \left[\frac{\tau_{oct}}{P_a} + 1\right]^{k'_3} \quad \text{(D.1)}$$

$$MR = k_1 P_a \left[\frac{\theta}{P_a}\right]^{k_2} \left[\frac{\tau_{oct}}{P_a} + 1\right]^{k_3} \quad \text{(D.2)}$$

Relationship between the nonlinear regression parameters of these two models had to be developed so that the proposed relationships can be used conveniently by highway agencies. To achieve this goal, 1000 random combinations of k' parameters was generated using a discrete uniform distribution. To simulate lab MR tests, the resilient moduli of more than a dozen loading sequences recommended by AASHTO T-307 were calculated using Equation D.1. The regression parameters for the MEPDG model (k_1, k_2 and k_3 in Equation D.2) were then backcalculated using the nonlinear optimization algorithm used in conjunction with lab MR tests.

A one-to-one relationship between parameters k_3 and k'_3 was obtained (i.e., $k'_3 = k_3$). Figure D.1 shows the relationship between parameter k_2 from the MEPDG model and k'_2 from Ooi model for the 1000 cases. The following equation can be used to estimate k'_2 from k_2:

$$k'_2 = 1.88\, k_2 \quad \text{(D.3)}$$

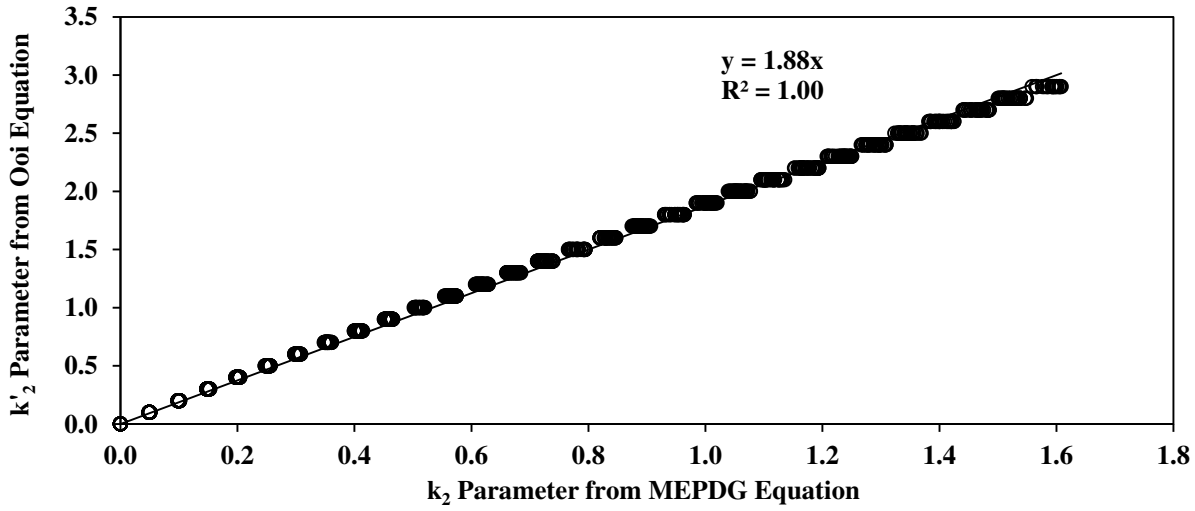

Figure D.1 - Relationship between k_2 Parameter from MEPDG Model and k'_2 Parameter from Ooi Model

Figure D.2 shows the relationship between k_1 and k'_1. A global trend between these two parameters is not evident. Upon further analysis, the scatter in the data could be related to parameter k_2. Some examples of the relationships between k_1 and k'_1 for several discrete values of k_2 are presented in Figure D.3. A strong linear relationship between k_1 and k'_1 is observed for each discrete value of k_2. The variation in the slope of these lines (denoted as "a") with parameter k_2 is shown in Figure D.4.

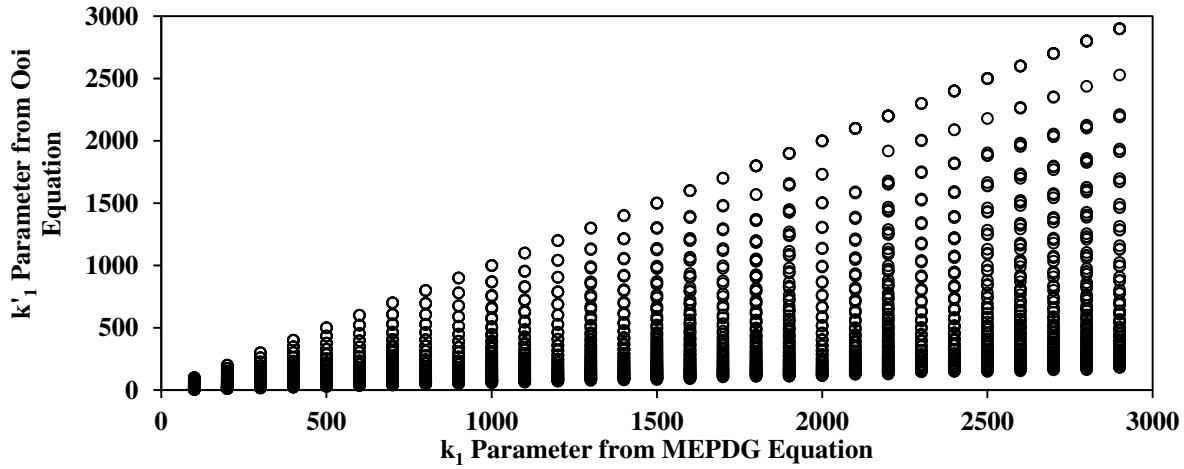

Figure D.2 - Relationship between k_1 Parameter from MEPDG Model and k'_1 Parameter from Ooi Model

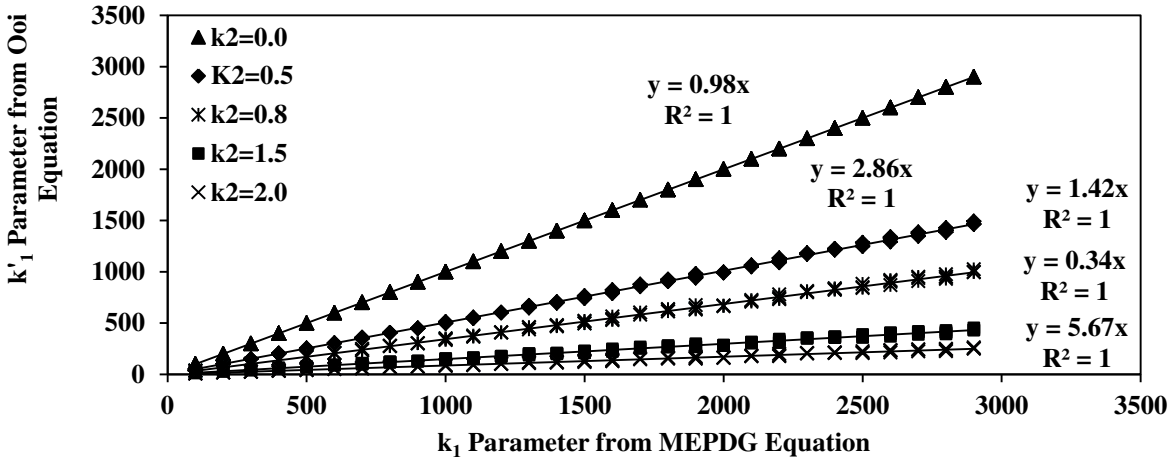

Figure D.3 - Relationships between k_1 Parameter from MEPDG Model and k'_1 Parameter from Ooi Model for Discrete Values of k'_2

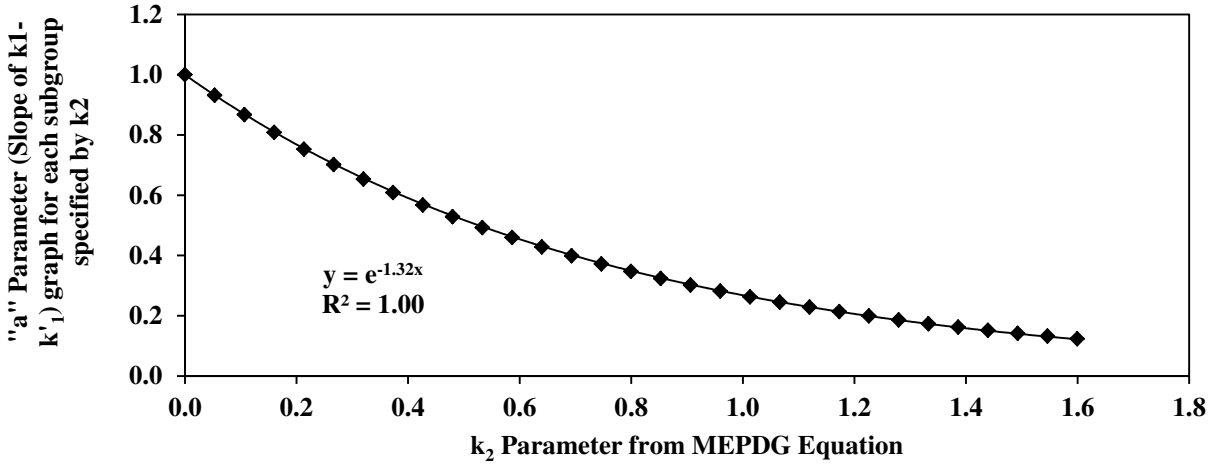

Figure D.4 - Relationship between Slope of k_1-k'_1 Linear Regression "a" from Figure D.3 and k_2

Based on Figures D.3 and D.4, the following relationship can be used to estimate k'_1:

$$k'_1 = k_1 e^{-1.32\,k2} \quad \text{(D.4)}$$

For further validation of the proposed models, the results of lab MR tests from CL, CH and ML geomaterials prepared at different moisture contents using the constant energy and constant density methods (See Section 3.2) were reduced independently with Equations D.1 (Ooi model) and D.2 (MEPDG model). The k'_1 and k'_2 values directly obtained from the laboratory data are compared in Figure D.5 with those estimated from the MEPDG k_1 and k_2 values along with Equations D.3 and D.4. The outcomes from the two processes are quite comparable given the inevitable experimental errors. As reflected in Figure D.5c, the representative lab MR moduli from the two processes are for all practical purposes the same.

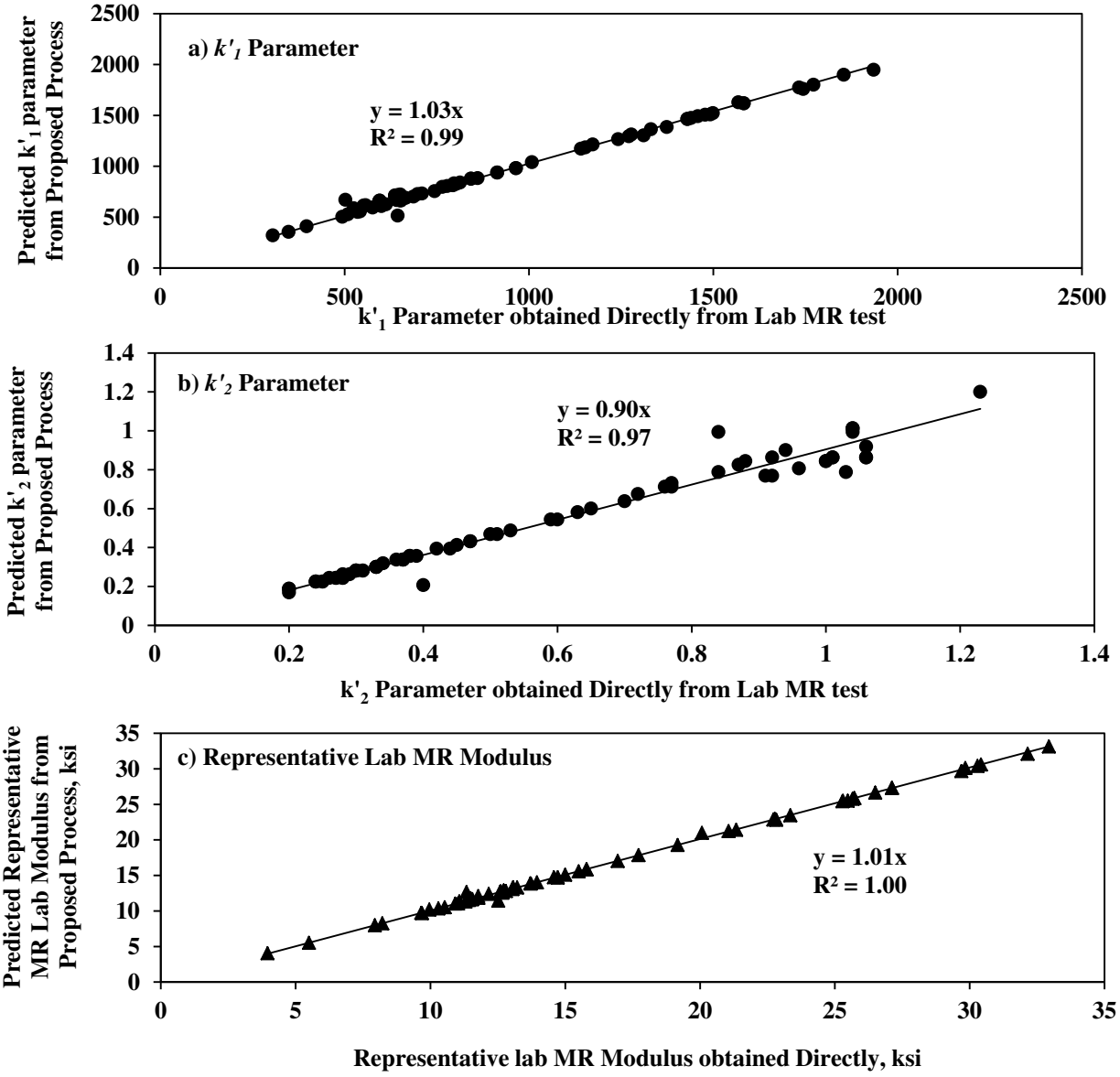

Figure D.5 - Verification of Developed Process to Calculate Ooi Nonlinear Regression Parameters (k'_1 and k'_2) from MEPDG Nonlinear Regression Parameters (k_1 and k_2)

Appendix E

IMPACT OF MOISTURE VARIATION ON MODULUS-BASED DEVICE MEASUREMENTS (SMALL-SCALE STUDY)

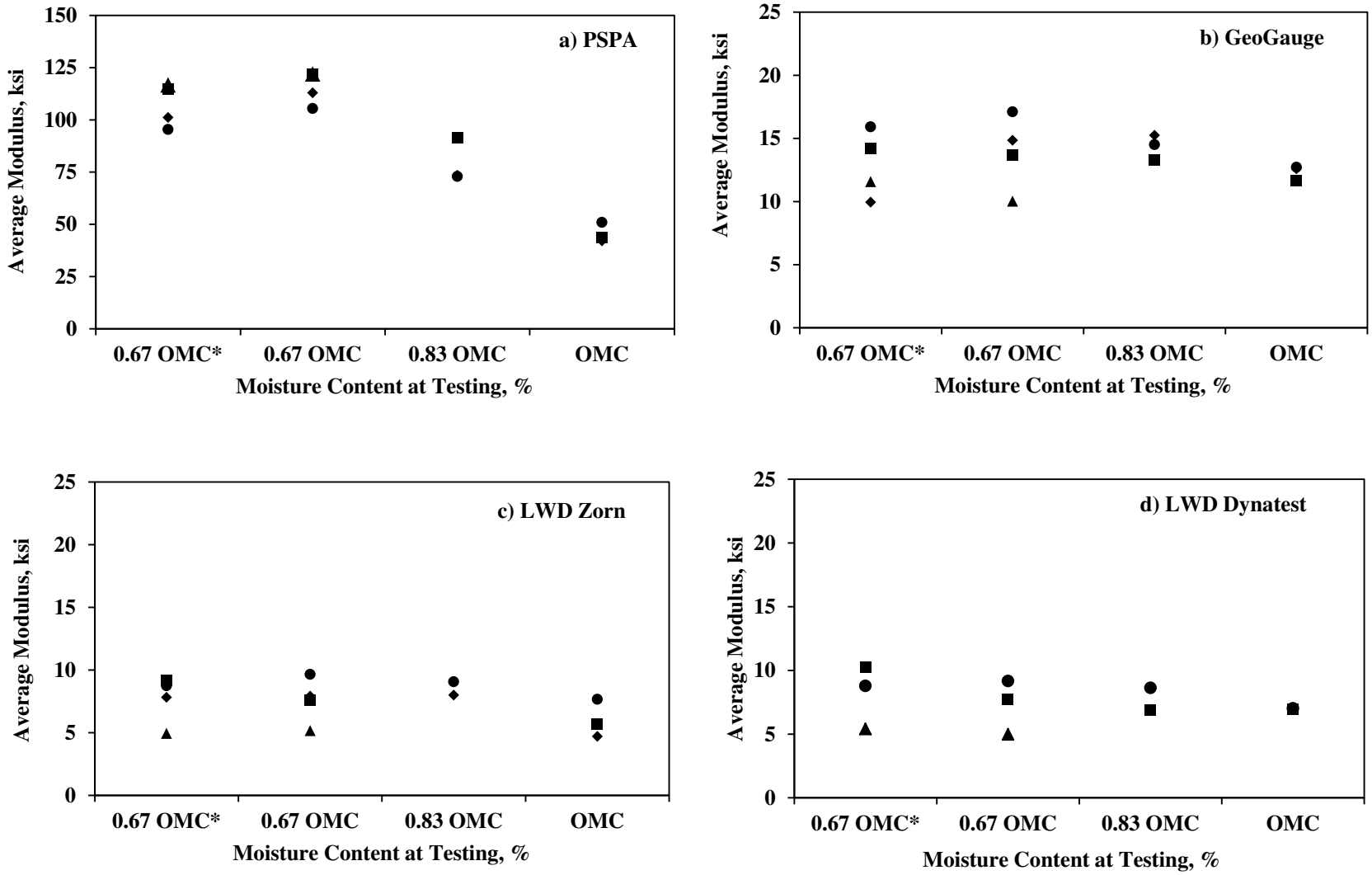

- Note: 0.67 OMC* = Base is dried to 0.67 OMC and subgrade is then saturated

Figure E.1 - Average Moduli from Different Modulus-based Devices at Various Moisture Contents (GW materials)

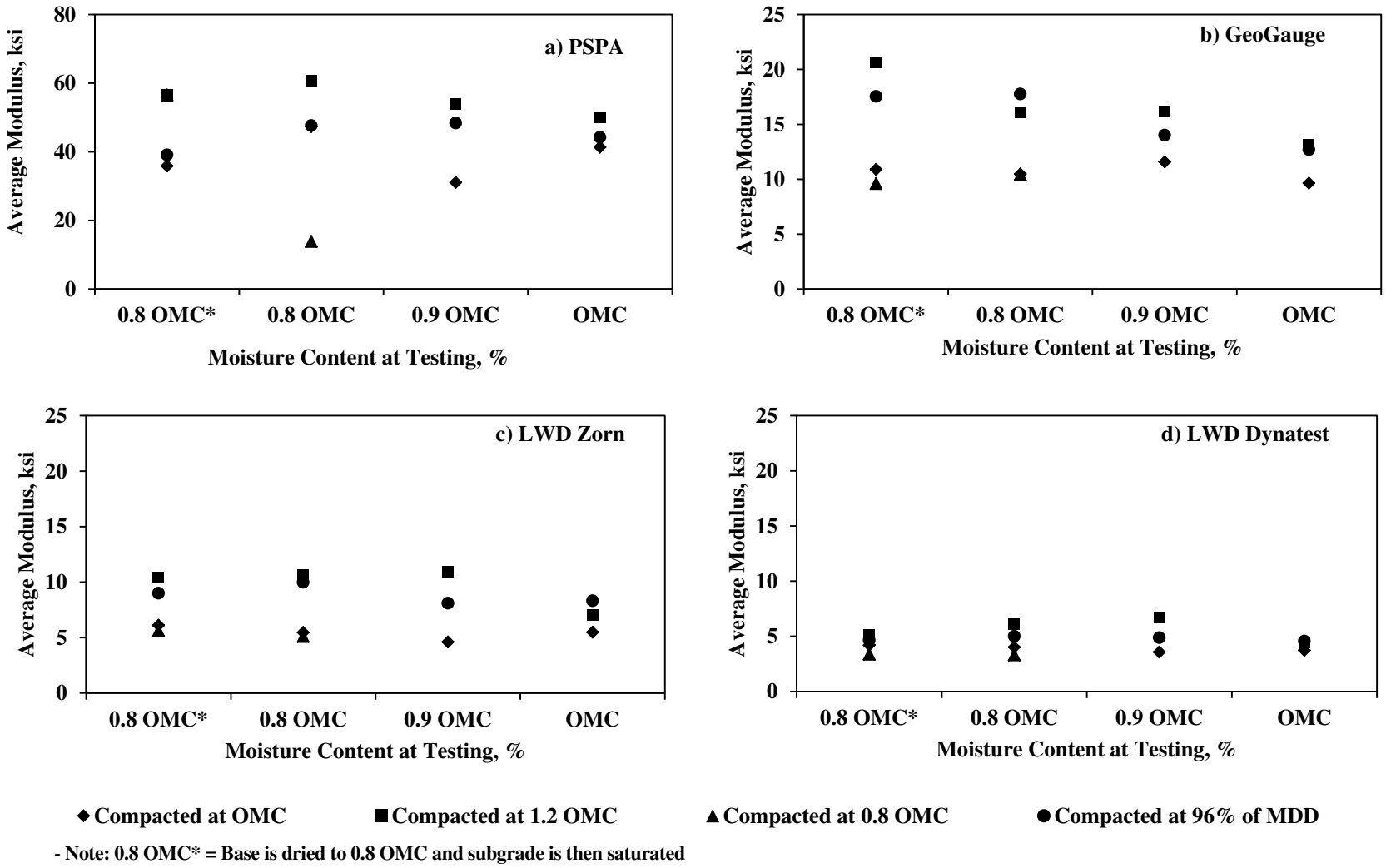

Figure E.2 - Average Moduli from Different Modulus-based Devices at Various Moisture Contents (CL materials)

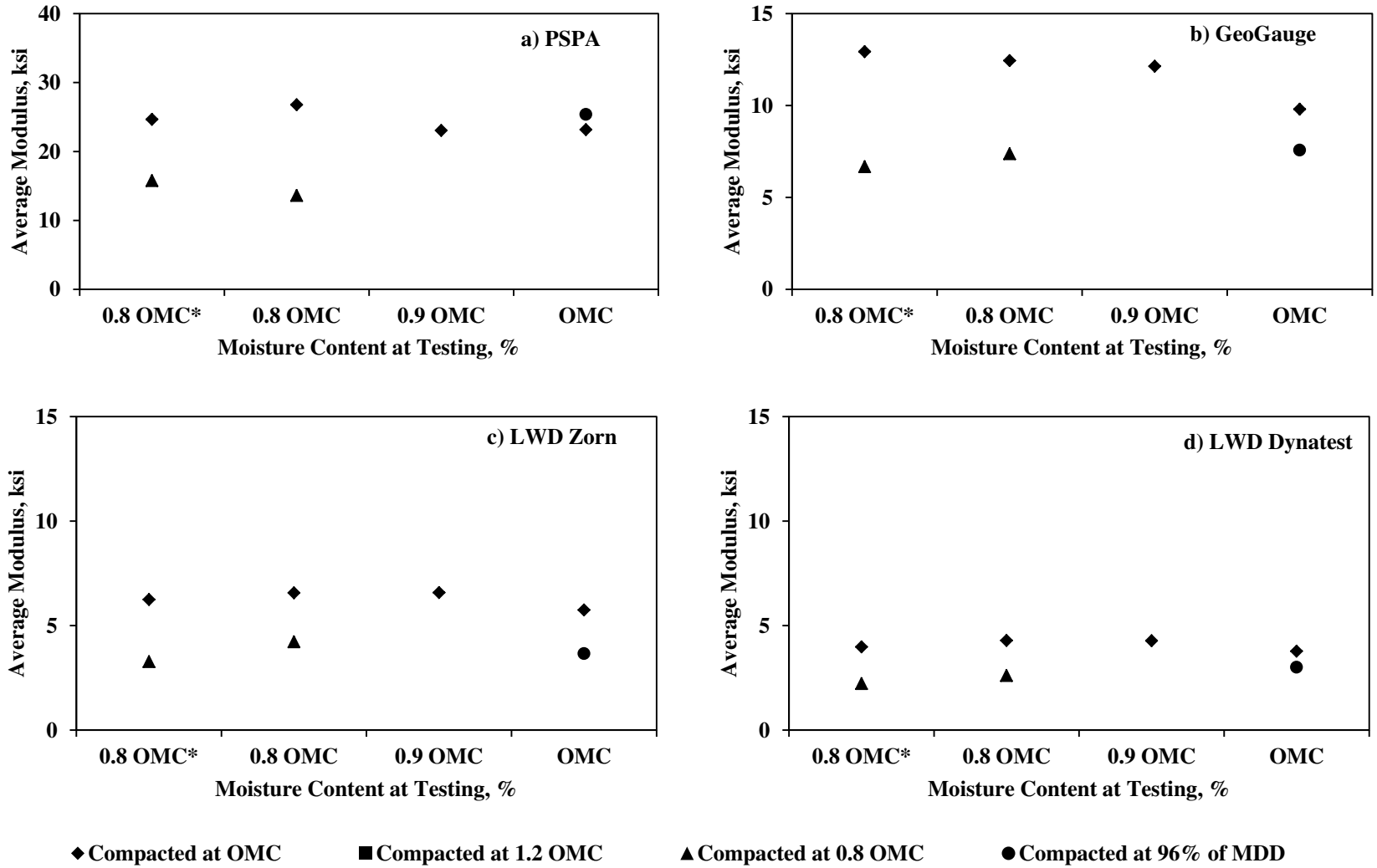

- Note: 1) 0.8 OMC* = Base is dried to 0.8 OMC and subgrade is then saturated,

Figure E.3 - Average Moduli from Different Modulus-based Devices at Various Moisture Contents (CH materials)
(Due to excessive cracking of specimens, some of data points are missing)

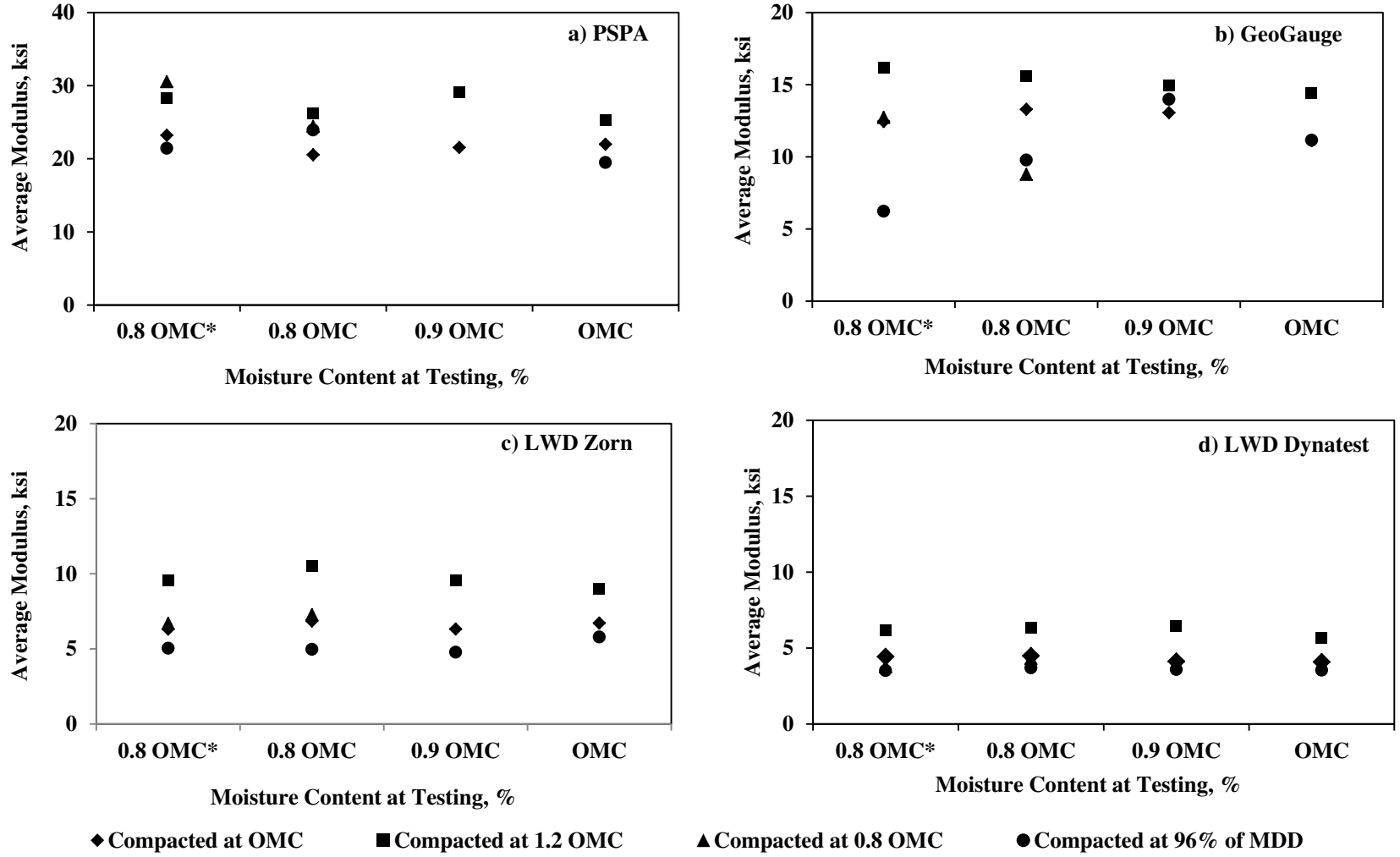

Figure E.4 - Average Moduli from Different Modulus-based Devices at Various Moisture Contents (ML materials)

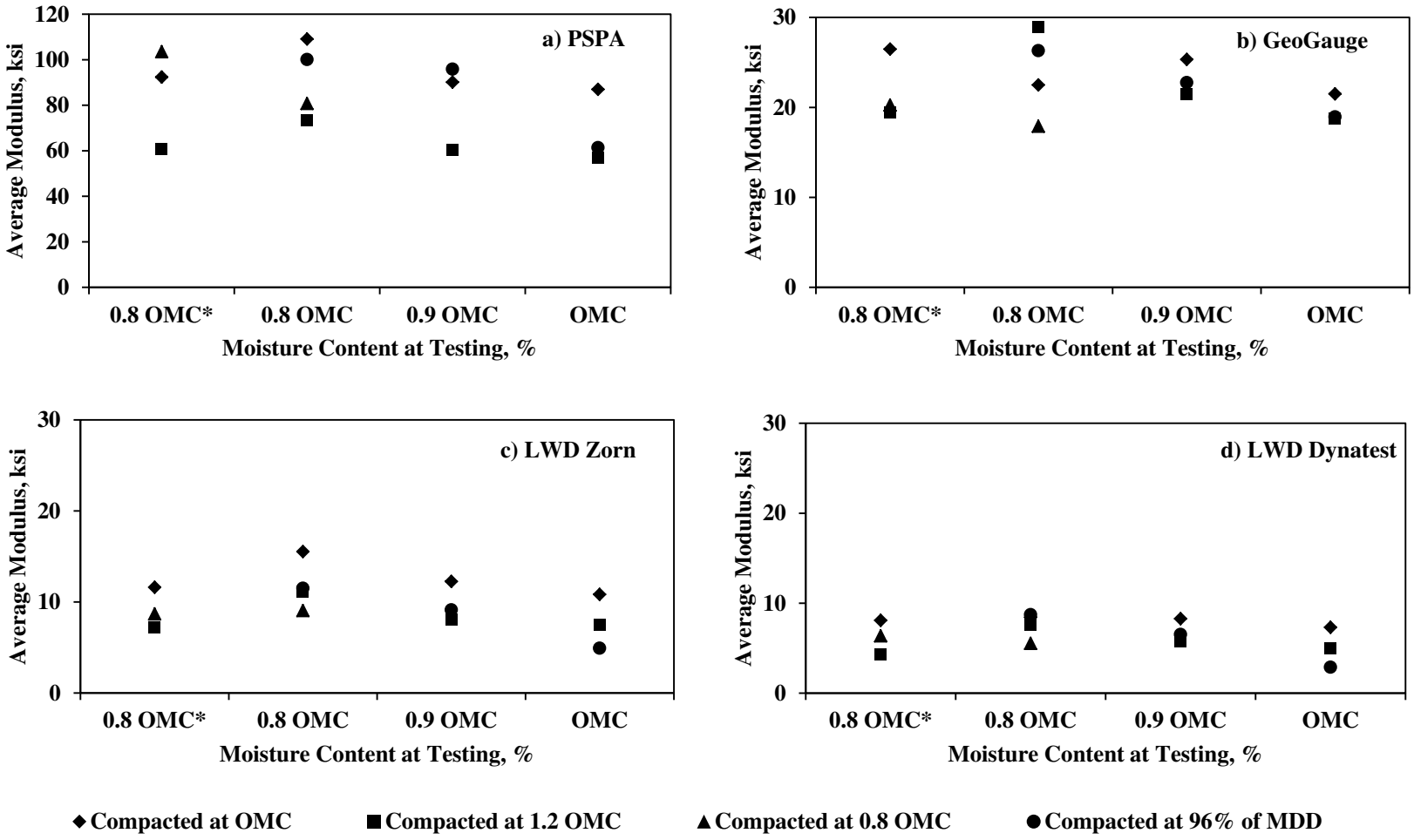

- Note: 0.8 OMC* = Base is dried to 0.8 OMC and subgrade is then saturated.

Figure E.5 - Average Moduli from Different Modulus-based Devices at Various Moisture Contents (SC materials)

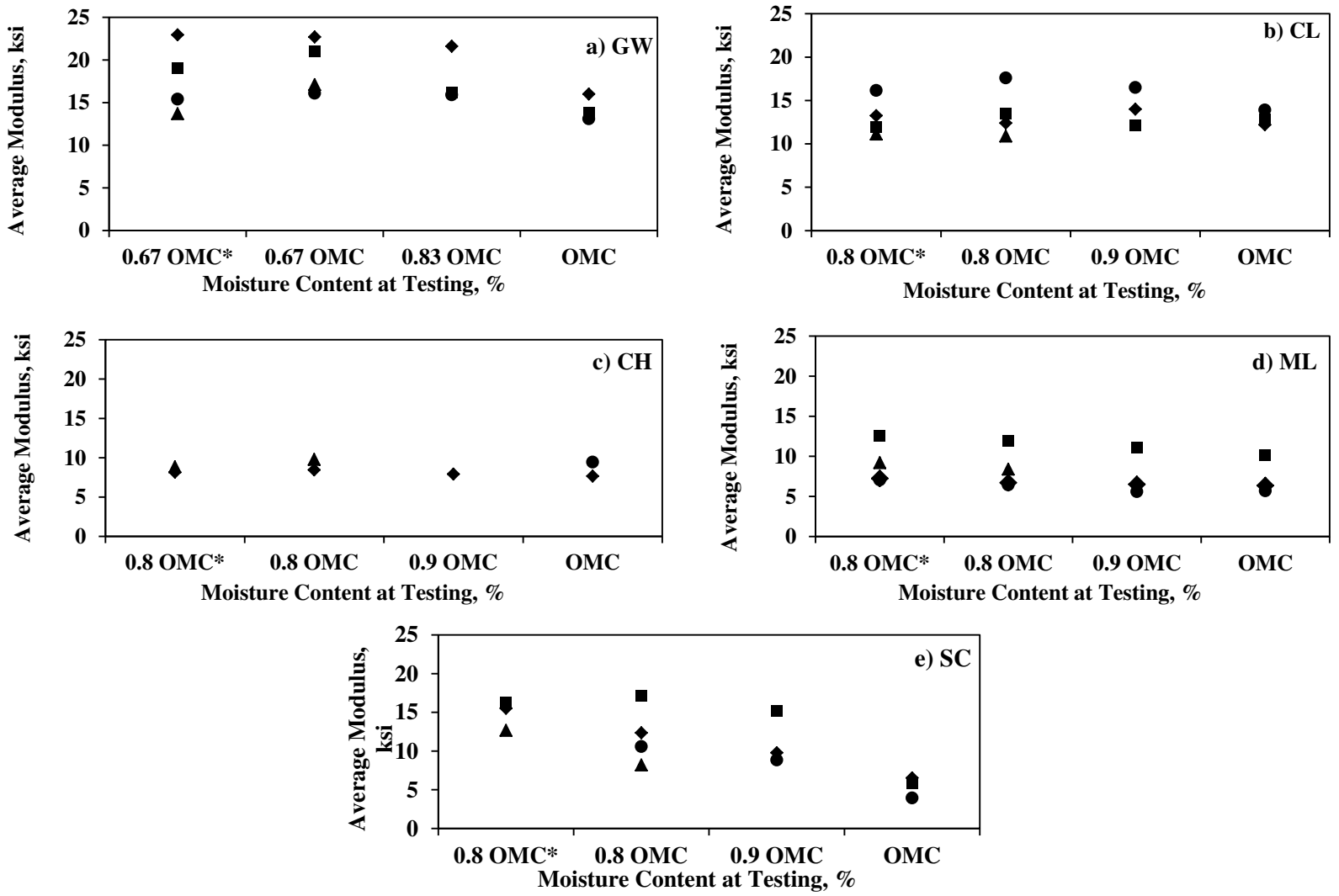

- Note: 0.8 OMC* = Base is dried to 0.8 OMC and subgrade is then saturated.

Figure E.6 – Average Moduli from DCP Device at Various Moisture Contents (GW, CL, CH, ML, and SC)

Appendix F

EVALUATION OF NUMERICAL MODELS WITH EXPERIMENTAL RESPONSE OF PAVEMENT THROUGH SMALL-SCALE TESTING

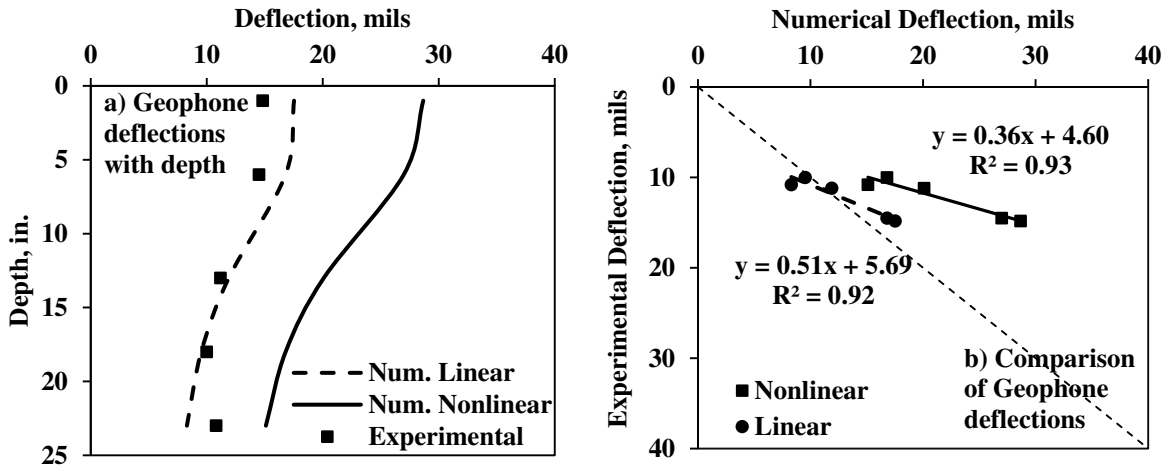

Figure F.1 - Comparison of Experimental and Numerical Deflections during LWD Tests (GW Materials Compacted and Tested at OMC)

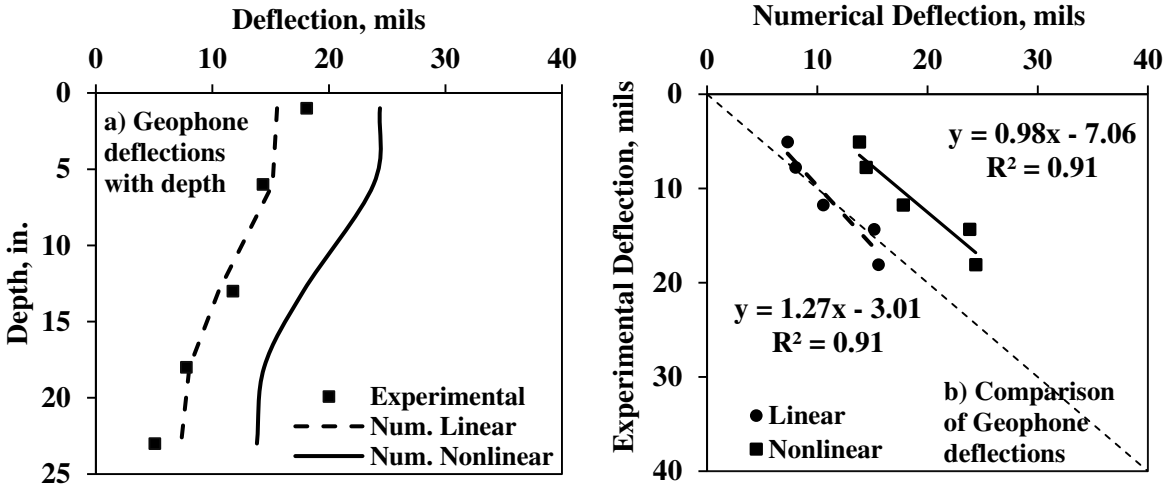

Figure F.2 - Comparison of Experimental and Numerical Deflections during LWD Tests (CL Materials Compacted and Tested at OMC)

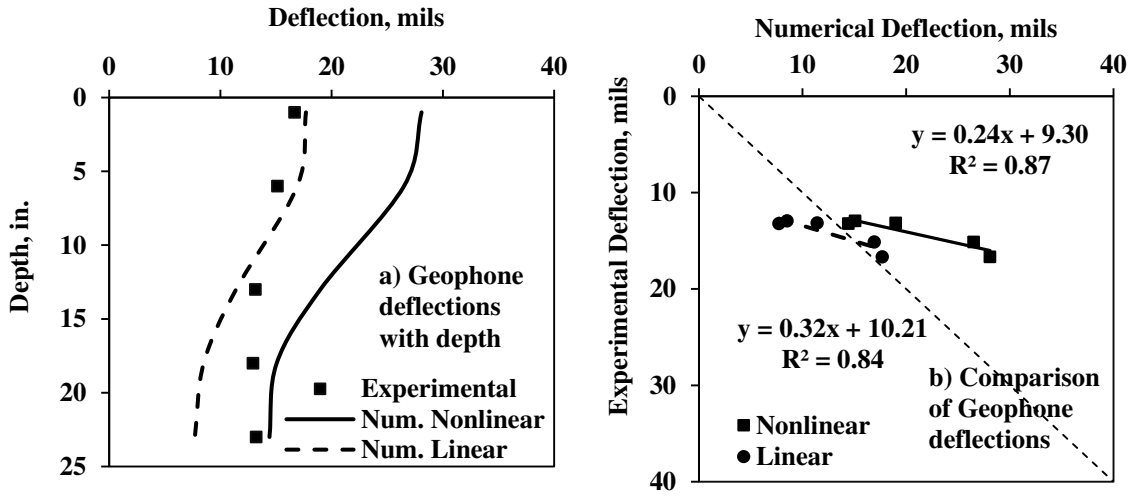

Figure F.3 - Comparison of Experimental and Numerical Deflections during LWD Tests (ML materials compacted and Tested at OMC)

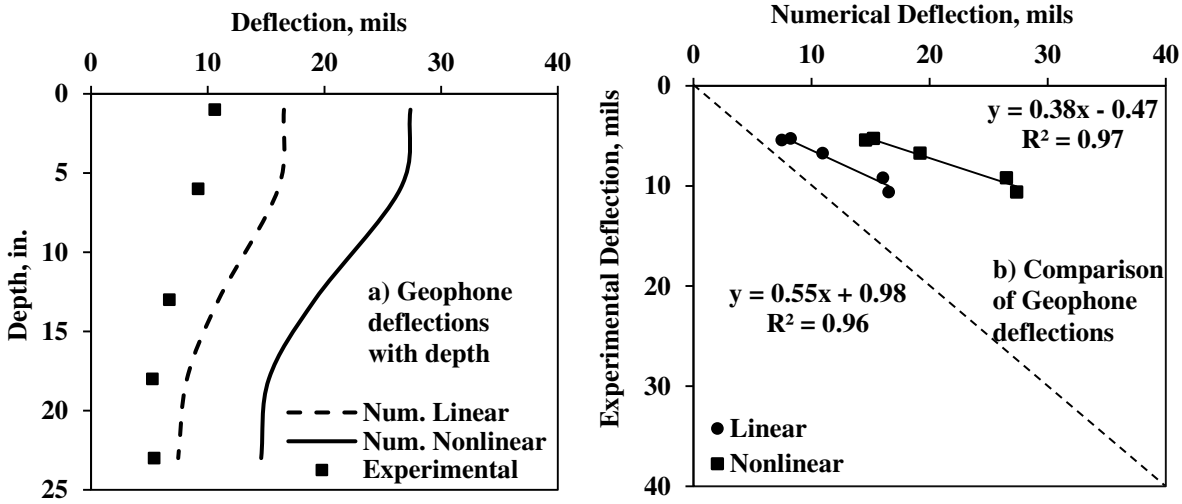

Figure F.4 - Comparison of Experimental and Numerical Deflections during LWD Tests (SC Materials Compacted and Tested at OMC)

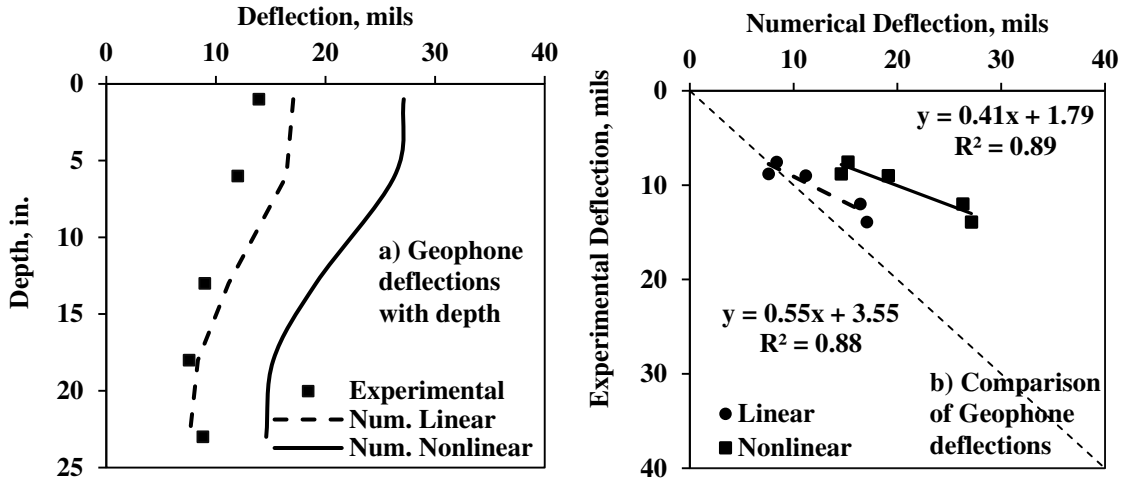

Figure F.5 - Comparison of Experimental and Numerical Deflections during LWD Tests (CH Materials Compacted and Tested at OMC)

Appendix G

FIELD EVALUATION AT LOUISIANA TRANSPORTATION RESEARCH CENTER

G.1 Introduction

The processes and relationships developed in this study were applied to a construction site. Several test sections constructed at the Louisiana Transportation Research Center (LTRC) in Port Allen, Louisiana. Those results are presented in this Appendix.

G.2 Louisiana Transportation Research Center Field Layout

Six test sections (three sections for subgrade and three for base layer) were constructed at the Pavement Research Facility (PRF) of the Louisiana Transportation Research Center (LTRC) in Port Allen, Louisiana (see Figure G.2.1). Test sections were built with full-scale construction equipment to simulate normal highway construction as per the Louisiana Department of Transportation and Development (LADOTD) specifications. The following construction sequences were used:

1. Preparation of the existing embankment platform to proper grade and initial testing.
2. Placement of necessary amount of subgrade geomaterial at each of the three nominal moisture levels (optimum, dry of optimum and wet of optimum), compaction of the section, and subsequent testing.
3. Compaction of the subgrade material layer to the optimum moisture content/density prior to the placement of the base layer.
4. Placement of necessary amount of base material at each of the three moisture levels (optimum, dry of optimum and wet of optimum), compaction of the section, and subsequent testing.

The test program was initiated on December 17, 2012 with the intention of completing the test program in one week. However, due to unseasonably repeated severe precipitation and flooding of the PRF, each layer and most sections had to be reworked numerous times extending the field tests until March 6, 2013. These unanticipated episodes resulted in some complications in the execution of the field plan and consequently the analyses of the data. These complications are discussed further when appropriate.

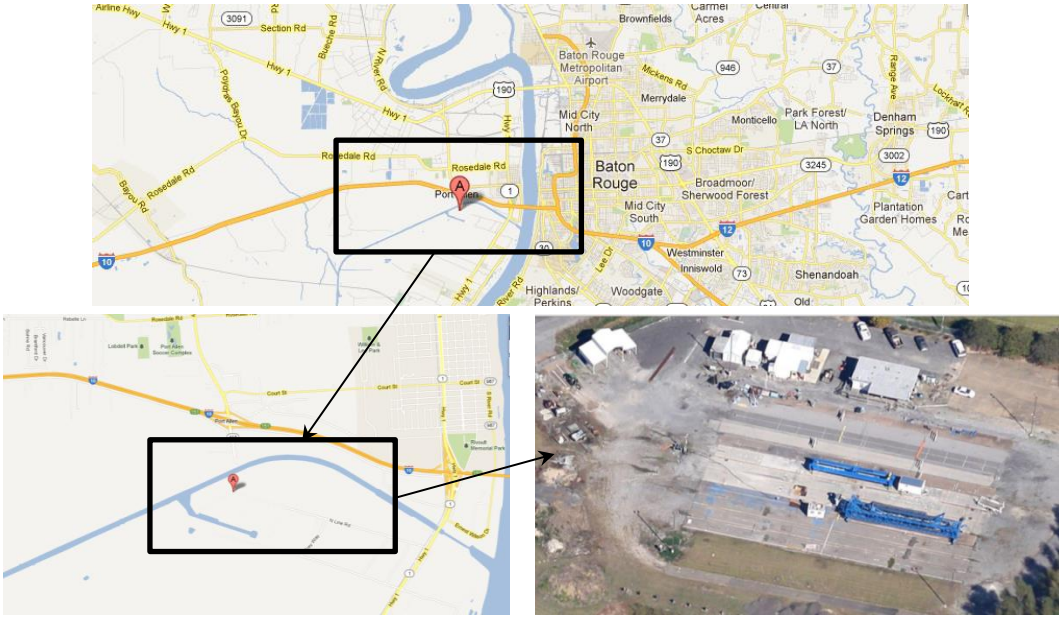

Figure G.2.1 – Location of the LTRC Field Testing Section

A typical test section is depicted in Figure G.2.2. Figure G.2.3 shows a typical layout along with test points. The test pad was divided into three 12-ft-wide by 60-ft-long sections to test the compacted layers at various moisture contents. Each section was then divided into twelve 6 ft by10 ft subsections along two

strips (Zone A and Zone B). Three test points were randomly selected within each subsection, resulting in a 36 test point for each section.

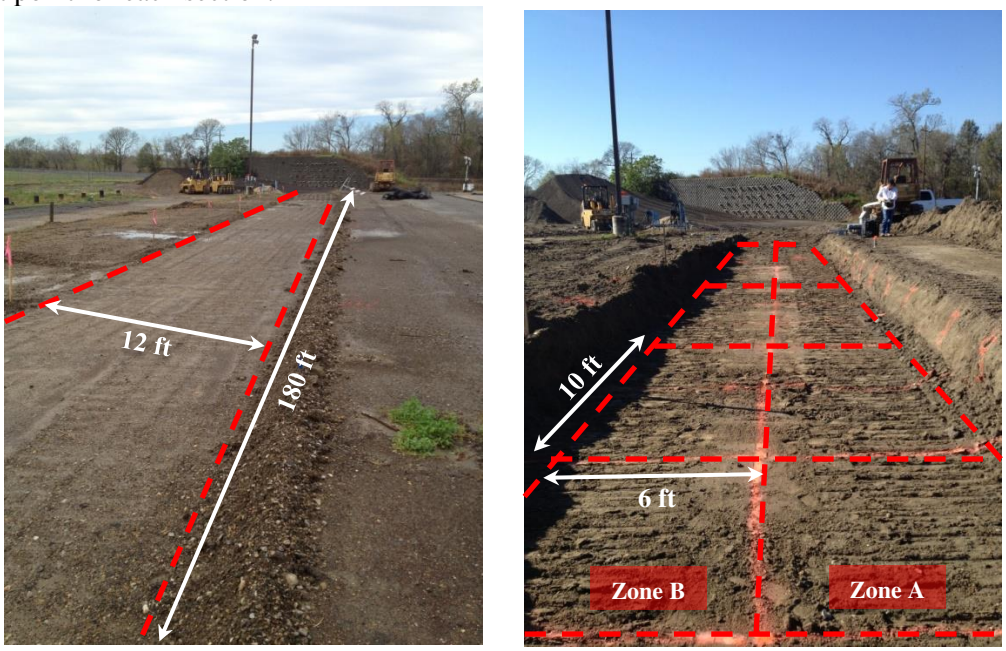

Figure G.2.2 – Typical LTRC Test Section

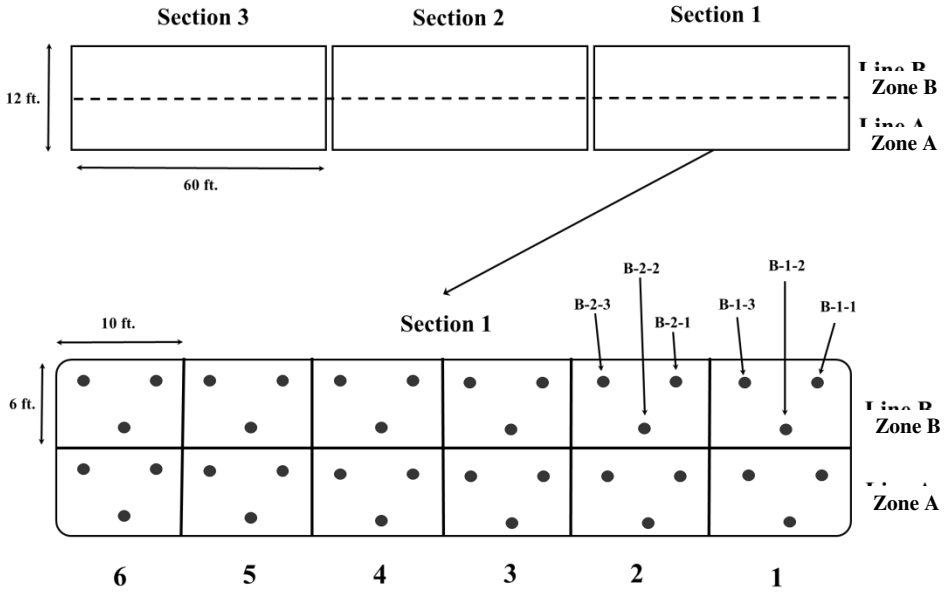

Figure G.2.3 – Location of Test Stations along the LTRC Test Section and Testing Lots (Base and Subgrade Layers)

Embankment Layer: The top soil layer was removed first as illustrated in Figure G.2.2b. After the preparation of the embankment layer to the proper grade, the following tests were performed on top of the embankment layer (see Figure G.2.4):

- Soil Density Gauge (SDG)
- Portable Seismic Pavement Analyzer (PSPA)

- Zorn Light Weight Deflectometer (LWD)

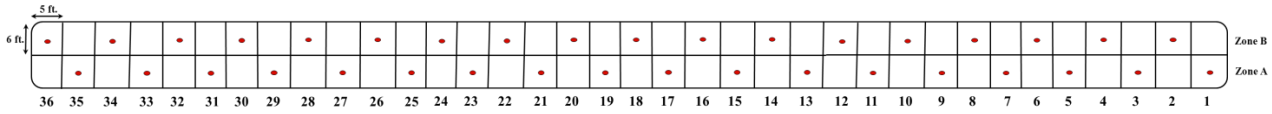

Figure G.2.4 – Location of Random Testing Points on Embankment Layer

Subgrade Layer: The subgrade layer was placed at different nominal moisture contents of OMC, wet of OMC and dry of OMC. Figure G.2.5 shows different testing devices used. The following tests (one after another) were performed subsequent to achieving the desired levels of moisture content and dry density of the subgrade layer (see Figure G.2.3 for testing lots and stations):

- ***Geogauge,*** triplicate testing at each station and three stations at each subsection (the device was moved and rotated slightly between readings).
- ***Soil Density Gauge (SDG),*** triplicate testing at each station and three stations at each subsection.
- ***PSPA,*** three times at each station and three stations at each subsection (the device was slightly moved and rotated between readings)
- ***Zorn and Dynatest LWDs,*** according to ASTM specifications (three seating drops followed by three reading drops). The test was repeated at three stations within each subsection.
- ***Nuclear Density Gauge (NDG),*** once at each subsection (for the OMC section) and three times at each subsection (for the dry and wet of OMC sections).
- ***Oven Moisture Content,*** random soil samples were extracted at different spots from the compacted layer to determine the laboratory oven dried moisture content.

An additional section of the subgrade at moisture contents near saturation was also tested. The results of that section are also reported.

Base Layer: the base layer was placed after the reworking and compacting the subgrade layer nominally to OMC for all three sections. The same procedure as the subgrade layer was followed on top of the compacted base layer.

G.3 Laboratory Results

The index properties of the embankment and subgrade soil samples are summarized in Table G.3.1 and the gradation curves are depicted in Figure G.3.1. The optimum moisture contents and maximum dry unit weights obtained from the standard Proctor tests for the embankment and subgrade and modified Proctor tests for the base are also reported in Table G.3.1. Properties of the base layer are the same as the GW base in Table 3.3.1 (Chapter 3).

Table G.3.1 - Index Properties of LTRC Geomaterials

Geomaterial	Gradation %				USCS Class.	Specific Gravity	Atterberg Limits			Moisture/Density	
	Gravel	Coarse Sand	Fine Sand	Fines			LL	PL	PI	OMC,* %	MDUW,** pcf
Embankment and Subgrade	0	21	8	71	CL	2.74	37	18	19	13.8	113.3
Base	51	31	15	3	GW	2.65	Non-Plastic			8.7	129.0

*OMC = Optimum Moisture Content, **MDUW = Maximum Dry Unit Weight

Figure G.2.5 – Nondestructive Testing of Compacted Pavement Layer at LTRC Test Sections

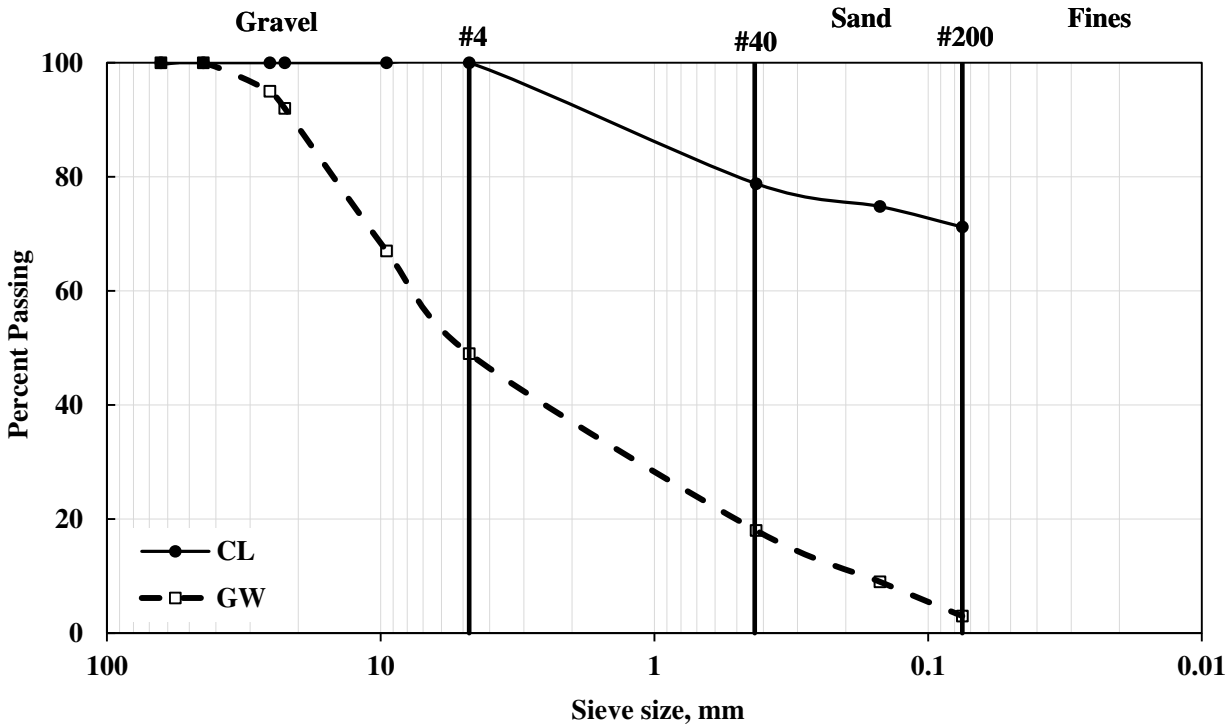

Figure G.3.1 – Gradation Curves of LTRC Geomaterials

The laboratory MR and FFRC tests (as described in Section 3.2), were performed on specimens prepared and compacted under the laboratory conditions at different moisture contents. The results of those tests are summarized in Table G.3.2. The laboratory results for base materials were also presented earlier in this report (see Table 3.1.1 for GW materials).

Table G.3.2 – Laboratory Results of MR and FFRC Tests of LTRC Geomaterials

Geomaterial	Target Moisture Content	Actual Moisture Content, %	Dry Density, pcf	FFRC Modulus, ksi	Nonlinear Parameters			Representative MR, ksi*
					k'_1	k'_2	k'_3	
Subgrade (CL)	0.8 OMC	10.9	111.5	46	1026	0.28	-0.05	18
	0.9 OMC	12.6	113.3	43	1231	0.19	-0.26	19
	1.0 OMC	14.4	113.4	39	672	0.23	-0.05	11
	1.1 OMC	15.2	112.5	21	908	0.44	-1.48	13
	1.2 OMC	16.7	112.8	7	98	1.53	-2.78	2
	1.4 OMC	19.0	110.7	2	76	0.97	-3.00	1
Base (GW)	0.8 OMC	6.5	125.6	24	1087	0.53	-0.10	28
	0.9 OMC	7.7	129.6	23	952	0.70	-0.10	30
	1.0 OMC	8.5	131.0	18	897	0.50	-0.10	22
	1.1 OMC	9.9	126.4	16	618	0.52	-0.10	16
	1.2 OMC	10.4	126.1	15	480	0.61	-0.10	14

* from Eq. 3.2.1 based on τ_{oct} and θ values of 7.5 psi and 31 psi for base and 3 psi and 12.4 psi for subgrades as recommended by NCHRP Project 1-28A.

G.4 Moisture Devices

The calibrated moisture contents from the SDG tests carried out on the embankment are compared with the average oven-dried moisture contents in Figure G.4.1. The average oven-dried moisture content of the embankment was 20.5%, which is 6.7% greater than the OMC from the standard Proctor tests. The average and standard deviation of the raw SDG moisture contents were 9.2% and 0.6%. The raw SDG results were systematically and significantly lower than the oven-dried moisture contents by a factor of 2, indicating the need for a rigorous pre-testing calibration of the SDG before utilization in a project. The average SDG moisture content after calibration was 20.6%.

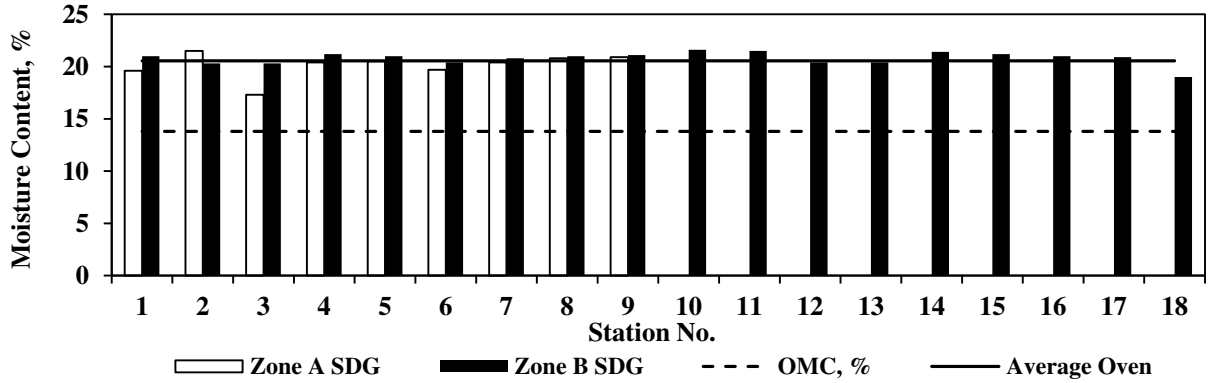

Figure G.4.1 –Calibrated SDG Moisture Contents for Embankment Layer

Figure G.4.2 depicts the variation of the dry density of the embankment layer measured with the SDG device. The SDG dry densities on average were about 12 pcf less than the laboratory MDD with a standard deviation of 2.5 pcf.

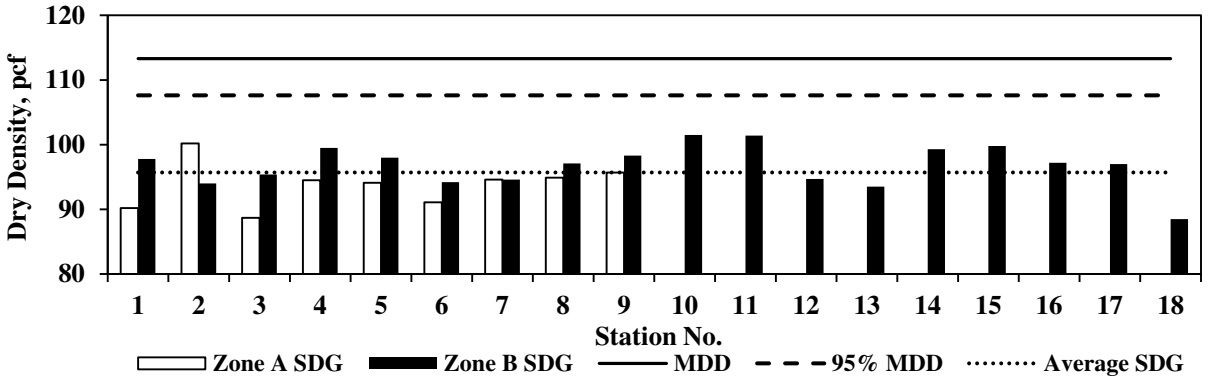

Figure G.4.2 – SDG Dry Density (Embankment Layer)

The results from the NDG and SDG for the 12-in.-thick subgrade layer (tested with the pattern shown in Figure G.2.3) are summarized in Figure G.4.3 and Table G.4.1. The average NDG moisture contents for the nominally dry, optimum, wet and saturated sections were 10.7% (3% dry of OMC), 15.3% (1.5% above OMC), 16.9% (3% above OMC) and 19.0% (5% above OMC), respectively. The calibrated SDG moisture contents were 10.5%, 15.8%, 16.2% and 18.8% for the nominally dry, optimum, wet and saturated sections, respectively. The standard deviation of measured moisture contents at each lot is also depicted in Figure G.4.3 as error bar. The average standard deviations on lot basis are 0.2% for the SDG and 0.5% for the NDG. As reflected in Table G.4.1, the oven-dried moisture contents of the subgrade sections were quite uniform since the COVs are 6% and less.

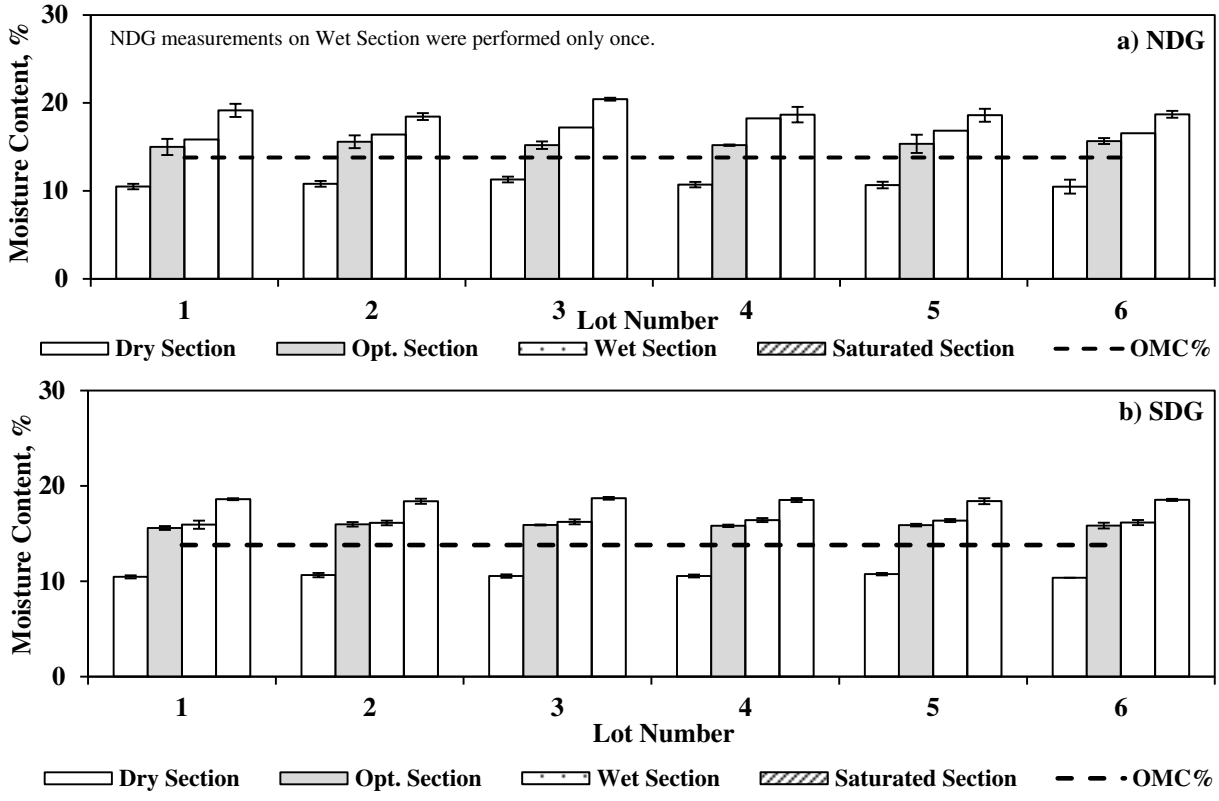

Figure G.4.3 –NDG and Calibrated SDG Moisture Contents after Compaction of Subgrade

Table G.4.1 – Spatial Averages and Coefficients of Variation (COV) of NDG and SDG Moisture Contents and Dry Densities of Base and Subgrade Layers

Layer	Parameter	Section	Nuclear Density Gauge		Soil Density Gauge		Oven Moisture Content	
			Average	COV, %	Average	COV, %	Average	COV, %
Subgrade	Calibrated Moisture Content, %	*Saturated*	19.0	7	18.8	3	18.8	4
		Wet	16.9	7	16.2	3	16.2	3
		Optimum	15.3	7	15.8	2	15.8	4
		Dry	10.7	8	10.5	2	10.8	6
	Raw Dry Density, pcf	*Saturated*	103.5	2	93.7	2		
		Wet	108.4	2	95.7	2		
		Optimum	109.7	2	94.9	2		
		Dry	111.6	3	94.0	2		
Base*	Calibrated Moisture Content, %	*Wet*	11.1	5	12.1	5	12.0	3
		Optimum	9.3	7	N/A*	N/A	9.6	3
		Dry	5.8	6	5.9	2	5.9	5
	Raw Dry Density, pcf	*Wet*	125.4	1	101.7	4		
		Optimum	132.2	1	N/A	N/A		
		Dry	122.5	1	91.7	1		

*SDG data for the optimum section was not collected due to time constraint

Figure G.4.4 summarizes the dry densities and corresponding standard deviations of each lot estimated with the NDG and SDG on top of the subgrade. The spatial average of densities and their corresponding COVs are also included in Table G.4.1. The dry, optimum and wet sections achieved their necessary degrees of compaction of 95% while this was not the case for the saturated section. The estimated dry densities with the SDG are systematically lower than expected indicating a need for a through calibration.

The variations of the average and standard deviation of the NDG moisture contents and dry densities for the base layers are summarized in Figure G.4.5. The moisture contents from the three sections are reasonable as per their nominal values (wet of optimum, optimum and dry of optimum). Furthermore, the dry densities of the sections are within the specification limits of 95% relative compaction. The spatial averages of the moisture contents and their corresponding COVs are included in Table G.4.1. The nominally dry, optimum and wet sections of base layer were about 2.8% dry of OMC, 0.9% above OMC and 3.3% above OMC, respectively.

Figures G.4.6 and G.4.7 summarize the correlations between the NDG and SDG measurements with the oven-dried moisture contents for the base and subgrade layers. Based on the limited available data, the uncertainties in moisture estimation are typically 15% or less of the measured values for both devices.

G.5 Modulus-Based Devices

The Zorn LWD and PSPA were used on top of the embankment layer at up to 36 spots. The average modulus of the embankment layer was about 1.6 ksi according to the Zorn LWD measurements with a standard deviation of 0.4 ksi and a COV of about 28%. The results from the PSPA were outside the operational limits of the device, and as such not reported.

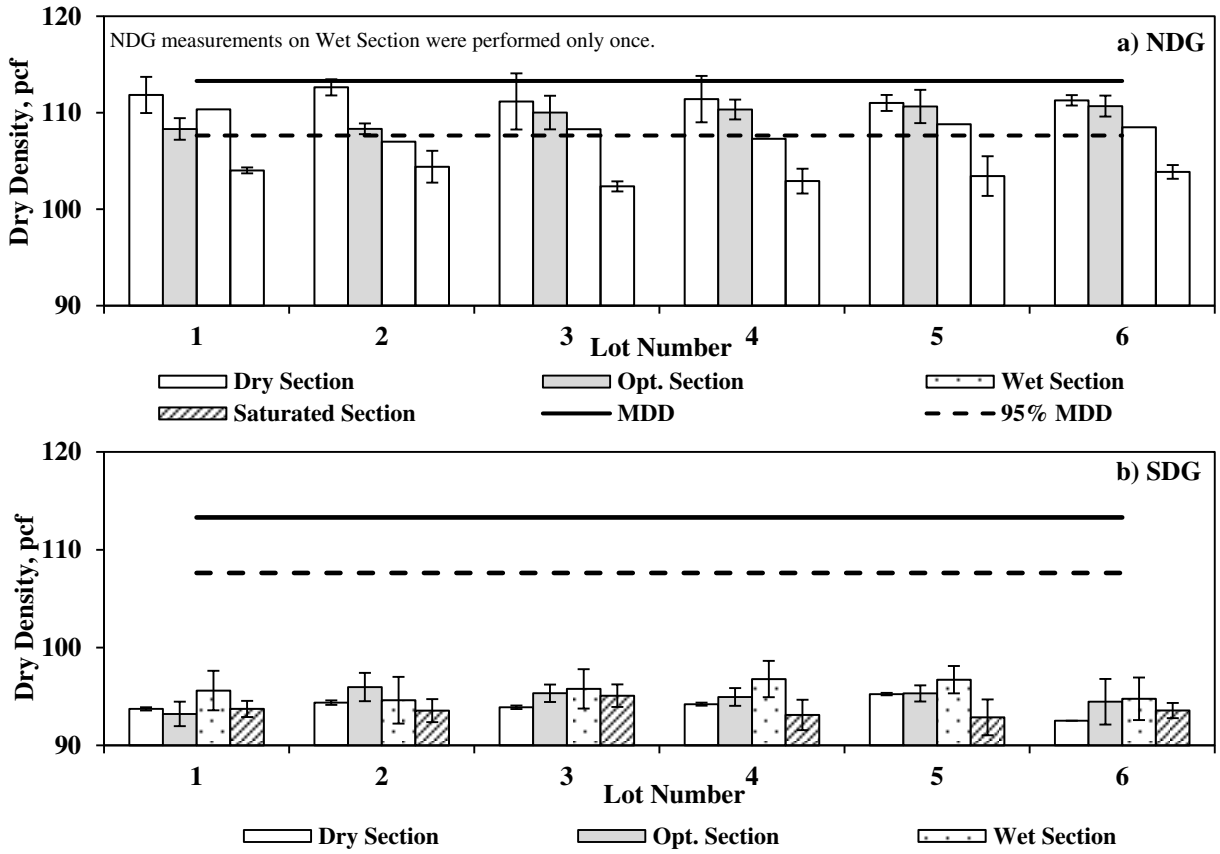

Figure G.4.4 – NDG and SDG Dry Densities after Compaction of Subgrade

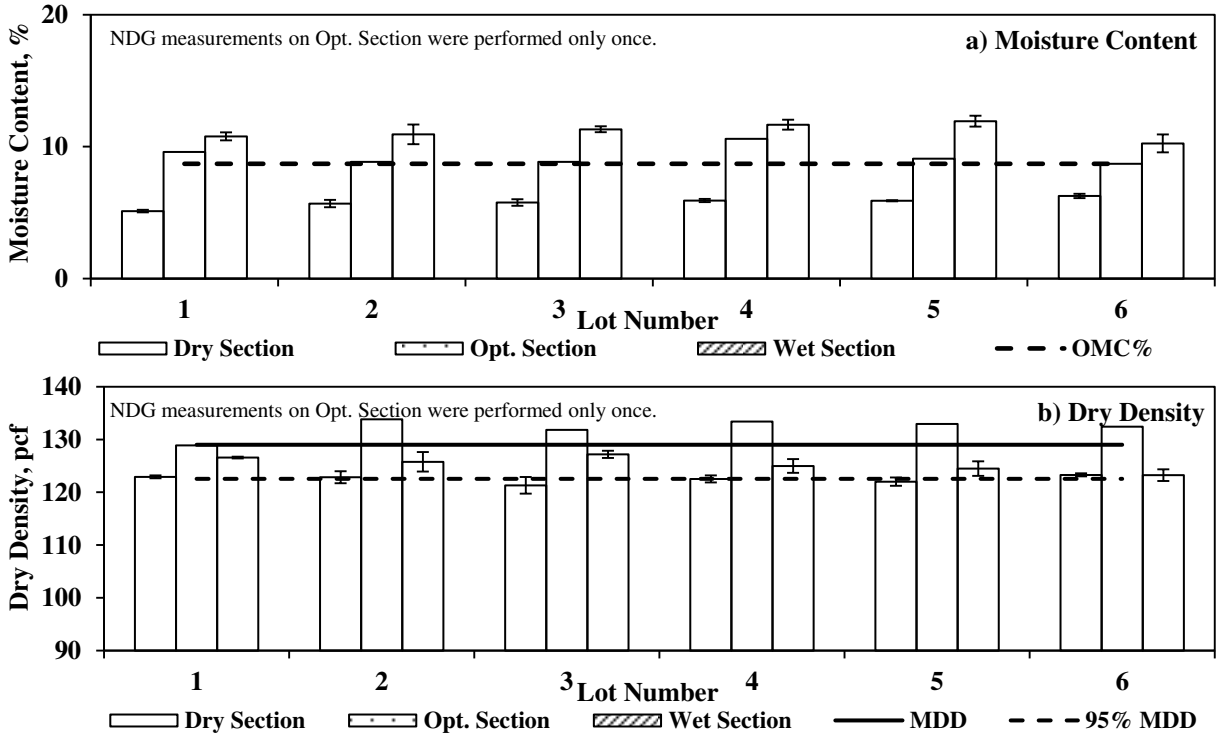

Figure G.4.5 –NDG Moisture Content and Dry Density after Compaction of Base Layer

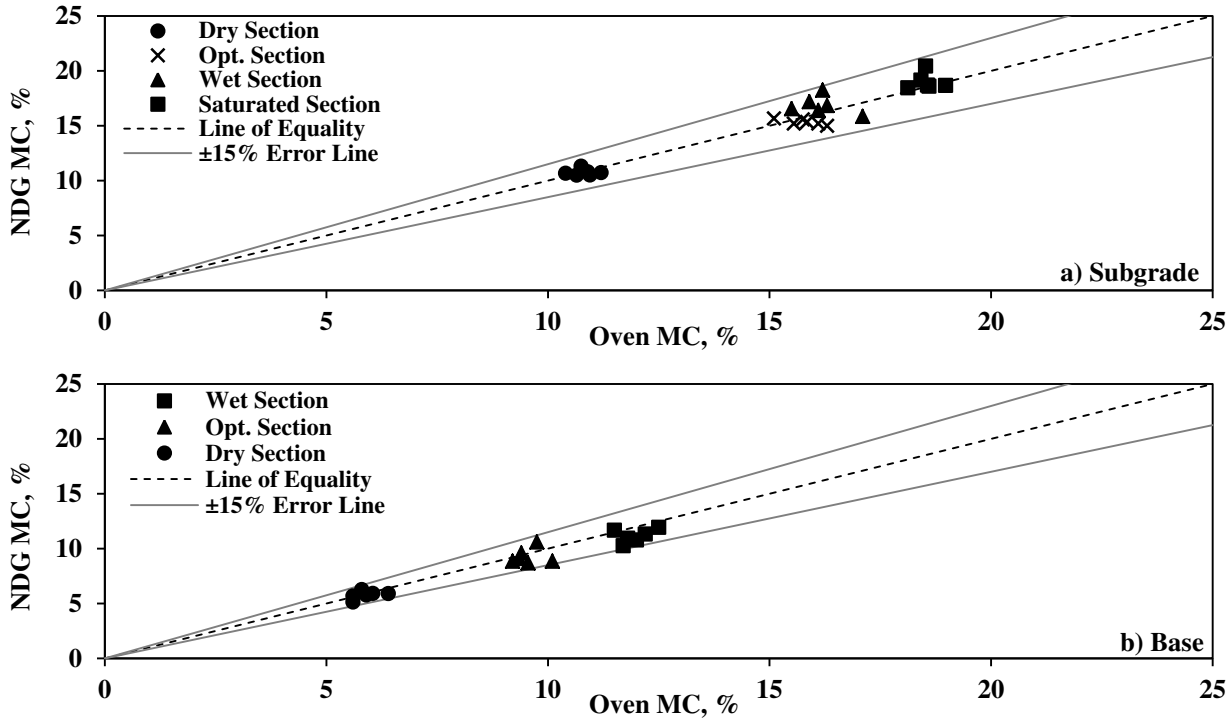

Figure G.4.6 – Comparison of Oven Moisture Contents with NDG Results for Base and Subgrade Layers

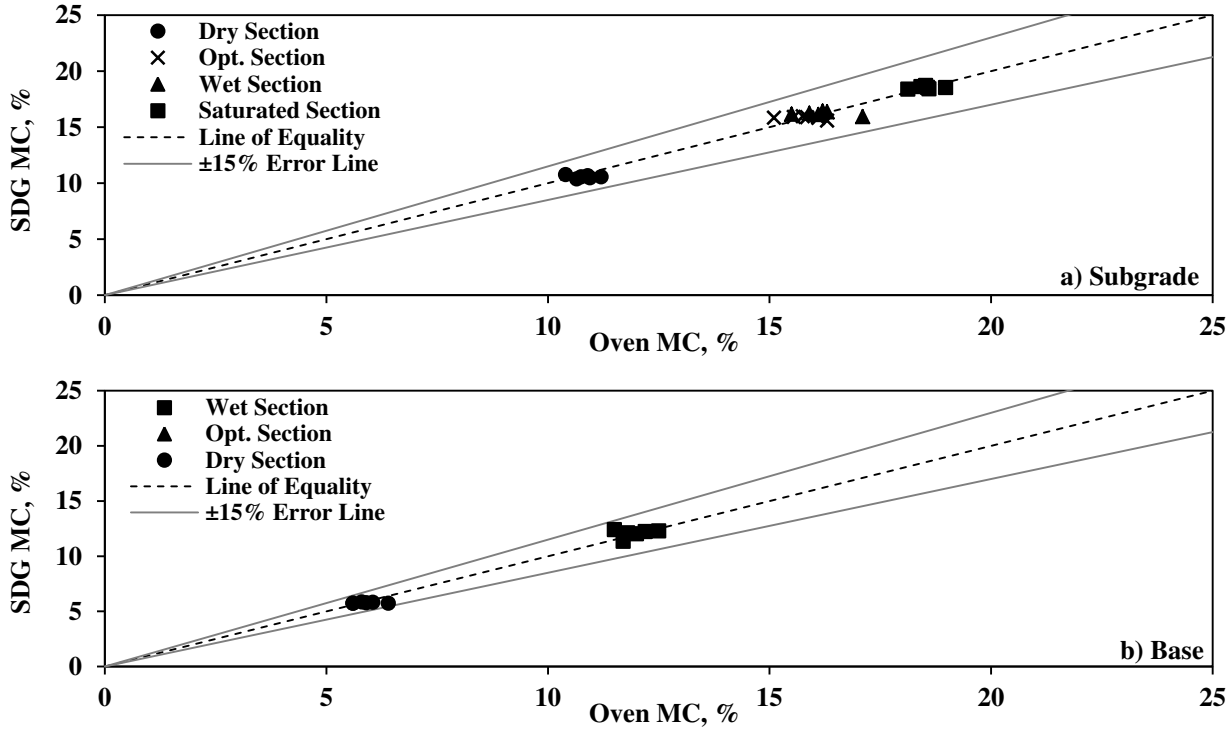

Figure G.4.7 – Comparison of Oven Moisture Contents with Calibrated SDG Results for Base and Subgrade Layers

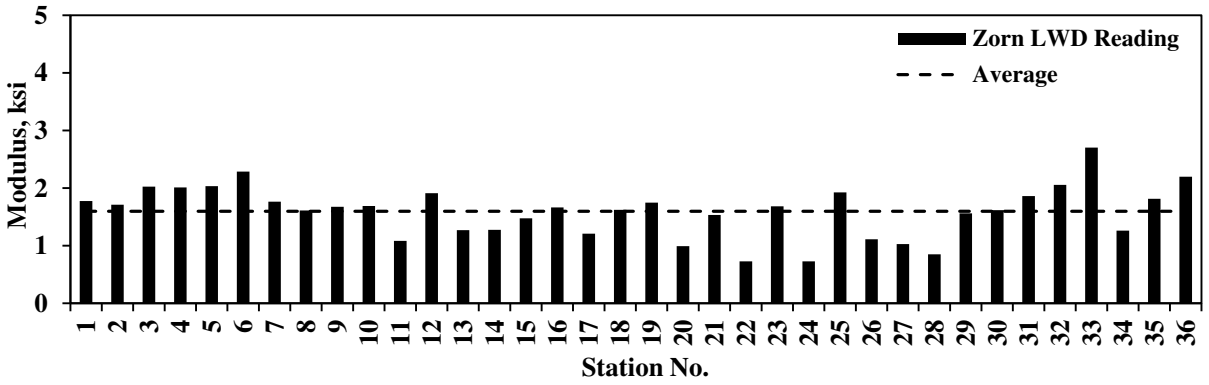

Figure G.5.1 – Spatial Variation of Zorn LWD Modulus of Embankment Layer

The averages and standard deviations (shown as error bars) of moduli from different devices for Zones A and B of the subgrade layer are summarized in Figure G.5.2. The PSPA moduli for the saturated section are not reported again since that section was too wet to be within the operational limits of the device. As expected, the dry section typically exhibited the greatest moduli for all devices followed by the optimum section, wet and saturated sections. The standard deviations of the moduli are greater for the stiffer materials for all devices. As illustrated in Figure G.5.3, the variation in DCP modulus also following the same pattern as observed in Figure G.5.2 for other devices.

As depicted in Figure G.5.2, the average PSPA modulus on the dry section is 1.8 times greater than the average modulus of the optimum section. The Dynatest LWD depicted even more increase in the modulus from the optimum to the dry with a factor of about seven. Relative to the optimum condition, the Zorn LWD average modulus of the dry section increased by about four times relative to the optimum section. The average DCP modulus of the dry section, similar to the PSPA, increases by a factor of about 1.4 as compared to the average modulus of the optimum section. In summary, the two layer-specific measurements (i.e., DCP and PSPA) exhibit less sensitivity to moisture content variation than the two LWDs that measure the response of the system. The patterns from the layer-specific measurements are more in agreement with the ones observed from the laboratory tests. The moduli from the wet and saturated sections are essentially the same with all devices. As indicated in Figure G.5.2b, the Geogauge exhibited high variation in modulus estimation with no clear pattern from different sections.

The variation in subgrade modulus with the NDG moisture content for each device is presented in Figure G.5.4. Figure G.5.5 illustrates the variations in subgrade modulus from different devices with the degree of saturation. The moduli from all devices (except Geogauge) correlate reasonably well with both moisture content and degree of saturation.

To compare the results with other relationships proposed earlier in this report, the variations in normalized modulus with normalized degree of saturation (S-S_{opt} as described in Section 4.4) and with normalized moisture content (defined as *[MC-OMC]/OMC* as described in Section 4.4) are shown in Figures G.5.6 and G.5.7, respectively. To estimate the moduli at the optimum moisture content (M_{opt}) the best-fit equations in Figures G.5.4 and G.5.5 were employed, respectively. As a reminder, similar correlations were also developed for the small-scale studies in Section 4.3. The MEPDG and Cary and Zapata (2010) relations for *wPI*=0 and *wPI*=13 (corresponding to the materials' index properties) are also included in Figure G.5.6. For data points much drier than the OMC, the MEPDG model for fine-grained soils match the data better than the other models, especially for the DCP and PSPA. For the conditions close to and wet of OMC, the Cary and Zapata model with *wPI*=0 match the field data better.

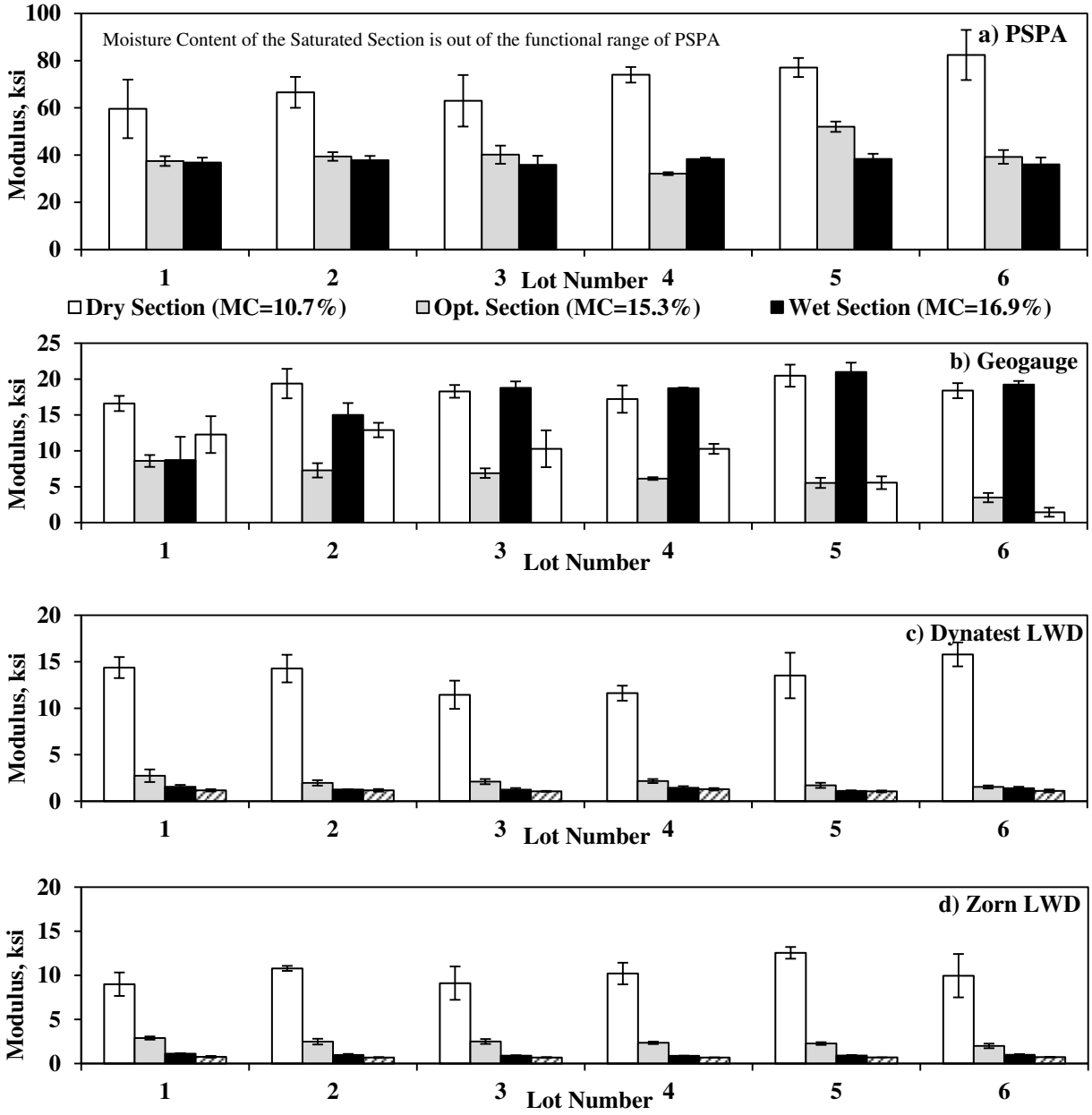

Figure G.5.2 –Variations of Moduli after Compaction of Subgrade

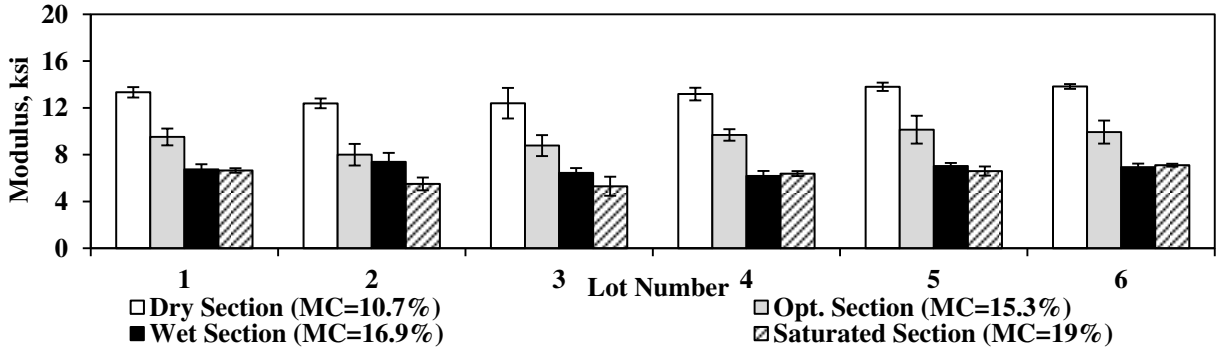

Figure G.5.3 –DCP Moduli after Compaction of Subgrade

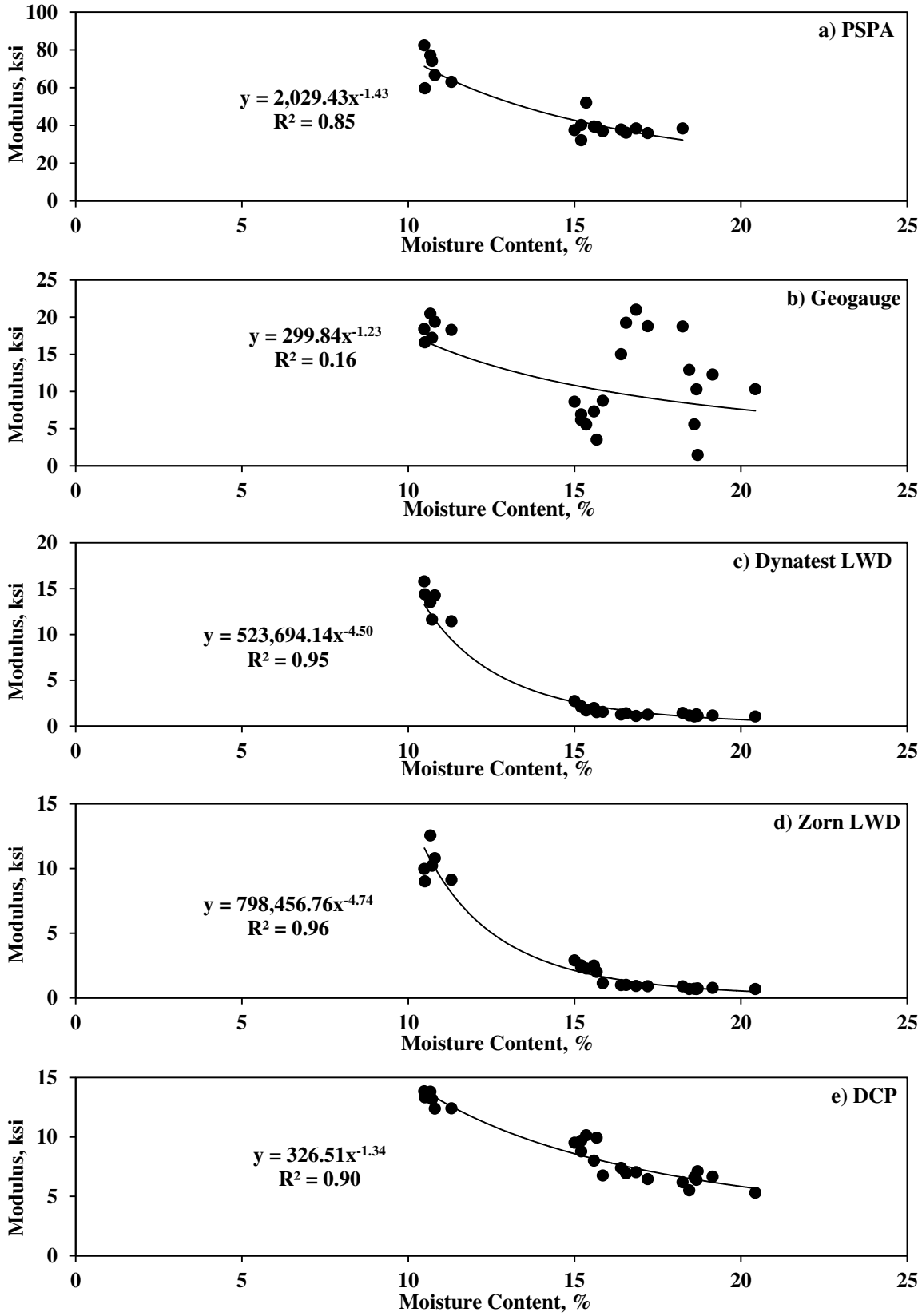

Figure G.5.4 – Variations in Field Modulus with Moisture Content of Subgrade Layer

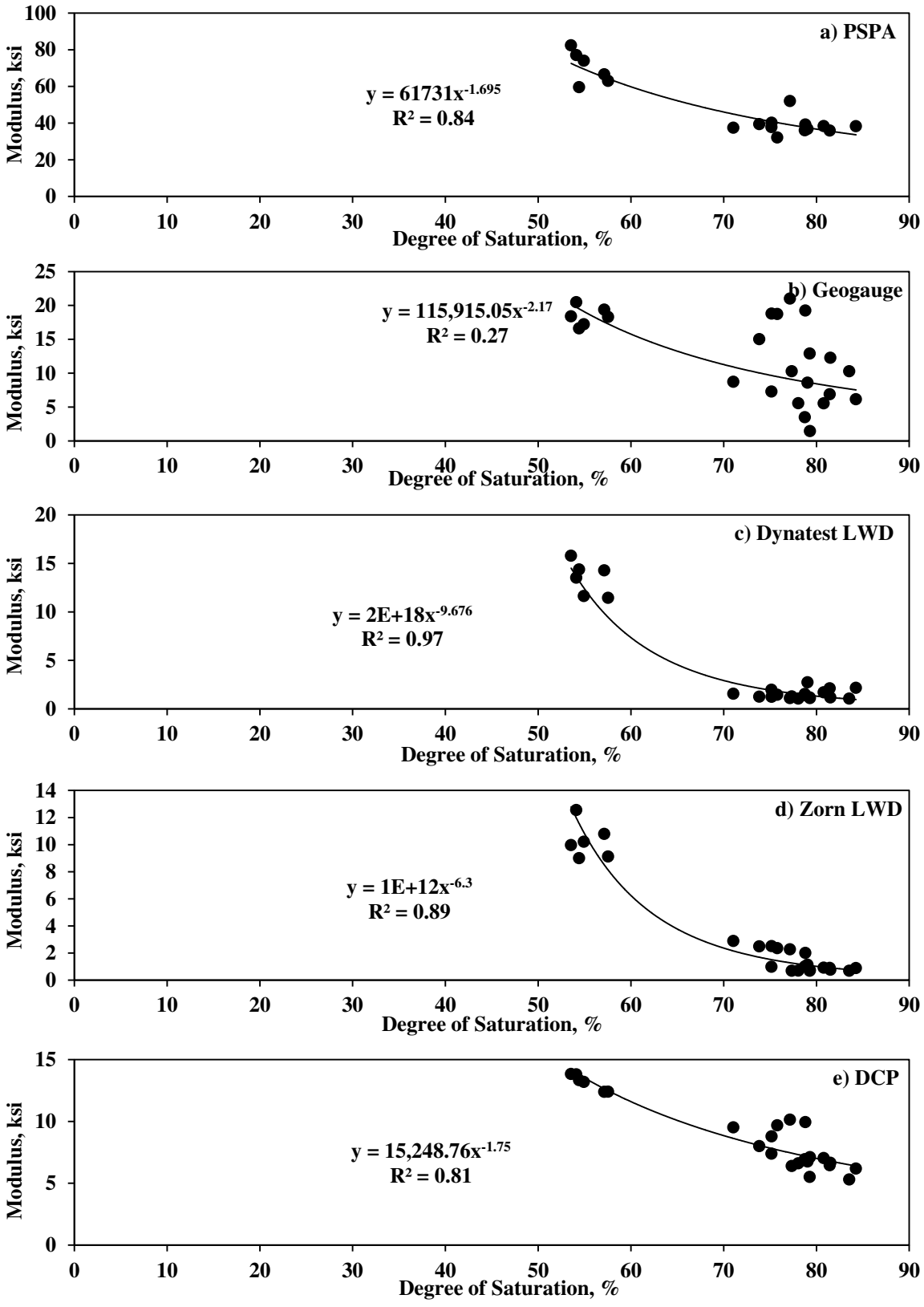

Figure G.5.5 – Variations in Field Modulus with Degree of Saturation of Subgrade Layer

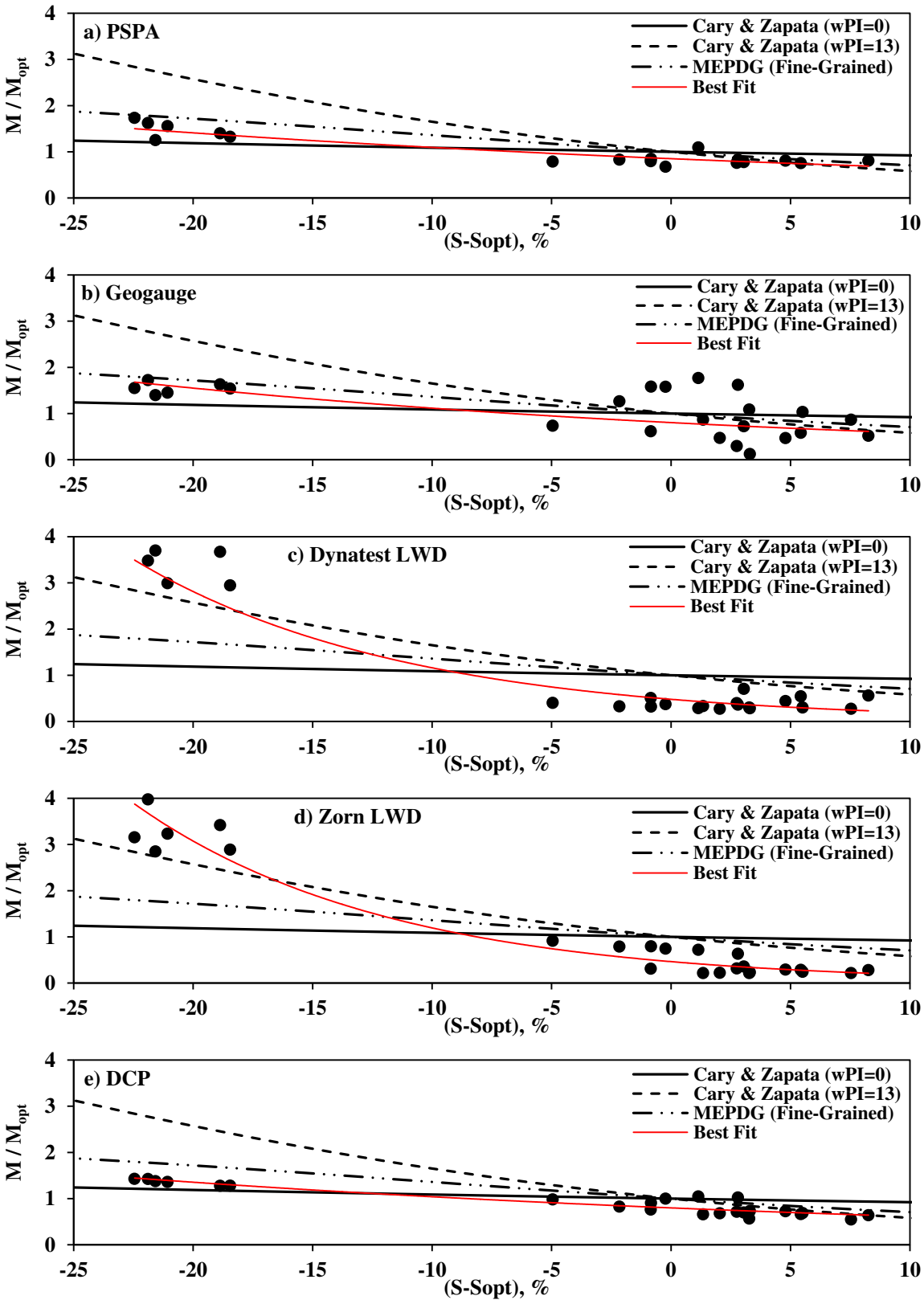

Figure G.5.6 – Variations in Normalized Field Modulus with Normalized Degree of Saturation of Subgrade Layer

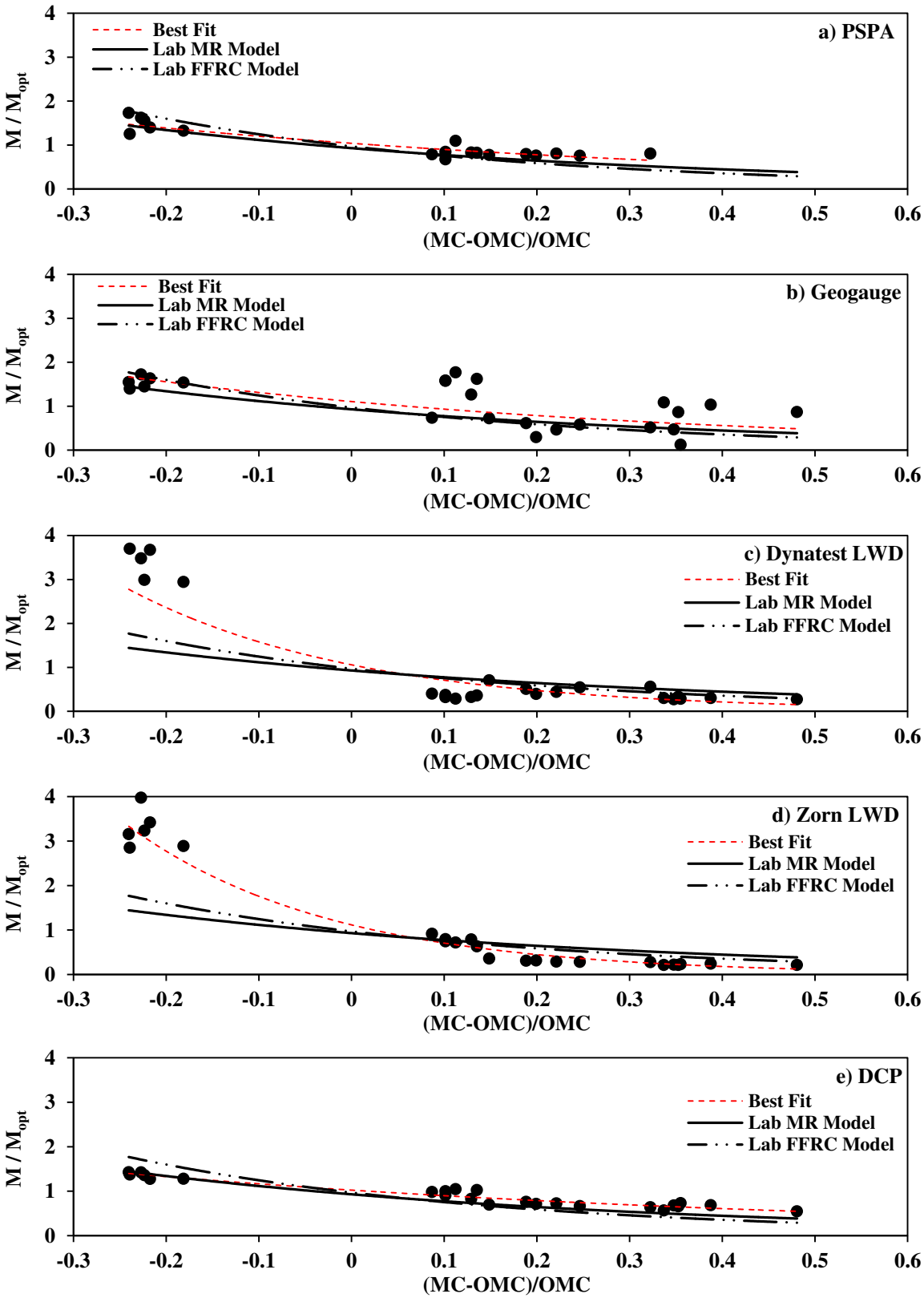

Figure G.5.7 – Variations in Field Modulus with Normalized Moisture Content of Subgrade Layer

As reflected in Figure G.5.7, the variations in the normalized moduli from the laboratory and field with the normalized moisture content are similar for the two layer-specific devices (DCP and PSPA) but not for the two LWD's. This is attributed to the fact that the LWD measurements are also impacted by the moduli of the underlying layers as discussed before.

The next step was to estimate and compare the target moduli (as discussed in Chapter 6) with the field moduli for different devices. This exercise was not carried out for the Geogauge due to scatter in the data. Figure G.5.8 depicts the target and field moduli for the PSPA. The optimum and wet sections did not achieve the desired acceptance limits, while the dry section marginally passed the specified target modulus. The anticipated moduli for each moisture condition based on the laboratory FFRC results are also shown in Figure G.5.8. The PSPA moduli are greater than moisture-adjusted anticipated modulus for the wet section, are similar for the optimum section and are less for the dry section. This trend confirms the trends relating the lab and field moduli in Section 4.5.

In terms of the target modulus based on the laboratory MR tests at OMC, all sections tested with the Dynatest LWD failed significantly (see Figure G.5.9) except for the dry section that passed marginally. Two sets of anticipated target moduli based on laboratory MR tests for each moisture condition are shown in Figure G.5.9, (1) assuming that the subgrade is a uniform layer, and (2) assuming a two-layer system with 12 in. of subgrade over the embankment. As the subgrade gets drier, these two anticipated moduli differ more significantly.

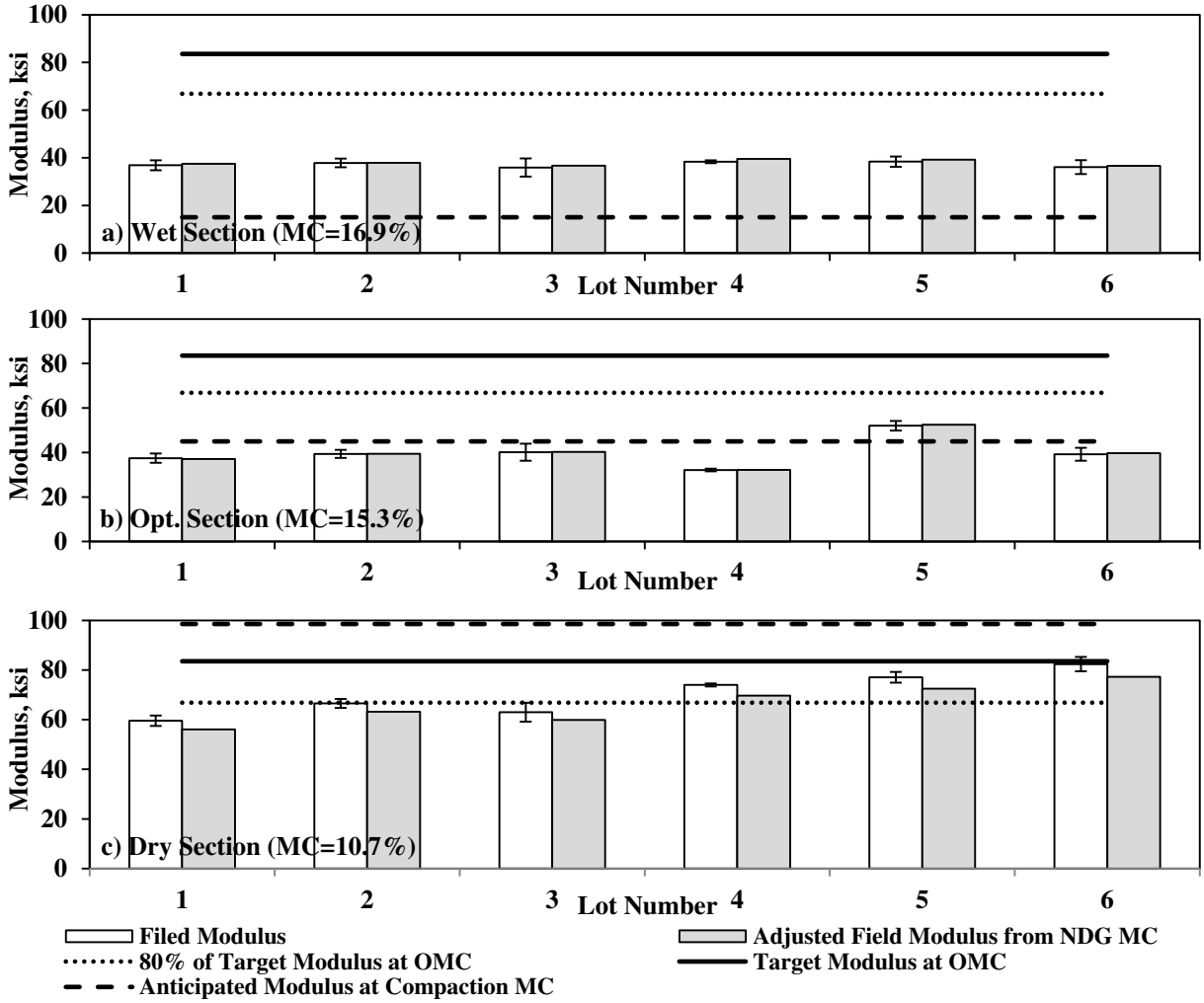

Figure G.5.8 – Comparison of Field PSPA and Corresponding Target Moduli for Subgrade Layer

The results from the Zorn LWD depict the same patterns as the Dynatest LWD as illustrated in Figure G.5.10. The main difference between the two LWD results is the significant differences in the measured moduli for the dry section.

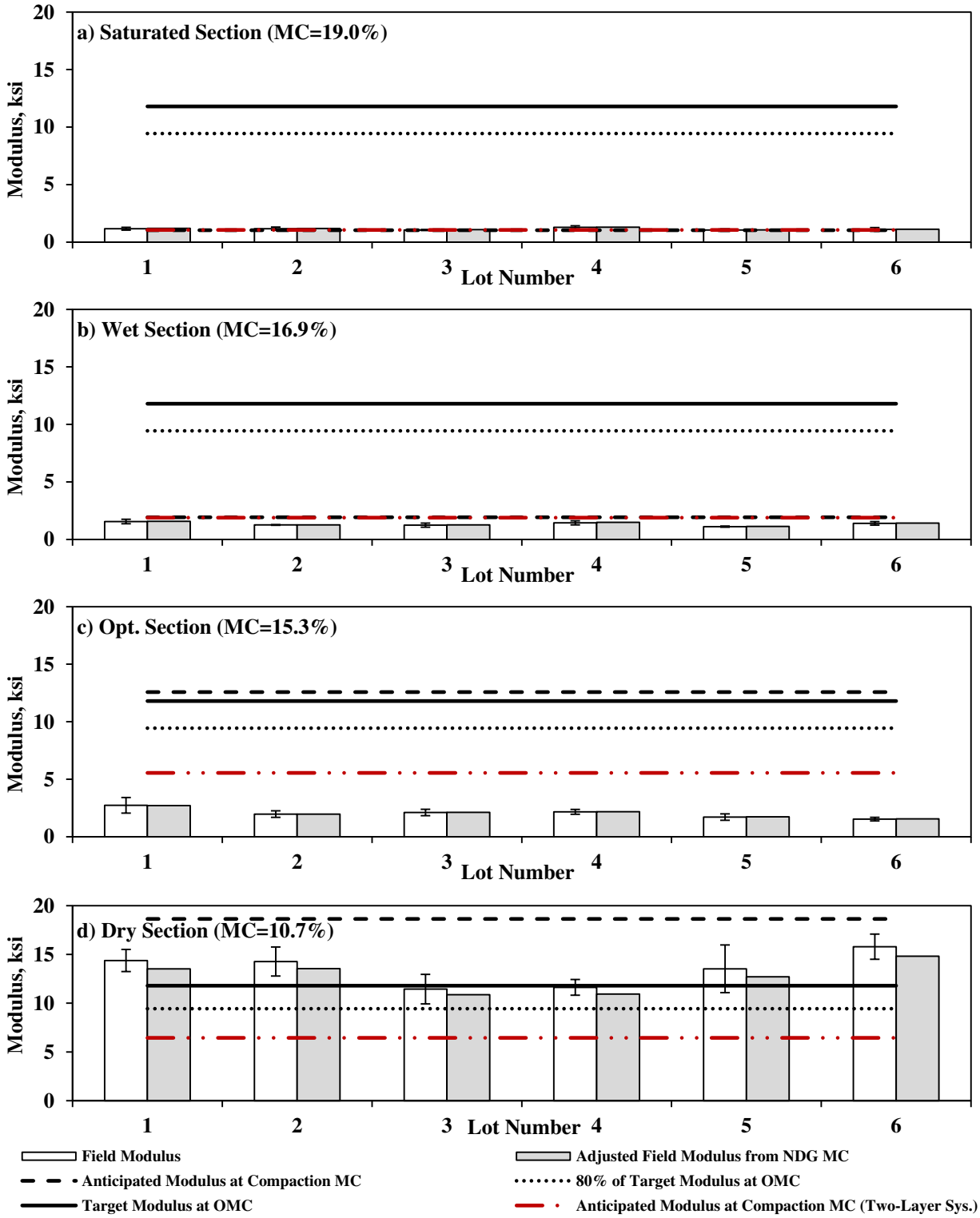

Figure G.5.9 – Comparison of Field Dynatest LWD and Corresponding Target Moduli for Subgrade Layer

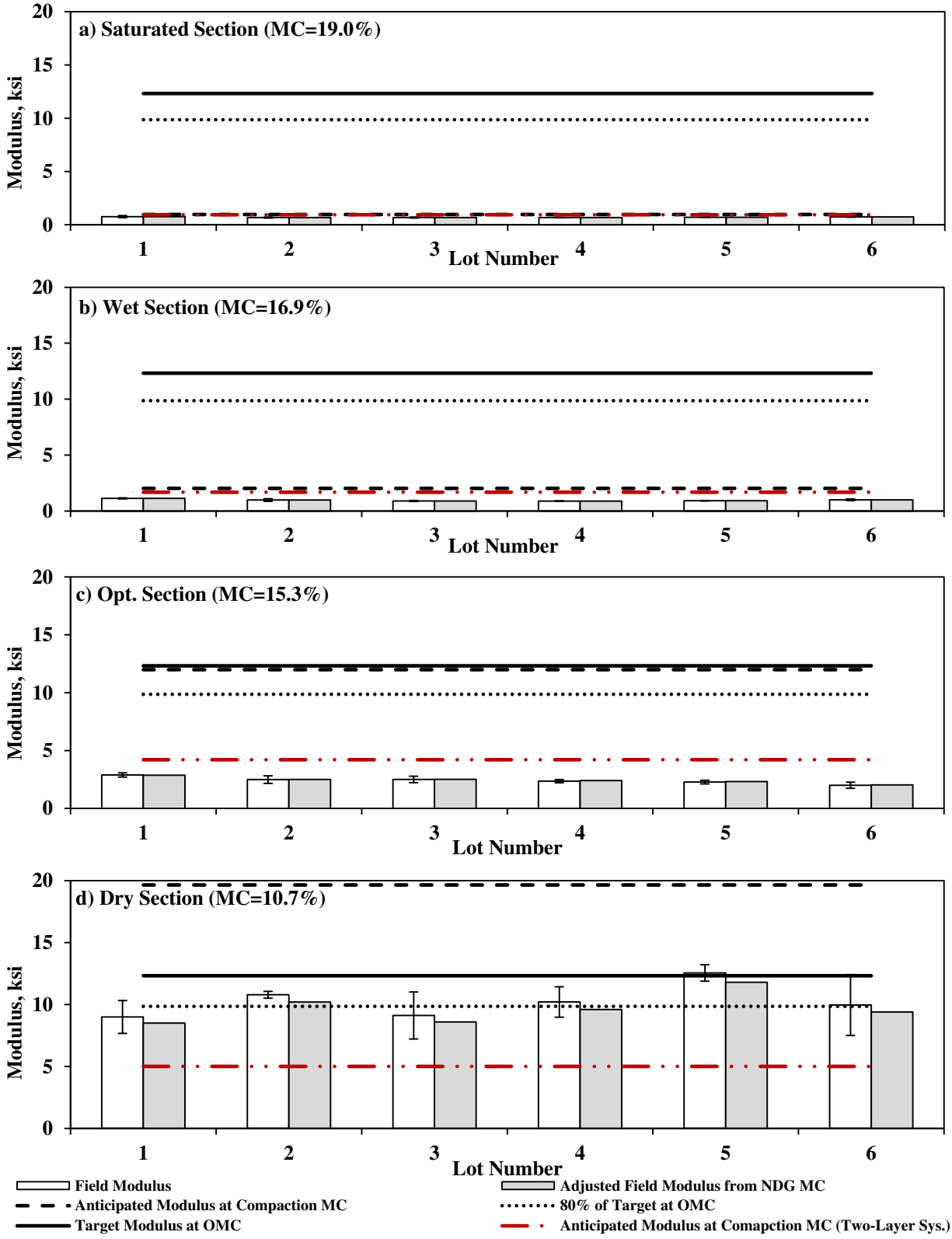

Figure G.5.10 – Comparison of Field Zorn LWD and Corresponding Target Moduli for Subgrade Layer

Figure G.5.11 illustrates the results from different devices at three nominal moisture contents of dry, optimum and wet on top of the base layer. The moduli estimated from different devices somewhat contradict one another. According to the PSPA, the dry and optimum sections yielded similar moduli with the moduli from the wet section being about 2.2 times less than that from the optimum section. The same pattern, but not as drastic, was observed in the laboratory FFRC tests. Based on the Geogauge measurements (Figure G.5.11b), the average modulus of the dry section is up to four times greater than the average modulus from the optimum section. As reflected in Table G.3.2, such a large variation in modulus is not supported by the lab MR results. The two devices that measure the responses of the pavement system (i.e. Zorn LWD and Dynatest LWD) yielded moduli that were greater for the optimum section relative to the wet and dry sections. The average modulus of the optimum section was up to 1.7 times greater than the average moduli of the wet or dry sections for the Dynatest LWD and about 1.5 times for the Zorn LWD.

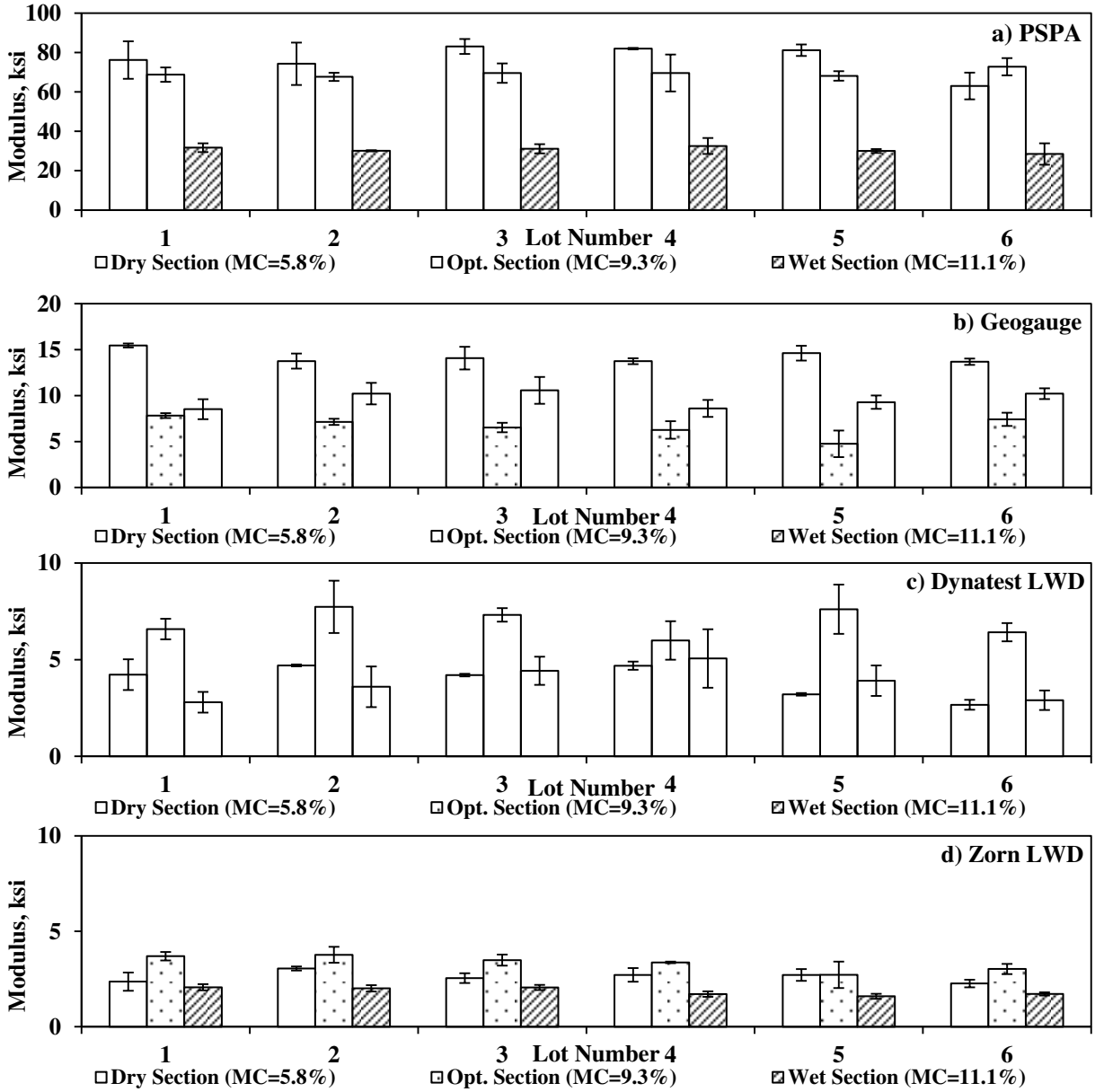

Figure G.5.11 – Spatial Variation of Modulus from Different Devices after Compaction of Base Layer

As reflected in Figure G.5.12, the pattern in estimated modulus with the DCP was similar to the ones observed with the LWDs. In this case, the average DCP modulus of the optimum section was up to 1.2 times the ones of the wet or dry sections.

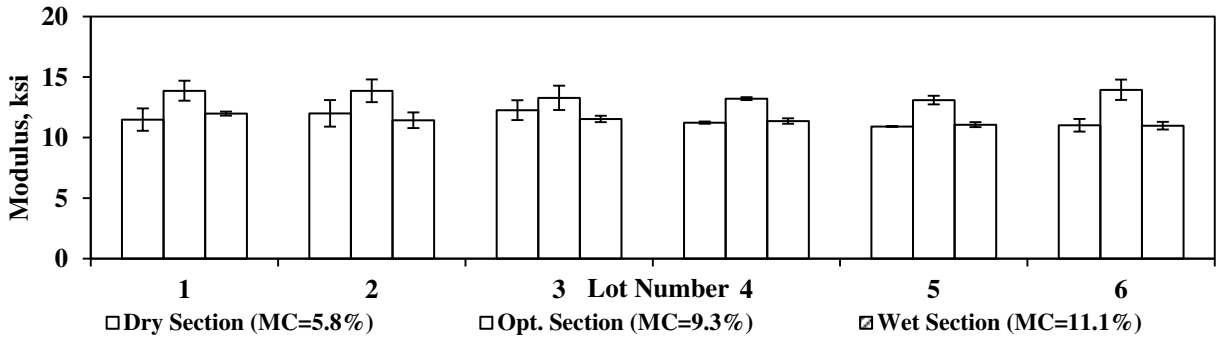

Figure G.5.12 – Spatial Variation of Modulus from DCP after Compaction of Base Layer

The variations in the field modulus with moisture content for different devices are shown in Figure G.5.13 and with degree of saturation in Figure G.5.14. A mild relationship between the modulus of the PSPA and moisture content is observed. This can be partially attributed to the uncertainties in measuring the moisture content and density with the NDG and partly to the performance of the devices.

Similar to the results from the subgrade layer, the normalized moduli from different devices were also compared with normalized degree of saturation. The moisture-modulus models proposed by the MEPDG and Cary and Zapata are also superimposed on the field results in Figure G.5.15. Except for the Dynatest LWD and the DCP, the field moduli from in-situ devices match closer with the Cary and Zapata model for non-plastic materials (*wPI=0*). Figure G.5.16 depicts the variation in normalized field modulus with normalized moisture content (as proposed in Section 3.3). The PSPA and Geogauge results marginally follow the trend developed based on the laboratory MR and FFRC values. Again, such discrepancy in the results could be associated to uncertainties with the NDG moisture and density estimations and the impact of the underlying layers.

Same as for the subgrade layer, the target moduli at OMC for different devices were calculated utilizing the algorithm discussed in Chapter 6. The target moduli for the Geogauge and the two LWDs were estimated from a composite pavement system of 12-in.-thick subgrade layer and 8-in.-thick base layer. The results of such analyses are summarized in Figure G.5.17 through G.5.20 for different devices.

As reflected in Figure G.5.17, all three sections, especially the dry and optimum sections, passed the modulus requirements with the PSPA. The Geogauge field moduli were also in the acceptable range for the dry and wet sections (Figure G.5.18). The Geogauge moduli from the optimum section were not in the acceptable range of defined target modulus which could be because of high variability in the results.

Based on the Zorn LWD field measurements, none of the test sections passed according to the proposed modulus-based specification (see Figure G.5.19). The contradictory patterns between the PSPA and Zorn LWD measurements may be explained in the following manner. According to the PSPA measurements the base layers were placed and compacted with a reasonable quality. However, the Zorn moduli indicate that the underlying layers were of low moduli because of repeated flooding.

The moduli measured with the Dynatest LWD indicate that the optimum section passed the modulus-based requirements, but the wet and dry sections were of marginal to low quality (see Figure G.5.20). The reasons for the differences in the moduli measured by the two LWD's require further study.

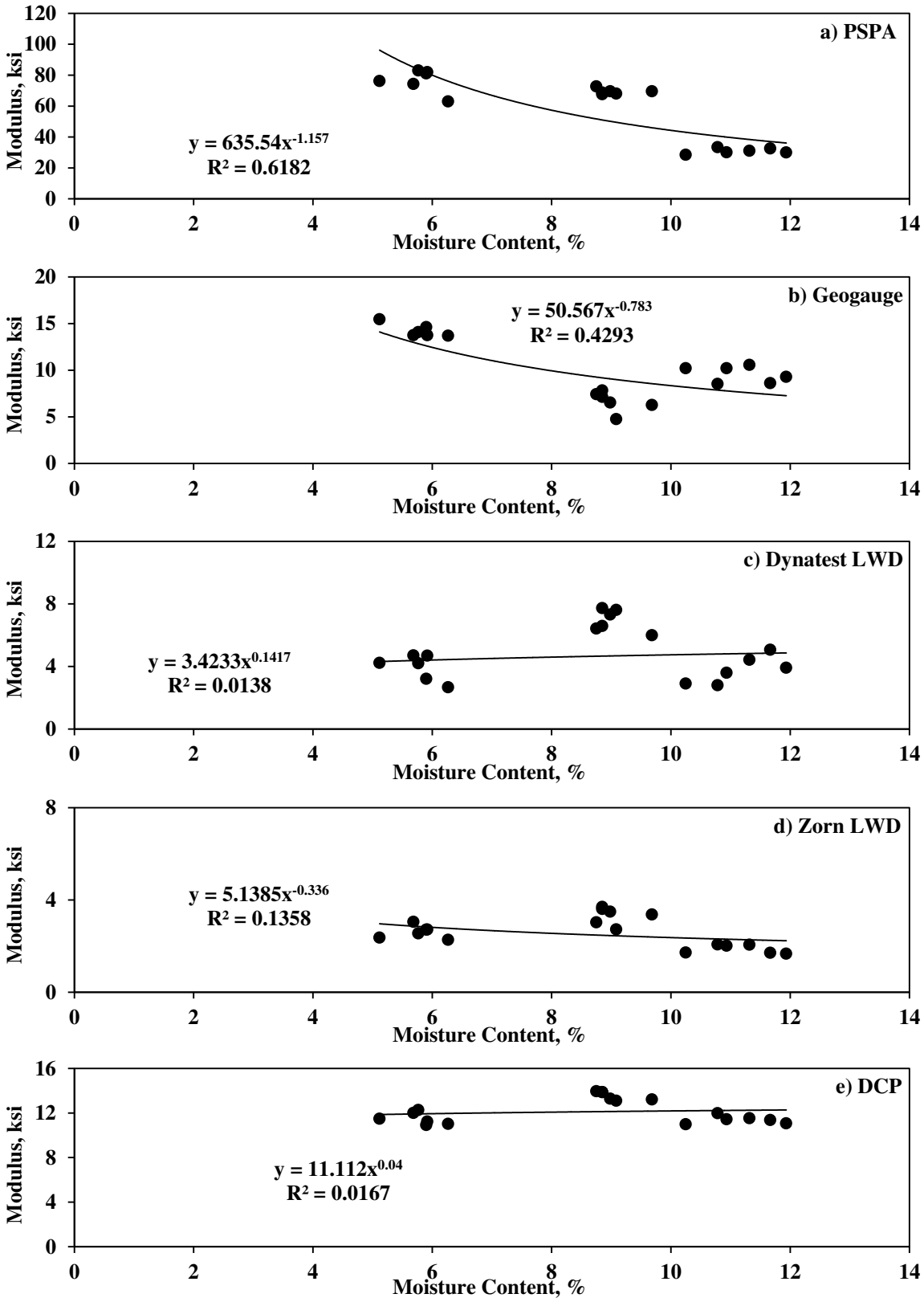

Figure G.5.13 – Variations of Field Modulus with Moisture Content (Base Layer)

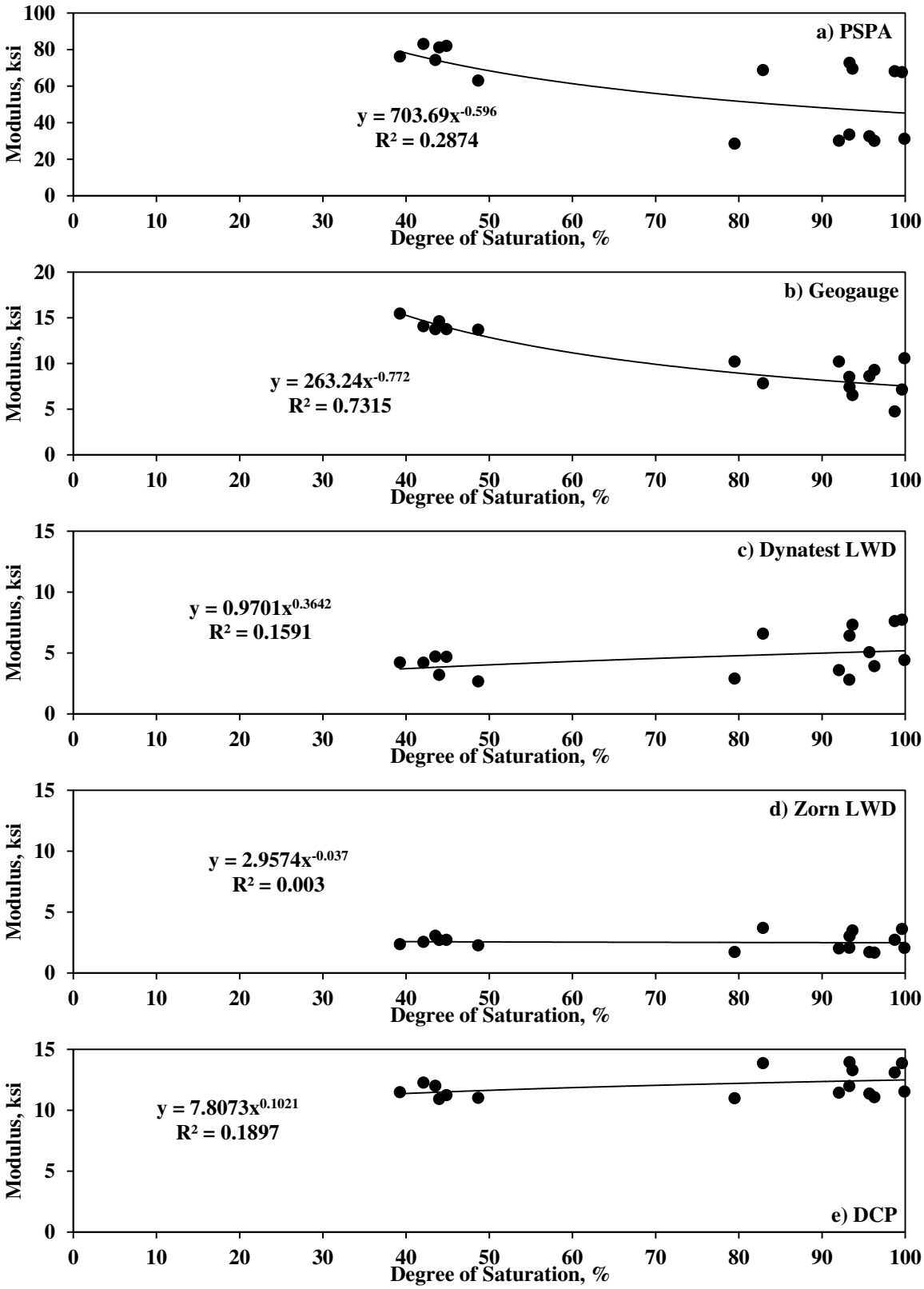

Figure G.5.14 – Variations of Field Modulus with Degree of Saturation (Base Layer)

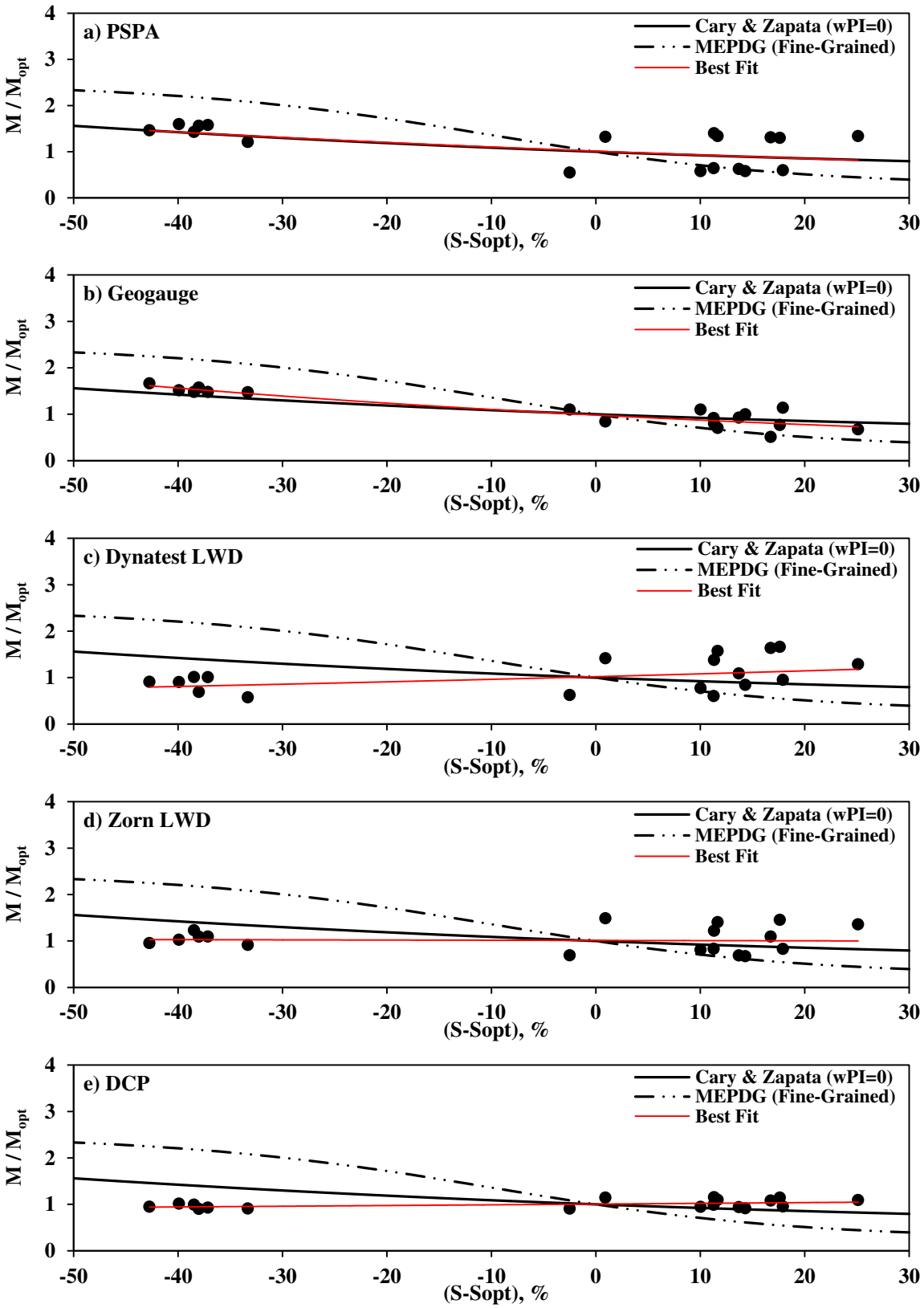

Figure G.5.15 – Variations of Normalized Field Modulus with Normalized Degree of Saturation (Base Layer)

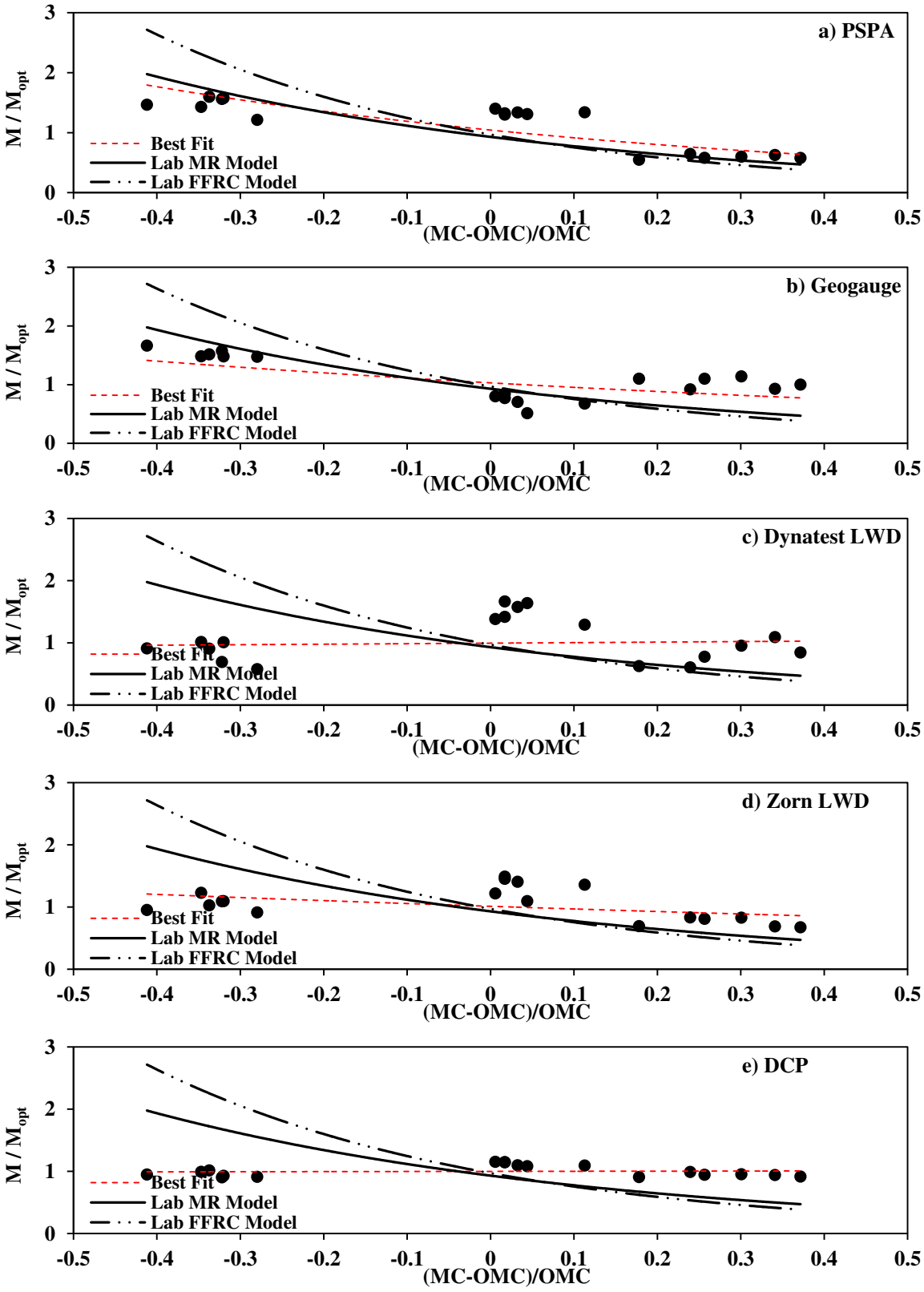

Figure G.5.16 – Variations of Normalized Field Modulus with Normalized Moisture Content (Base Layer)

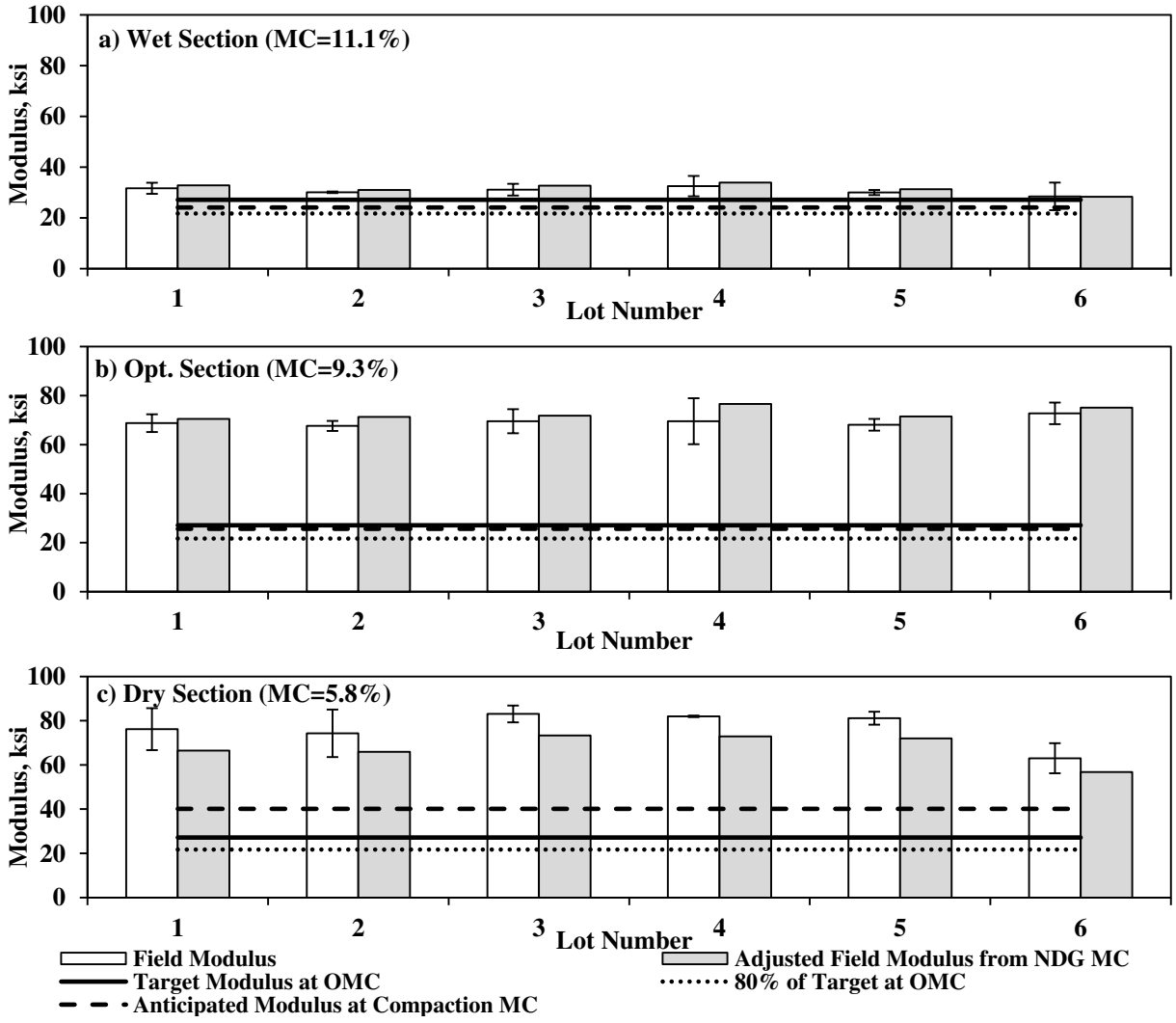

Figure G.5.17 – Field and Target Moduli from PSPA after Compaction of Base Layer

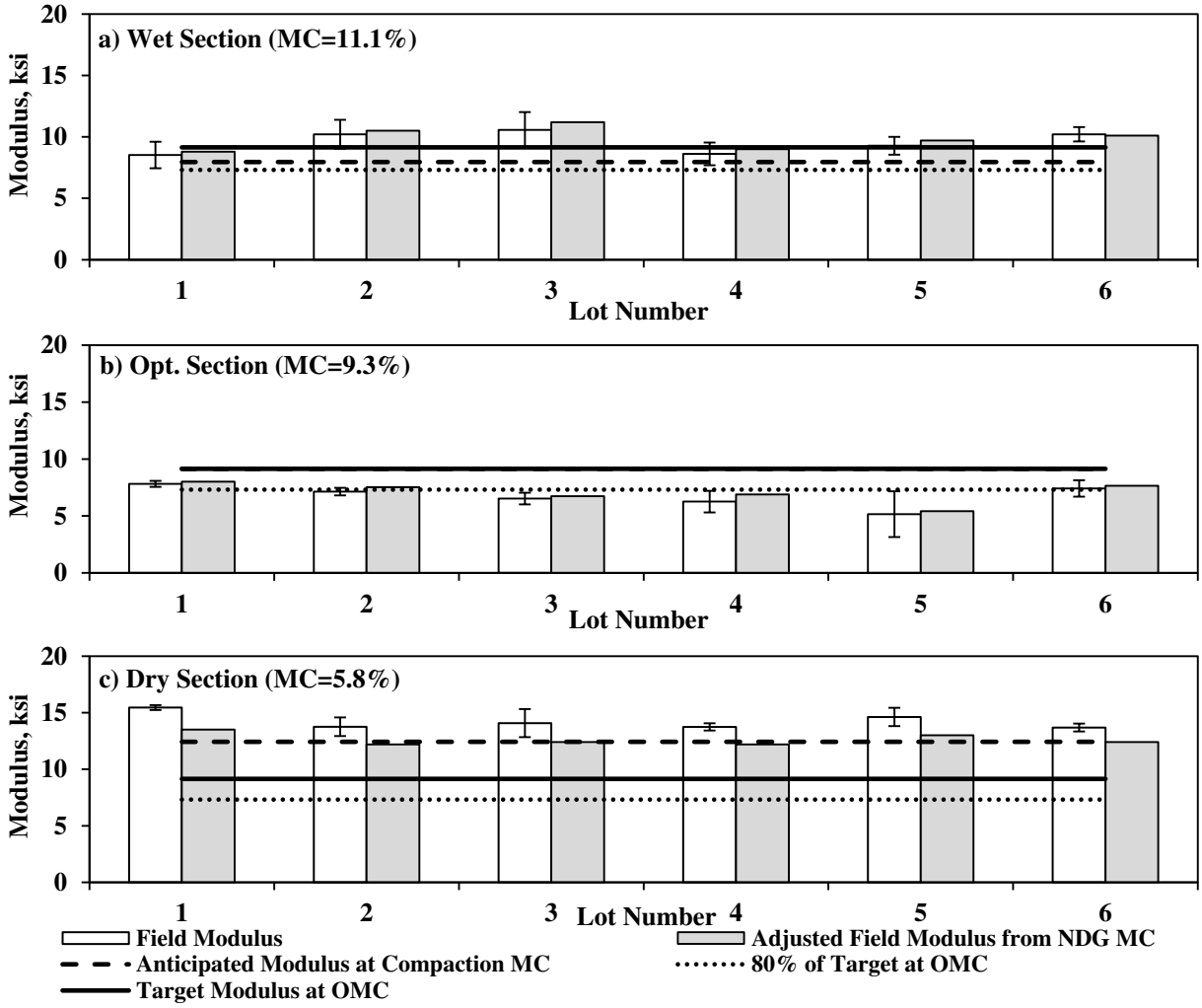

Figure G.5.18 – Field and Target Moduli from Geogauge after Compaction of Base Layer

The measured field moduli in Figures G.5.17 through G.5.20 were also adjusted to account for the difference between the laboratory and field moisture conditions. Since according to the laboratory tests, the base layer modulus was not very moisture dependent, the differences between the raw and adjusted moduli are rather small.

As a side case study, the Zorn LWD tests were repeated 24 hours after compaction on the optimum base section to estimate the effect of moisture variations on modulus of compacted layer due to differences between compaction and testing moisture contents. As shown in Figure G.5.21, the average moisture content decreased by about 1% after 24 hours. Such difference in moisture content should result in higher field moduli measured 24 hours after compaction relative to the values measured at compaction. The measured field moduli at compaction and 24 hours after compaction are shown in Figure G.5.22. Field moduli after 24 hrs increased by about 25% as compared to those at the time of compaction. The moisture adjustment algorithm included in the specification in Appendix A predicts an increase of about 35% in modulus.

As discussed in Appendix A, the target moduli can be calculated either from laboratory tests or can be estimated from index properties of the geomaterials. The estimated target moduli from the two approaches are compared in Table G.5.1. The method of estimating k' parameters impacts the target moduli.

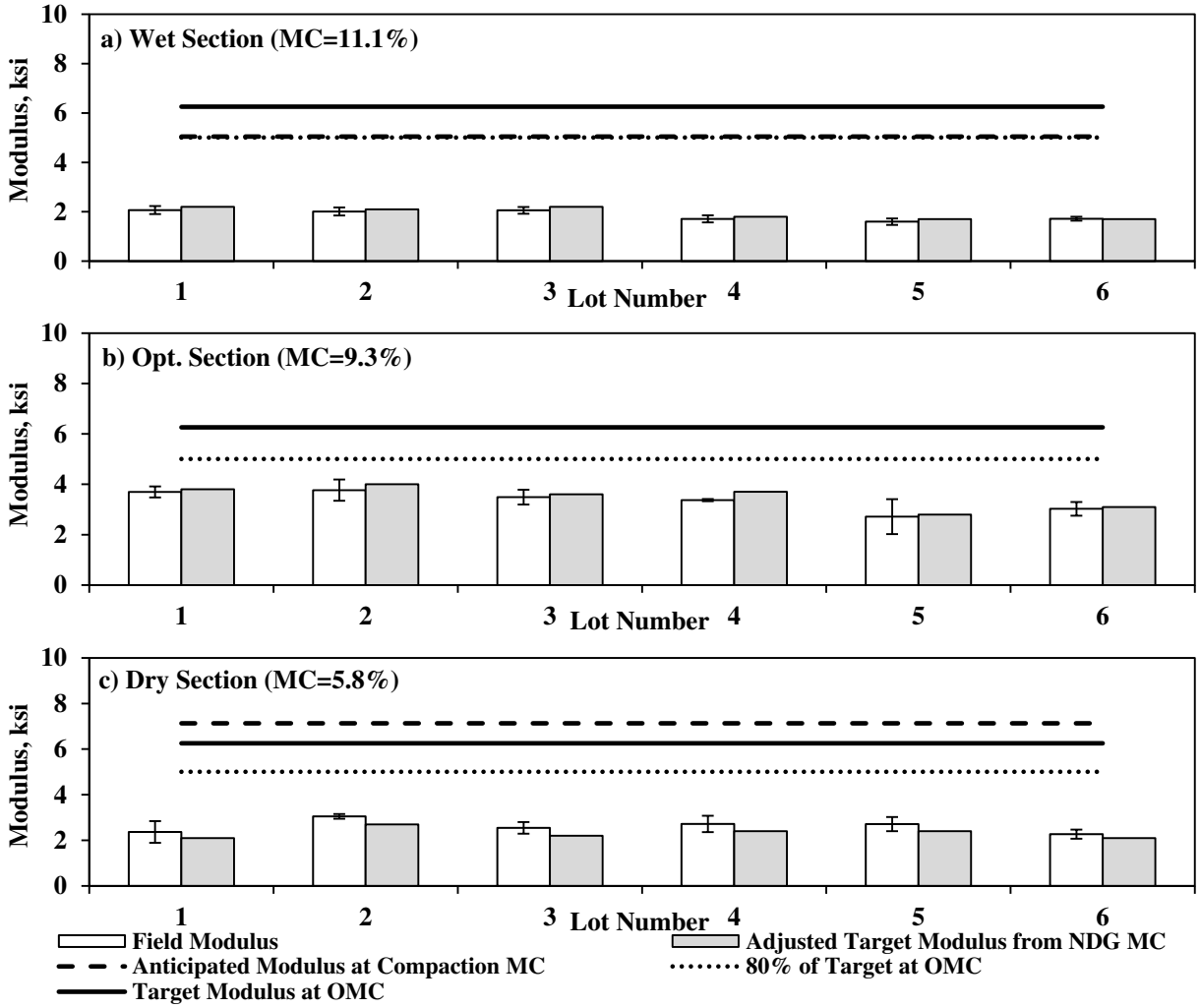

Figure G.5.19 – Field and Target Moduli from Zorn LWD after Compaction of Base Layer

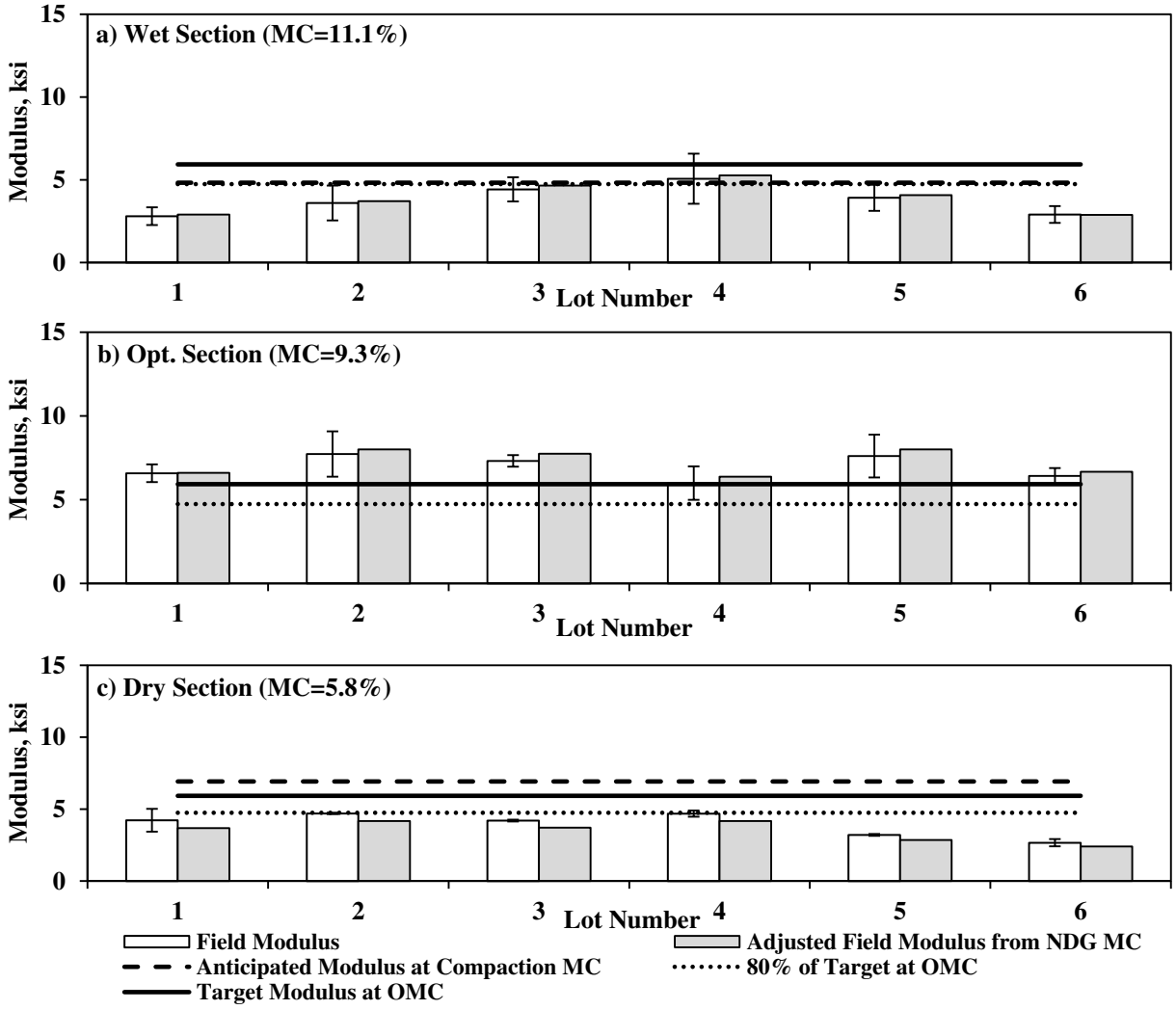

Figure G.5.20 – Field and Target Moduli from Dynatest LWD after Compaction of Base Layer

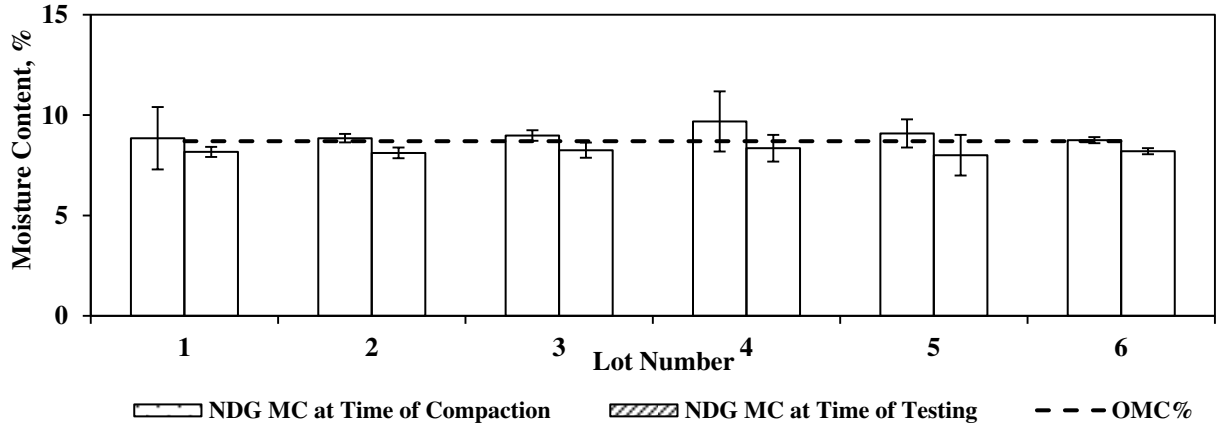

Figure G.5.21 – Comparison of NDG Moisture Content at the Time of Compaction and the Time of Testing (after 24 hrs.) on Optimum Section of Base Layer

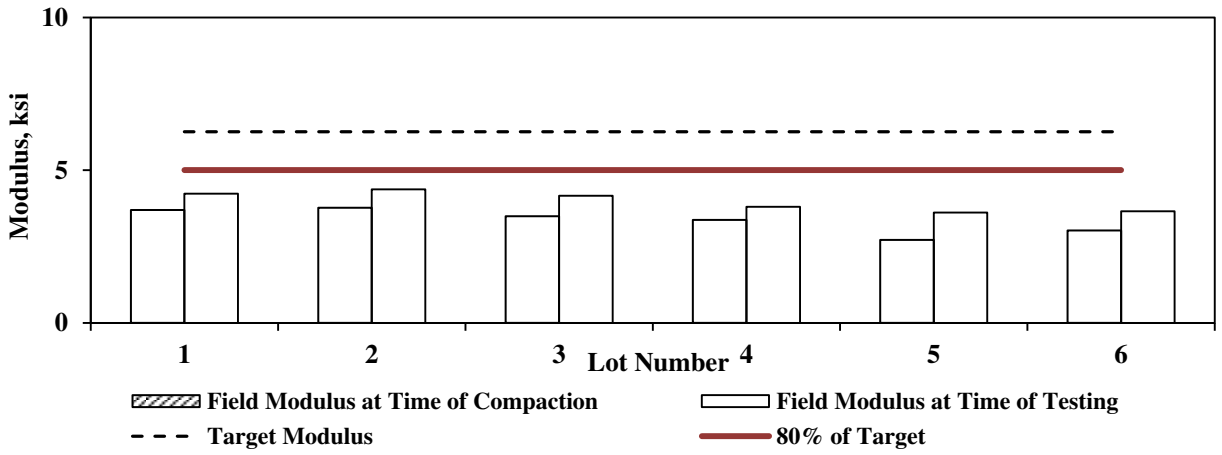

Figure G.5.22 – Comparison of Field Moduli Measured at the Time of Compaction and the Time of Testing with Zorn LWD on Optimum Section of Base Layer

Table G.5.1 – Estimated Target Modulus of Different Devices for Base and Subgrade Layer

Layer	Device	Target Modulus, ksi									
		Using Lab-Derived Parameters					Using Estimated[a] Parameters				
		at Lab Optimum Moisture Content	at Average Field Moisture Content				at Lab Optimum Moisture Content	at Average Field Moisture Content			
			Sat.	Wet	Opt.	Dry		Sat.	Wet	Opt.	Dry
Subgrade	PSPA	83.6	4.3	15.0	45.0	98.6	N/A				
	Geogauge	20.5	2.4	3.2	28.0	31.4	21.6	16.1	18.3	20.1	25.0
	Zorn LWD	12.3	1.0	2.0	12.0	19.7	7.6	5.2	6.1	6.9	9.2
	Dynatest LWD	11.8	1.0	1.9	12.6	18.6	8.4	5.8	6.8	7.6	10.1
Base	PSPA	27.1	N/A	24.1	25.7	40.1	N/A				
	Geogauge	9.1		7.9	9.1	12.4	6.9	N/A		6.9	
	Zorn LWD	6.3		5.0	6.3	7.1	5.9			5.9	
	Dynatest LWD	5.9		4.8	5.9	6.9	5.4			5.4	

[a] Estimated from index properties of materials as discussed in Appendix A
[b] Equations in Appendix A for base materials does not include the sample moisture or density as an independent variable

The small-scale moduli reported in Chapter 4 are compared with the field moduli for the base section placed at OMC in Figure G.5.23-a. The patterns from the Zorn LWD, PSPA and Geogauge are similar, with the small-scale moduli being 1.5 times greater than the field moduli. The differences can be attributed to the differences in the placement moisture contents as reported in the figure. The DCP results from the two tests vary by about 10%. The patterns for the dry sections (see Figure G.5.23-b) are reasonable as well given the uncertainties about condition of underlying layers and differences in the moisture contents. The results for the wet sections are not shown since the small-scale specimen was too soft to test.

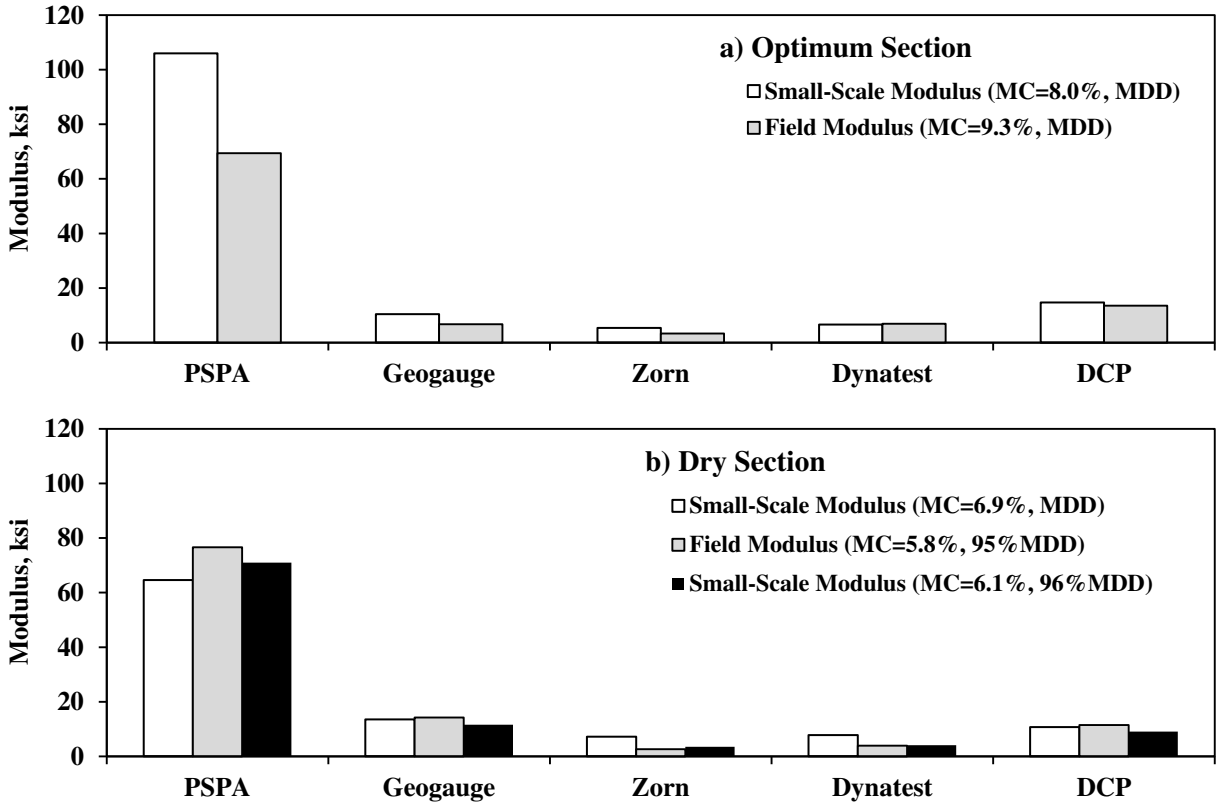

Figure G.5.23 – Comparing Field Modulus with the Modulus from Small-Scale Specimens at Optimum and Dry Conditions of Base Layer

G.6 Variability of In-Situ Modulus Devices

To study the variability of different modulus-based devices for in-situ tests, the coefficient of variation (COV) of triplicate measurements at each testing spot was calculated and compared with their corresponding modulus at various test sections. Figure G.6.1 illustrates the variation of COV of each device relative to the measured modulus for subgrade layer. The Geogauge exhibits the highest variability followed by the PSPA, Dynatest LWD, DCP and Zorn LWD. For the PSPA and DCP, the measured moduli at the optimum section exhibit relatively higher COVs than the other sections. For the Geogauge and Dynatest LWD, the wet and saturated sections had higher variability in measured moduli.

The same process was repeated for the results from the modulus devices on top of the base layer. Such results are summarized in Figure G.6.2. The PSPA exhibited higher variability on the wet section of the base layer while such pattern was not evident for other devices. The DCP, Geogauge followed by Zorn LWD illustrated less variation due to moisture changes in the compacted base layer. The Dynatest LWD exhibited relatively high variations in modulus estimation especially on wet and optimum sections.

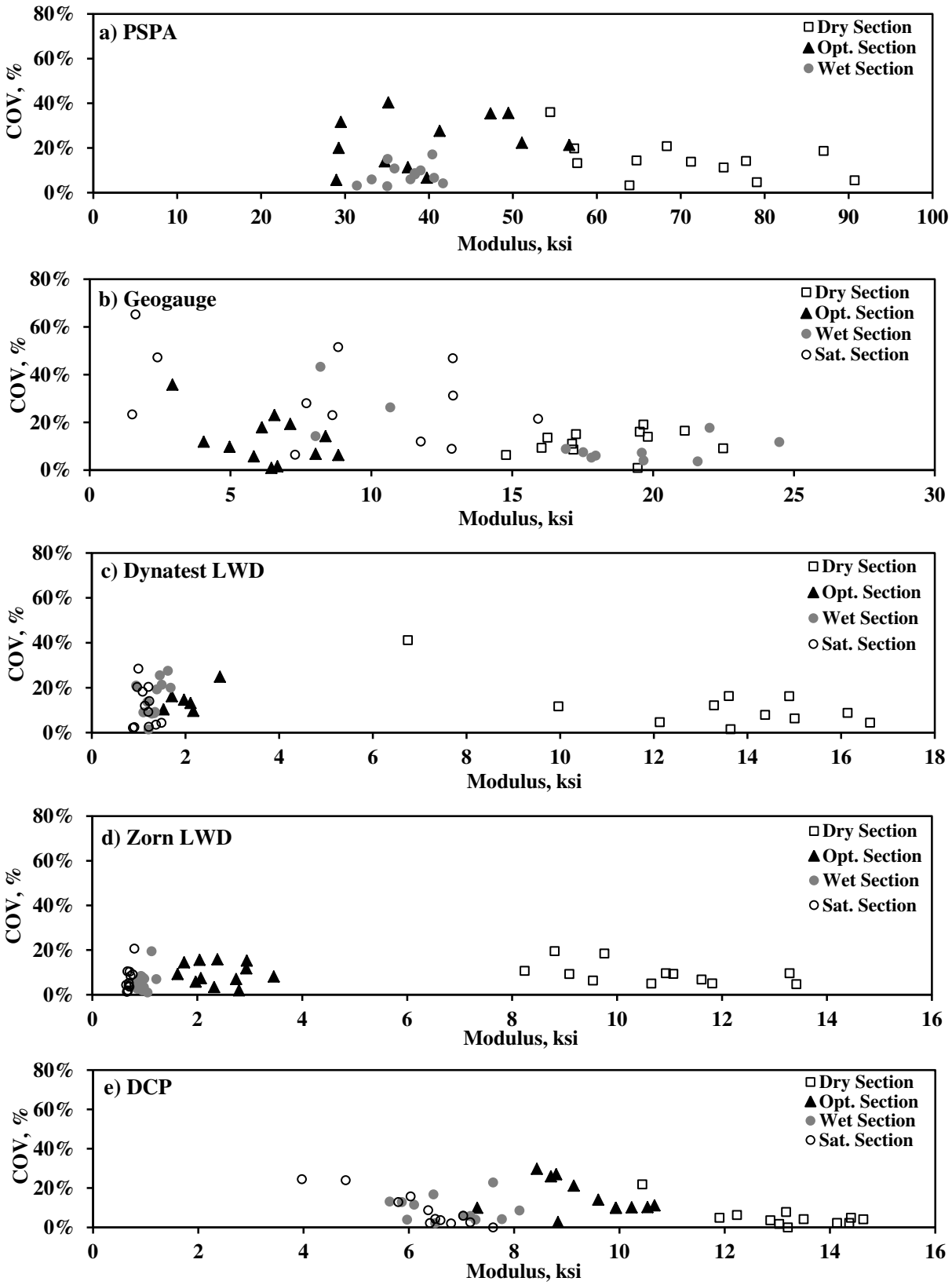

Figure G.6.1 – Variability of Modulus Measurements with Different Devices (Subgrade Layer)

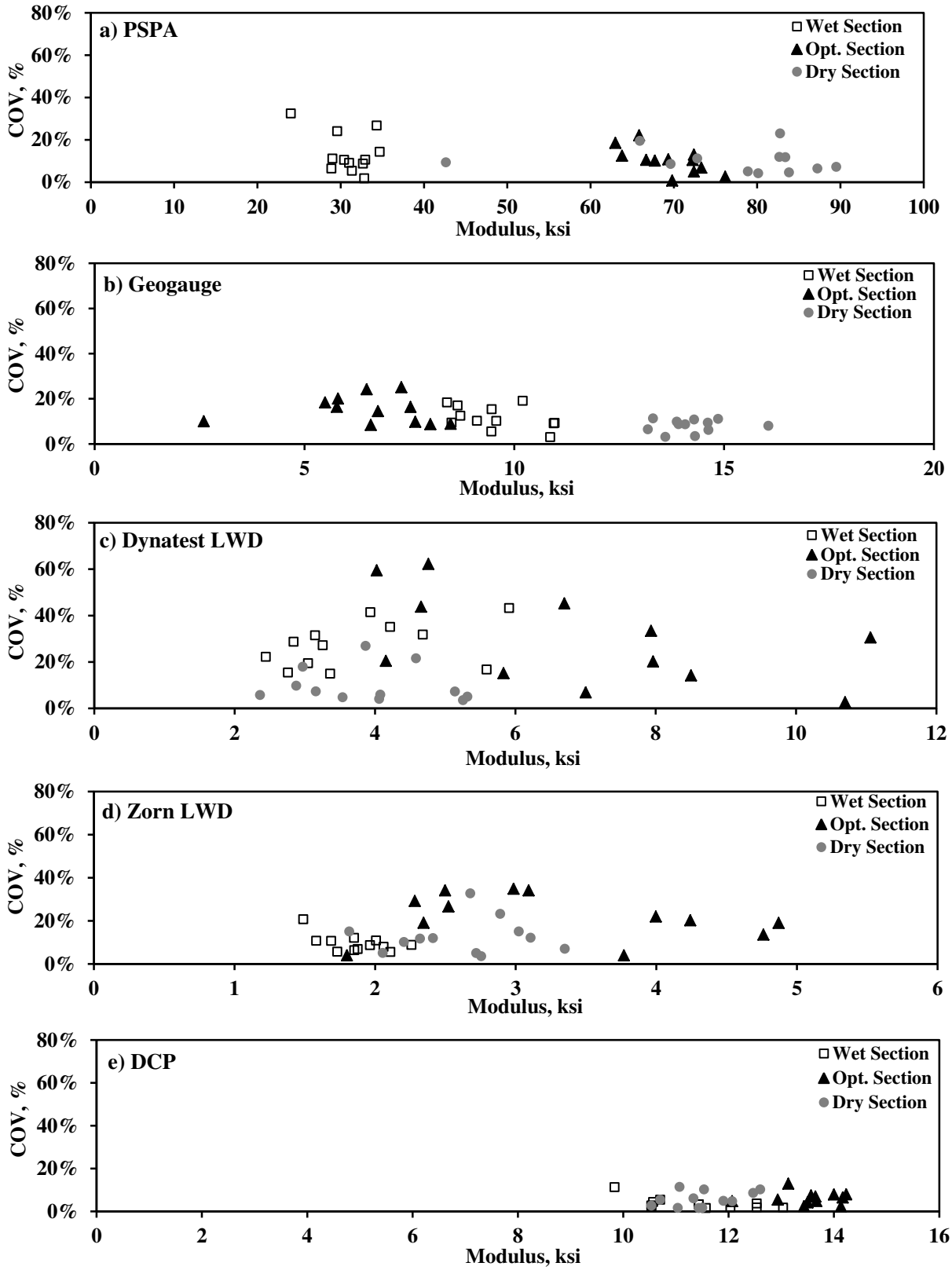

Figure G.6.2 – Variability of Modulus Measurements with Different Devices (Base Layer)

The moduli from different devices and their variations on subgrade and base layers are summarized in Table G.6.1. For compacted subgrade layer, the Geogauge has the highest variability followed by the PSPA, Dynatest LWD, DCP and Zorn LWD. The Dynatest LWD exhibited the highest COV (22%) on the base layer followed by the Zorn LWD (COV=15%), Geogauge (COV=12%), PSPA (COV=11%), and DCP (COV=5%). Considering the overall variability of the devices (on both subgrade and base layers for different moisture conditions), the Dynatest LWD showed higher COV as compared to the Geogauge, PSPA, and Zorn LWD, respectively. The DCP had the lowest variability (COV=8%) among all devices.

Table G.6.1 – Variation of Different Devices during In-Situ Modulus Estimations

Layer	Parameter	PSPA		Geogauge		Dynatest LWD		Zorn LWD		DCP	
		Modulus, ksi	COV, %	Modulus, ksi	COV, %	Modulus, ksi	COV, %	Modulus, ksi	COV, %	Modulus, ksi	COV, %
Subgrade	Min.	29.0	3%	1.5	1%	0.9	1%	0.6	1%	4.0	0%
	Max.	90.7	40%	24.5	65%	16.6	41%	13.4	21%	14.6	30%
	Avg.	52.9	13%	12.6	17%	4.6	13%	3.7	8%	8.9	10%
Base	Min.	24.0	1%	2.6	3%	2.4	3%	1.5	4%	9.8	2%
	Max.	89.5	32%	16.1	25%	11.1	62%	4.9	35%	14.2	13%
	Avg.	59.0	11%	10.1	12%	4.9	22%	2.6	15%	12.1	5%

Appendix H

OBSERVATIONS FROM IMPLEMENTATION OF SPECIFICATION

Site I.1

H.1 Introduction

The first field evaluation was carried out at a construction site near Dublin, Texas at three locations as reflected in Figure H.1.1. Figures H.1.2 depicts the test sections. The first location was dedicated to evaluating the placement of a subgrade layer. The focus of the second location was the placement of a base layer, while the third section consisted of the placement of a lime-treated layer (even though outside the scope of this project).

H.2 Laboratory Results

The index properties of the subgrades and base are summarized in Table H.2.1, and their gradation curves are presented in Figure H.2.1. Two slightly different geomaterials (namely Subgrade A and Subgrade B) were used in the first location. Both subgrades were classified as low-plasticity clay as per Unified Soil Classification System (USCS). The base was classified as well-graded gravel. The treated layer was primarily constructed with Subgrade A with nominally 5% lime. The optimum moisture contents and maximum dry unit weights obtained as per standard Proctor tests (AASHTO T99) for the subgrades and as per modified Proctor tests (AASHTO T180) for the base are also reported in Table H.2.1.

Table H.2.1 - Index Properties of Dublin Geomaterials

Soil Type	Gradation %				USCS Class.	Specific Gravity	Atterberg Limits			Moisture/Density	
	Gravel	Coarse Sand	Fine Sand	Fines			LL	PL	PI	OMC,* %	MDUW,** pcf
Subgrade A	0	4.0	10.0	86.0	CL	2.75	41	14	27	16.7	107
Subgrade B	0	5.0	11.8	83.2	CL	2.75	36	13	23	16.9	109
Lime-Treated Subgrade	0	4.0	10.0	86.0	CL	2.75	35	26	9	18.7	95
Base	51.8	29.0	15.0	5.0	GW	2.68	28	16	12	10.4	120

*OMC = Optimum Moisture Content, **MDUW = Maximum Dry Unit Weight

The resilient modulus (MR) and FFRC tests were performed on laboratory specimens prepared at the OMC, dry of OMC and wet of OMC as summarized in Table H.2.2. Figure H.2.2 illustrates the variations of the FFRC moduli and representative MR values with moisture content. Despite similar index properties, Subgrades A and B exhibit slightly different moduli.

H.3 Field Testing Program

Slightly different test programs were implemented at different locations as discussed below.

Subgrade Layer: As illustrated in Figure H.3.1, field testing was carried out along three side-by-side sections. The embankment at the site had been prepared before the research team arrived at the site. The first activity was to map the embankment before the subgrade layer was placed. The following tests were performed on the embankment layer of the three sections along Rows A and C:

- Soil Density Gauge (SDG)
- Zorn Light Weight Deflectometer (LWD) as per ASTM E2835
- Portable Seismic Property Analyzer (PSPA)
- Nuclear Density Gauge (NDG)

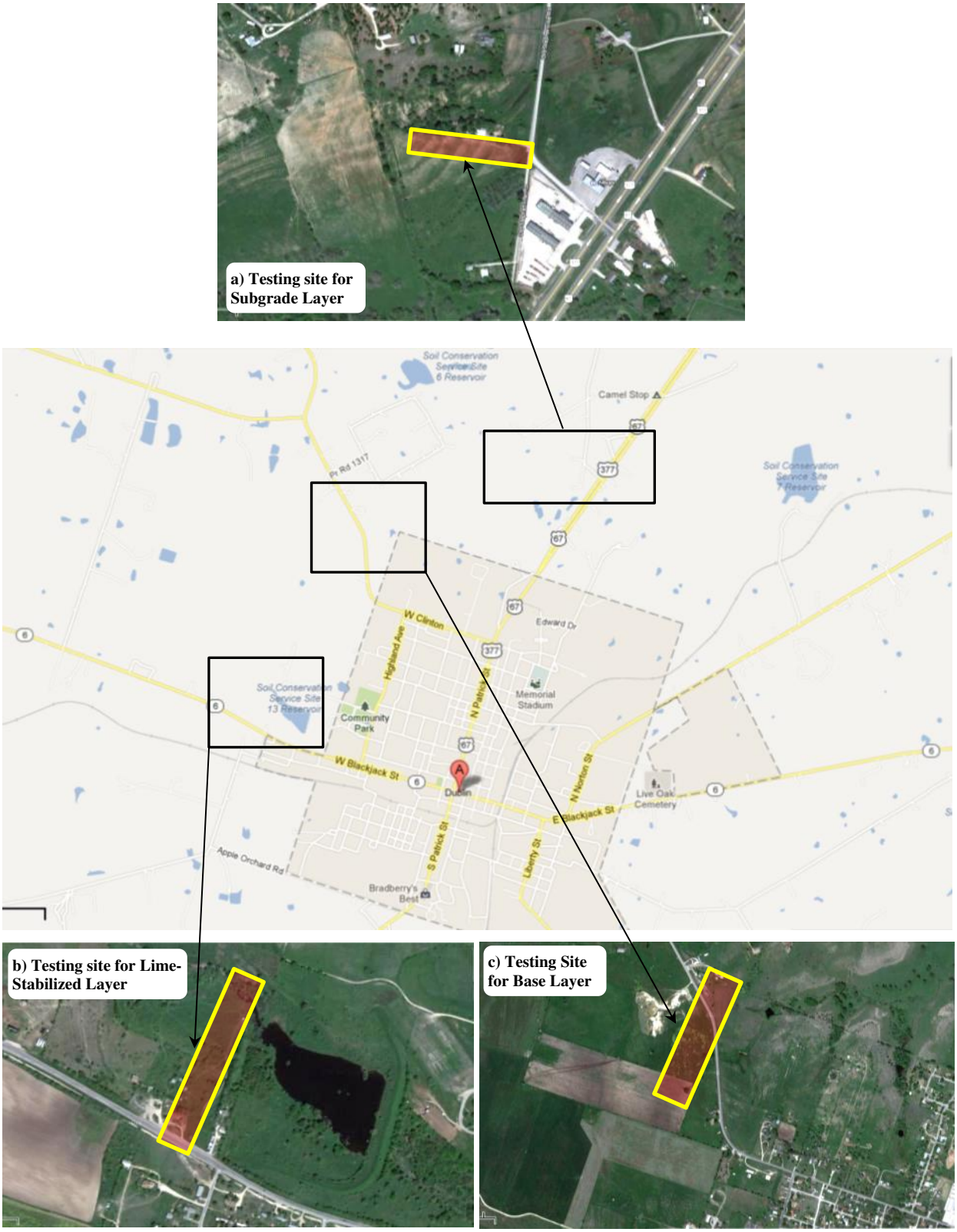

Figure H.1.1 – Location of Field Evaluation Sites in Dublin, TX (Subgrade Layer, Base Layer and Lime-Stabilized Layer)

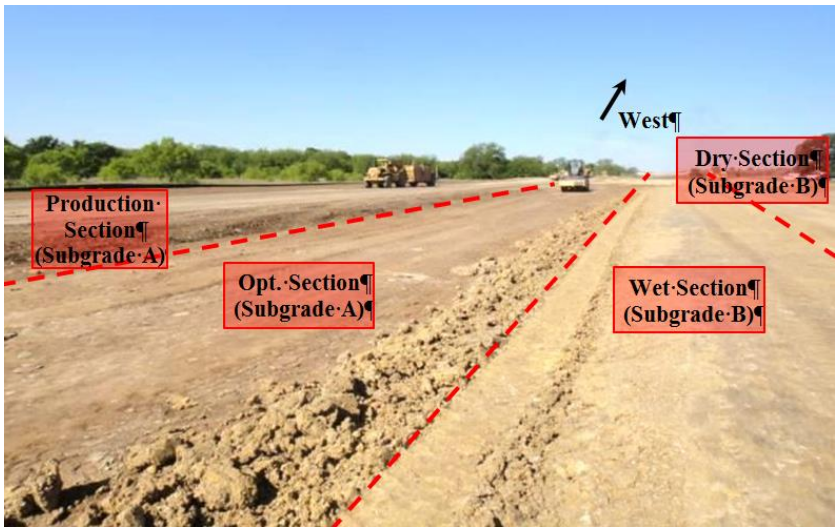

a) Subgrade

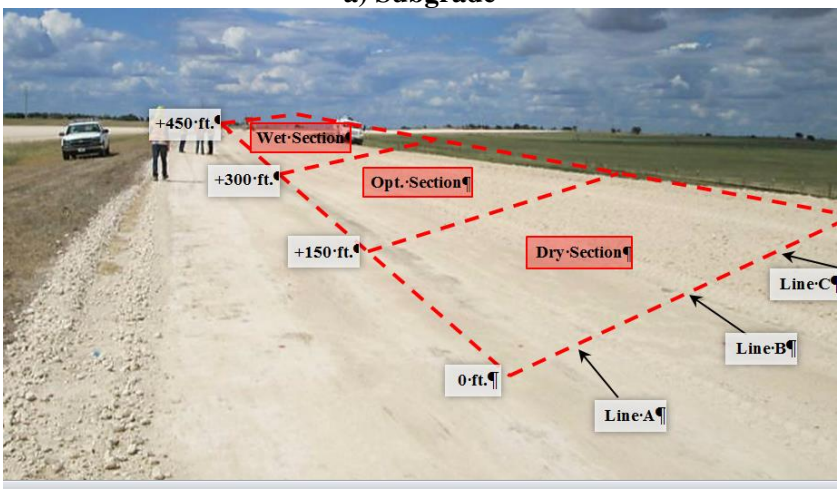

b) Base Layer

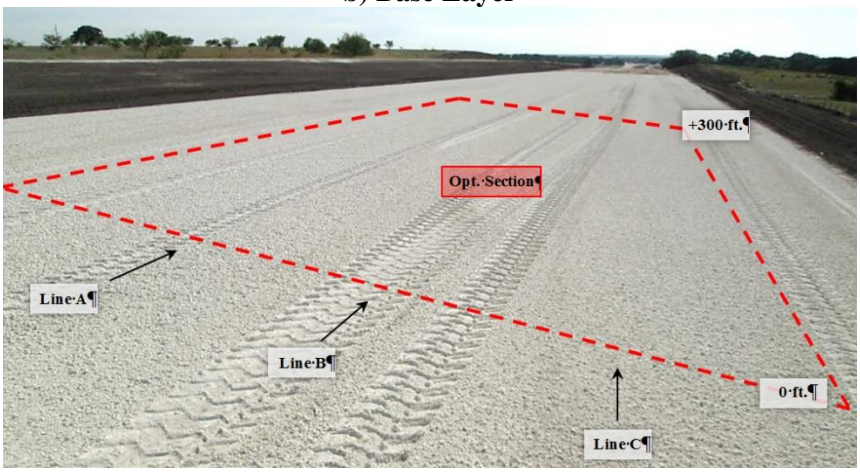

c) Lime-Treated Subgrade

Figure H.1.2 – Illustration of Test Section in Dublin, TX

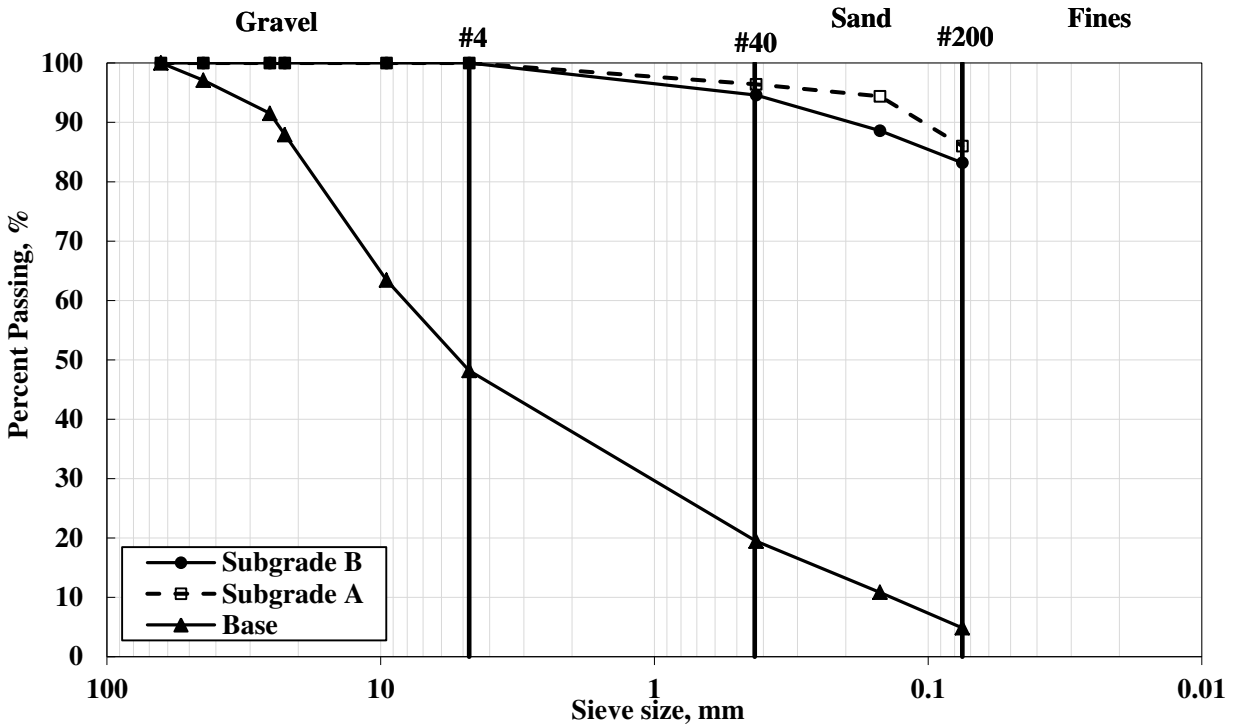

Figure H.2.1 – Gradation Curves of Dublin Geomaterials

Table H.2.2 – Laboratory Results of MR and FFRC Tests of Dublin Geomaterials (Subgrades, Base and Lime-Treated Subgrade)

Type	Target Moisture Content	Actual Moisture Content, %	Dry Density, pcf	FFRC Modulus, ksi	Nonlinear Parameters			Representative MR, ksi*
					k'_1	k'_2	k'_3	
Subgrade A	OMC-2	13.0	104.8	41.6	1304	0.14	-0.56	18.9
	OMC-1	14.6	106.3	38.4	1169	0.15	-0.37	17.6
	OMC	16.7	108.6	37.6	935	0.17	-0.35	14.2
	OMC+1	18.6	105.7	26.3	926	0.15	-0.96	12.5
	OMC+2	20.5	103.5	17.8	491	0.34	-1.47	6.8
Subgrade B	OMC-2	13.3	105.5	27.1	920	0.20	-0.92	12.9
	OMC-1	14.9	107.0	24.2	859	0.21	-0.72	12.5
	OMC	16.9	108.2	24.5	829	0.23	-0.71	12.3
	OMC+1	18.2	106.4	15.5	724	0.21	-0.87	10.2
	OMC+2	20.2	105.2	7.7	216	0.91	-3.00	3.2
Base	OMC-2	9.6	122.0	115.0	1117	0.67	-0.25	31.7
	OMC-1	10.8	123.4	72.0	1042	0.71	-0.22	31.2
	OMC	11.5	126.0	30.0	875	0.74	-0.23	27.1
	OMC+1	12.5	125.1	11.4	525	0.85	-0.05	19.7
	OMC+2	13.2	124.5	12.9	536	0.87	-0.08	20.5
Lime-Treated Subgrade	OMC	18.7	94.7	29.6	1554	0.34	-0.18	27.2

* from Eq. 3.2.1 based on τ_{oct} and θ values of 7.5 psi and 31 psi for base and 3 psi and 12.4 psi for subgrades as recommended by NCHRP Project 1-28A.

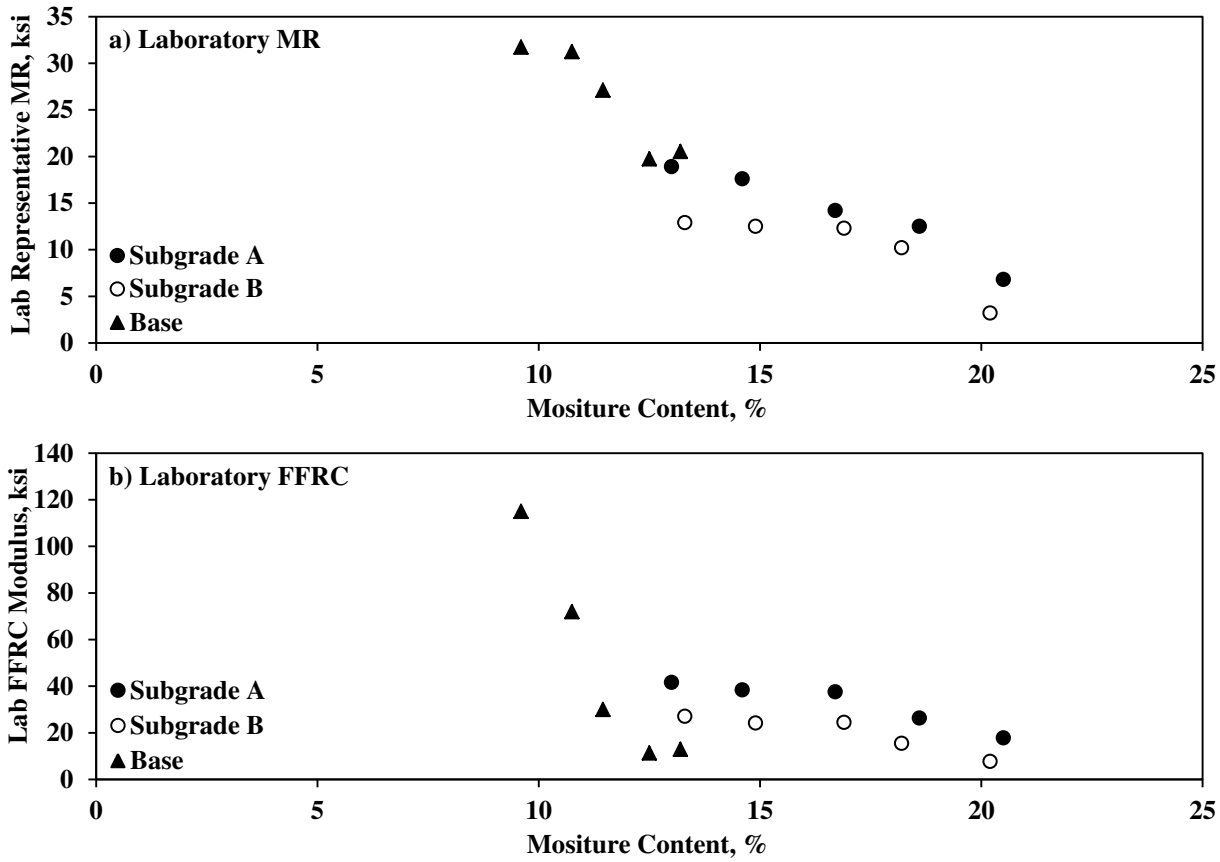

Figure H.2.2 – Variations of Laboratory MR and FFRC Moduli with Moisture Content

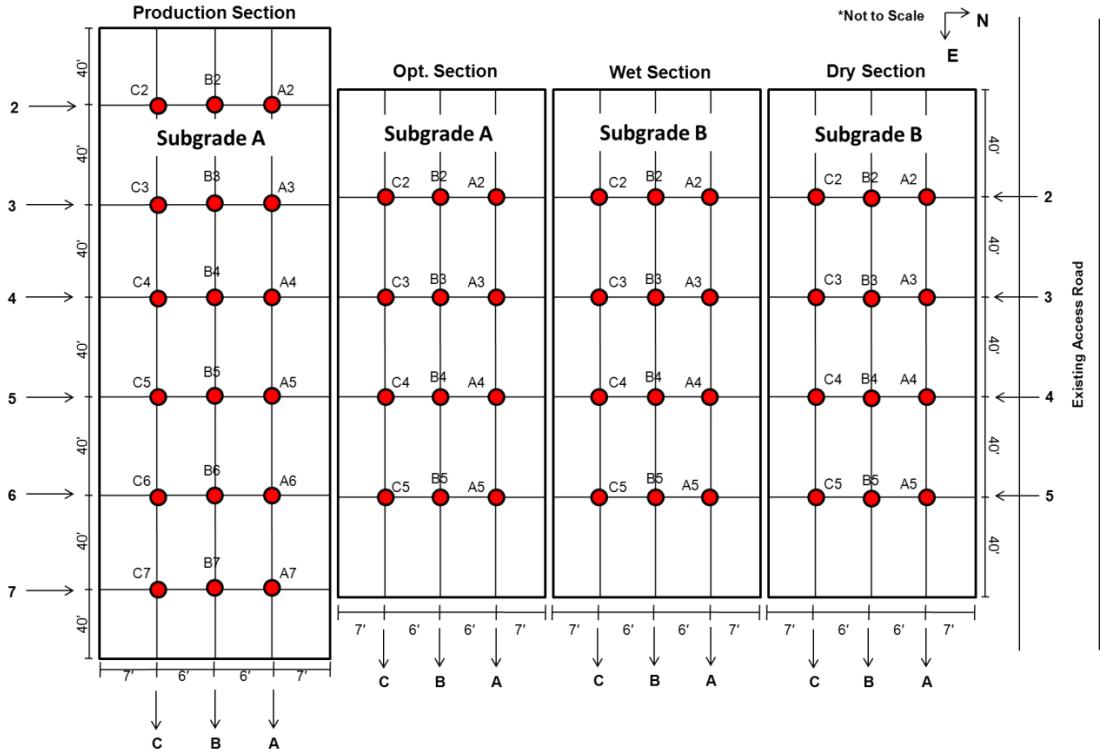

Figure H.3.1 – Test Locations on Subgrade Layer

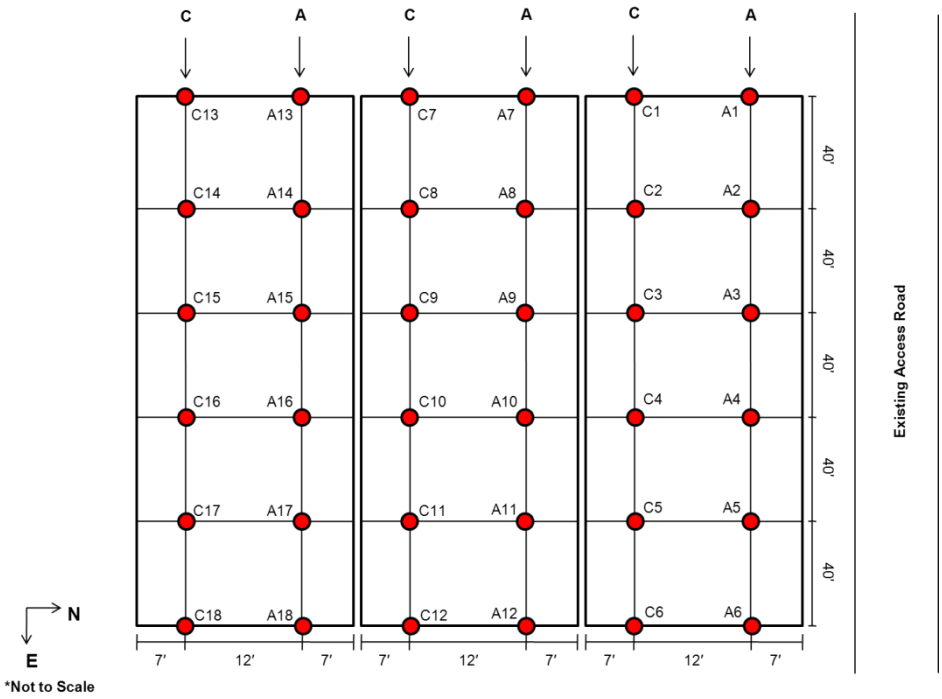

Figure H.3.1, cont. - Test Locations on Embankment Layer

A 12-in.-thick subgrade layer was then placed along each of the three sections. Both a sheep foot roller and a vibratory Intelligent Compaction (IC) roller were utilized in this project to compact the materials. One pass of single wheel smooth drum roller with the IC kit was used after every two passes of the sheep foot roller to measure the layer response. The first section with Subgrade B (which is adjacent to the existing access road) was placed dry of the OMC, the second section (with Subgrade B) was placed wet of OMC, and the third section (with Subgrade A) was placed close to OMC. The following tests were performed on the compacted subgrade layers along Rows A, B and C (see Figure H.3.1):

- Soil Density Gauge (SDG): one test per point
- Zorn Light Weight Deflectometer (LWD) in triplicate as per ASTM E2835
- Geogauge in duplicate as per ASTM D6758
- Portable Seismic Property Analyzer (PSPA) in triplicate
- Nuclear Density Gauge (NDG) one test per point
- Dynamic Cone Penetrometer (DCP) one test per point

In addition, soil samples were extracted from the compacted subgrade layer at most points to estimate their oven-dried moisture contents. A fourth section was selected as a "Production" section in order to evaluate the routine compaction process performed by the contractor. The spot tests were carried out after the completion of the compaction and mapping with intelligent compaction roller.

Base Layer: Prior to the placement of the base layer, the underlying support condition of the subgrade was mapped with the IC roller and modulus-based spot test devices. The 10-in.thick base layer was compacted using single wheel smooth drum roller with IC kit. The roller pattern was maintained the same as the subgrade. As illustrated in Figure H.3.2, the first section was placed at dry of OMC, the second section close to OMC, and the third section at wet of OMC. The following tests were performed on the subgrade before compaction and on compacted base layers:

- Soil Density Gauge (SDG): one test per point
- Zorn Light Weight Deflectometer (LWD) in triplicate as per ASTM E2835

- Geogauge: in duplicate as per ASTM D6758
- Portable Seismic Property Analyzer (PSPA) in triplicate
- Nuclear Density Gauge (NDG one test per point)
- Dynamic Cone Penetrometer (DCP) one test per point

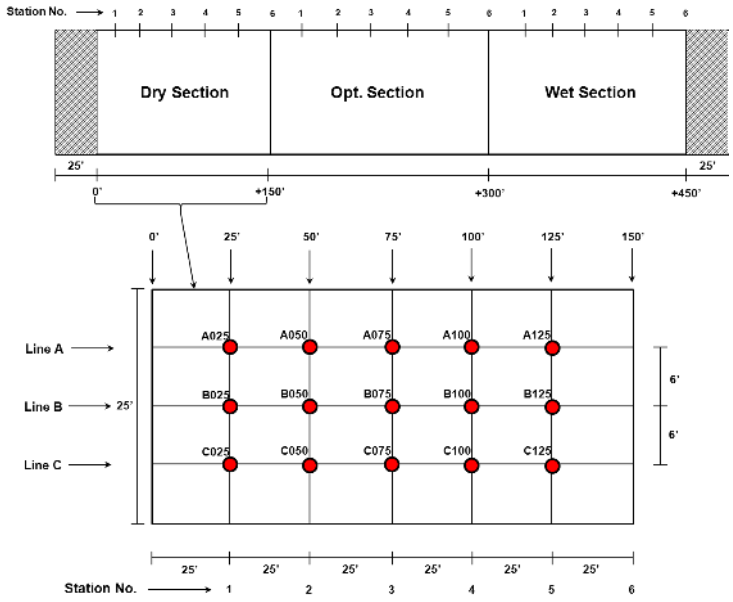

Figure H.3.2 – Test Locations on Base Layer

Lime-Treated Subgrade: A 300-ft-long and 50-ft-wide test section was selected to evaluate a 10-in.-thick lime-treated subgrade soil (see Figure H.1.2). Five percent (by weight) of quick lime was mixed with the compacted subgrade layer, and sealed with a pass of a pneumatic roller. The sealed layer was milled after 48 hrs, mixed with water, and compacted with the combination of a pneumatic and a single wheel smooth drum IC roller. The same testing devices and testing routines adopted for the base layer (see Figure H.3.3) were repeated for the compacted lime-treated subgrade layer.

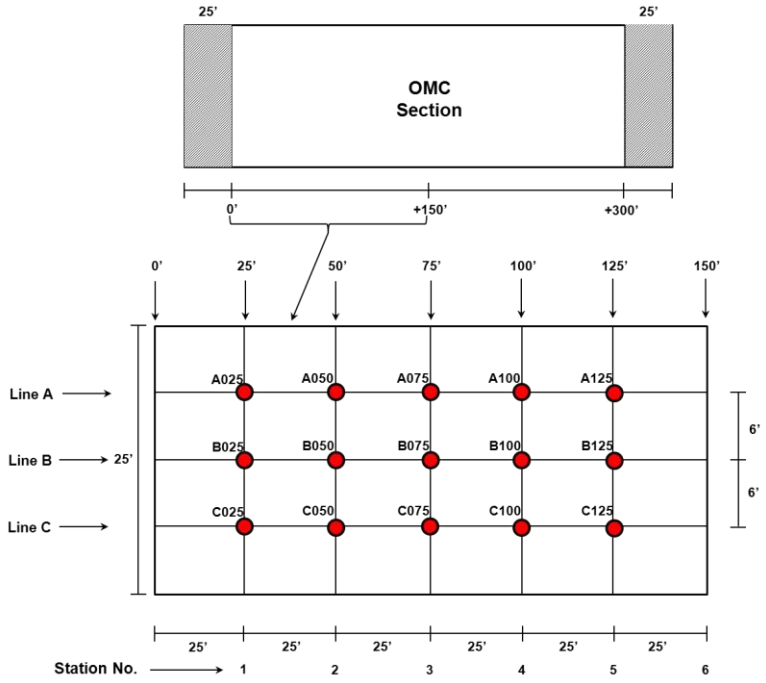

Figure H.3.3 – Test Locations on Lime-Treated Subgrade

H.4 Evaluation of Moisture-Density Devices

Embankment: The variations of the average moisture contents of the embankment measured with the SDG and NDG before the placement of subgrade are depicted in Figure H.4.1. The averages of the device readings from Lines A and C are shown for all three sections. The NDG data were not collected along the third section because of time constraints between construction phases. The overall average moisture content of the embankment from the NDG was 9.4% and from the SDG was 9.3%, which was about 7% less than the OMC from the standard Proctor tests.

Figure H.4.2 summarizes the dry densities measured with the SDG and NDG. The average dry density from the SDG was 88.7 pcf, while the average dry density estimated with the NDG was 115.8 pcf. The SDG results seem low based on the condition of the site. The embankment passed the density specification limit of 95% of MDD based on the NDG results.

Subgrade Layer: The average SDG and NDG moisture contents (average of the three readings from lines A, B and C) measured on top of the subgrade are summarized in Figure H.4.3 for all sections. The first and last rows of the compacted subgrade sections were not considered in the analysis to eliminate the effects of the construction boundaries. The SDG results do not reflect the changes in the moisture contents among the three sections (see Figure H.4.3a). As illustrated in Figure H.4.3b, the NDG results reflect the variations in moisture contents among different sections. The average NDG moisture content of the dry section was 12.8% (3.9% dry of OMC), the wet section was 18.3% (1.6% wet of OMC) and the optimum section was 17.6% (0.7% wet of OMC). Based on the NDG results, moisture contents of the test sections are close to their nominal values (dry of OMC, wet of OMC and close to OMC).

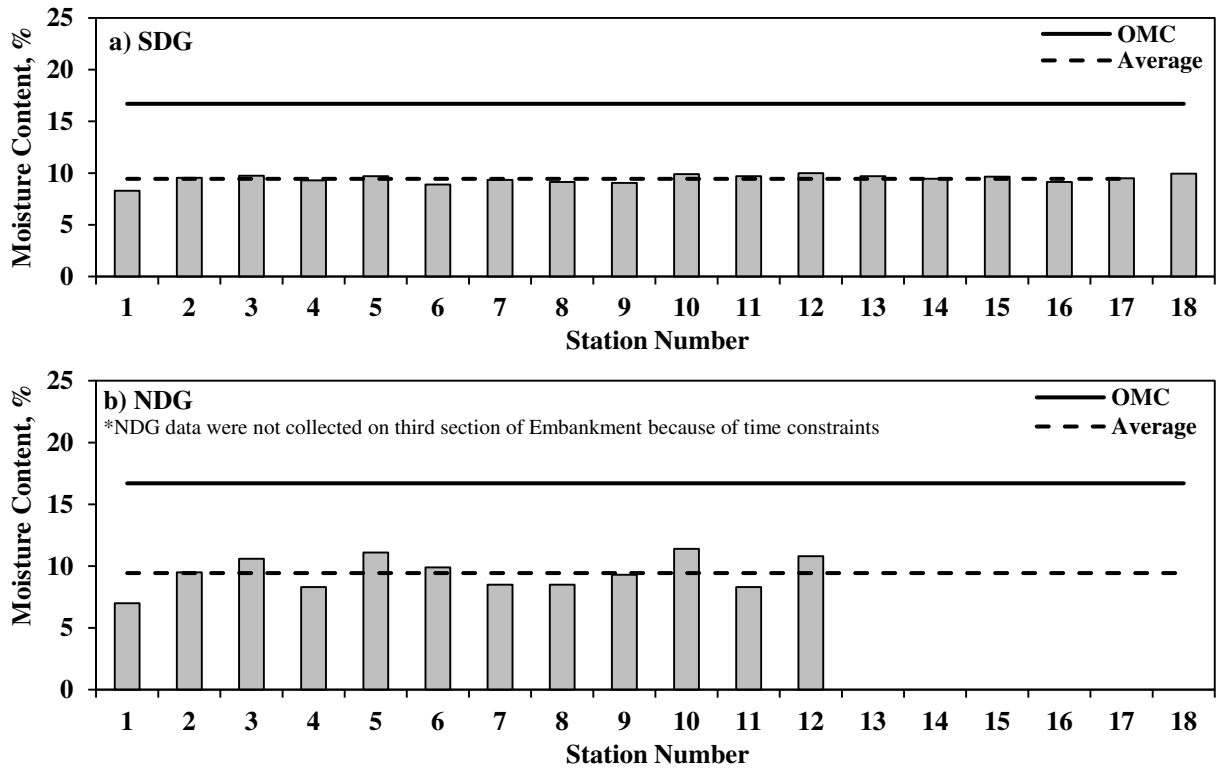

Figure H.4.1 – Spatial Variations of SDG and NDG Moisture Contents of Embankment

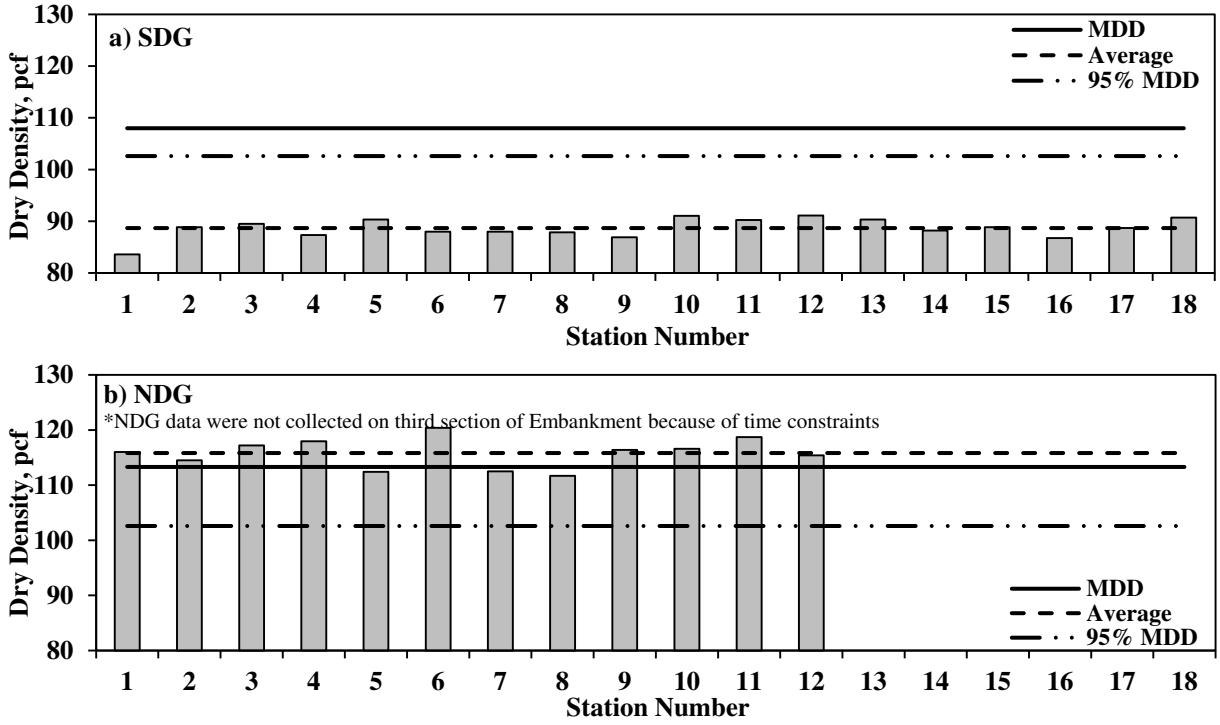

Figure H.4.2 – Spatial Variations of NDG and SDG Dry Densities of Embankment Layer

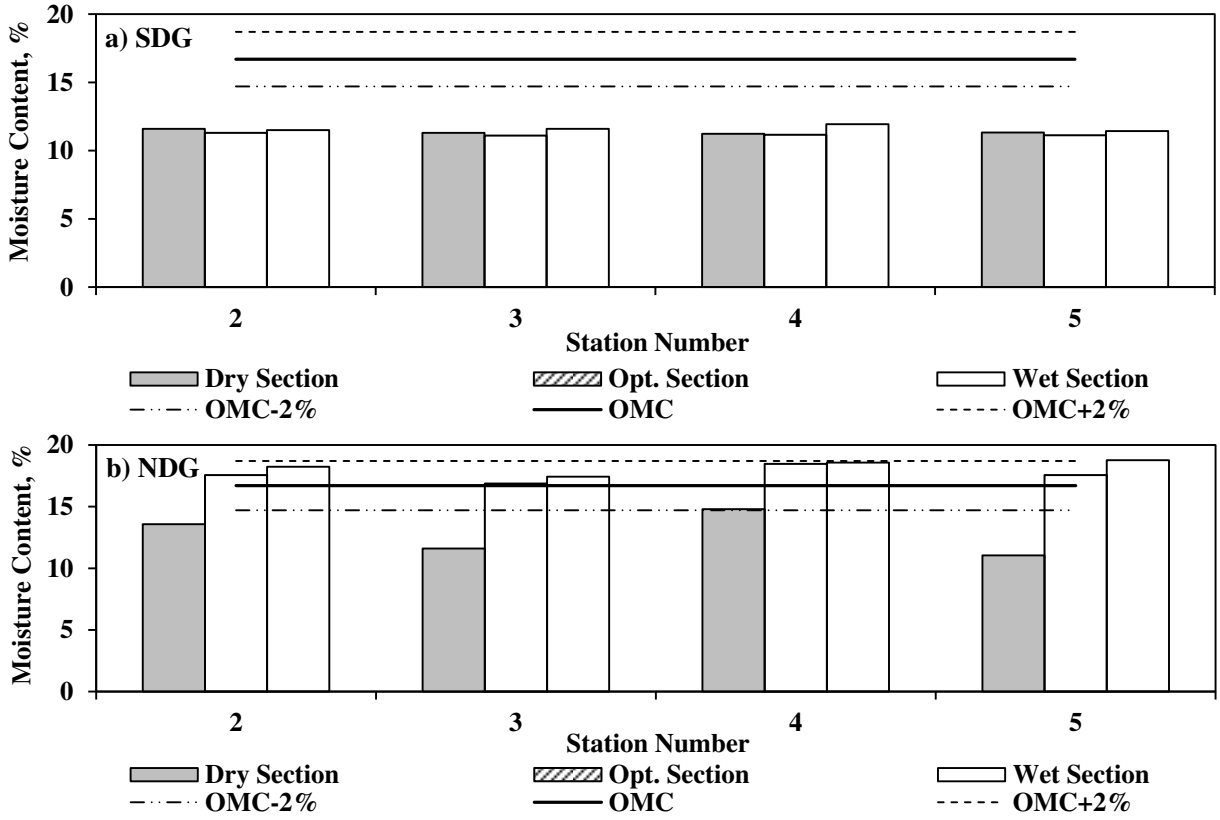

Figure H.4.3 – Spatial Variations of SDG and NDG Moisture Contents Immediately after Compaction of Subgrade

Soil samples were extracted to determine the oven moisture contents at most of the NDG and SDG test spots. Table H.4.1 summarizes the average SDG, NDG and oven-dry moisture contents for all sections. The oven-dry moisture contents were about 2% less than those measured with the NDG. Again, the SDG moisture readings do not reflect the variation in actual field conditions.

Figure H.4.4 summarizes the density estimations by the SDG and NDG immediately after compaction of the subgrade layer. The SDG results do not show the variation in dry density for different sections. According to the NDG results, almost all stations from the three sections passed the specification limit of 95% of MDD.

Table H.4.1 – Comparisons of Average Moisture Contents of Subgrade with Different Devices

Section (Nominal MC, %)	**Average Measured Moisture Content, %**			**Target Moisture Content, %**
	SDG	**NDG**	**Oven**	
Dry Section (OMC-2%)	11.4	12.8	11.4	14.7
Opt. Section (OMC)	11.2	17.6	15.3	16.7
Wet Section (OMC+2%)	11.6	18.3	16.2	18.7

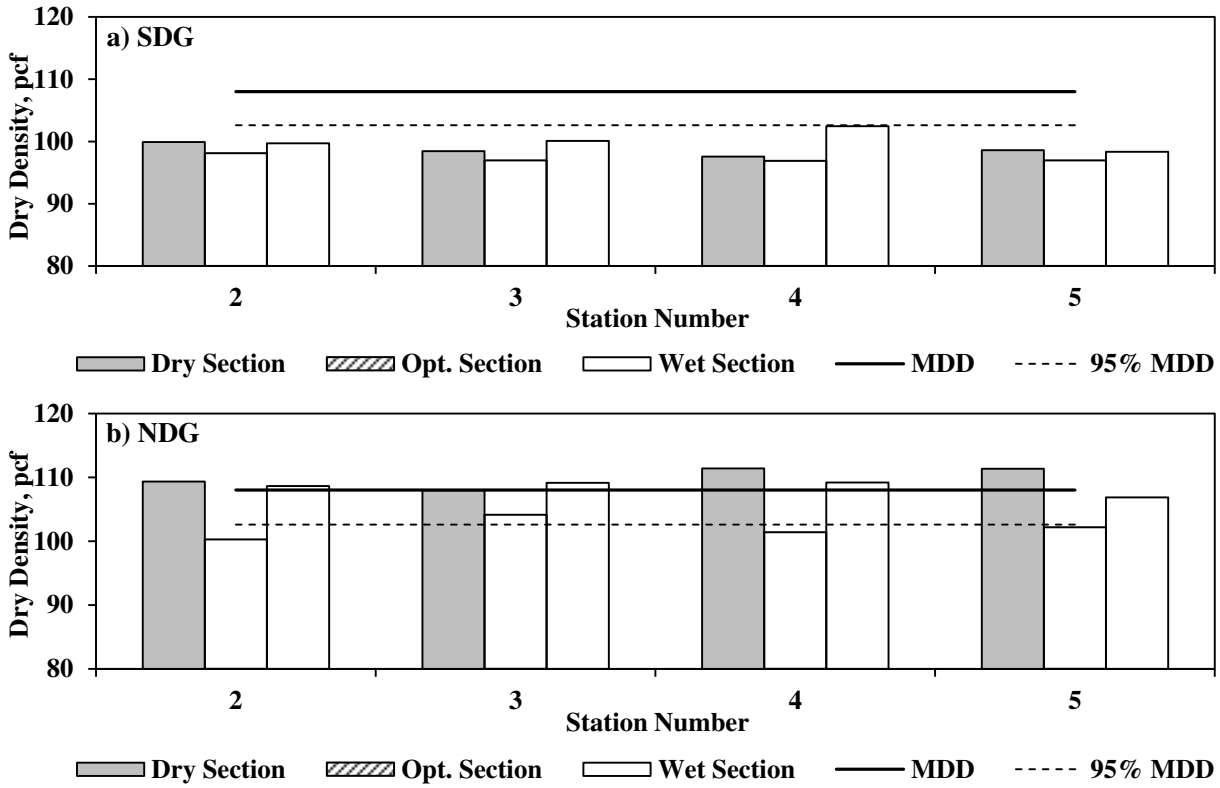

Figure H.4.4 – Spatial Variations of NDG and SDG Dry Densities Immediately after Compaction of Subgrade Layer

Figure H.4.5 illustrates the variations in the NDG dry density and moisture content of the subgrade layer for different passes of the IC roller. With a few exceptions, the dry densities increase with the increase in the number of roller passes. Considering the uncertainties in the NDG readings, the changes in the moisture contents between the passes are for the most part small.

The average NDG moisture contents and dry densities after different passes of the IC roller are summarized in Figure H.4.6. Except for the wet section, the dry densities of the sections increased with

more passes of the roller. On the other hand, the moisture contents of the compacted layers decreased slightly between successive passes of the roller. The rates of changes in dry density and moisture content are minimal for the wet section and more evident for the dry section. The gradient of density and moisture changes for the optimum section is intermediate.

Figure H.4.7 summarizes the same results from the SDG device. As discussed earlier, the SDG results do not reflect the changes in neither moisture content nor dry density of the compacted layer between the passes of the IC roller. The average SDG readings on the three sections (dry, wet and optimum) are depicted in Figure H.4.8. Even the average of dry densities and moisture contents do not reflect any changes between passes of roller and even between three sections.

Production Section: A 280-ft-long production section was also tested. Figure H.4.9 summarizes the NDG and SDG moisture contents from the production section. The average NDG moisture content is 18.1% (as compared to the OMC of 16.9%) while the average SDG moisture content is 9.8% (about 7% less than OMC). Figure H.4.10 depicts the dry densities measured on the production section with the SDG and NDG. Based on the NDG results, all test stations are in the range of acceptance limit for density of 95% of MDD. The SDG dry densities are high (with the average of 143 pcf) which is not reasonable when compared to the maximum dry density of 108 pcf from the laboratory Proctor tests.

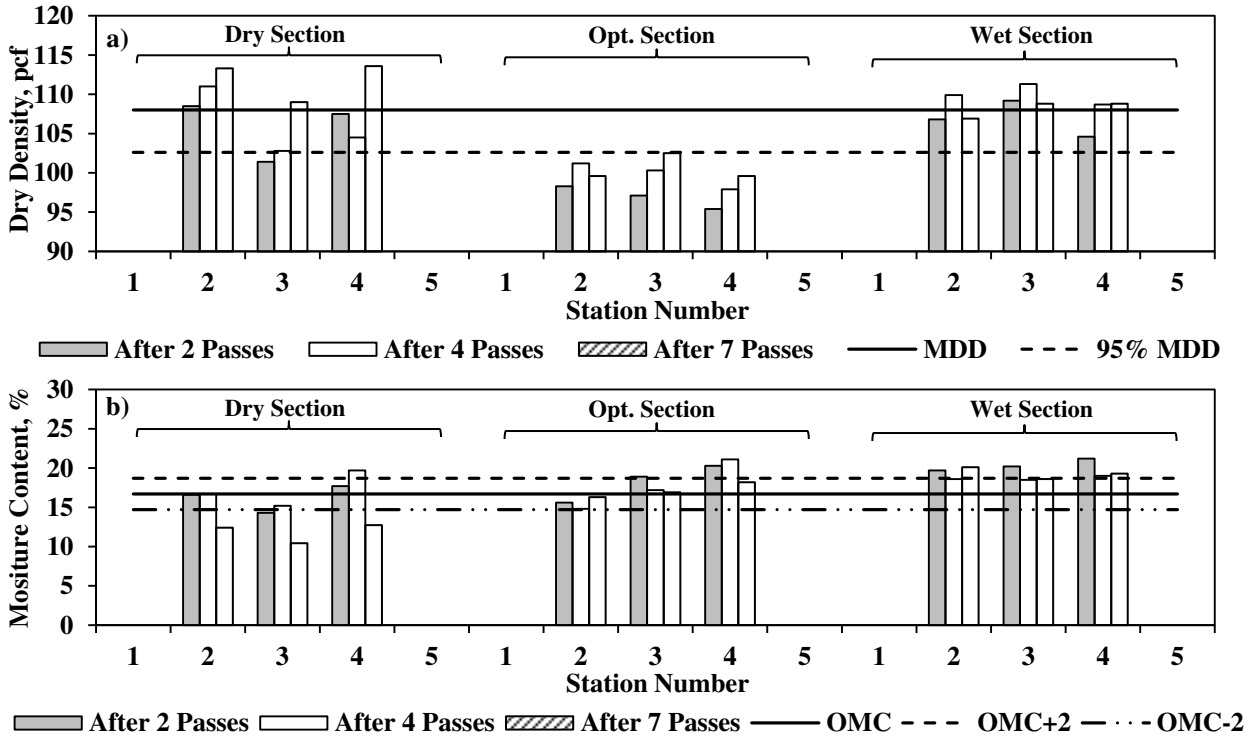

Figure H.4.5 –Variations of NDG Readings with Number of Passes of Roller during Compaction of Subgrade Layer

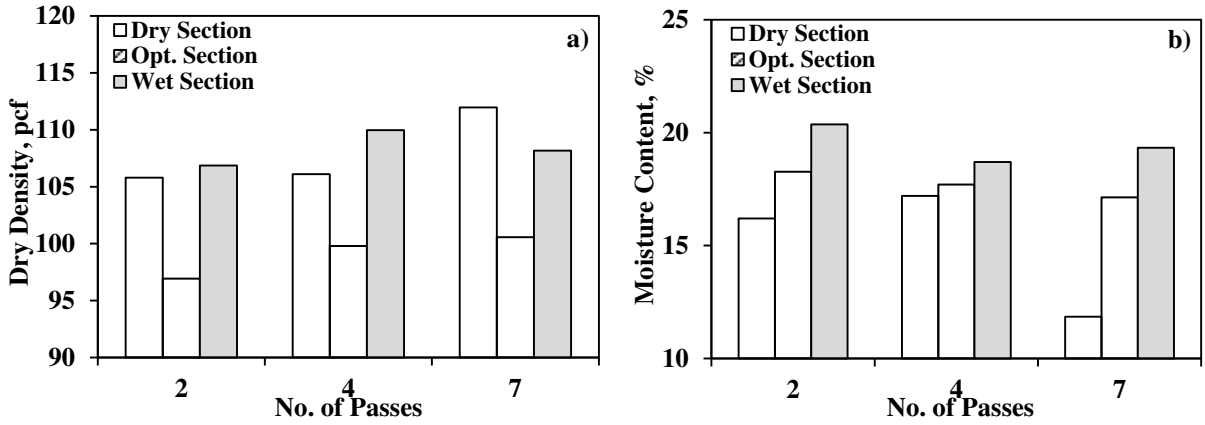

Figure H.4.6 – Variations of Average NDG Moisture Contents and Dry Densities with Number of Passes of Roller during Compaction of Subgrade Layer

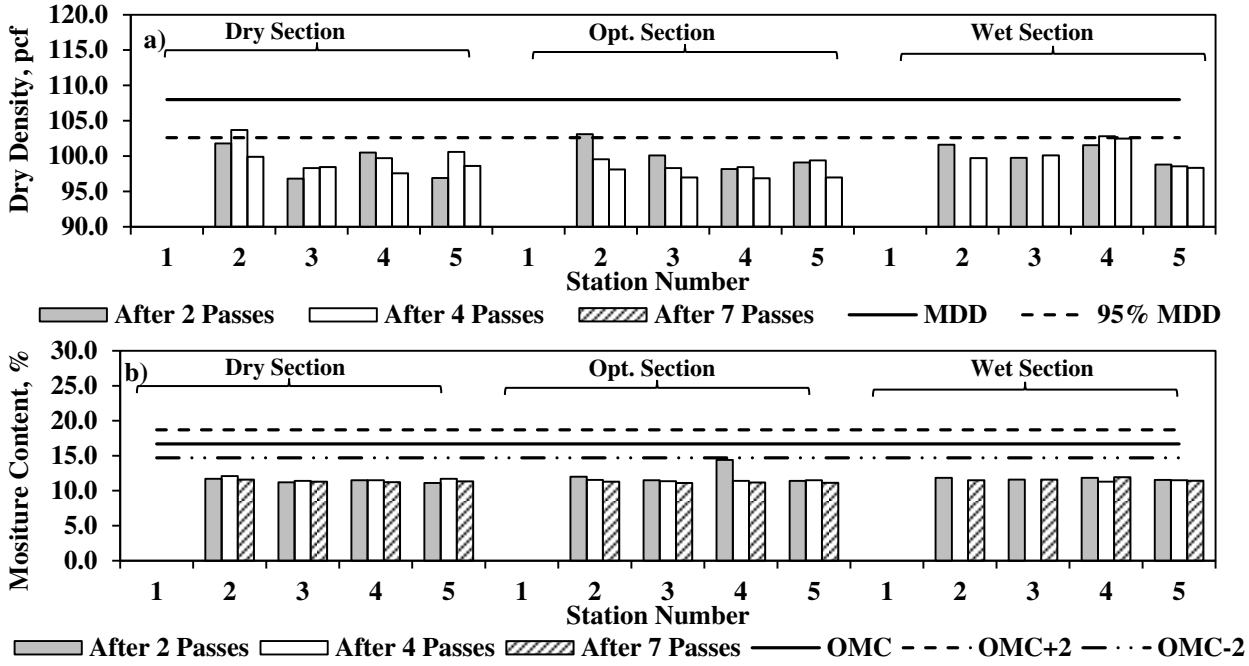

Figure H.4.7 –Variations of SDG Dry Densities and Moisture Contents with Number of Passes of Roller during Compaction of Subgrade Layer

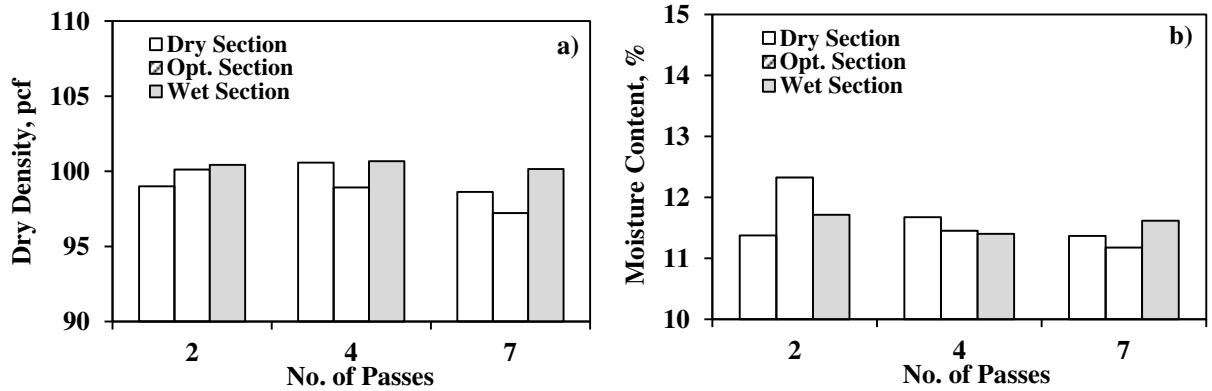

Figure H.4.8 – Variations of Average SDG Moisture Contents and Dry Densities with Number of Passes of Roller during Compaction of Subgrade

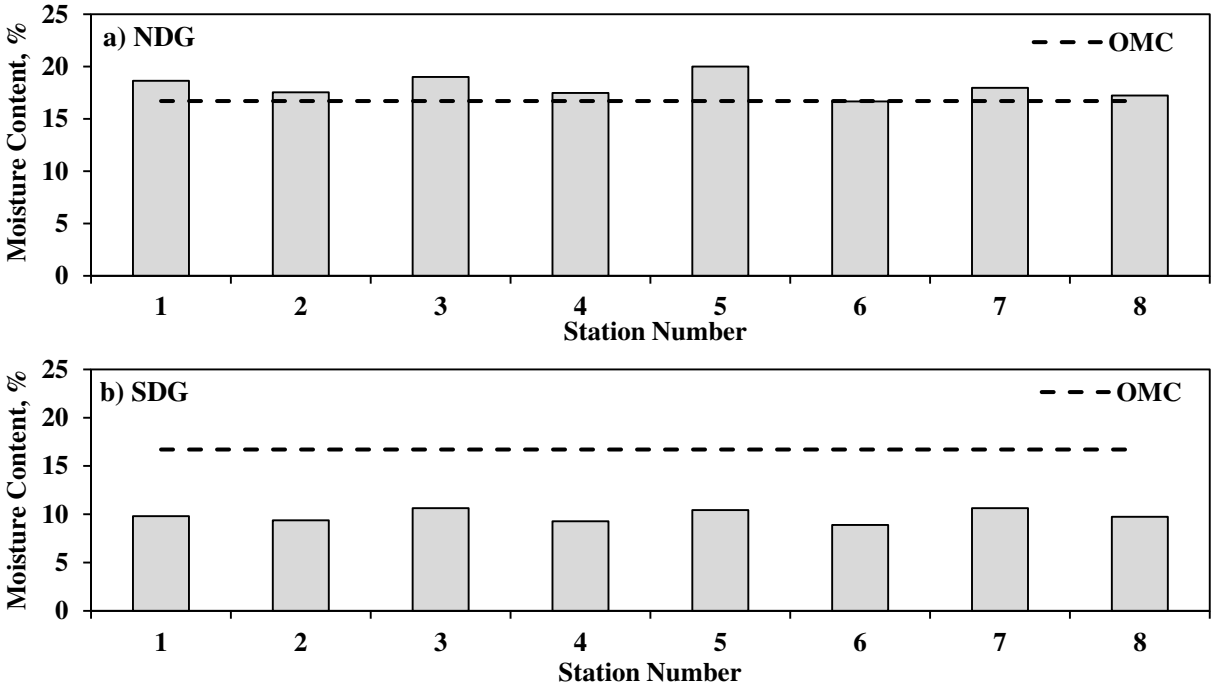

Figure H.4.9 – Variation of Average NDG and SDG Moisture Content of Production Section of Subgrade Layer

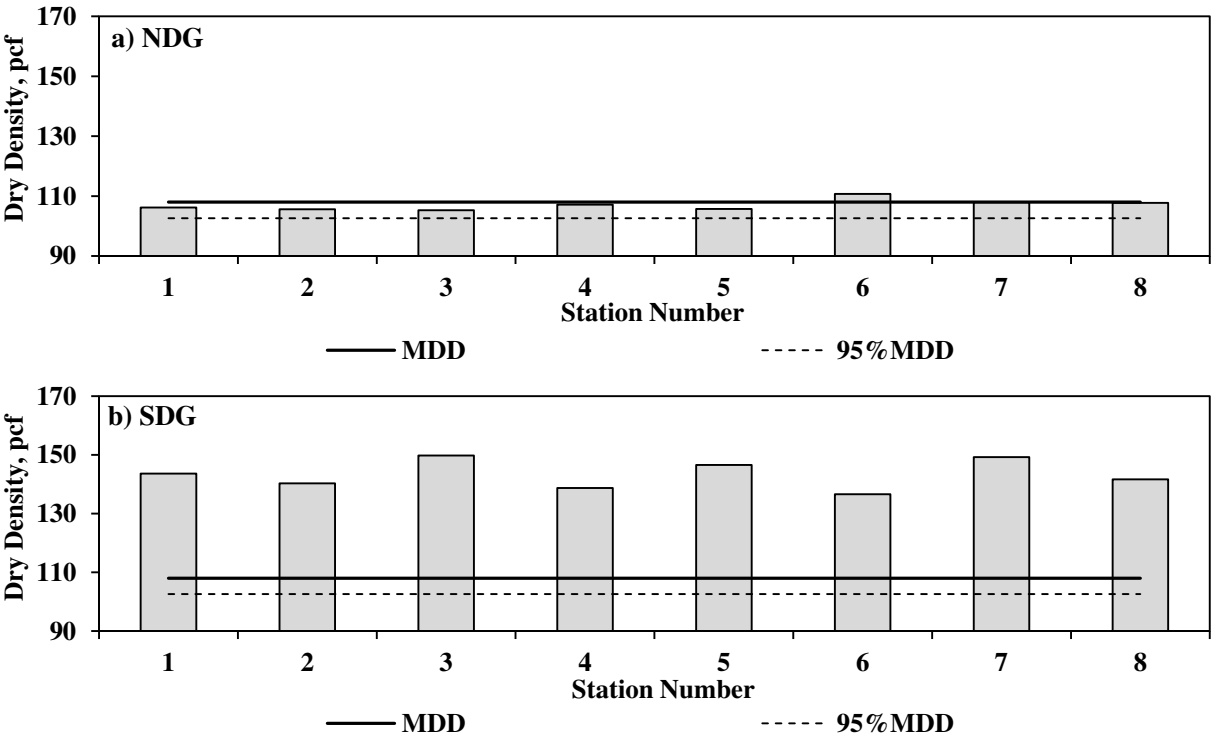

Figure H.4.10 – Variations of Average NDG and SDG Dry Densities of Production Section of Subgrade Layer

Base Layer: Figure H.4.11 illustrates the variations in the NDG and SDG moisture contents of the embankment layer before the placement of the base. The average moisture content of the embankment layer was 16.0% with the SDG and the more realistic value of 8.4% with the NDG. The NDG tests were not carried out on some stations due to time constraint.

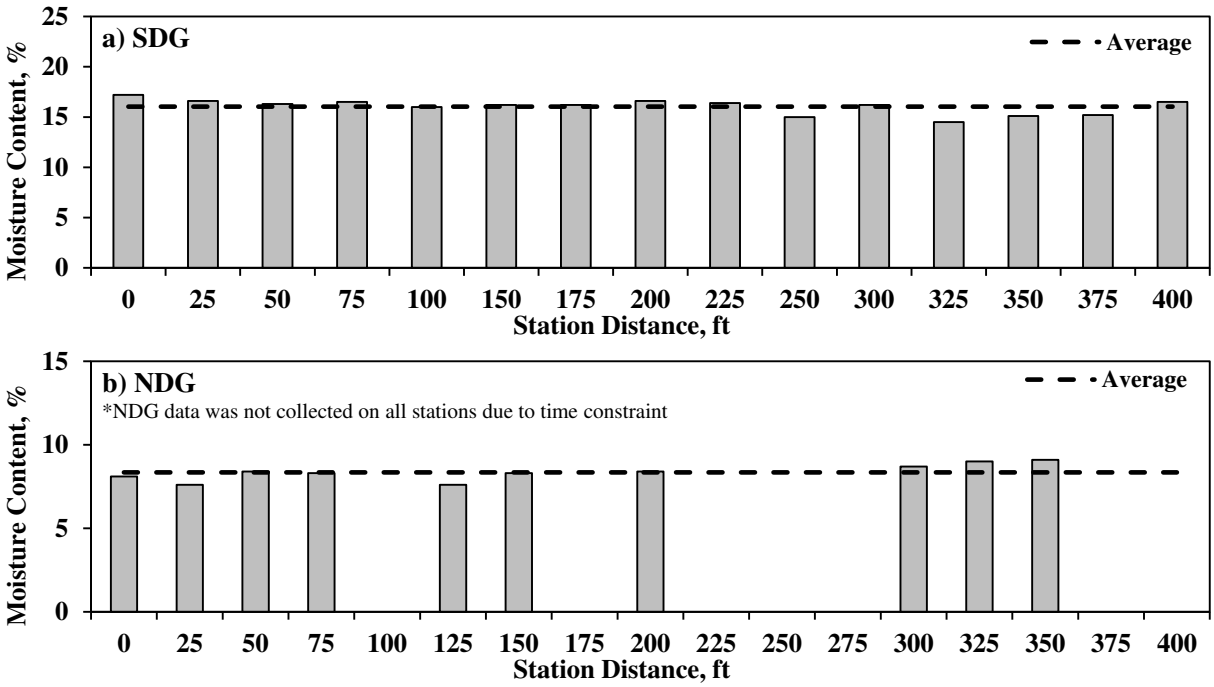

Figure H.4.11 – Spatial Variations of SDG and NDG Moisture Contents on Embankment Layer before Placement of Base

Figure H.4.12 summarizes the SDG and NDG density readings on the embankment layer before the placement of the base. The average SDG and NDG dry densities were both 124 pcf.

As shown in Figure H.3.2, three different sections (dry, optimum and wet) were constructed. The NDG and SDG were utilized immediately after the compaction of the base layer to determine the moisture contents and dry densities. The results of those tests are summarized in Figures H.4.13 and H.4.14. Based on the SDG results (Figure H.4.13a), the average moisture content of the dry section was 11.4%, the optimum section was 11.7% and the wet section was 15.3%. The optimum moisture content from the laboratory modified Proctor tests was 10.4% (see Table H.2.1). According to the NDG results (Figure H.4.13b), the average moisture content of the dry section was 7.0%, the optimum section was 9.0% and the wet section was 11.3%. Some of the stations were not tested due to time constraint. Table H.4.2 summarizes the average SDG and NDG moisture contents compared to oven dry moisture data.

Figure H.4.14 summarizes the dry densities from the SDG and NDG of the compacted base layer. The SDG dry densities were less than 95% of the MDD except for the wet section. The NDG results show that all test stations were for the most part between 95% and 100% of the MDD. The SDG and NDG data were not collected at some stations due to the malfunction of SDG and unavailability of the NDG.

Table H.4.2 – Comparisons of Average Moisture Contents of Base with Different Devices

Section (Nominal MC, %)	**Average Measured Moisture Content, %**			**Target Moisture Content, %**
	SDG	**NDG**	**Oven**	
Dry Section (OMC-2%)	11.4	7.0	6.6	8.4
Opt. Section (OMC)	11.7	9.0	8.8	10.4
Wet Section (OMC+2%)	15.3	11.3	11.0	12.4

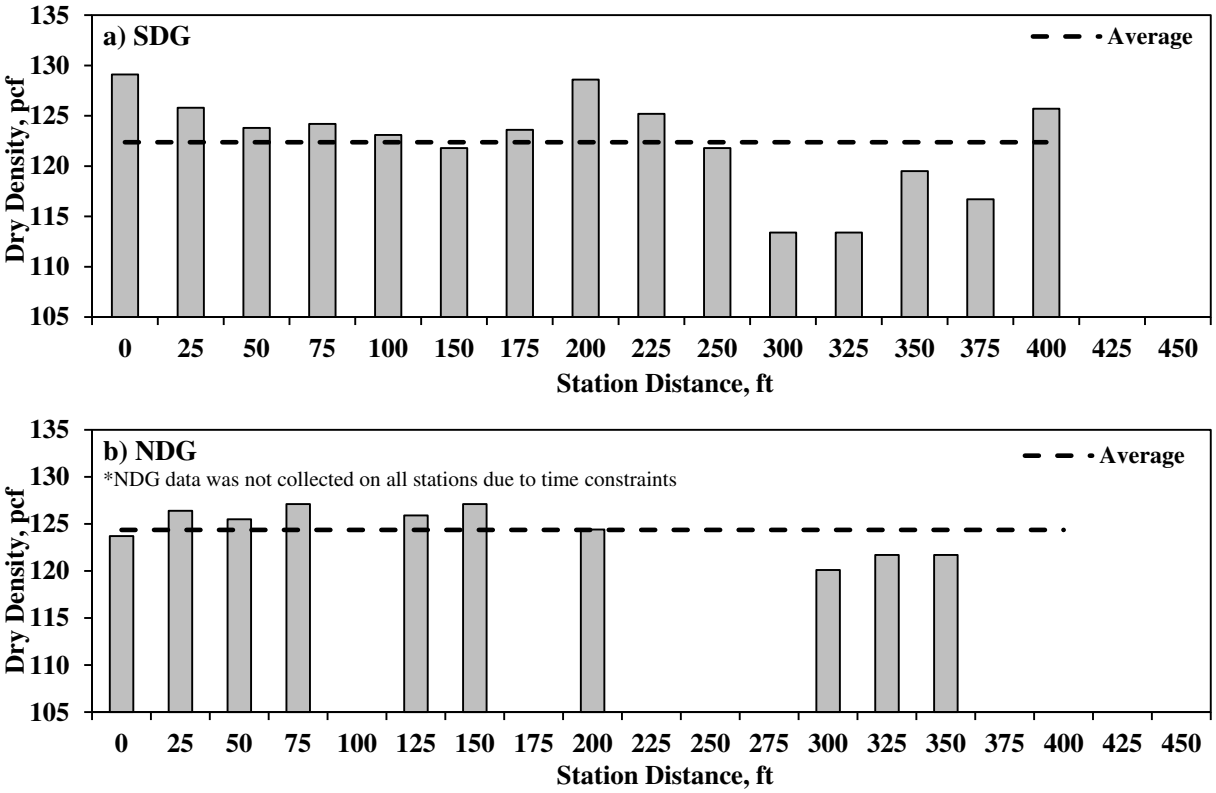

Figure H.4.12 – Spatial Variations of SDG and NDG Dry Densities on Embankment Layer before Placement of Base

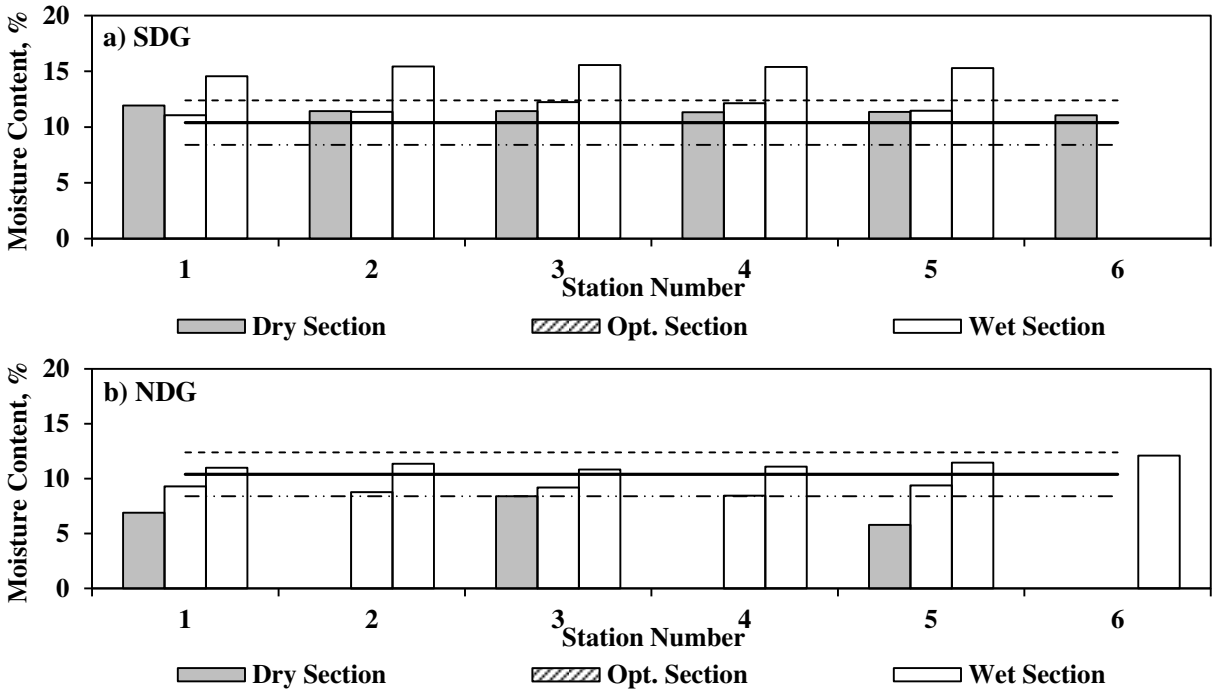

Figure H.4.13 – Spatial Variations of SDG and NDG Moisture Contents Immediately after Compaction of Base Layer

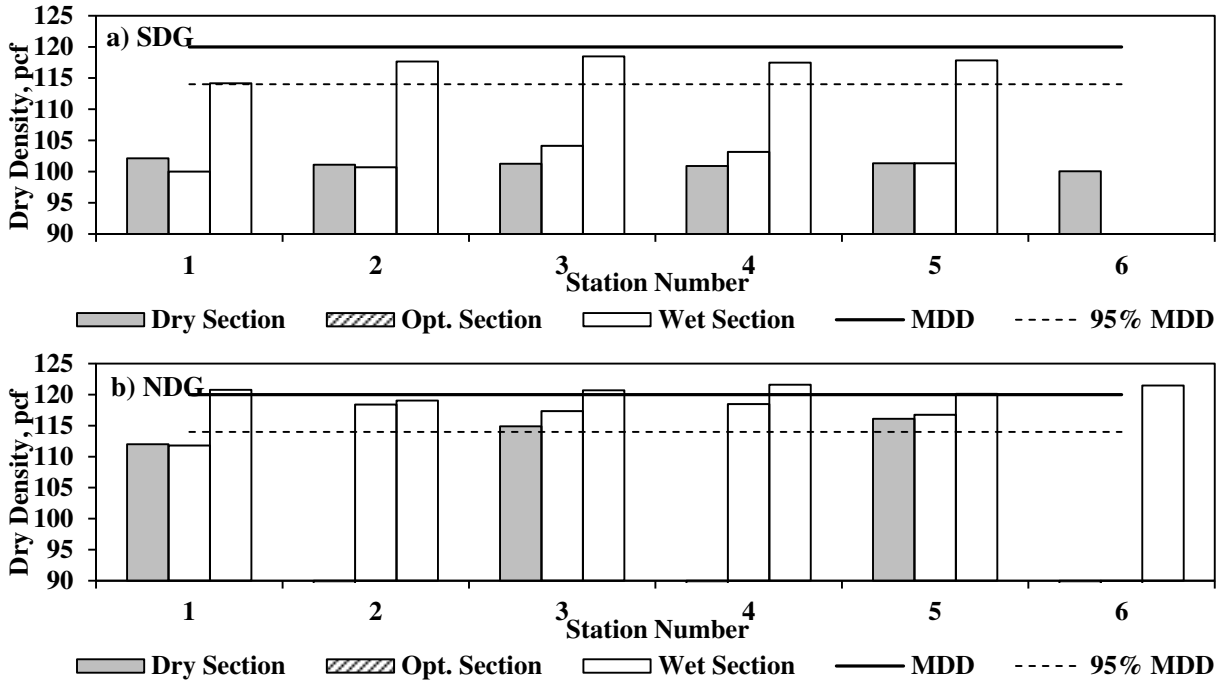

Figure H.4.14 – Spatial Variations of NDG and SDG Dry Densities Immediately after Compaction of Base Layer

Lime-Treated Subgrade Layer: Moisture contents and dry densities of the compacted lime-treated subgrade as a function of the passes of the roller and after completing the compaction process are summarized in Figures H.4.15 and H.4.16. Figure H.4.15a illustrates the variations of the SDG moisture contents between the passes of the IC roller. A clear pattern is not apparent in the data. The changes in the SDG moisture contents immediately after compaction and 24 hours after compaction are small (see Figure H.4.15b). Figure H.4.16 summarizes the SDG density readings during and after the compaction process. Again, a significant pattern is not observed (see Figure H.4.16a).

Figure H.4.17 summarizes the NDG readings at the same stations of the compacted lime-treated subgrade. The NDG data were collected only after the compaction process was completed. Furthermore, due to functional problems of the device and construction time constraints, it was not possible to collect all the required data. On average, the moisture content was 2% greater than the OMC and the dry density was close to 95% of the MDD.

H.5 Evaluation of Modulus-Based Devices

Subgrade Layer: A Zorn LWD and a PSPA were used on top of the embankment layer along Lines A and C shortly before the placement of the subgrade layer. The average moduli from lines A and C for each station are illustrated in Figure H.5.1. The average LWD modulus was 15±8 ksi (Figure H.5.1a), and the average PSPA modulus was 45±24 ksi (Figure H.5.1b).

Table H.5.1 and Figure H.5.2 contain the results of the measurements with the PSPA, Geogauge, LWD and DCP after the compaction of the subgrade layer. The variations in the average modulus among the three sections with the PSPA is rather small as supported by the laboratory modulus test results presented in Table H.2.2 for the range of moisture contents varying from 13% to 17% for subgrade layer.

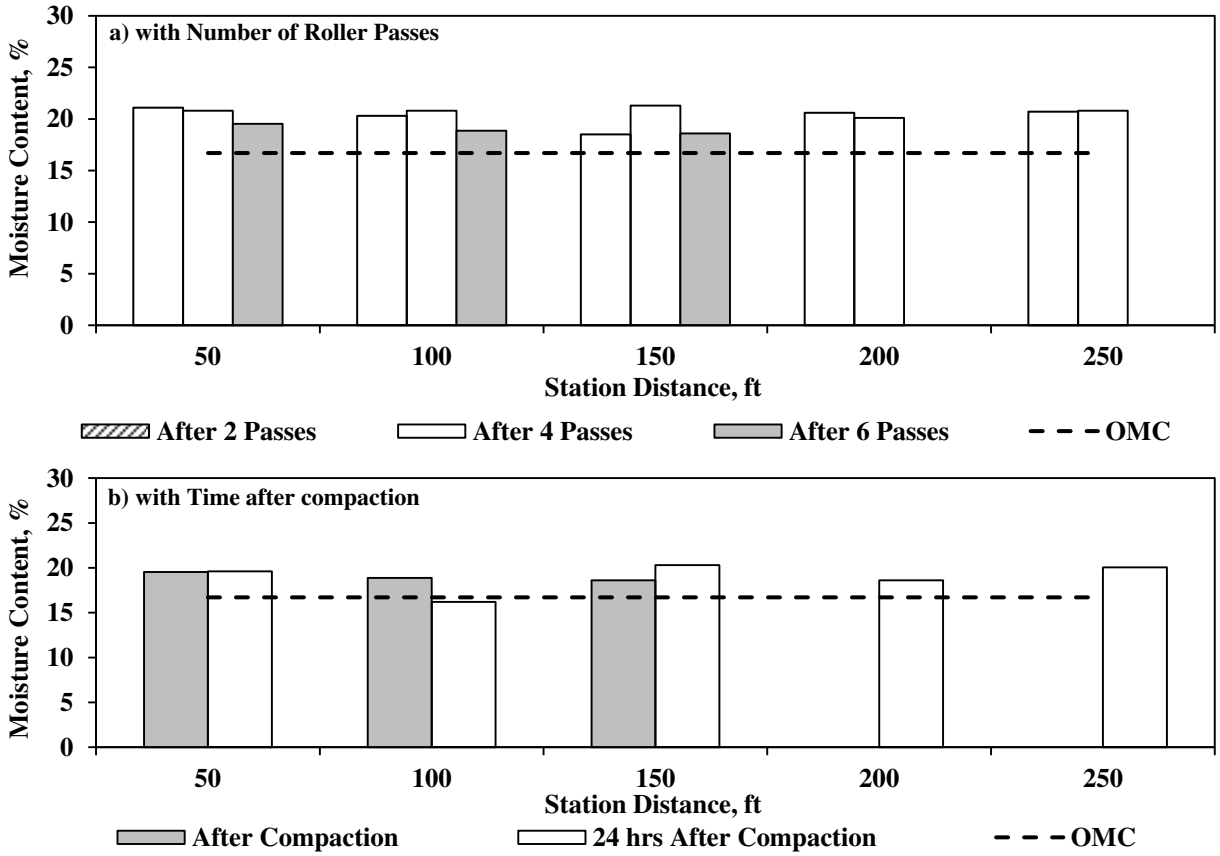

Figure H.4.15 – Spatial Variations of SDG Moisture Contents for Lime-Treated Subgrade

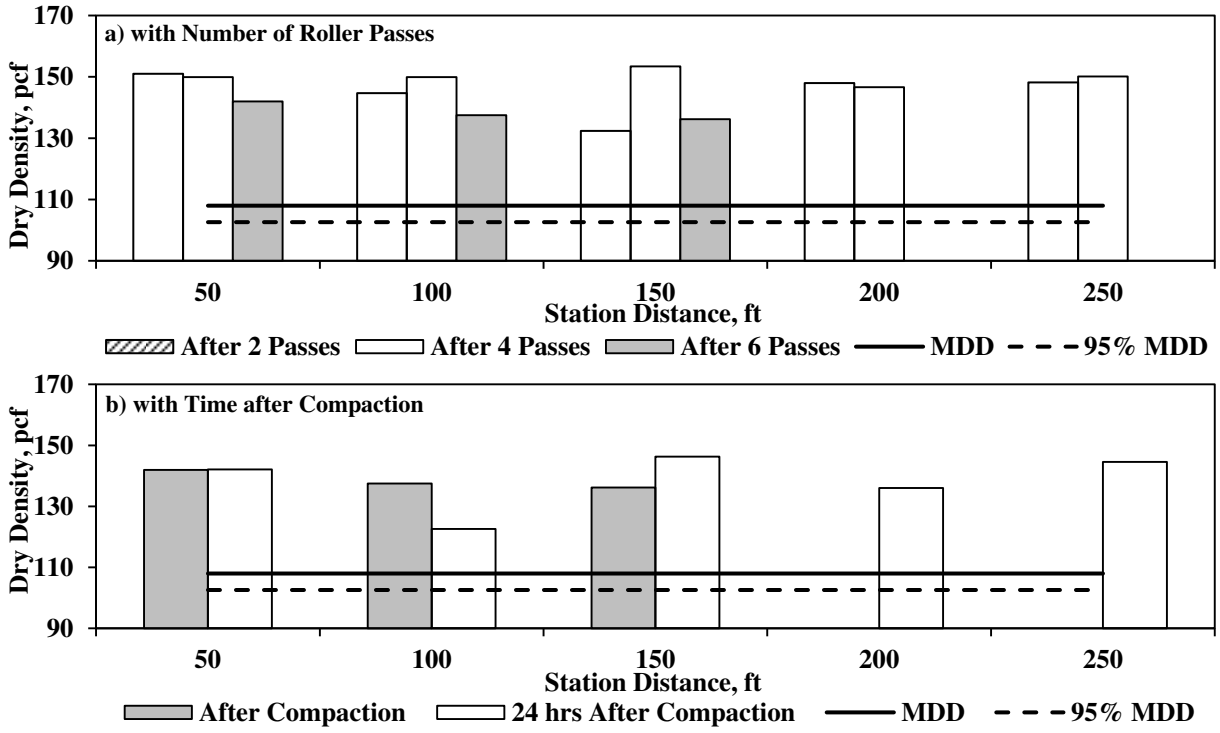

Figure H.4.16 – Spatial Variations of SDG Dry Densities for Lime-Treated Subgrade

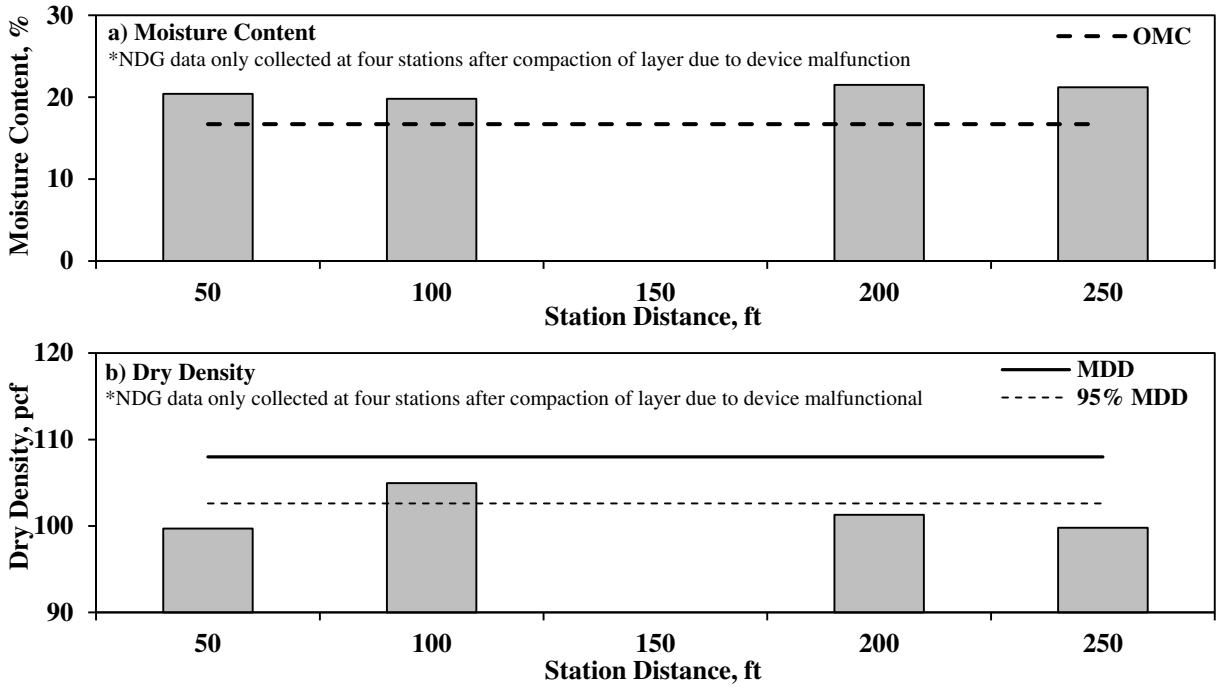

Figure H.4.17 – Spatial Variations of NDG Moisture Contents and Dry Densities after Compaction of Lime-Treated Subgrade

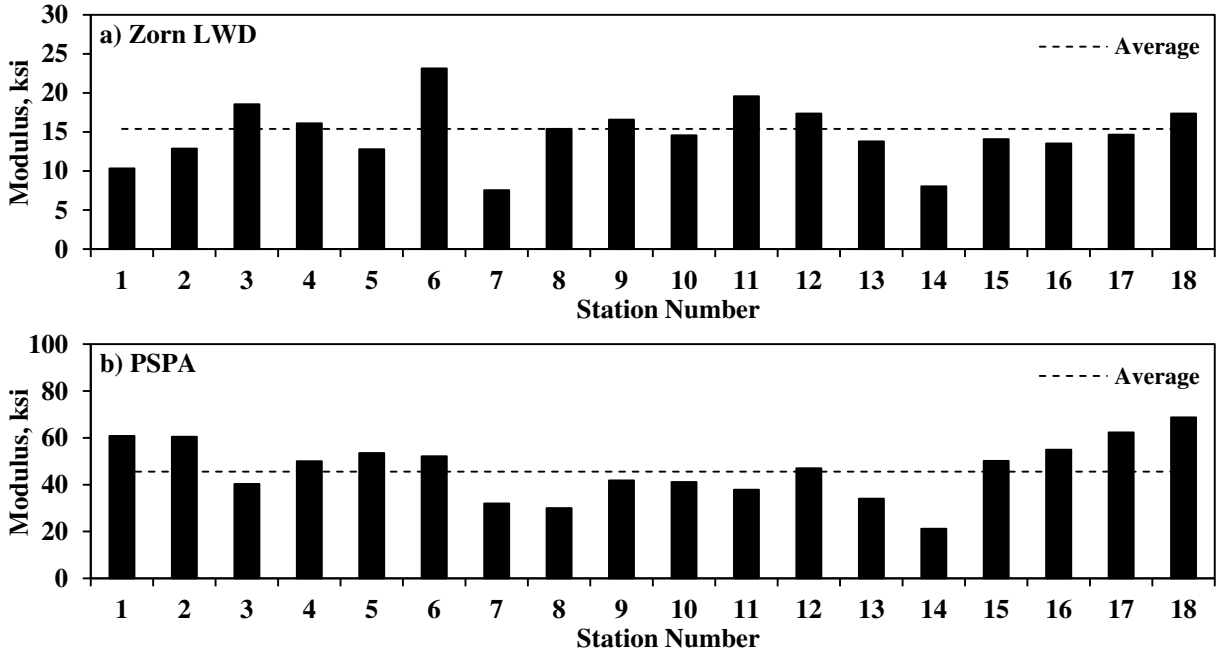

Figure H.5.1 –Variations of Measured Moduli of Embankment Layer

Table H.5.1 – Average Moduli from Different Sections

Field Section	Average Modulus, ksi						Average Oven MC, %
	PSPA		Geogauge	LWD		DCP	
	Subgrade	Embankment	Subgrade	Subgrade	Embankment	Subgrade	
Dry Section	38	53	48	8	15	17	11.4
Opt. Section	34	40	61	9	12	13	14.9
Wet Section	33	36	47	5	14	8	16.2

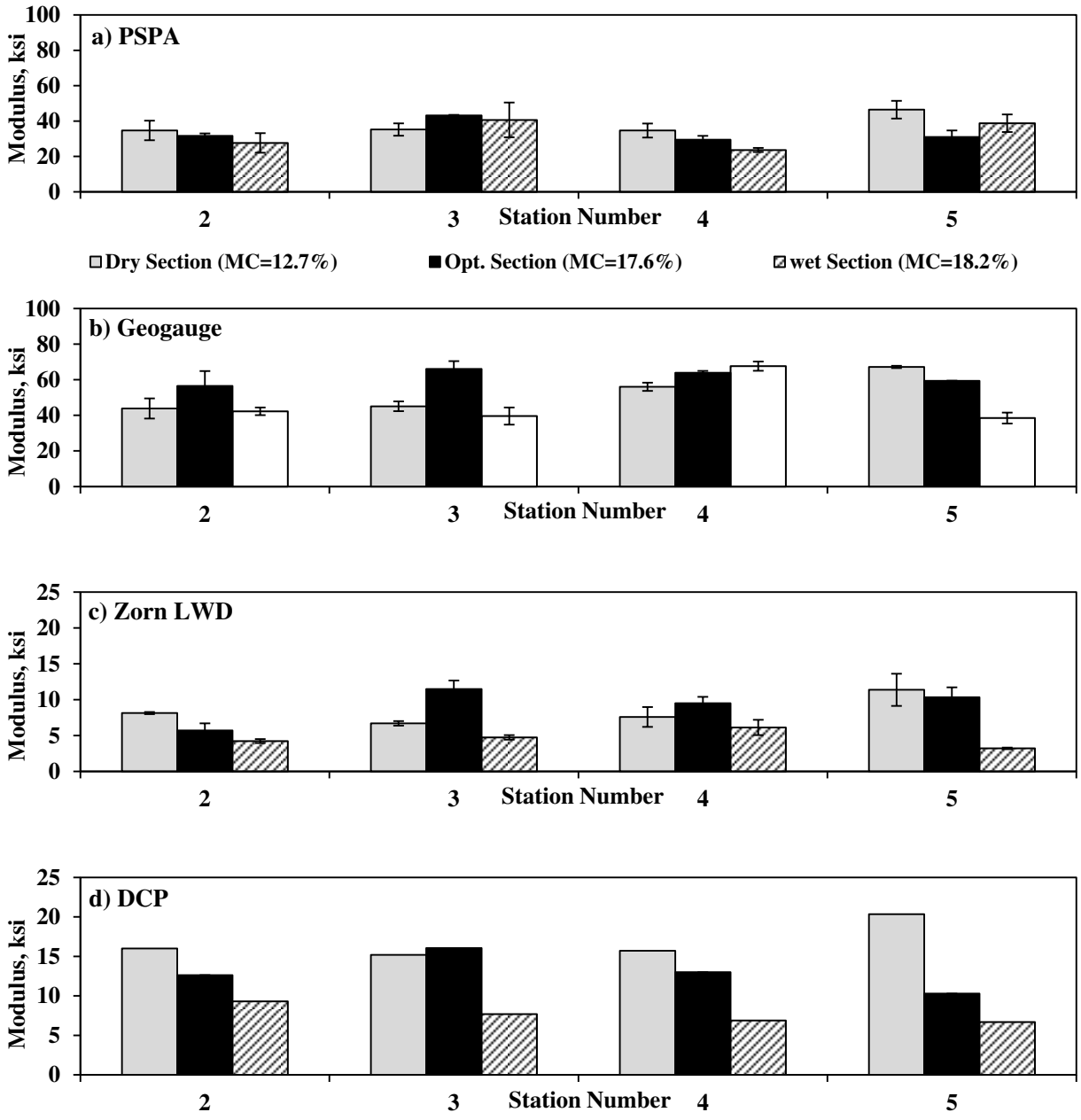

Figure H.5.2 – Spatial Variations of Measured Moduli immediately after Compaction of Subgrade (Average of Lines A, B, and C)

Figure H.5.3 summarizes the variations of the LWD and PSPA moduli between the passes of the IC roller during compaction of the subgrade layer. The modulus of the compacted layer increases for the most part with more passes of the roller.

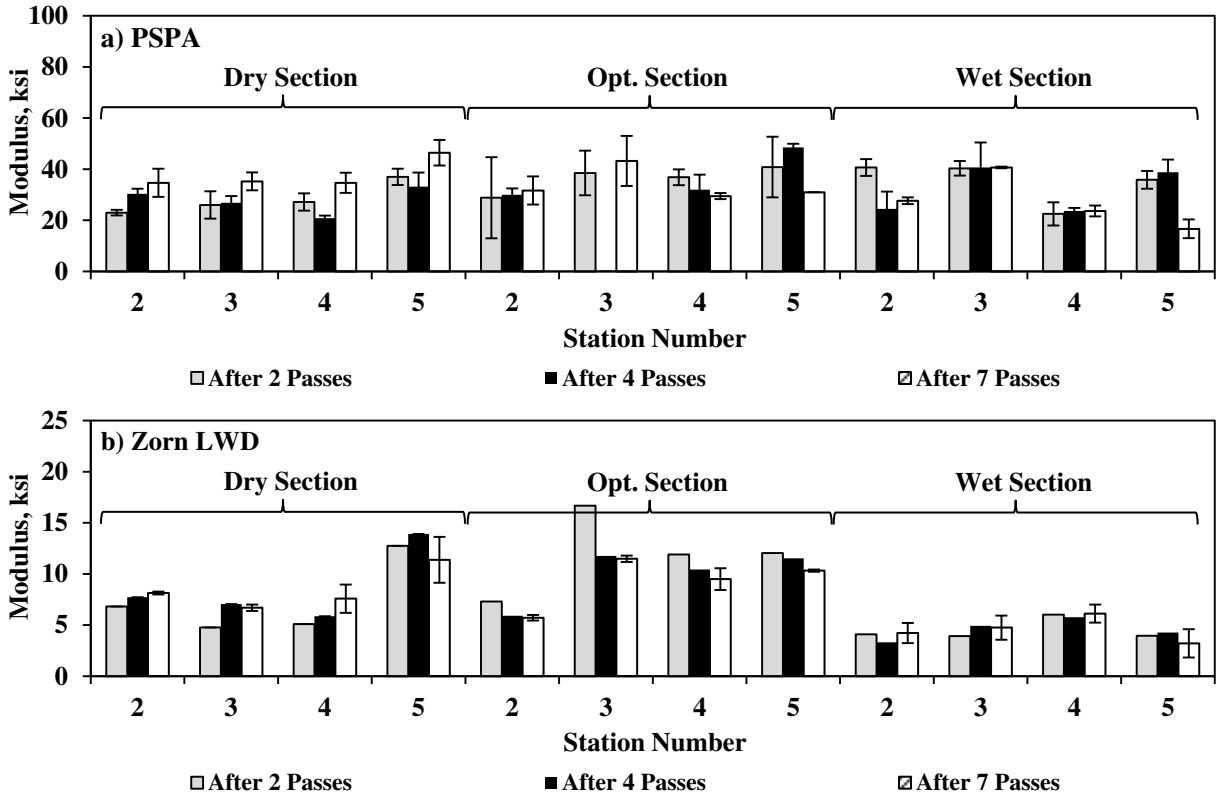

Figure H.5.3 –Variations of Measured Moduli between Passes of IC Roller during Compaction of Subgrade Layer

The results of the modulus-based devices on compacted subgrade layer from the production section are summarized in Figure H.5.4. The moduli of the compacted section from different devices are mostly consistent. The average PSPA modulus is 42 ksi, the Geogauge is 70 ksi, the LWD is 14 ksi and the DCP is 17 ksi. The production section is stiffer than the other subgrade sections. This can be attributed to numerous passing of reclaimers and water tanks in addition to the compactors over that section. Such construction traffic was avoided for the other three sections. The standard deviations of replicate tests on the same stations are illustrated as error bars in Figure H.5.4. DCP data was not collected at all test points due to time constraints.

Base Layer: The results from the PSPA, LWD and DCP tests on subgrade before the placement of the base layer are summarized in Figure H.5.5. The average PSPA modulus is 58 ksi while the average LWD modulus is 15 ksi. The average DCP modulus is 33 ksi. The variations in modulus from the three devices follow similar patterns. Stations 0, 200, 250, 300 and 450 are less stiff as compared to the other ones.

The results from the modulus testing of the three base sections are summarized in Figure H.5.6. Based on the LWD results (Figure H.5.6a), the average modulus for the dry section is 19 ksi, for the optimum section is 19 ksi and for the wet section is 12 ksi. Such results for the PSPA are 76 ksi, 75 ksi, and 50 ksi, respectively. There is not much difference between the LWD and PSPA moduli of the dry and optimum sections. For both devices, the modulus of wet section decreased by about 35%. Such pattern was not observed from the DCP data in which the average moduli of the dry, optimum and wet sections were 24, 26 and 26 ksi, respectively. As compared to the representative laboratory MR values (reported in Table H.2.2), the lab modulus increases by about 15% for dry samples and decreases by about 24% for wet

samples, respectively. As compared to the sample tested at OMC, the laboratory FFRC moduli increased by 74% and decreased by 57% for the dry and wet samples, respectively.

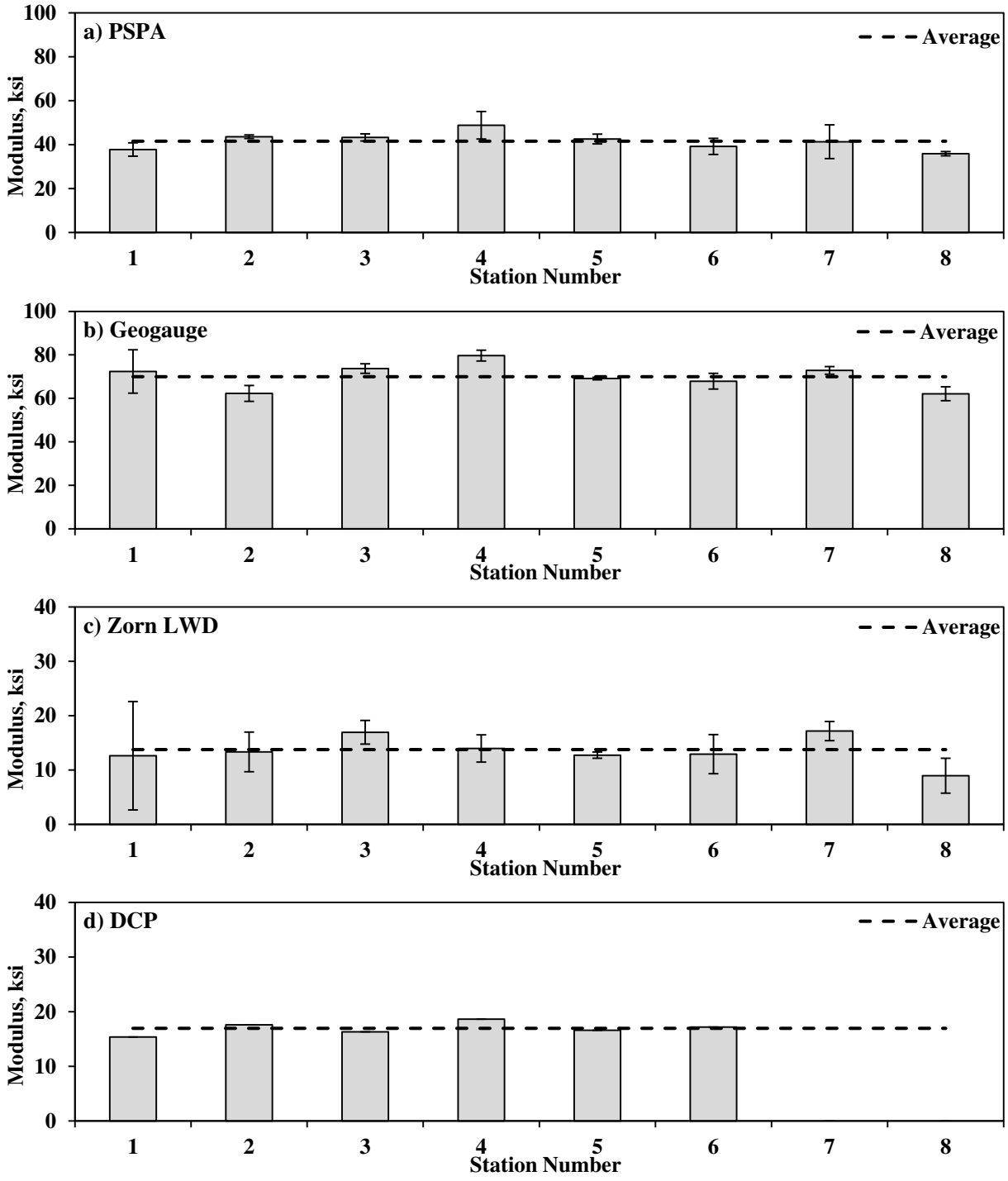

Figure H.5.4 – Spatial Variations of Measured Moduli immediately after Compaction of Subgrade at Production Section

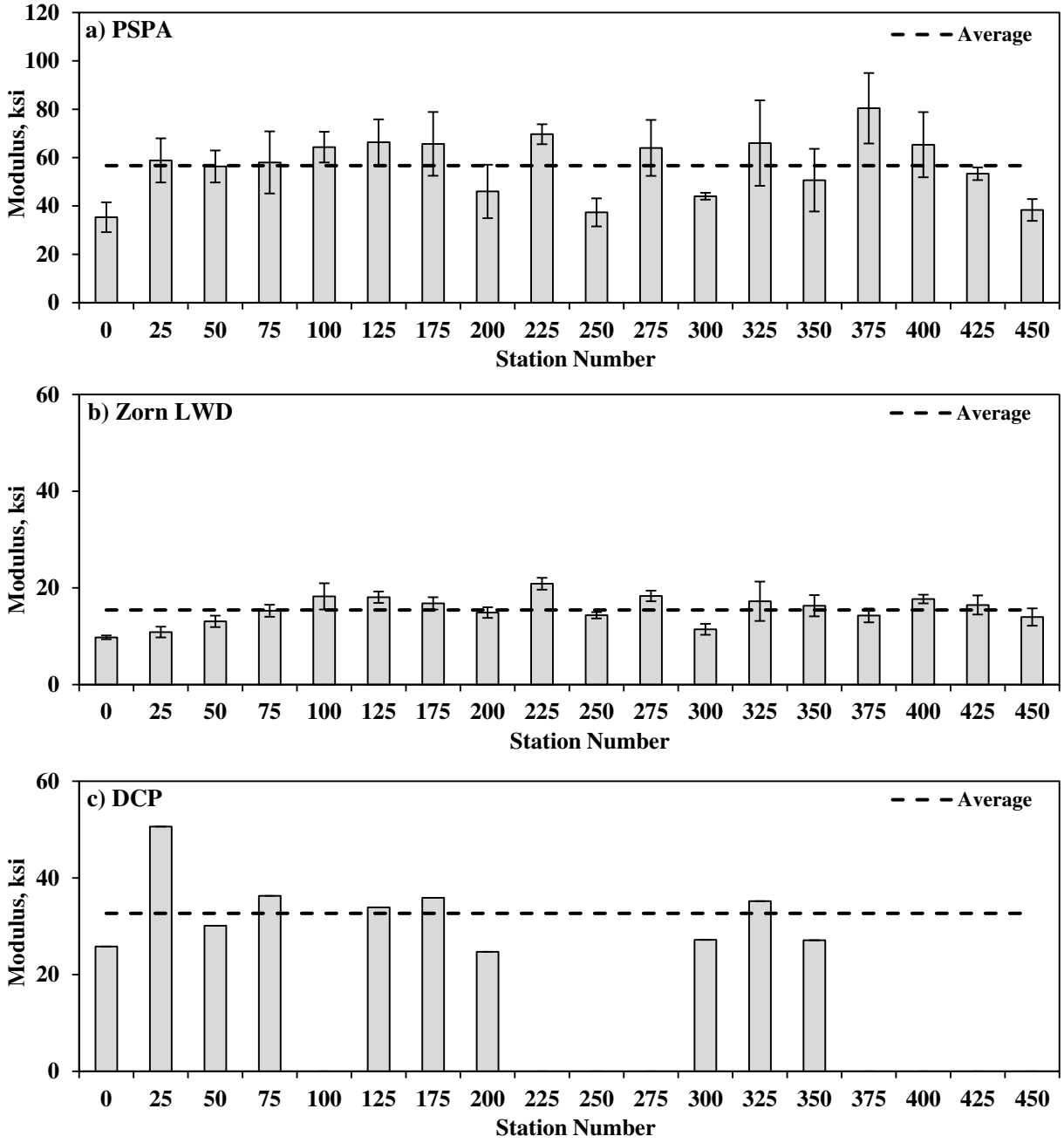

Figure H.5.5 – Spatial Variations of Measured Modulus of Subgrade before Placement of Base

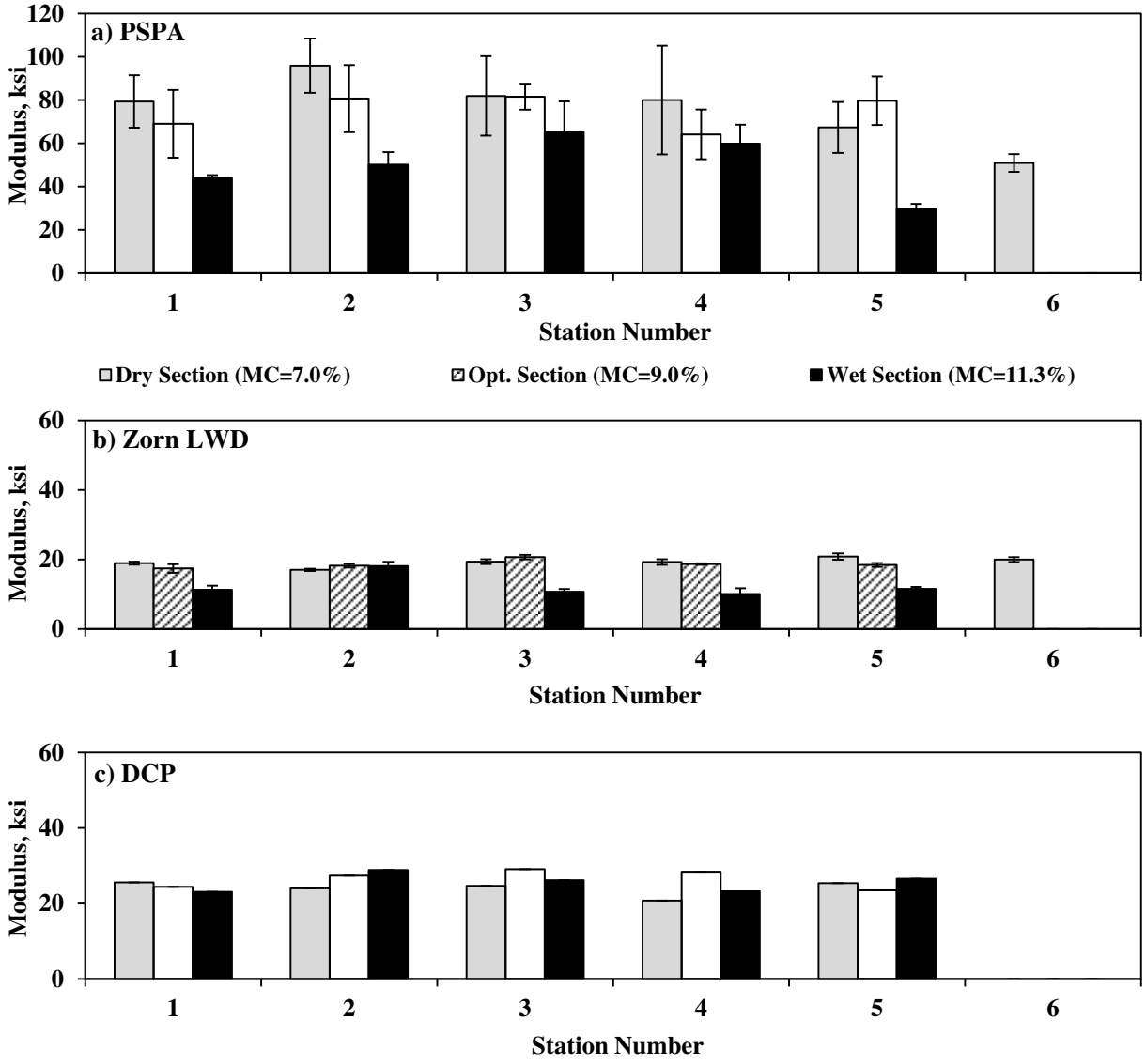

Figure H.5.6 – Spatial Variations of Measured Modulus immediately after Compaction of Base

Lime-Treated Subgrade Layer: Figure H.5.7 illustrates the results of the modulus measurements on the prepared subgrade layer before the treatment. The modulus variations among testing stations are similar with Stations 100 and 150 having slightly higher moduli as compared to the other stations. The average LWD modulus was 12 ksi and that of the PSPA was 51 ksi.

Figure H.5.8 summarizes the modulus measurements between the passes of the IC roller on the lime-treated subgrade and after the completion of the compaction process (6 passes of IC roller) for different devices. The DCP data were collected only after the final pass of the roller due to time constraints. Figure H.5.9 depicts the changes in measured moduli with different devices with respect to the passes of the IC roller. The stiffness of the compacted layer (from both the LWD and PSPA) increases with more passes of the roller.

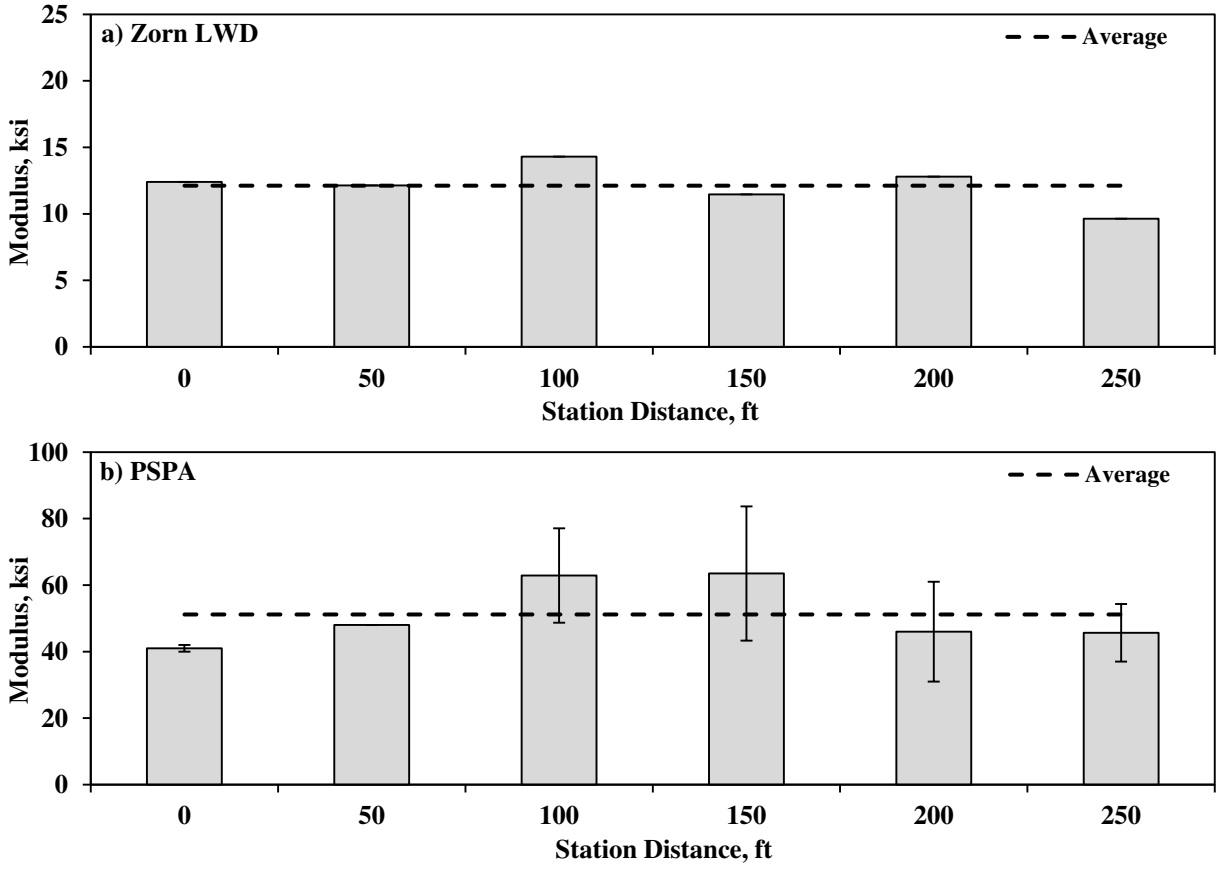

Figure H.5.7 – Spatial Variations of Measured Modulus before Stabilization of Subgrade Layer

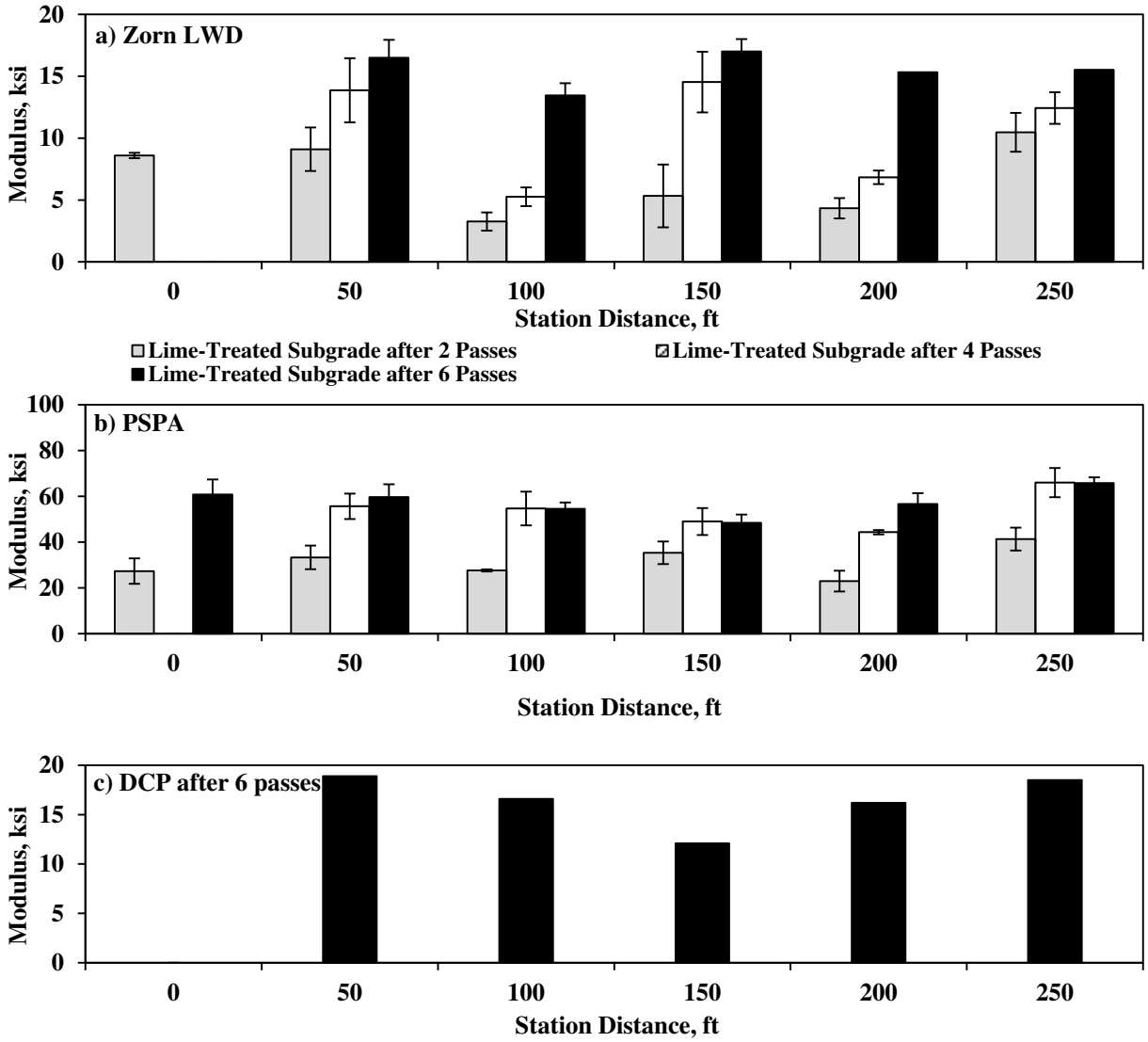

Figure H.5.8 – Spatial Variations of Measured Moduli between Passes of IC Roller and Immediately after Compaction of Lime-Treated Subgrade Layer

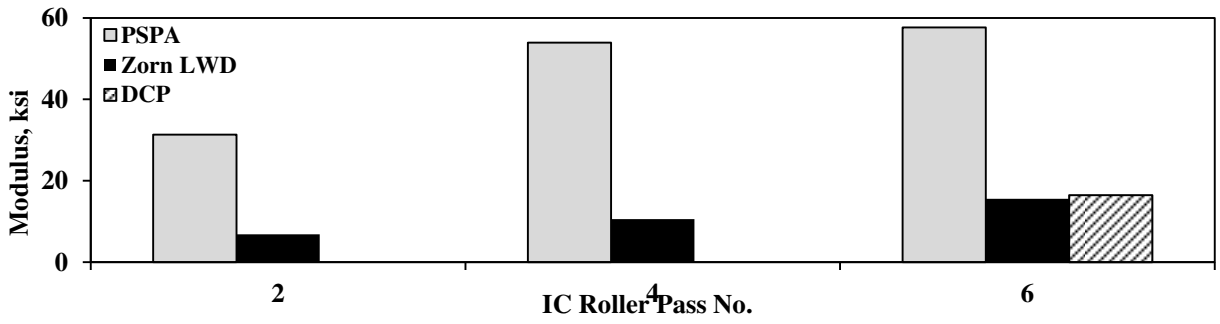

Figure H.5.9 – Variations of Moduli between Passes of IC Roller from Different Devices

H.6 Variability of Modulus-Based Devices

Subgrade Layer: In order to investigate the variability of modulus-based devices for in-situ modulus estimation, the coefficient of variation (COV) of the replicate tests at each test spot was calculated after the final pass of the IC roller. The distributions of the COVs with measured field moduli for the PSPA, Geogauge and LWD are summarized in Figure H.6.1. A clear trend between the average measured modulus and the COV cannot be observed for any of the devices. The maximum COVs for the PSPA and Geogauge were 49%, while such value for the LWD was 38%. The relatively high COVs might be because of the compaction nonuniformity among the test locations at each station as shown in Figure H.6.2.

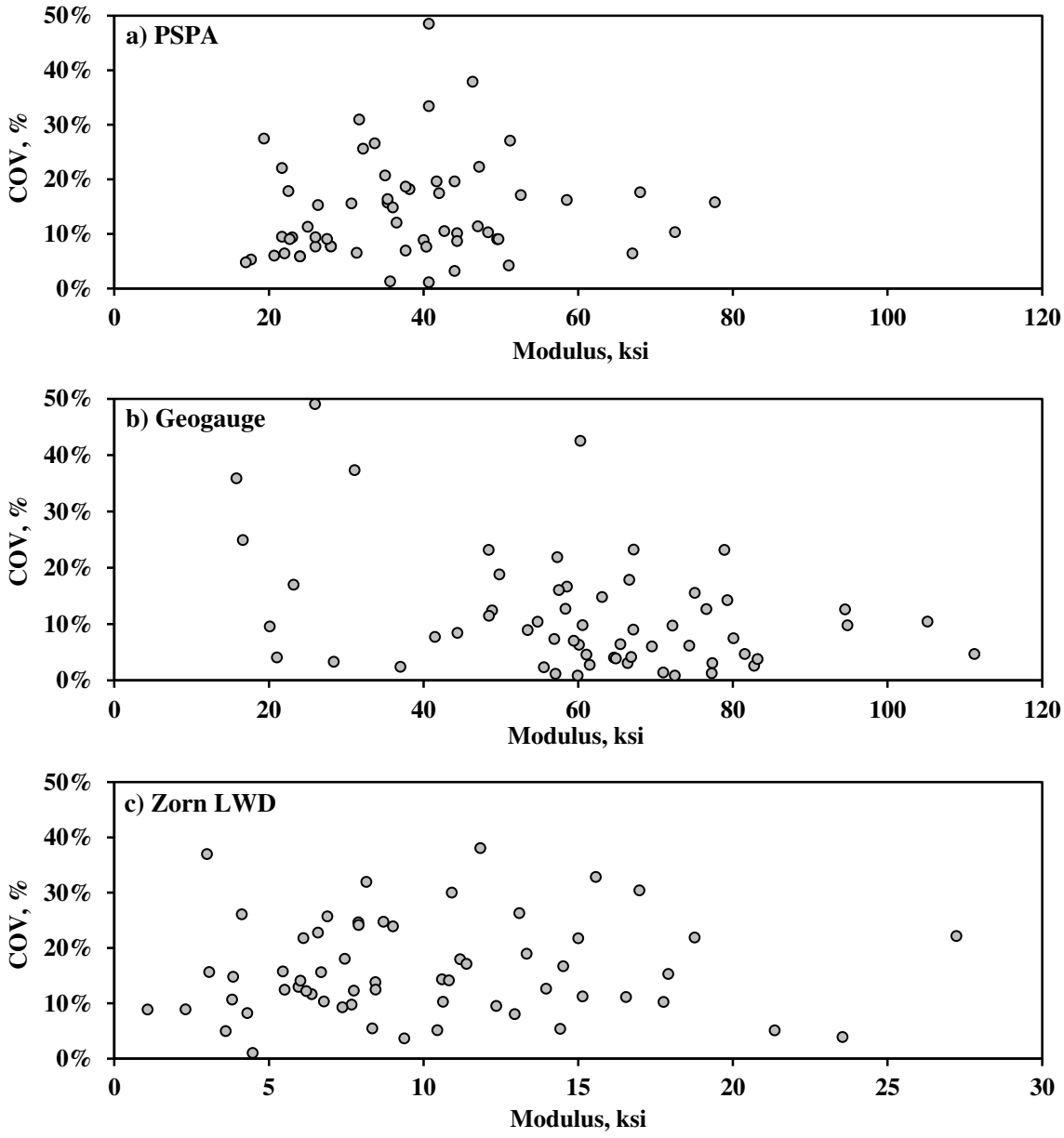

Figure H.6.1 – Variations in Coefficient of Variation (COV) of Modulus-based Devices with Average Measured Modulus of Subgrade Layer

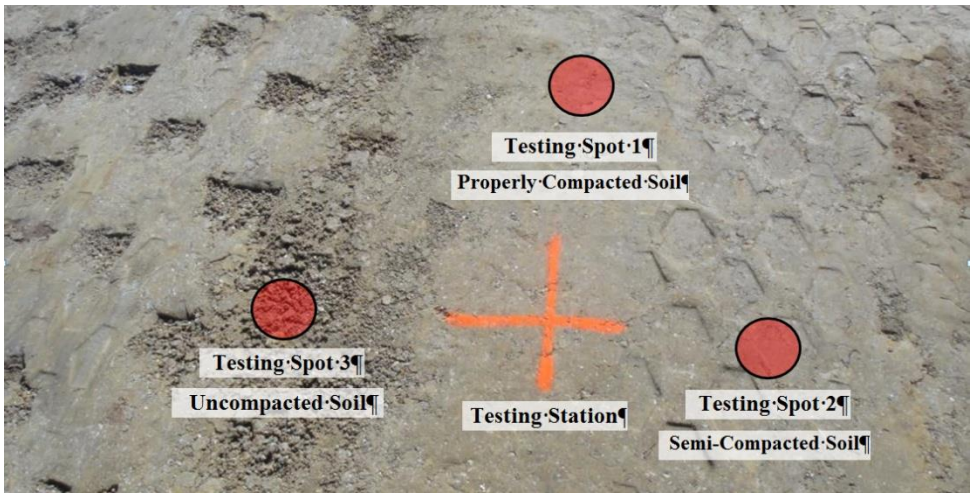

Figure H.6.2 – Compaction Discrepancy among Testing Spots around a Sample Station

Base Layer: Figure H.6.3 illustrates the distributions of the COVs for corresponding measured moduli with the LWD and PSPA. The average COV value for the LWD measurements is 7% with maximum COV of 29%. The maximum COV for the PSPA readings is 44% with an average of 16%. The differences in the COVs can be partially attributed to the fact that the LWD measures a composite modulus of the base and subgrade while the PSPA directly measures the modulus of the base layer.

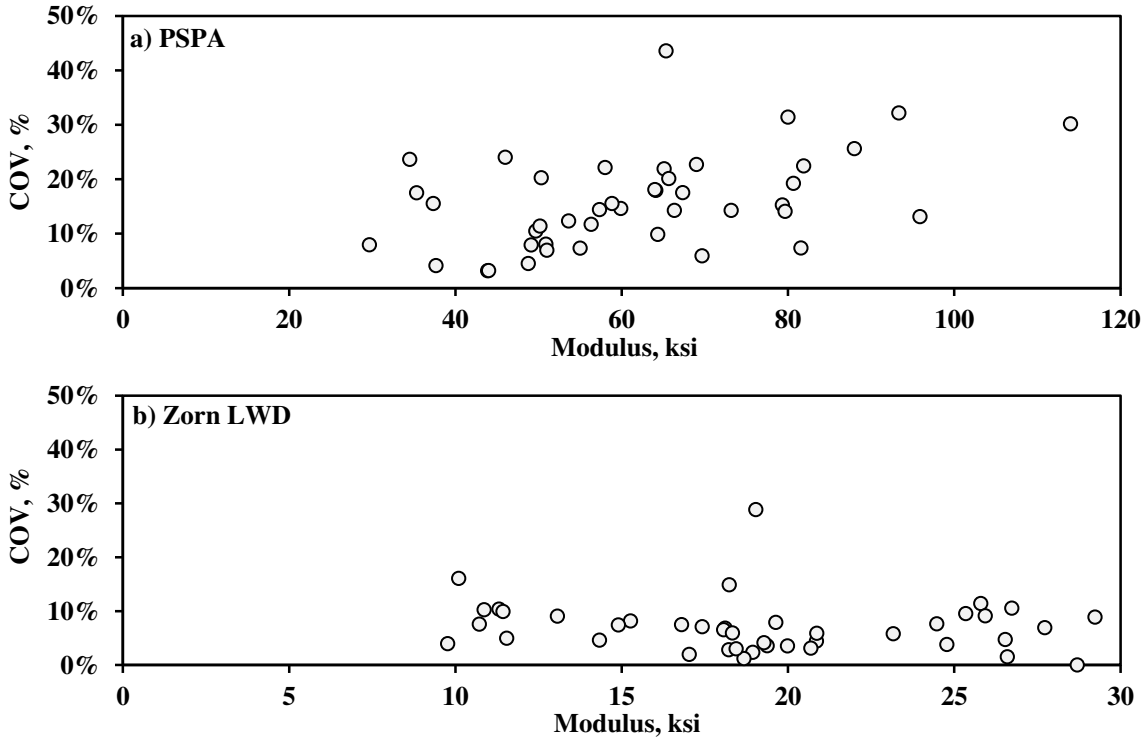

Figure H.6.3 – Variations in Coefficient of Variation (COV) of Modulus-based Devices with Average Measured Modulus of Base Layer

Lime-Treated Subgrade: The distributions of the COVs for the measured moduli of the lime-treated subgrade are summarized in Figure H.6.4 for the LWD and PSPA. The average PSPA COV is 13% with the maximum of 33% while such values for the LWD are 11% with maximum of 23%.

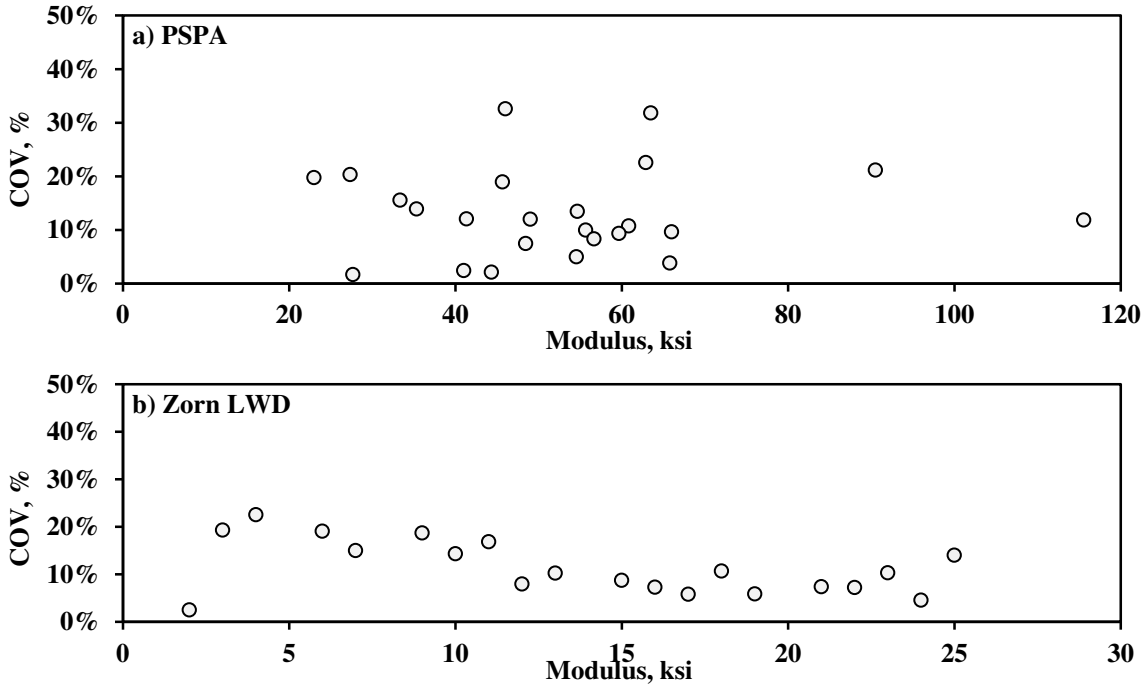

Figure H.6.4 – Variations in Coefficient of Variation (COV) of Modulus-based Devices with Average Measured Modulus of Lime-Treated Subgrade Layer

H.7 Moisture-Modulus Relationships

Subgrade Layer: Figure H.7.1 compares the NDG moisture contents with the oven dry moisture contents. On average, the NDG measurements are 2.6% greater than the oven-dry moisture contents.

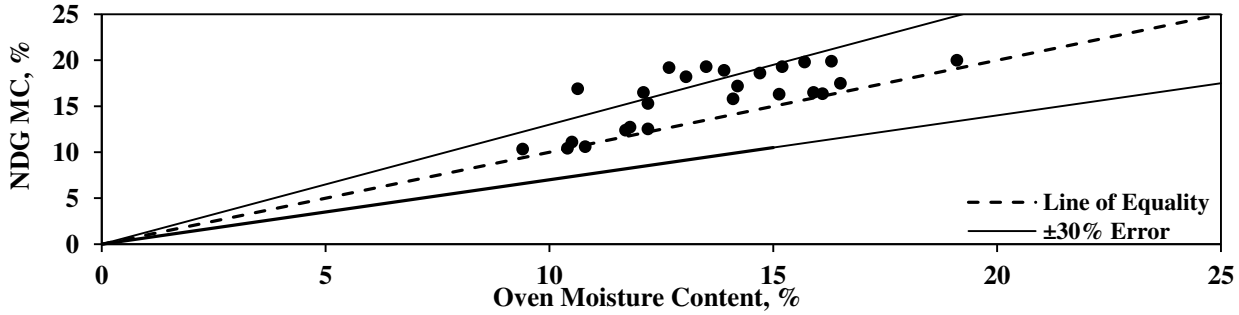

Figure H.7.1 – Relationship between Oven-Dry and NDG Moisture Contents after Compaction of Subgrade Layer

The relationships between the field moduli from different devices and their corresponding oven dry moisture contents are summarized in Figure H.7.2. The results from all devices except for the Geogauge are correlated reasonably. Similar results but with the NDG are summarized in Figure H.7.3. Due to uncertainties associated with the NDG results (as shown in Table H.4.1 and Figure H.7.1), the moisture-modulus correlations are not as strong as those in Figure H.7.2. Since the correlations illustrated in Figure H.7.2 were deemed more reliable, further investigations are limited to oven dry moisture contents.

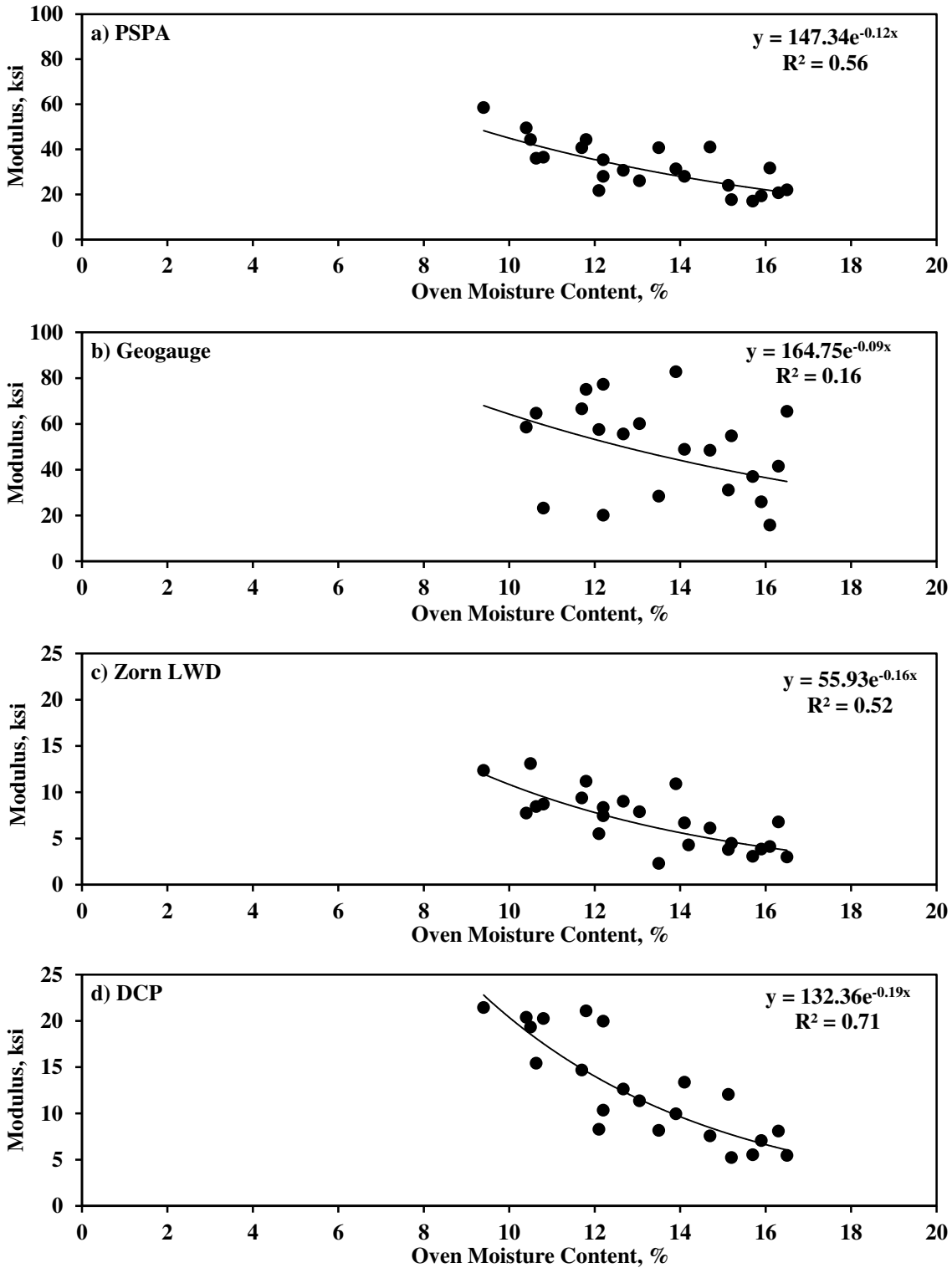

Figure H.7.2 – Relationships between Oven Moisture Contents and Measured Moduli of Subgrade Layer (for dry, optimum and wet sections)

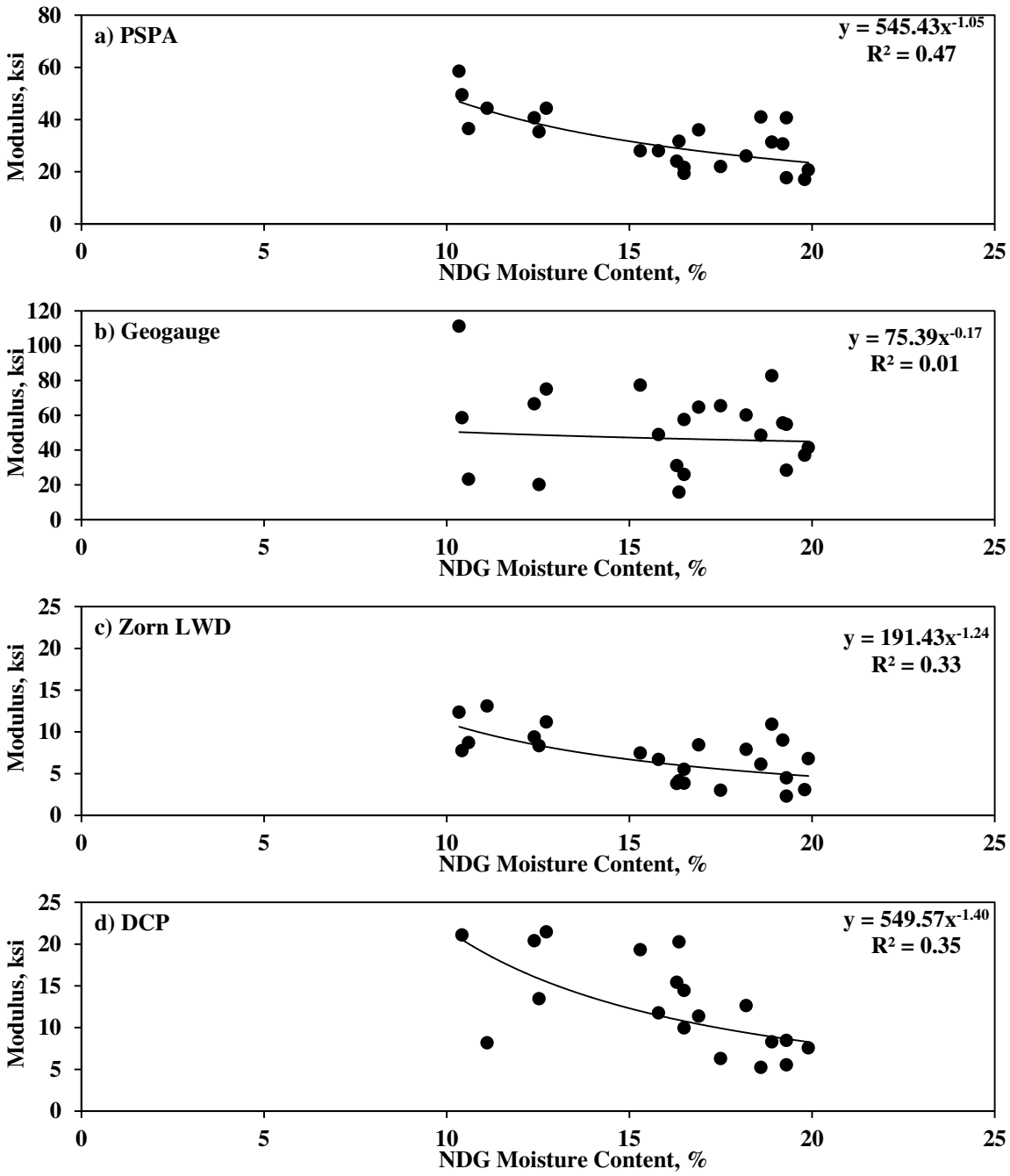

Figure H.7.3 – Relationships between NDG Moisture Contents and Measured Moduli of Subgrade Layer (for dry, optimum and wet sections)

The correlations developed in Figure H.7.2 were employed to predict the modulus at the optimum moisture content, M_{opt}. The relations between the normalized modulus, M/M_{opt}, and normalized oven moisture content, (MC–OMC)/OMC, are presented in Figure H.7.4. The measured field data are in agreement with the models developed based on the laboratory MR and FFRC moduli (see Chapter 3).

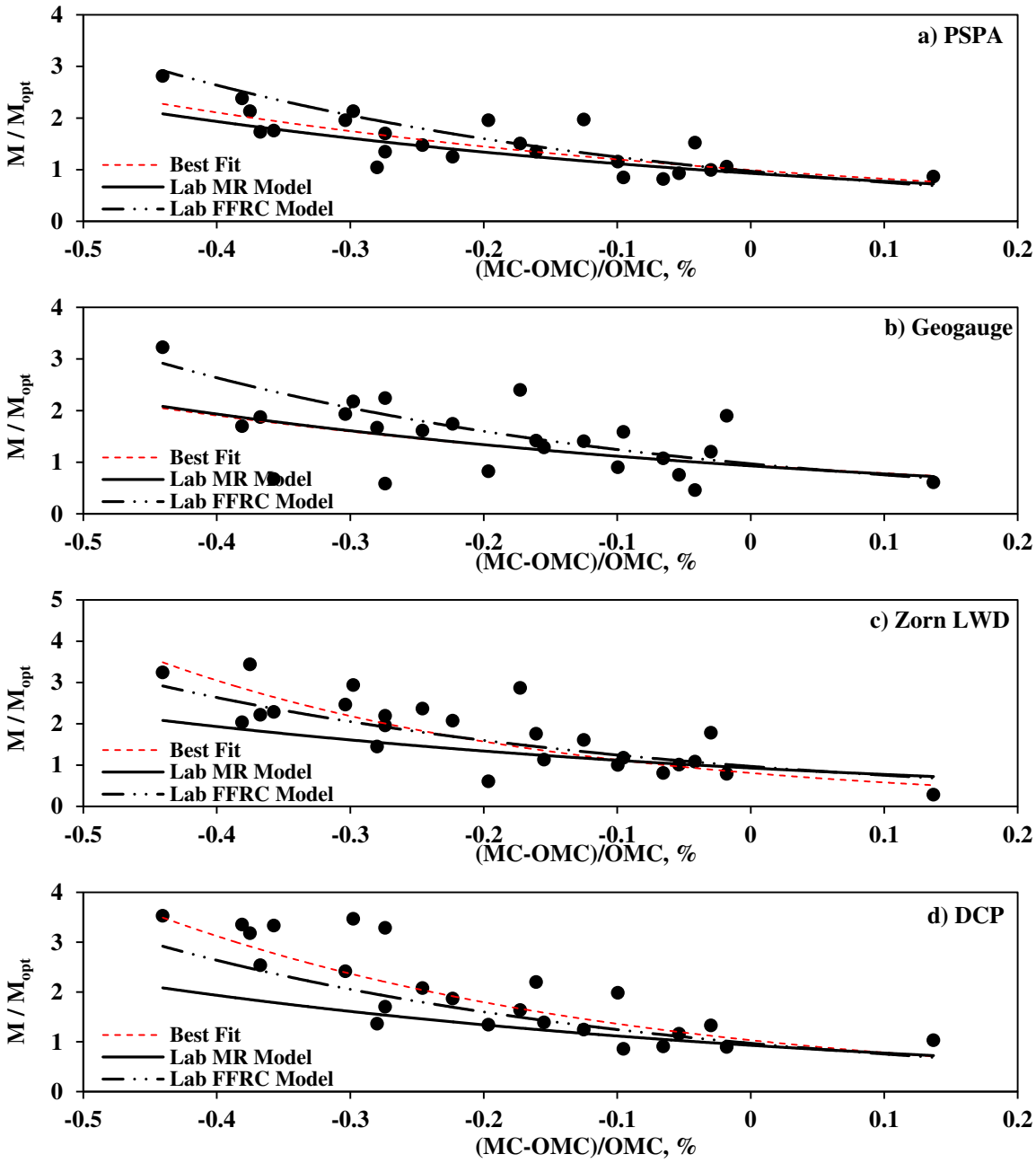

Figure H.7.4 – Correlation between Normalized Modulus and Normalized Oven Moisture Contents

The variations in the normalized modulus with the calculated normalized degree of saturation, S-S_{opt}, are summarized in Figure H.7.5. Except for the Geogauge, reasonable correlations between the measured in-situ moduli and the normalized degree of saturation are observed. The field data are also compared with the Cary and Zapata (using the corresponding *wPI* of the material) and the MEPDG models in Figure H.7.5. The best-fit curves of measured field data are closer to the MEPDG fine-grained model.

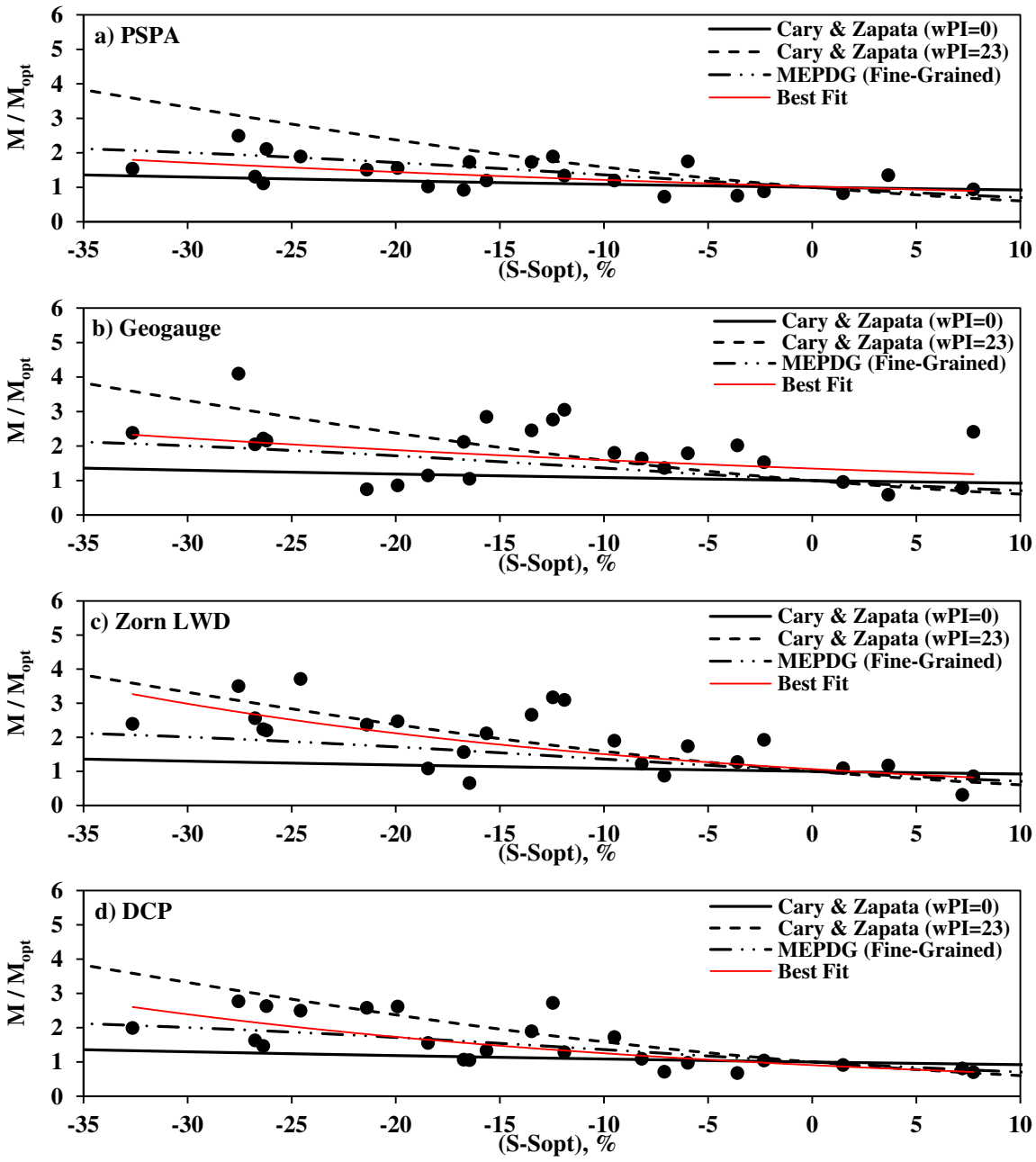

Figure H.7.5 – Correlations between Normalized In-Situ Moduli with Normalized Degree of Saturation

***Base Layer**:* The same process explained in previous section was applied to the data collected after the compaction of the base layer. The variations in the modulus with the NDG moisture content are shown in Figure H.7.6 and with the oven dry moisture content in Figure H.7.7. The numbers of data points in the two figures are different because the oven moisture contents were not measured for all test points. Again, the correlations based on the oven dry moisture contents are better defined than those based on the NDG moisture contents. Based on the oven moisture contents, the strongest correlation is obtained from the LWD data.

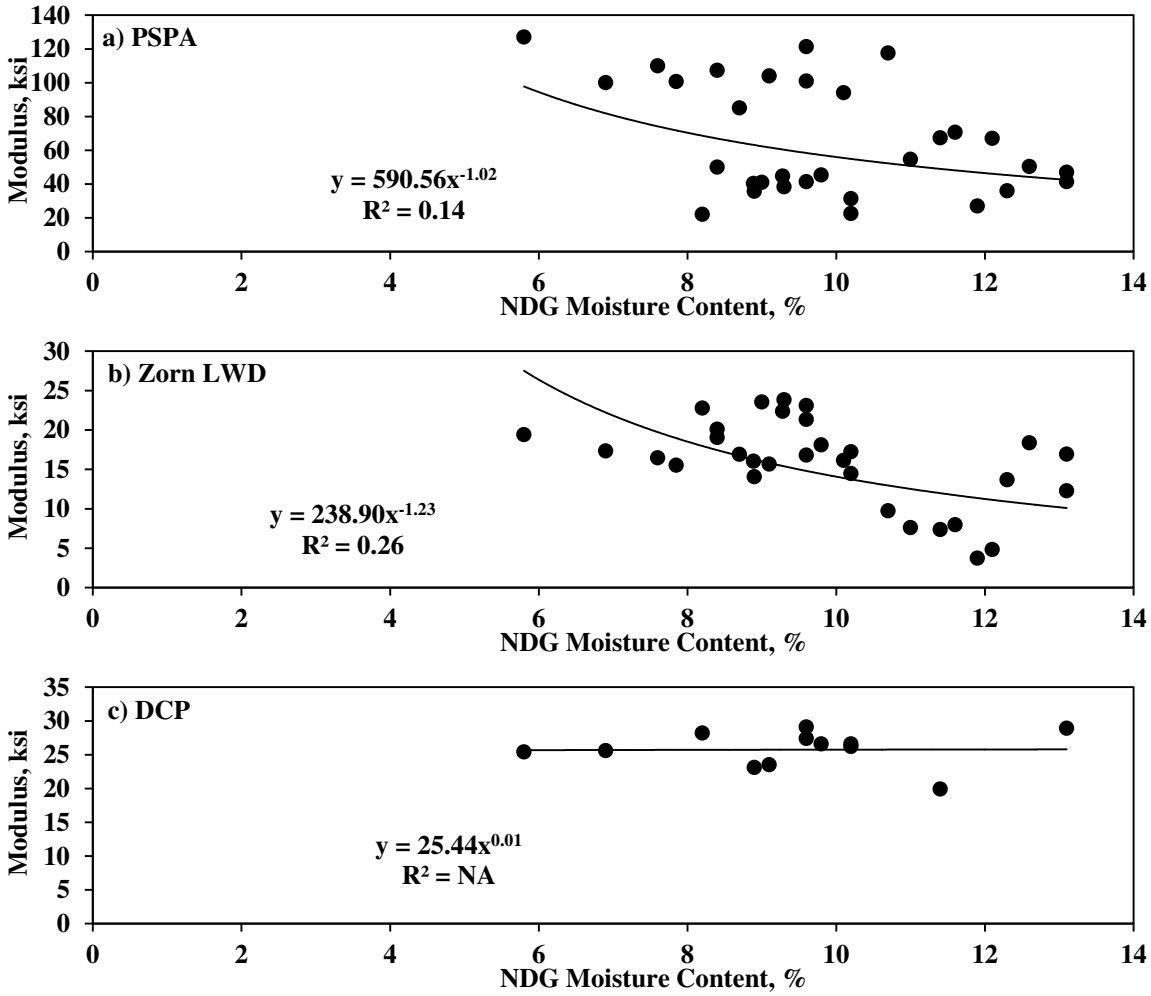

Figure H.7.6 – Measured Field Moduli Compared to NDG Moisture Contents for Base Layer

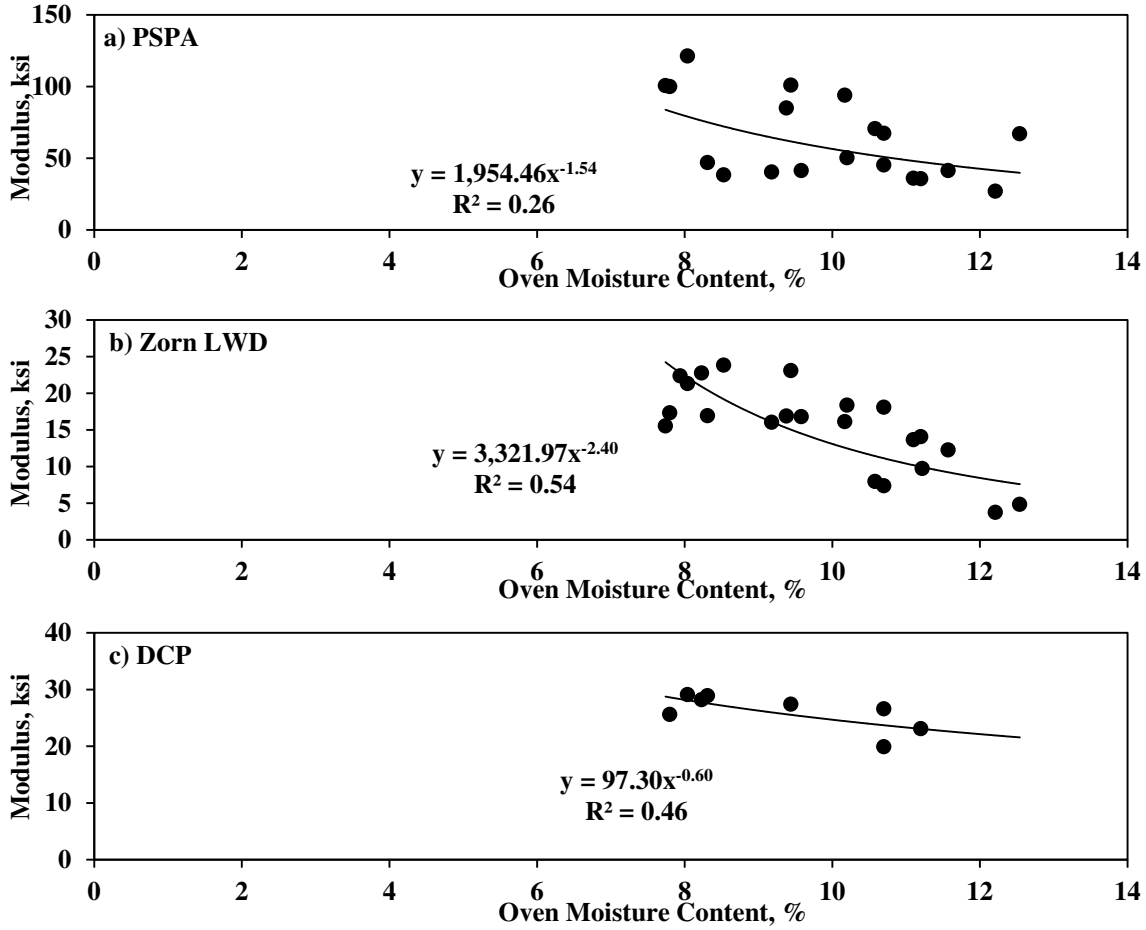

Figure H.7.7 – Measured Field Moduli Compared to Oven-Dry Moisture Contents for Base Layer

Figure H.7.8 depicts the relations between normalized moduli, M/M_{opt}, and normalized oven moisture contents, (MC-OMC)/OMC, and the correlations developed in Chapter 3. The relationship for the DCP follows the model developed from the laboratory MR results in Chapter 3 better, while the model developed from the FFRC moduli explains the LWD and PSPA data better.

Figure H.7.9 summarizes the correlations between the normalized modulus and the normalized degree of saturation, $S\text{-}S_{opt}$. Due to scatter in measured moduli, the predicted moduli at optimum content for different devices contain some uncertainty. The LWD data better match the MEPDG coarse-grained model, and the DCP and PSPA data show better correlation with Cary and Zapata model with *wPI*=0.

H.8 Establishing Field Target Moduli and Adjustment Factors

Subgrade: The target moduli for the subgrade were established for the LWD and Geogauge as discussed in Chapter 6. Laboratory-measured resilient modulus parameters (k'_1, k'_2 and k'_3) at OMC and MDD were used as input to these equations. Since PSPA directly measures the seismic properties of the layer, there is no need to use a relationship to establish the target modulus. Such value can be estimated directly from the Poisson's ratio and laboratory seismic modulus (see Chapter 6). The target moduli (at laboratory OMC) for the LWD, Geogauge and PSPA are reported in Table H.8.1. The estimated field moduli (based on the average field moisture contents, immediately after compaction) are also reported in Table H.8.1. Such values are not implemented in quality control process and are just an estimation of the anticipated field moduli (for each device) based on correlations developed in this project.

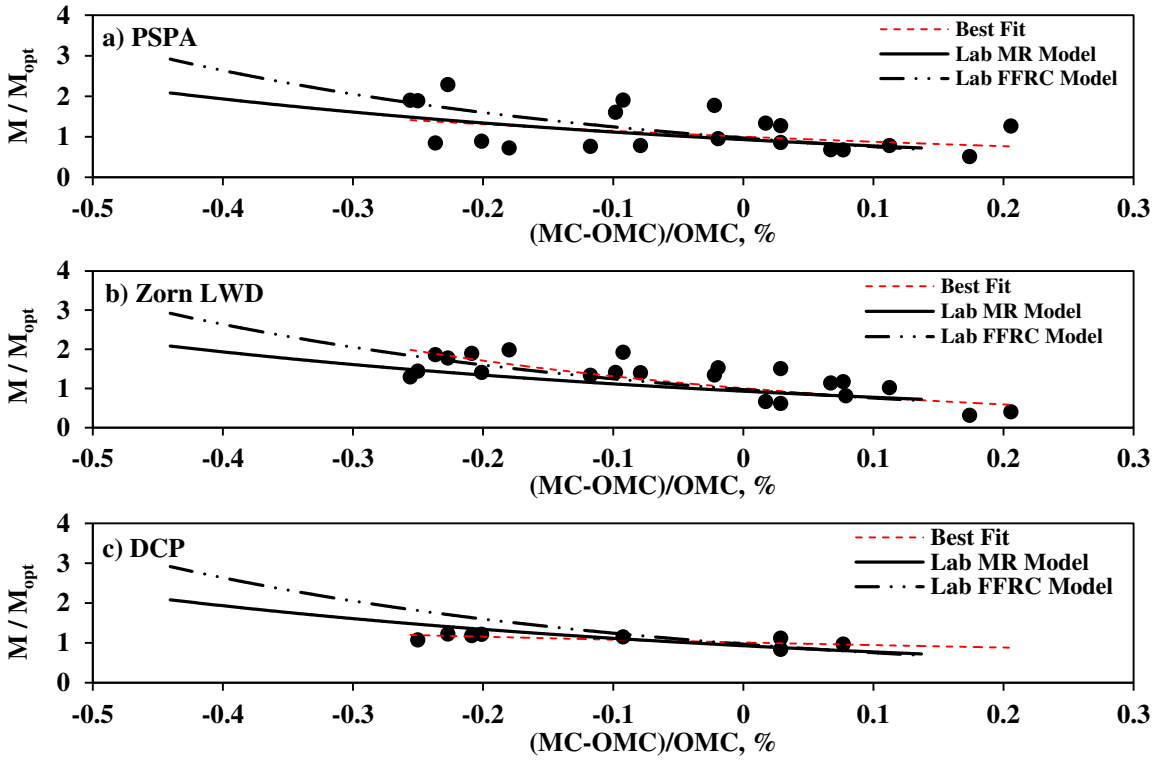

Figure H.7.8 – Correlation between Normalized Field Moduli and Normalized Oven Moisture Contents for Base Layer

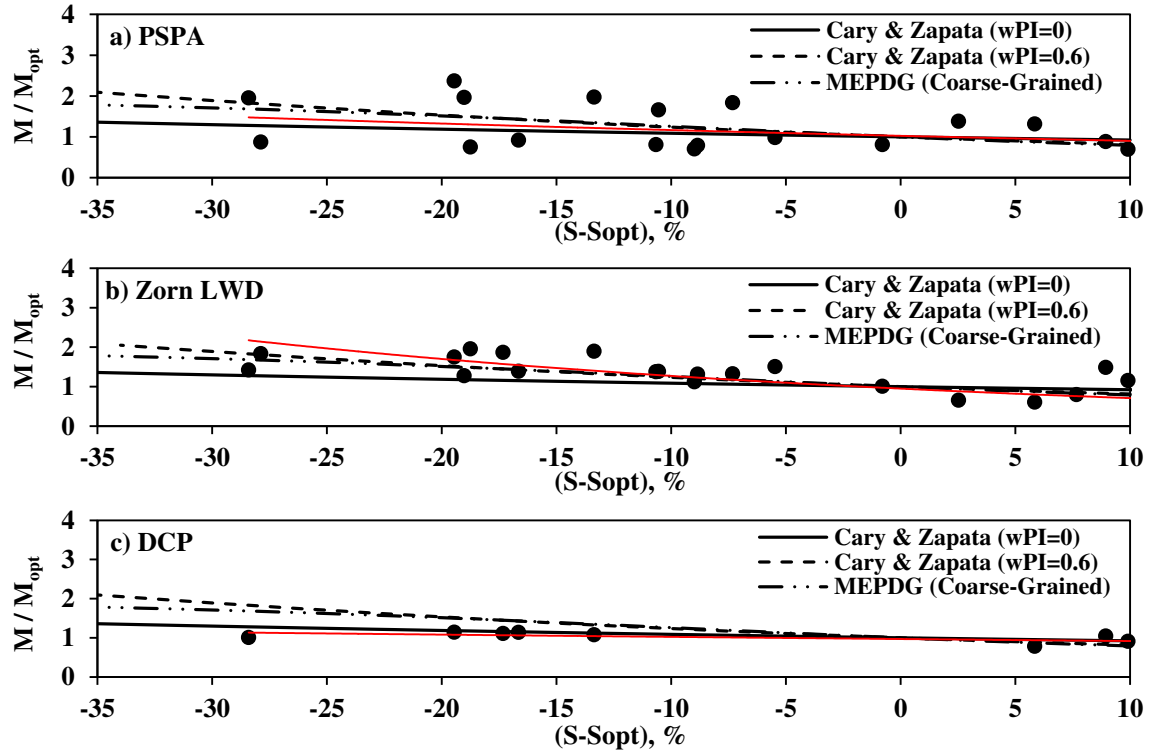

Figure H.7.9 – Correlation between Normalized Field Moduli and Normalized Degree of Saturation (using Oven moisture content) for Base Layer

Table H.8.1 – Estimated Target Moduli of Different Devices

Device	Target Modulus, ksi		Estimated Field Modulus at Compaction Moisture Content, ksi			
	Using Lab-Derived k' Parameters					
	Lab OMC-Soil A	Lab OMC-Soil B	Dry Section	Wet Section	Opt. Section	Production Section
PSPA	81	53	89	56	45	33
Geogauge	28	25	40	28	24	22
Zorn LWD	15	12	18	11	11	10
	Using Estimated[a] k' Parameters					
PSPA	NA	NA	NA	NA	NA	NA
Geogauge	14	14	17	12	13	12
Zorn LWD	4	4	5	4	4	4

[a] Estimated from index properties of materials

The k' parameters can also be estimated using index properties of the materials (see Appendix A). The target and estimated field moduli based on such k' parameters are also summarized in Table H.8.1. These moduli are marginally lower for the OMC moisture conditions and substantially less for the field moisture contents.

Base Layer: The target moduli for the LWD and PSPA for the base layer are summarized in Table H.8.2 using both the lab-derived k' parameters and the estimated ones from index properties. Estimated field moduli based on the NDG moisture results from field conditions (dry, optimum and wet sections) are also included in this table.

Table H.8.2 – Estimated Target Modulus of Different Devices for Base Layer

Device	Target Modulus, ksi	Estimated Field Modulus at Compaction Moisture Content, ksi		
	Using Lab-Derived k' Parameters			
	Lab OMC	Dry Section	Opt. Section	Wet Section
PSPA	154	246	64	28
Zorn LWD	26	27	22	16
	Using Estimated[a] k' Parameters			
PSPA	NA	NA	NA	NA
Zorn LWD	14	14	14	15

[a] Estimated from index properties of materials

Lime-Treated Subgrade: The target moduli and estimated field moduli for the PSPA and LWD for the lime-treated subgrade were also calculated using both lab-derived k' parameters and the ones estimated from the index properties. Since the moduli of lime-treated materials are not as sensitive to minor changes in moisture content, the target modulus at the average NDG field moisture content (20.5%) was considered the same as the target modulus at the laboratory OMC. Such value was 63 ksi for the PSPA and 30 ksi for the LWD.

H.9 Acceptance Scenarios for Modulus-Based Devices

Subgrade: Figure H.9.1 compares the average measured PSPA moduli (average of the three readings along line A, B and C considered as a lot) after compaction and about 24 hrs after compaction with the target moduli established from the lab-derived k' parameters at the OMC. The dry section marginally and the optimum and wet sections substantially fail the acceptance criterion of 80% of the target modulus at OMC. The estimated field moduli based on the compaction moisture contents are close to the measured field moduli for the wet and optimum sections, but significantly greater for the dry section.

Figure H.9.2 summarizes the field and target moduli from the Geogauge. The measured Geogauge moduli for all sections are greater than the target modulus. Such results might not be quite reliable due to high variability associated with the measurements at this site.

Figure H.9.3 summarizes the field results from the LWD. The dry and wet sections fail the established acceptance criteria marginally and the optimum section substantially. Having in mind that the embankment layer was stiff (see Figure H.5.1), the LWD and PSPA data can be considered complementary since the LWD measures the composite modulus of the subgrade and embankment while the PSPA measures the modulus of the subgrade layer only.

Figure H.9.4 compares the measured field moduli at the production section with the target moduli and estimated field moduli based on the laboratory results. As per LWD and Geogauge results, the section passes the acceptance criteria of 80% of established target modulus. According to the PSPA tests, the section fails. The estimated field moduli at the actual compaction moisture are close to the measured ones except for the Geogauge.

Base Layer: The same process of establishing the target moduli was applied to the base materials. Figure H.9.5 compares the PSPA field moduli with the established target moduli and the estimated field moduli at the field moisture contents. None of the sections passes the acceptance criteria. The estimated field moduli at the compaction moisture contents are fairly close to the measured field moduli for the optimum and wet sections but are significantly greater for the dry section. Unlike for the subgrade layer, the PSPA moduli of compacted layers typically decreased for measurements made 24 hours after the compaction of the base layer. This can be attributed to the extensive micro-cracks observed on the sections due to extremely hot July temperatures (in excess of 100^{o}F) and relatively high fine contents (about 20%) of the base.

Figure H.9.6 shows the same results as Figure H.9.5 but for the LWD. Based on the measurements immediately after compaction, all three sections marginally or substantially fail to meet the target modulus. The LWD moduli measured after 24 hours are typically greater the corresponding LWD moduli after compaction, especially for the wet section. Based on the measurements after 24 hours, all sections will meet the established target moduli.

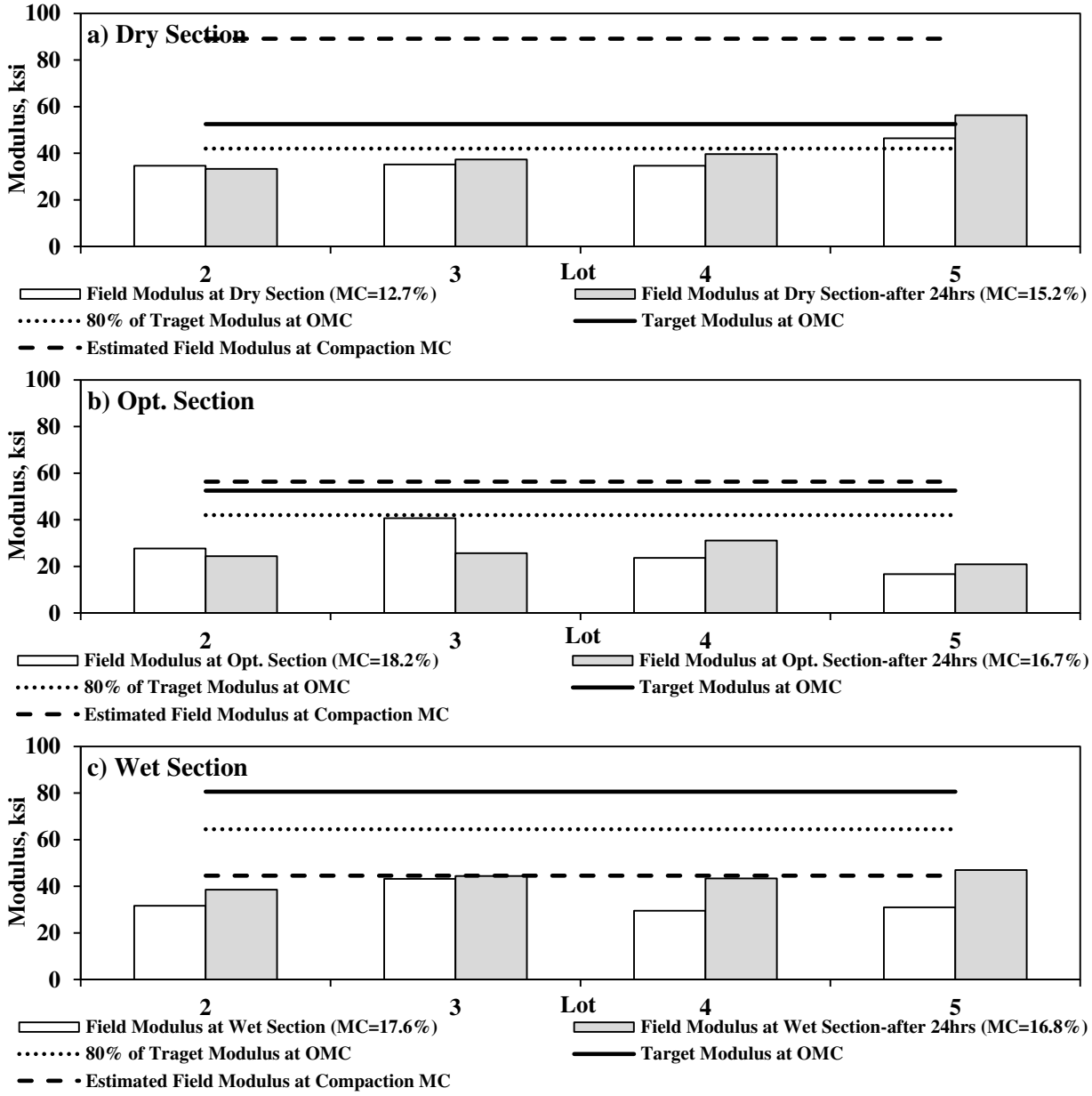

Figure H.9.1 – Comparisons of Field and Target Moduli of PSPA

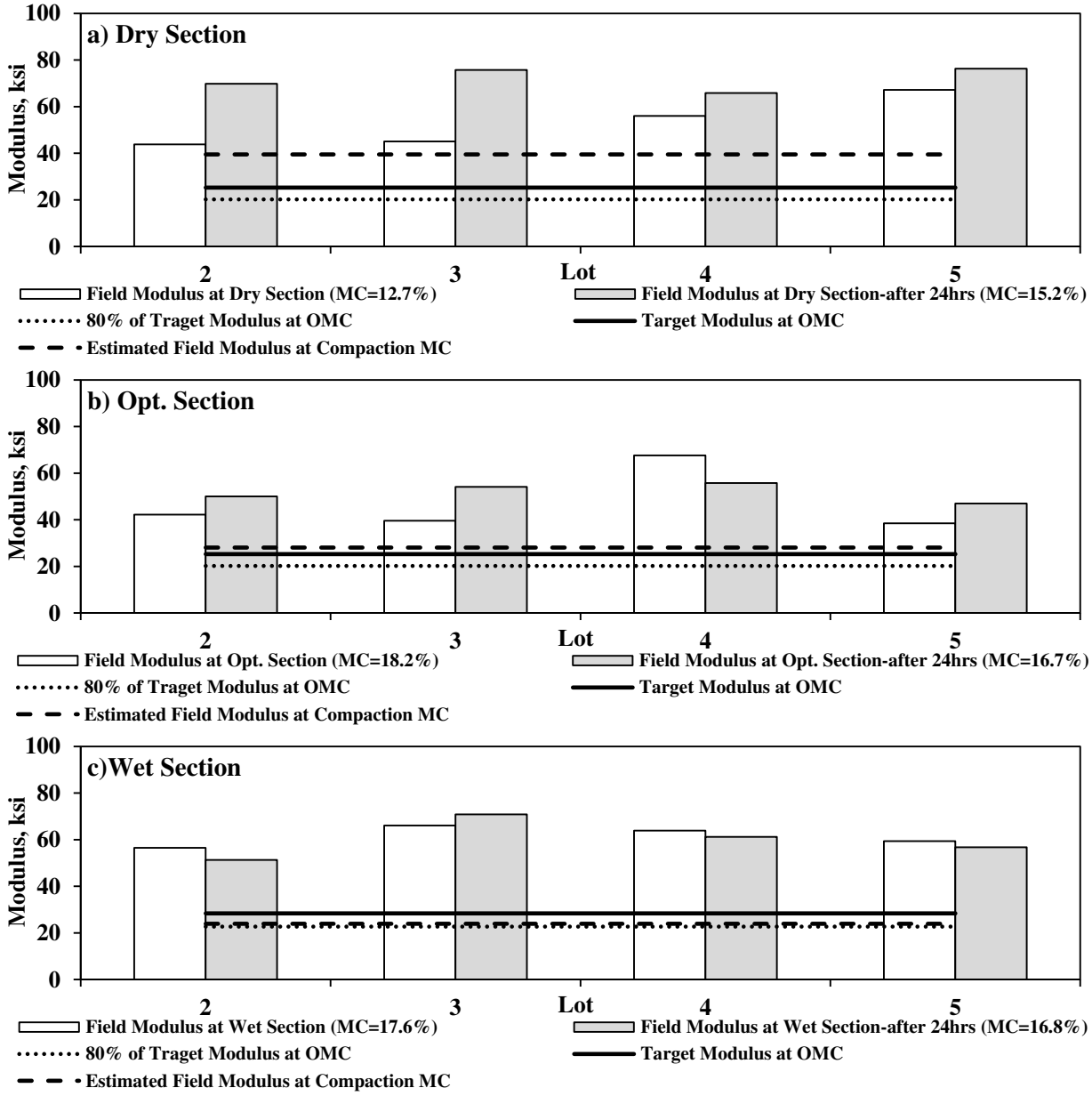

Figure H.9.2 – Comparisons of Field and Target Moduli of Geogauge

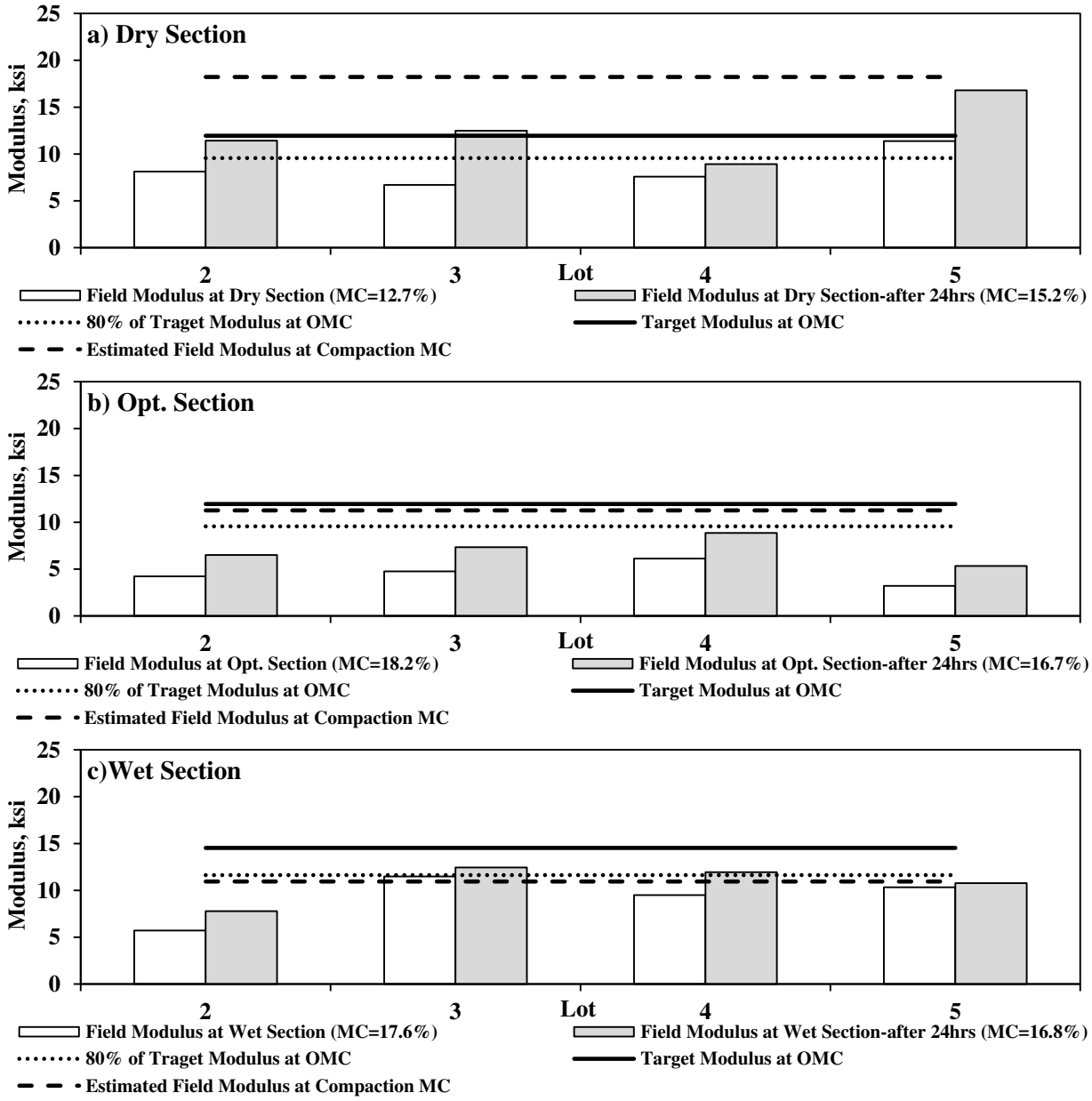

Figure H.9.3 – Comparisons of Field and Target Moduli of Zorn LWD

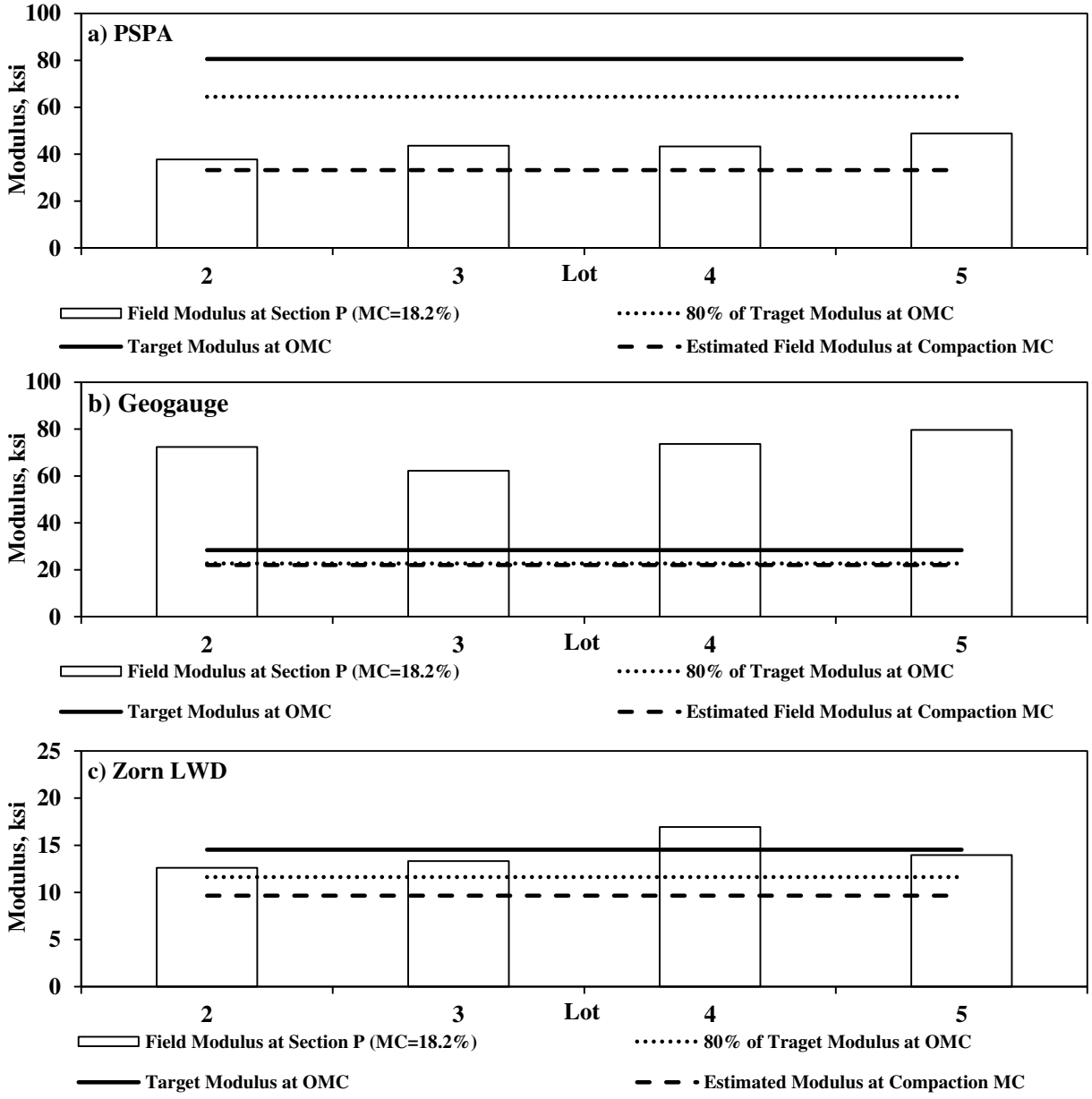

Figure H.9.4 – Comparisons of Field and Target Moduli of Devices on Production Section of Subgrade Layer

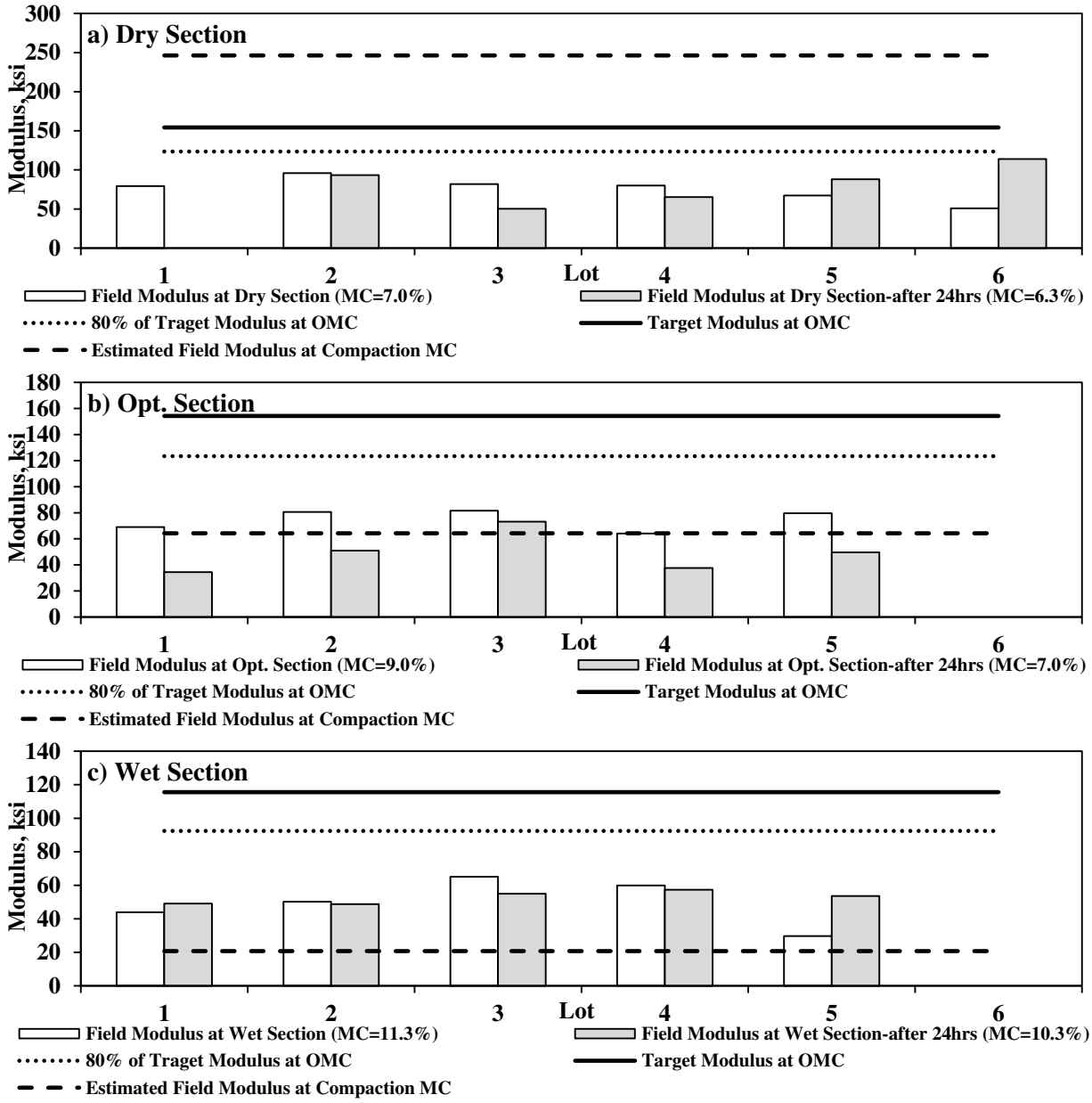

Figure H.9.5 – Comparisons of Field and Target Moduli of PSPA for Base Layer

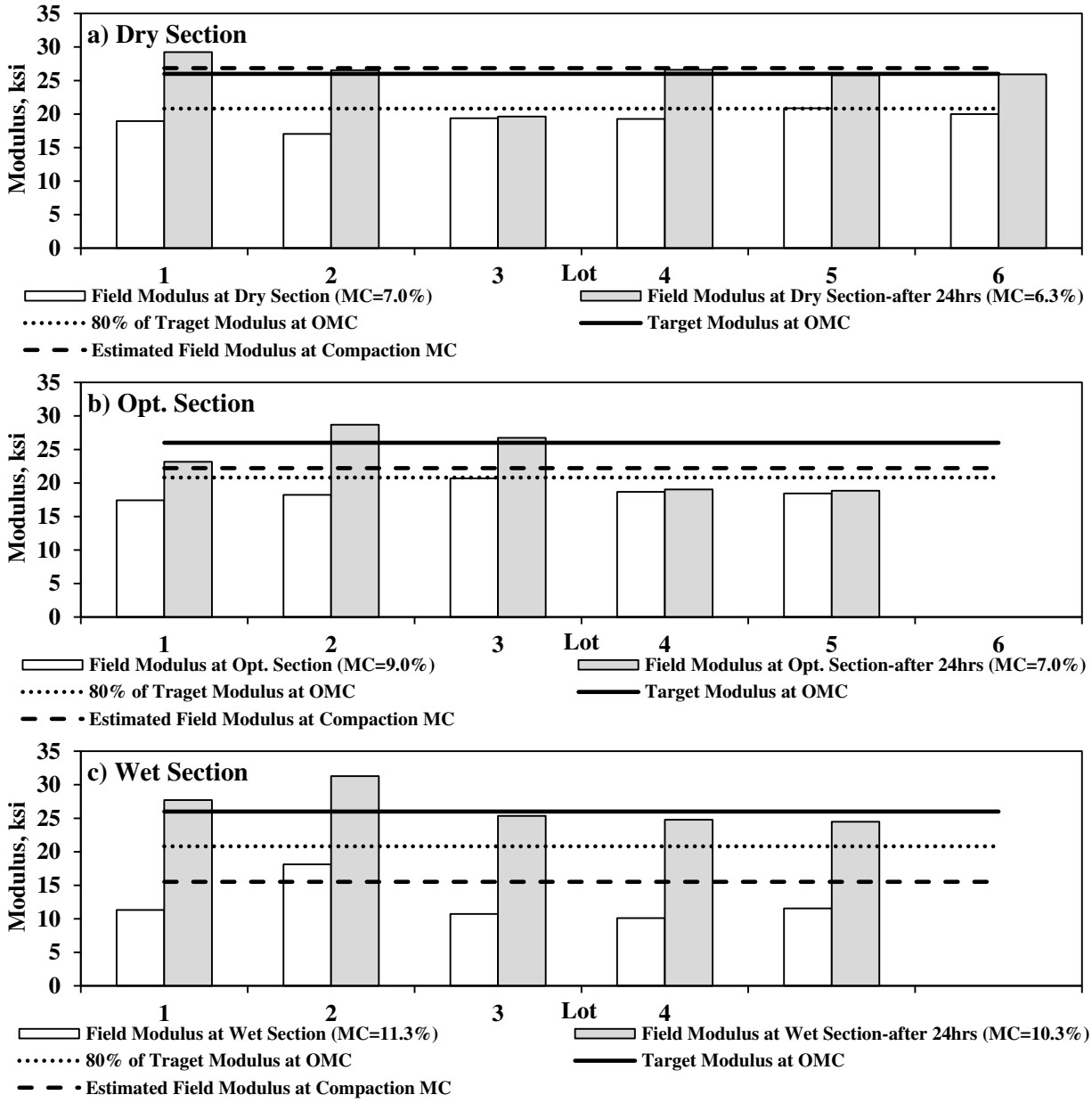

Figure H.9.6 – Comparisons of Field and Target Moduli of Zorn LWD for Base Layer

H.9 Intelligent Compaction

Subgrade Layer: This section presents the analysis and interpretation of the roller measurement values collected during the subgrade construction at Site I.1. The IC roller drum and the soil interaction to compaction process were captured using the Compaction Meter Value (CMV). The CMV technology uses an accelerometer to measure the roller drum vibration in response to the soil behavior during the compaction. Figure H.9.1 presents the distributions of the roller CMV with the number of roller passes for the three subgrade sections (Pass 3 in Figure H.9.1a means two passes of the sheep foot roller and one pass of the IC roller). From Figure H.9.1a, the CMV distribution for the dry section tends toward higher values with an increase in the compaction effort. From Figure H.9.1b, the CMV distributions for the OMC section after six and nine roller passes are close, indicating that six passes of the roller were optimal. Eleven roller passes were required to achieve the optimal compaction for the wet section. From

Figure H.9.1c, the variations in the distribution of the CMV measurements of the wet section are comparable to the dry and OMC sections. However, the CMV measurements decrease with the increase in the number of passes for the wet section.

The contribution of the subgrade layer placed on the embankment was explored by comparing the CMV distributions before and after the placement of the subgrade. From Figures H.9.2a and H.9.2b, the CMV distributions before (labeled Mapping) and after the placement of the subgrade layer were similar. Since the embankment and subgrade materials were similar, one can conclude that the subgrade layer was placed properly. However, the CMV distribution for the embankment support of the wet section in Figure H.9.2c is substantially greater than the CMV distribution after the subgrade placement. This signifies the influence of moisture control during compaction for quality management.

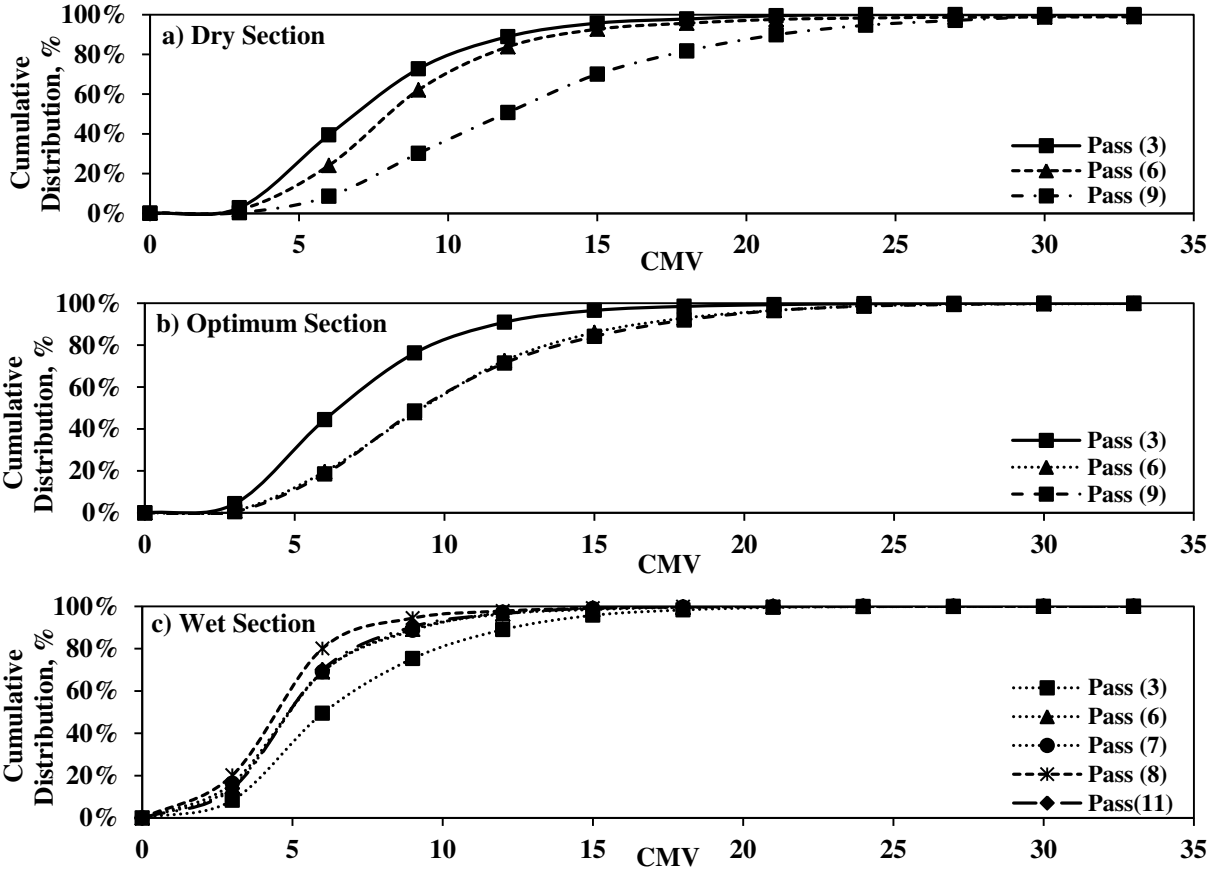

Figure H.9.1 – Distributions of CMVs with Passes for Different Subgrade Sections

The influence of the rolling pattern and time of testing for quality assurance was assessed by studying the roller responses immediately after and 16 to 24 hrs after compaction. The rolling patterns were varied from the normal sequence to a forward and reverse sequence (To-and-Fro) at different times. Figures H.9.3a and H.9.3b present the distributions of the CMV values for the final pass and 16 hrs later with regular and to-and-fro patterns of rolling. For the dry and OMC sections, the CMV distributions remain comparable at different times and rolling sequences. However, for the wet section (Figure H.9.3c), the distributions of the CMV values after 16 hrs are substantially greater as compared to 24 hrs later and to the final pass. Figure H.9.4 presents the distributions of the CMV values for the production section before and after subgrade compaction. The two CMV distributions are comparable since the embankment and the subgrade material used were similar.

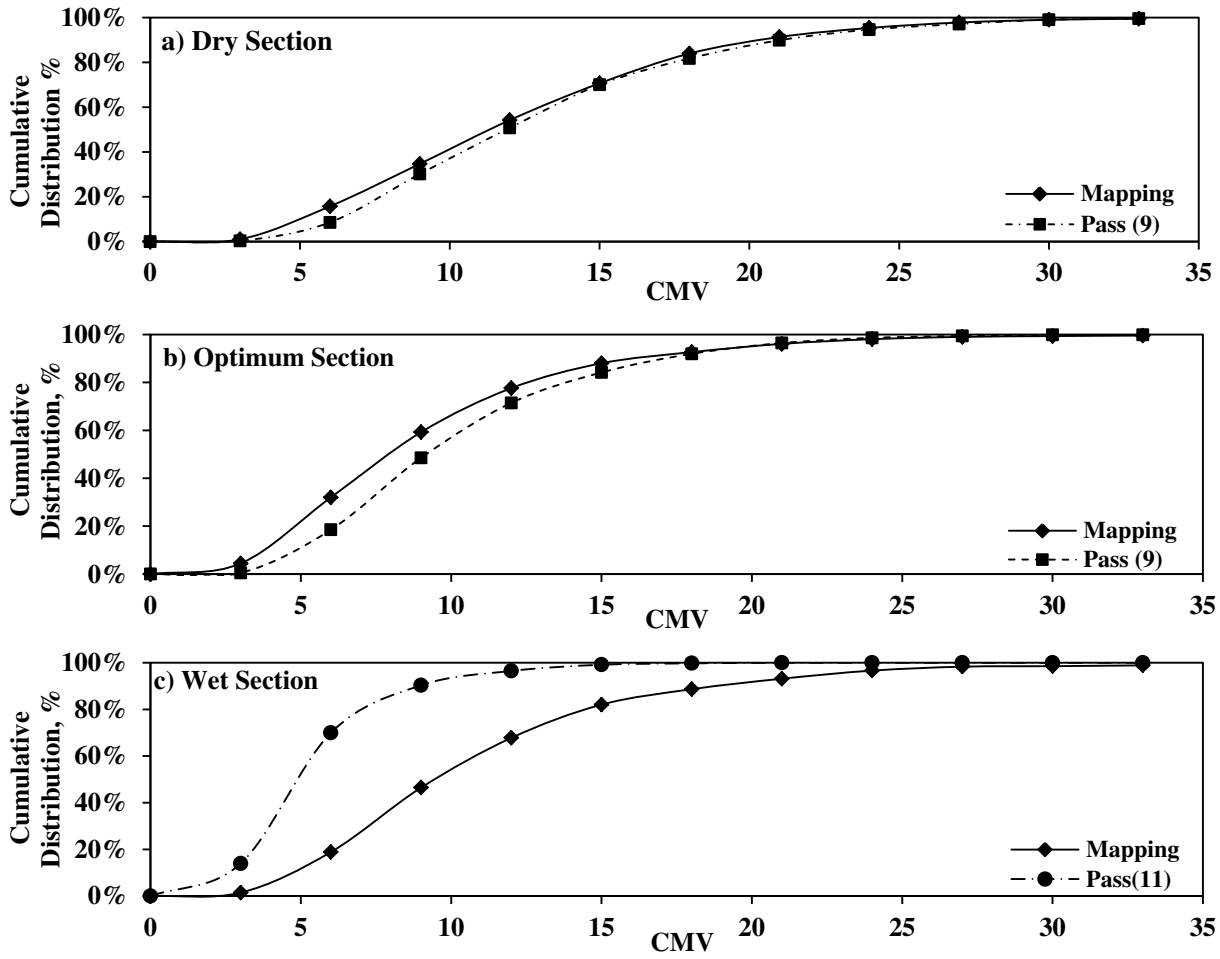

Figure H.9.2 – Impact of Subgrade Placement after Compaction of the Embankment Layer

Base: The construction sequence of the base layer was quite different as compared to the subgrade layers. The 10 in. thick layer of base material was compacted by placing 2 to 2 ½ in. thick successive lifts of base material. Each lift was graded and watered before rolling. Figure H.9.5 presents the distributions of the CMV measurements with the number of passes for the sections placed at different moisture contents. For the base layer constructed towards the dry side of the OMC in Figure H.9.5a, the increase in the roller passes (up to 8 passes) reduces the variability in the CMV distributions (i.e., a more uniform section). For both the dry and OMC sections, the CMV measurements are more uniformly distributed for Pass 6 and Pass 8 when compared to the lower and higher number of passes.

The wet section was reworked after 10 passes to achieve the required moisture content. Hence, four additional roller passes were required to meet the quality requirements similar in the dry and OMC sections. From Figure H.9.5c, the distributions of the CMV values remain similar until the 10^{th} roller pass. Substantial differences in the CMV distributions can be observed after the 12th and 14th passes. The differences in the CMV distributions can be attributed to the rework carried out and the base layer being compacted as a single lift. Hence, the CMV values are also substantially higher than Passes 2 to 10.

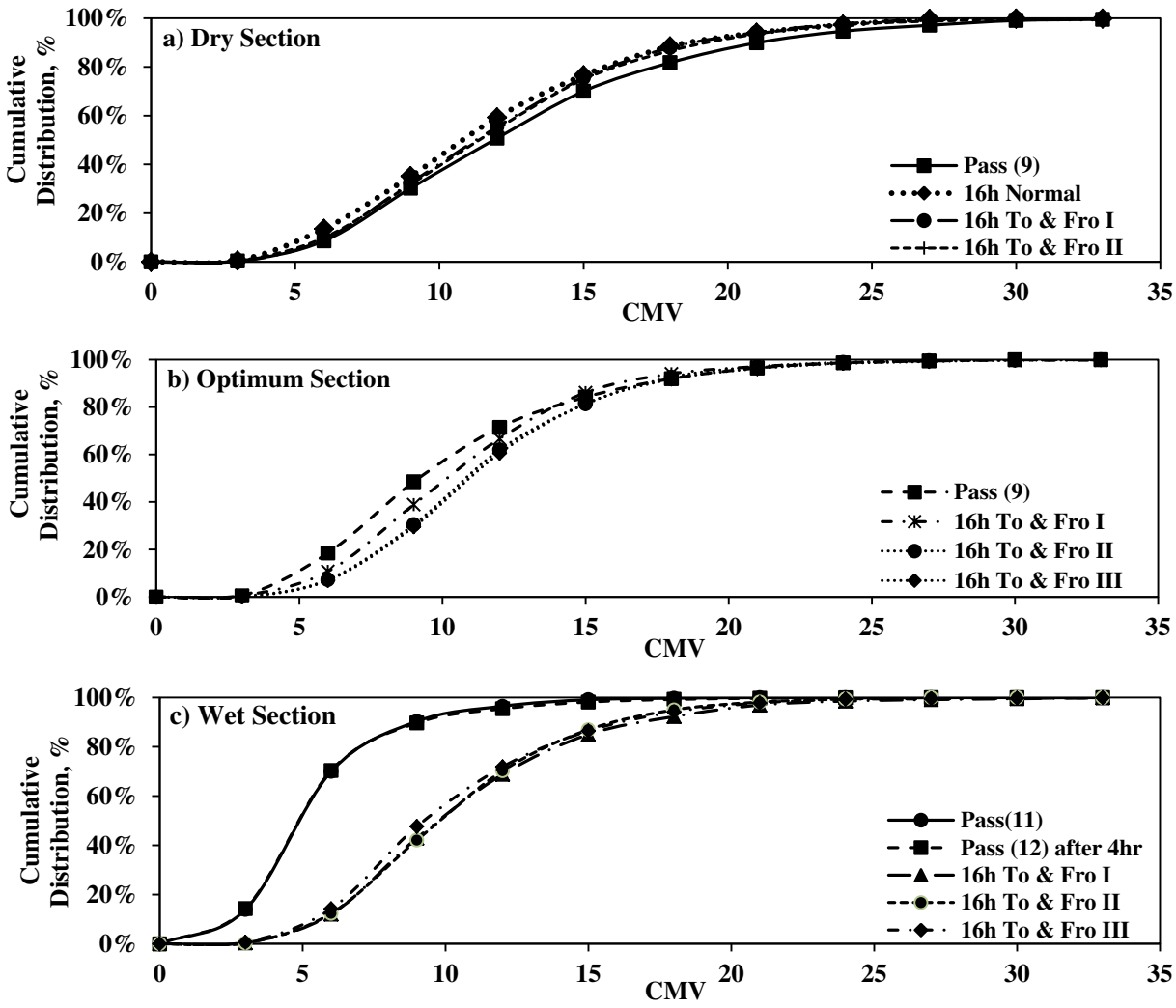

Figure H.9.3 - Influence of Time on Roller Measurement Values for Subgrade Sections

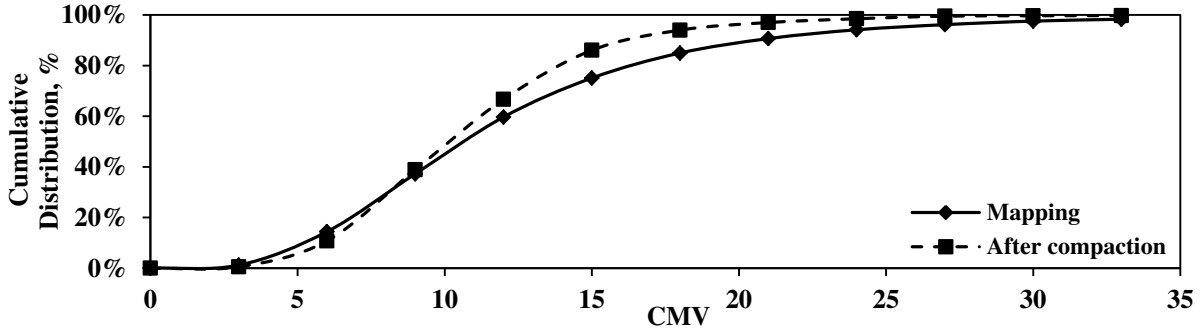

Figure H.9.4 - Distributions of CMV with Passes for Production Section

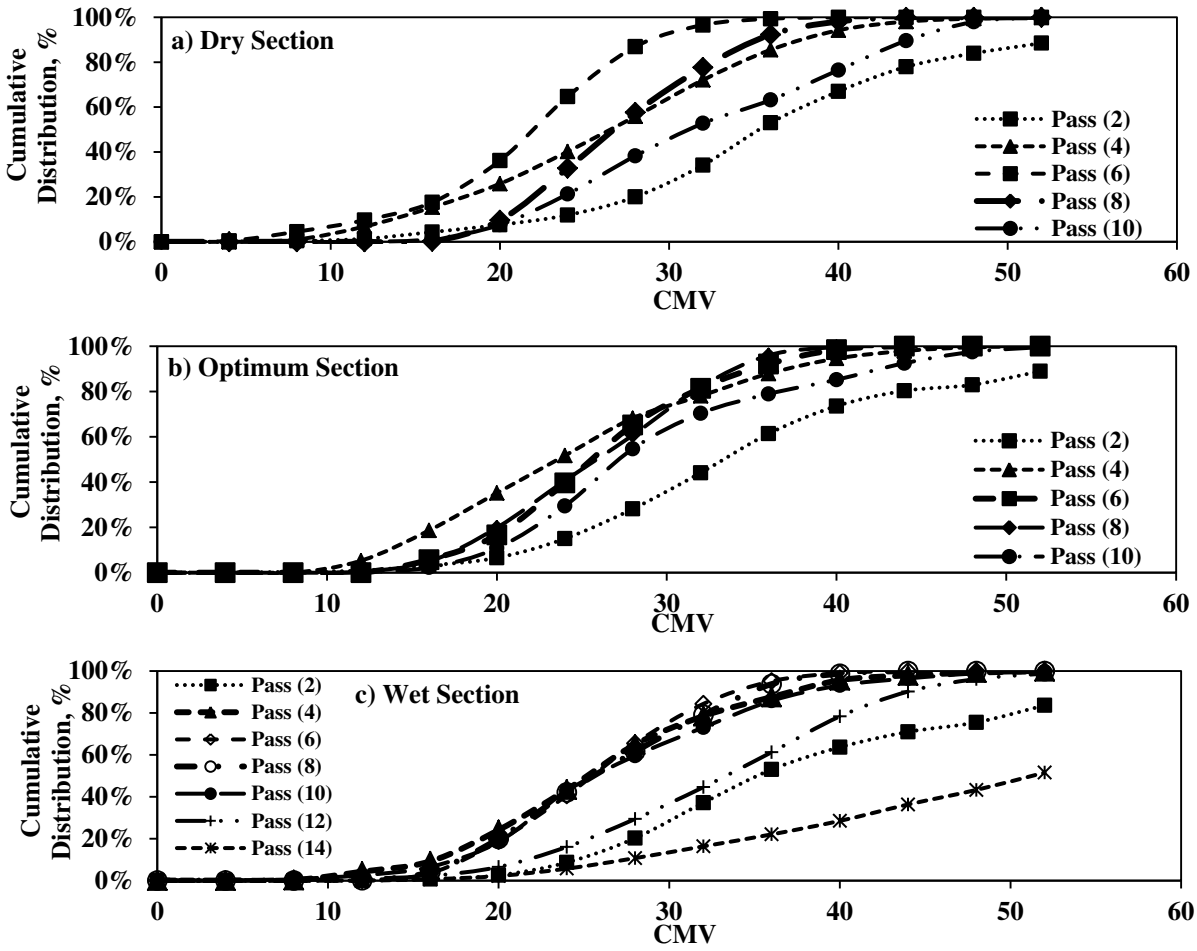

Figure H.9.5 - Distributions of CMV with Passes for different Base Sections

Figures H.9.6 and H.9.7 summarizes the correlations between CMV and NDG dry densities for all the testing sections on subgrade and base layer. There is not a strong relationship between these two parameters.

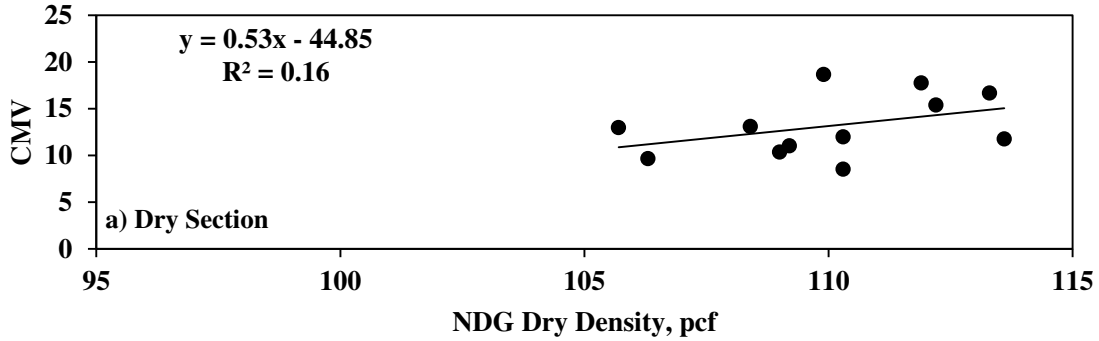

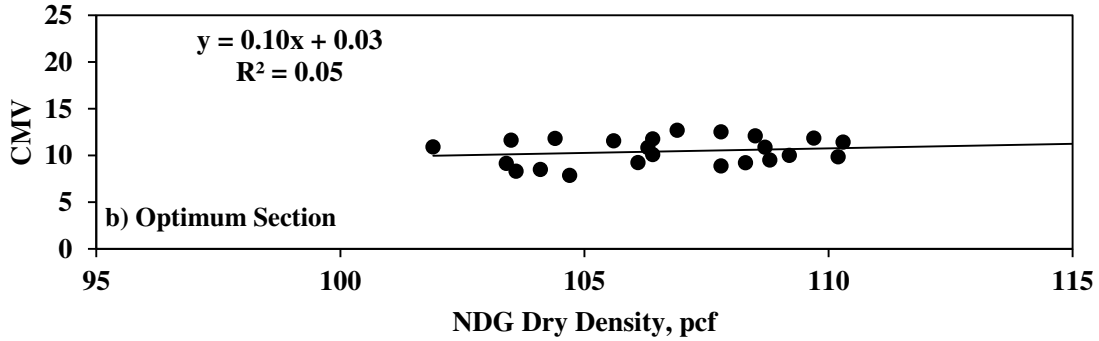

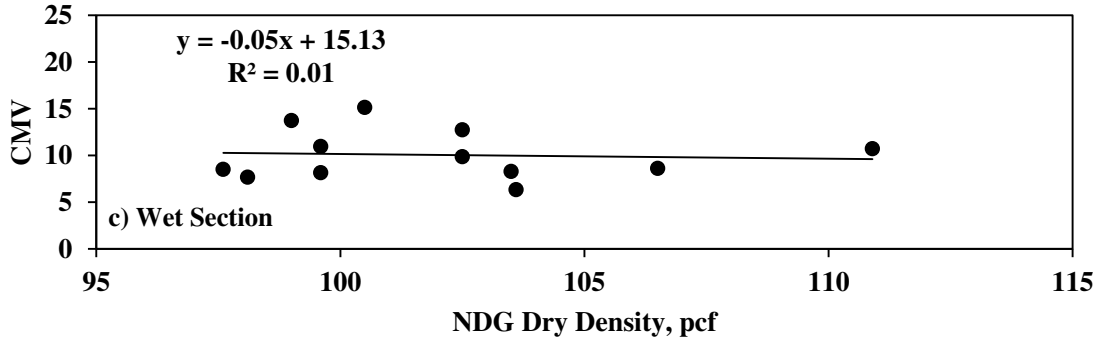

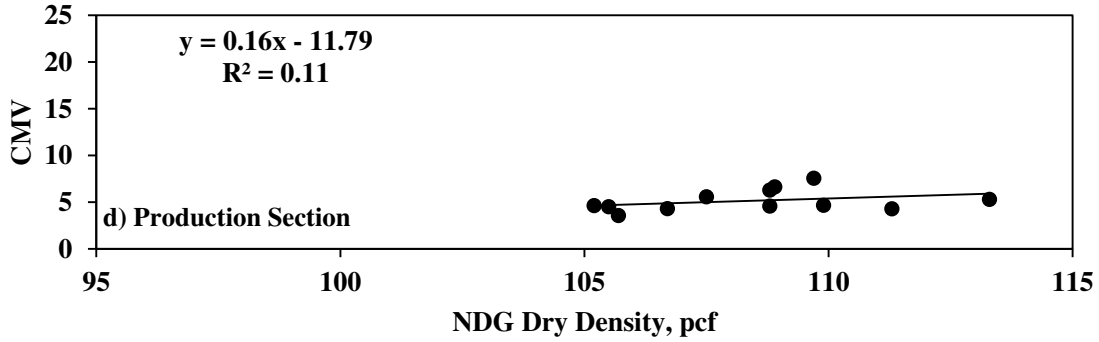

H.9.6 - Relations between the NDG Dry Density and the CMV for Subgrade Sections

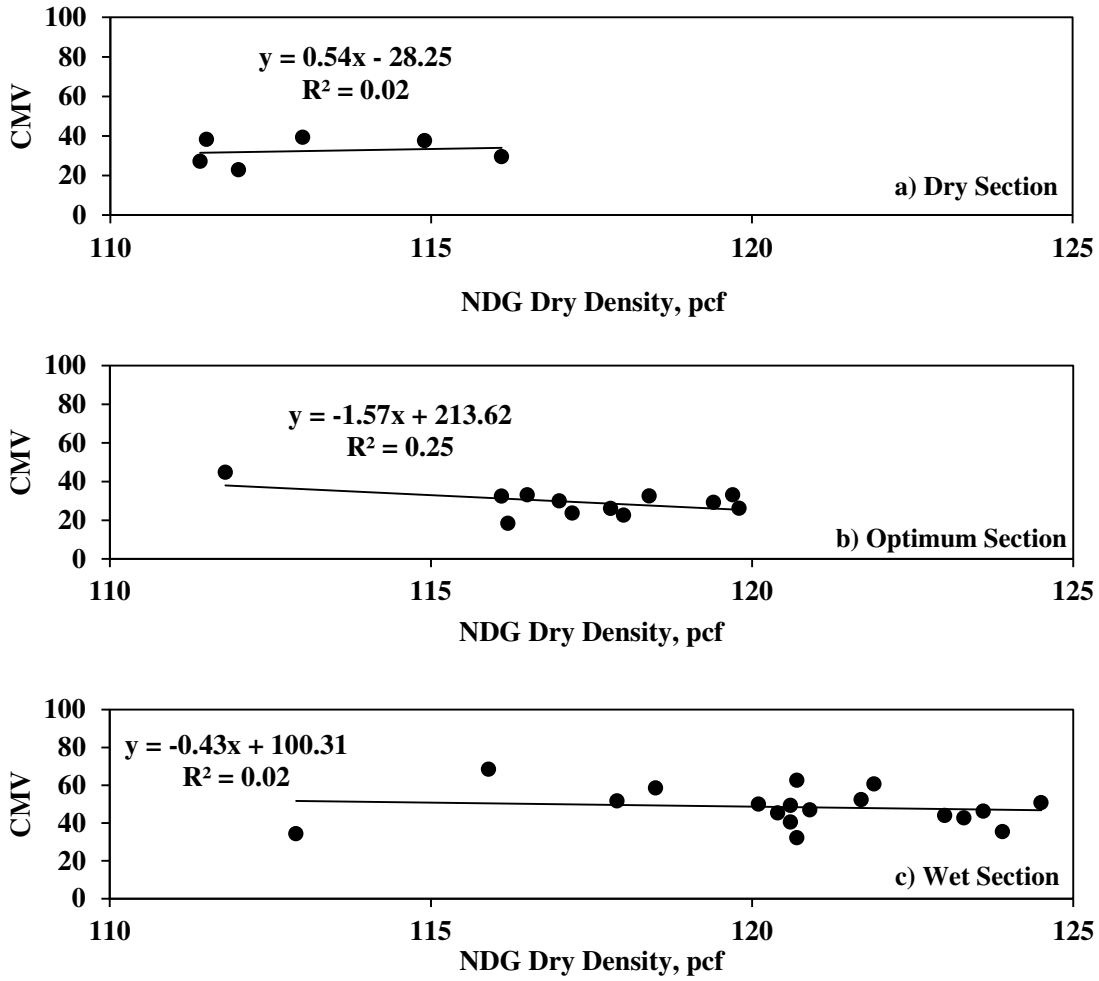

Figure H.9.7 - Relations between the NDG Dry Density and the CMV for Base Sections

Appendix I

OBSERVATIONS FROM IMPLEMENTATION OF SPECIFICATION

Site I.2

I.1 Introduction

The second field evaluation was carried out at a site in Tarrant County near Fort Worth, Texas. This project was a part of the reconstruction of the existing lanes and adding toll lanes along IH 35W in Fort Worth, TX. As reflected in Figure I.1.1, the project site is a bypass close to the intersection of IH 35W and State Highway 81.

Figure I.1.1 – Location of Field Evaluation Site on I-35W Fort Worth, TX

Only the subgrade layer was evaluated in this study. Figure I.1.2 depicts the embankment and subgrade layers during construction. The test spots were marked on the prepared embankment layer and then mapped to the compacted subgrade layer using GPS coordinates. Test segments on both the embankment and subgrade layers consisted of three 150-ft-long by 25-ft-width sections. An 8-in. thick subgrade layer was placed, leveled and compacted at three sections (dry of OMC, OMC and wet of OMC). Both a sheep foot roller and a vibratory IC roller were utilized to compact the materials. One pass of the IC roller was used after every two passes of the sheep foot roller to measure the layer responses. Following the completion of each construction phase by the contractor, the research team conducted the NDT tests followed by NDG tests performed by DOT staff.

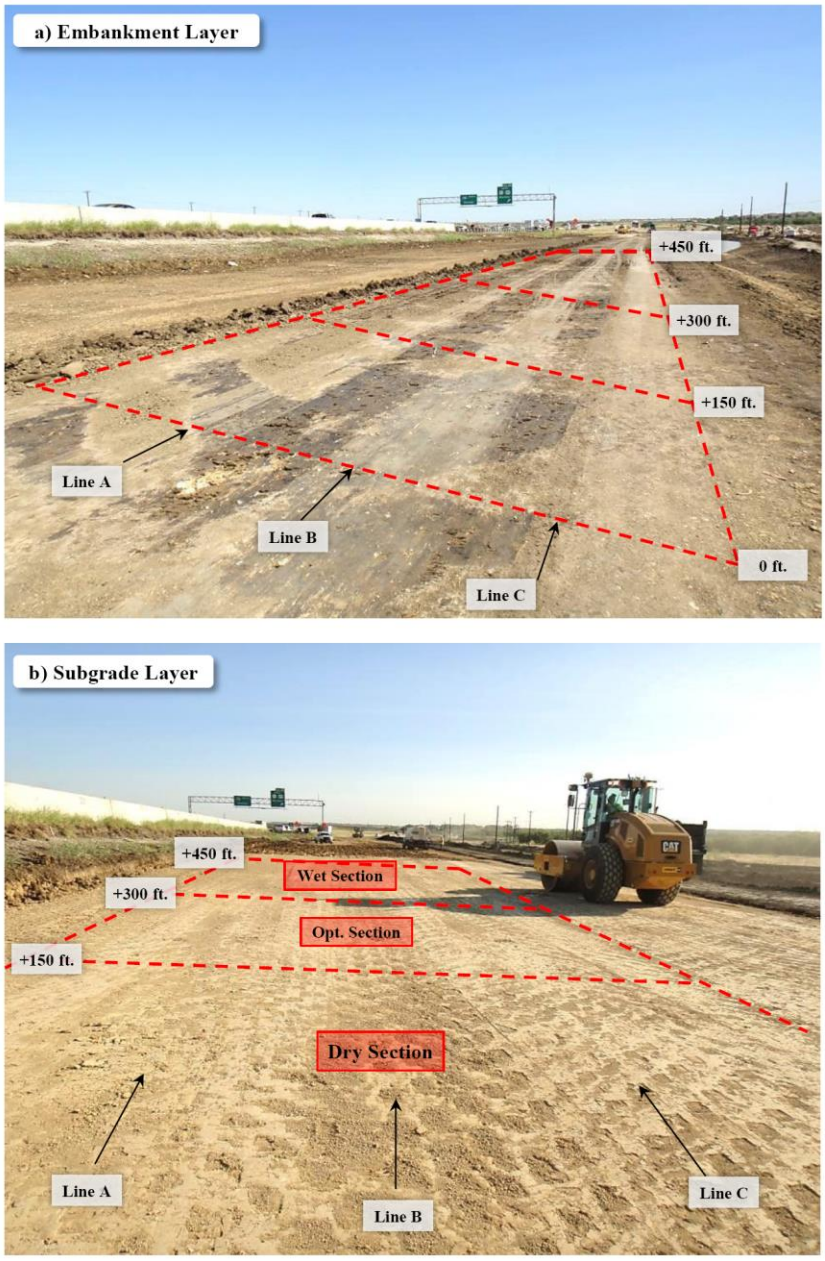

Figure I.1.2 – Test Sections along IH 35, Tarrant County, TX

I.2 Laboratory Results

Index properties of the subgrade are summarized in Table I.2.1. Gradation curve of the subgrade materials is depicted in Figure I.2.1. This material was classified as high-plasticity clay as per USCS. The optimum moisture content and maximum dry unit weight obtained as per standard Proctor tests (AASHTO T99) are also reported in Table I.2.1. Based on previous tests of the depot materials, the reported OMC was 16.3%. As such, the target OMC during field tests was 16.3% and not the 21.2% obtained from the actual material sampled.

Table I.2.1 - Index Properties of IH 35W Subgrade

Gradation %				USCS Class.	Specific Gravity	Atterberg Limits			Moisture/Density	
Gravel	Coarse Sand	Fine Sand	Fines			LL	PL	PI	OMC, %	MDUW,** pcf
0	8.0	2.5	89.4	CH	2.76	55	15	40	21.2	101.1

*OMC = Optimum Moisture Content, **MDUW = Maximum Dry Unit Weight

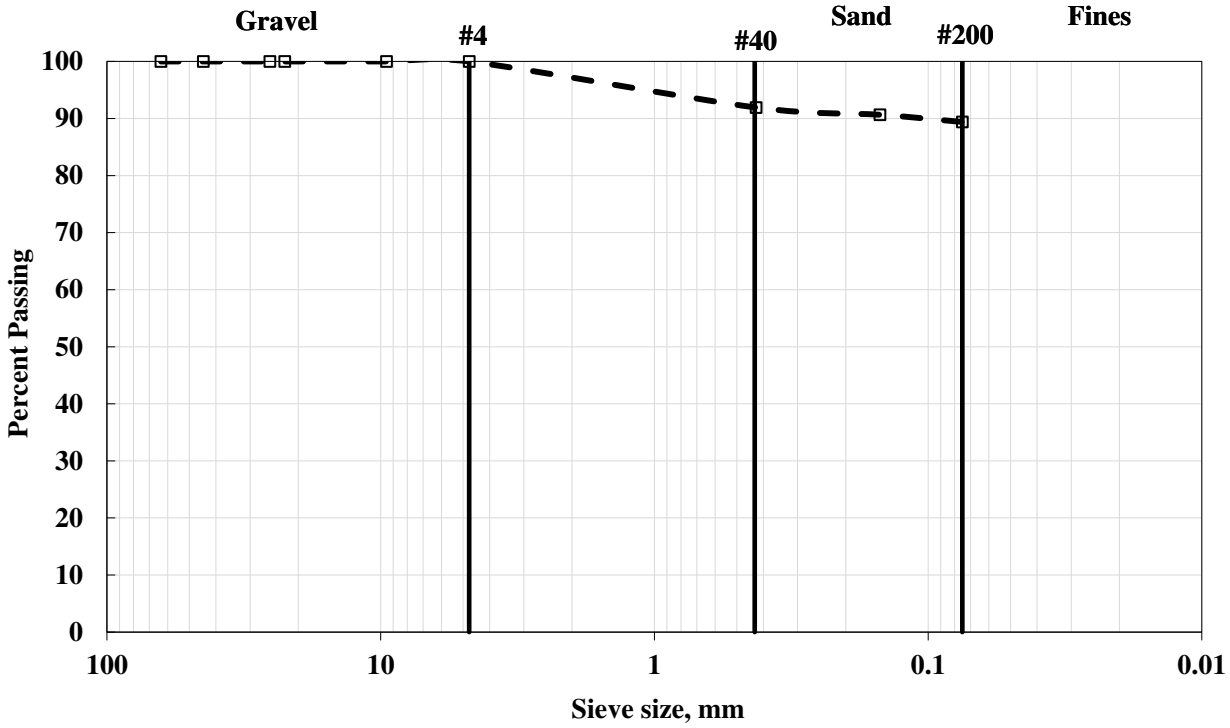

Figure I.2.1 – Gradation Curve of IH 35W Fort Worth Subgrade

The laboratory resilient modulus (MR) and FFRC tests were performed on specimens prepared and compacted under the laboratory conditions at the OMC, dry of OMC and wet of OMC, as summarized in Table I.2.2. Figure I.2.2 illustrates the variations of the laboratory FFRC moduli and representative MR values with moisture content. The two measured moduli decrease drastically when the specimens are prepared wet of OMC.

Table I.2.2 – Laboratory Results of MR and FFRC Tests of IH 35W Subgrade

Target Moisture Content	Actual Moisture Content, %	Dry Density, pcf	Degree of Saturation, %	FFRC Modulus, ksi	Nonlinear Parameters			Represent-ative MR, ksi*
					k'_1	k'_2	k'_3	
OMC-2	16.8	100.0	64	29	1075	0.27	-1.65	14
OMC-1	19.1	101.9	76	28	1012	0.22	-1.52	13
OMC	21.5	102.0	86	23	795	0.30	-2.91	8
OMC+1	23.8	101.0	93	9	127	0.68	-3.00	2
OMC+2	25.1	99.3	94	6	91	0.69	-3.00	1

* from Eq. 3.2.1 based on τ_{oct} and θ values of 3 psi and 12.4 psi for subgrades as recommended by NCHRP Project 1-28A.

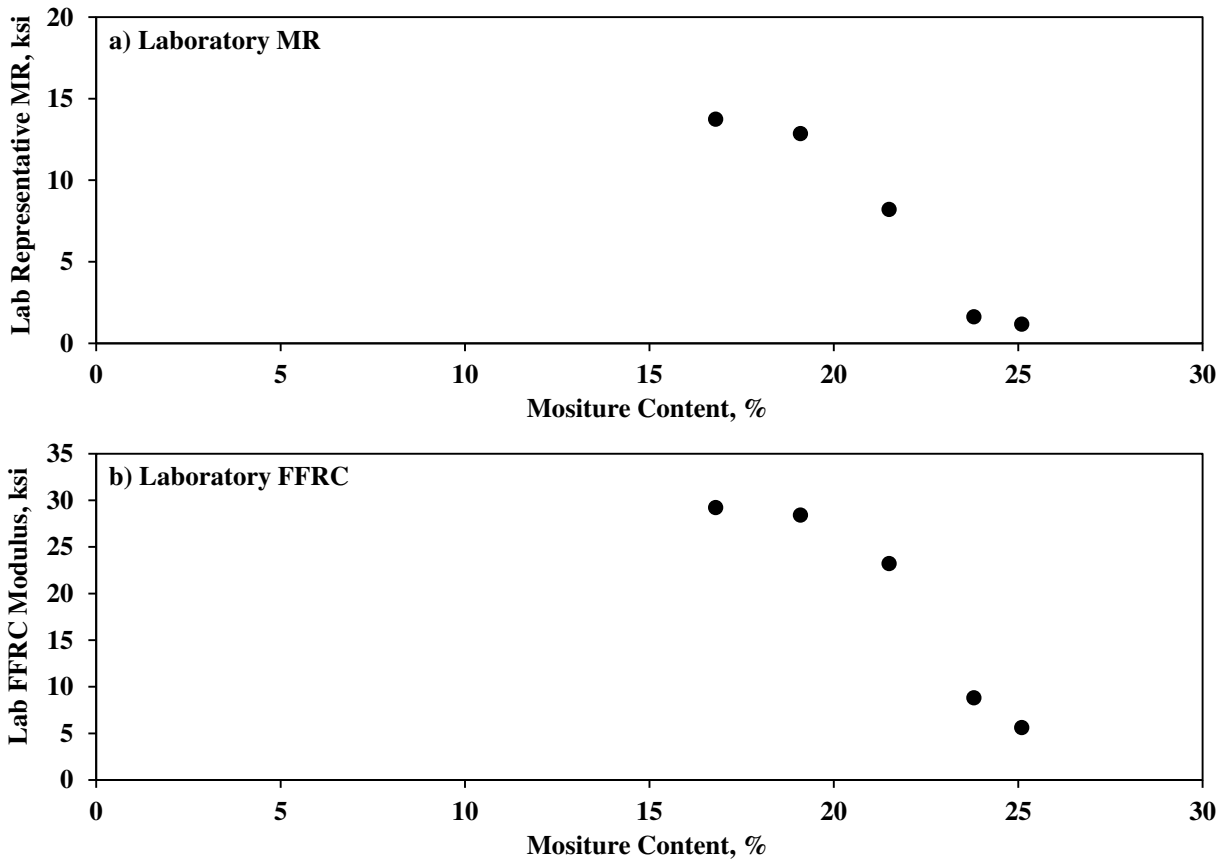

Figure I.2.2 – Variation of Laboratory MR and FFRC Modulus with Moisture Content

I.3 Field Testing Program

Embankment Layer - The prepared embankment layer was tested before the placement of the subgrade layer. As illustrated in Figure I.3.1, field-testing was carried out on three side-by-side sections to obtain the baseline information. An Intelligent Compaction (IC) roller was also utilized in this project to assess the quality of compaction. The following tests were performed on the three embankment sections along rows A and C:

- Soil Density Gauge (SDG)
- Zorn Light Weight Deflectometer (LWD) as per ASTM E2835
- Portable Seismic Property Analyzer (PSPA)
- Nuclear Density Gauge (NDG)
- Geogauge

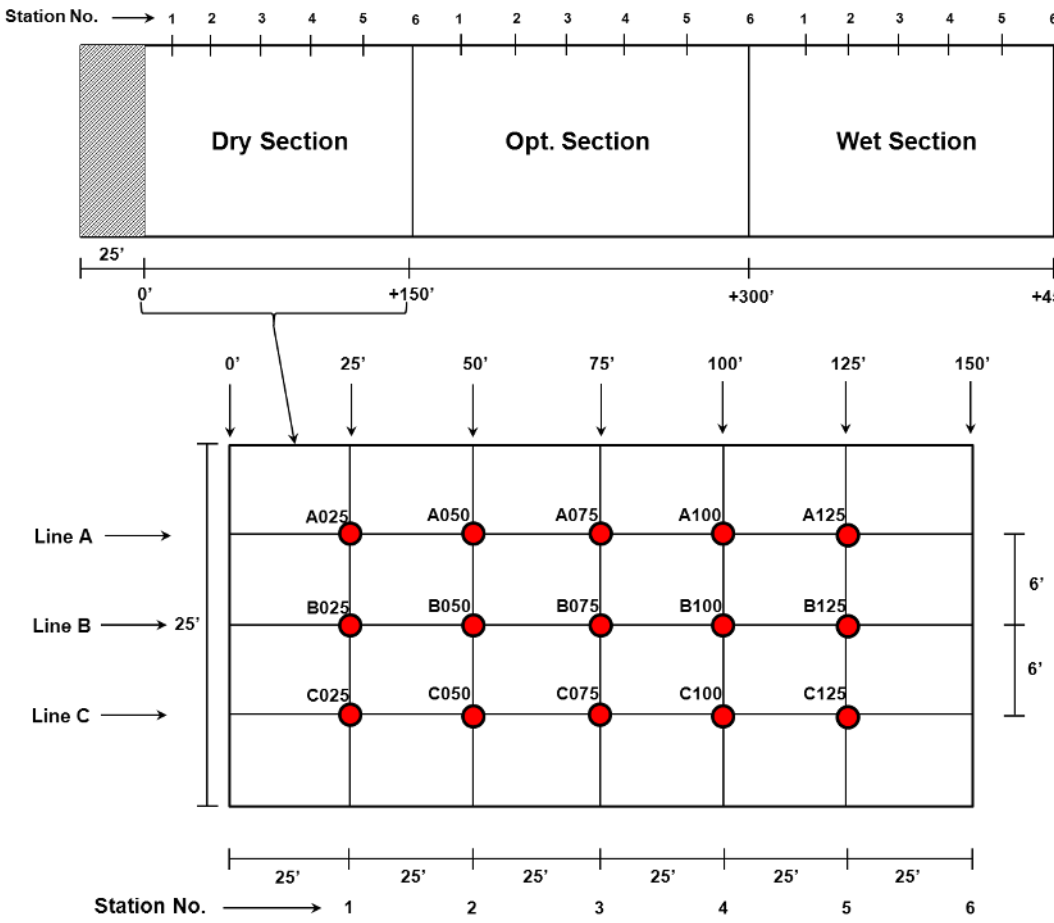

Figure I.3.1 – Test Locations on Embankment and Subgrade along IH 35W Section

Subgrade Layer - After testing of the embankment, the subgrade layer was placed, leveled and compacted for each of the three sections. The IC roller was also utilized to evaluate the subgrade layers. The first section of the subgrade layer was nominally placed at dry of OMC, the second section at OMC, and the third section at wet of OMC. The following tests were performed on the compacted subgrade layer along lines A, B and C (see Figures I.3.2):

- Soil Density Gauge (SDG): one test per point
- Zorn Light Weight Deflectometer (LWD) in triplicate as per ASTM E2835
- Geogauge: in duplicate as per ASTM D6758
- Portable Seismic Property Analyzer (PSPA): three to five readings
- Nuclear Density Gauge (NDG) one test per point
- Dynamic Cone Penetrometer (DCP) one test per point

In addition, soil samples were collected from the compacted subgrade layer at many points to estimate their oven-dried moisture contents.

I.4 Evaluating Moisture-Density Devices' Results

Embankment Layer - The NDG test results on top of the prepared embankment layer are shown in Figure I.4.1. The average NDG moisture contents was 17.6%, which was about 3.6% less than the actual OMC (from our laboratory tests) and 1.3% above the contractor's target OMC. The average dry density was 106.8 pcf, which was 5.7 pcf greater than the MDD.

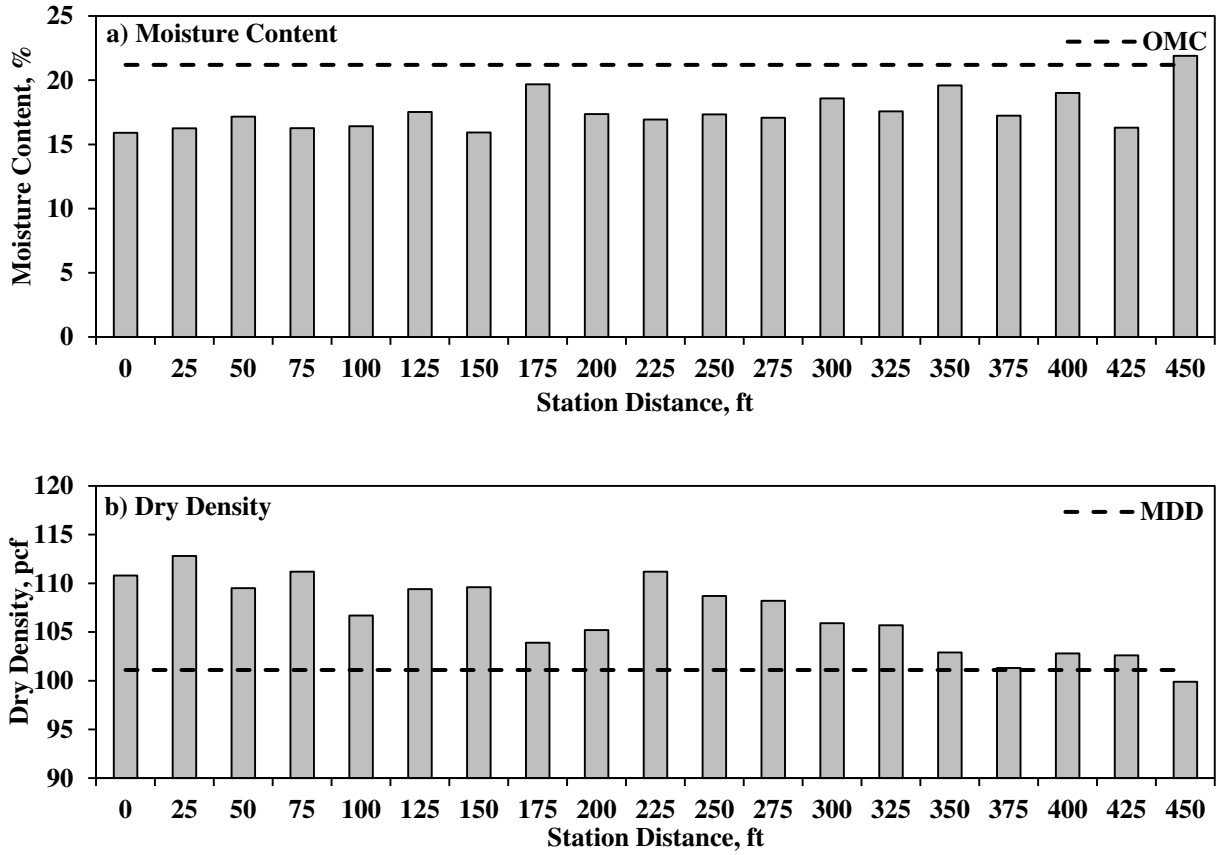

Figure I.4.1 – Spatial Variations of NDG Moisture Content and Dry Density of Embankment Layer

Subgrade Layer - The subgrade was prepared at three different moisture contents (wet of OMC, OMC, and dry of OMC) and compacted with a sheep foot compactor and a smooth drum IC roller. Figure I.4.2 depicts the NDG and SDG moisture contents immediately after the final pass of the IC roller. Based on the NDG results, the three sections were placed dry of OMC as compared to the actual Proctor tests (from our laboratory tests) and around the contractor's target OMC. The SDG results show more dispersion from the target moisture contents. The oven dry moisture contents from the field specimens exhibit nonuniform variation in moisture contents at the site.

Figure I.4.3 summarizes the NDG and SDG dry densities after the compaction of the subgrade layer. All test sections yielded dry densities that exceeded the acceptance limit of 95% of MDD. The average SDG dry densities were about 132 pcf, which is much greater than the NDG average dry density of 109.5 pcf.

Figure I.4.4 summarizes the NDG moisture contents during the passes of the IC roller. Considering typical uncertainties associated with the NDG, the moisture contents do not change appreciably between passes. The same process was repeated for the measured NDG densities in Figure I.4.5. It seems that the optimum number of passes is four.

The SDG and NDG moisture contents are compared with the oven moisture contents in Figures I.4.6 and I.4.7. Since the SDG data were collected only after the final pass of the IC roller, the number of data points illustrated in Figure I.4.6b is less than in Figure I.4.6a. Overall, the NDG readings are less than the oven moisture contents, while the SDG moisture contents are scattered about the oven moisture contents.

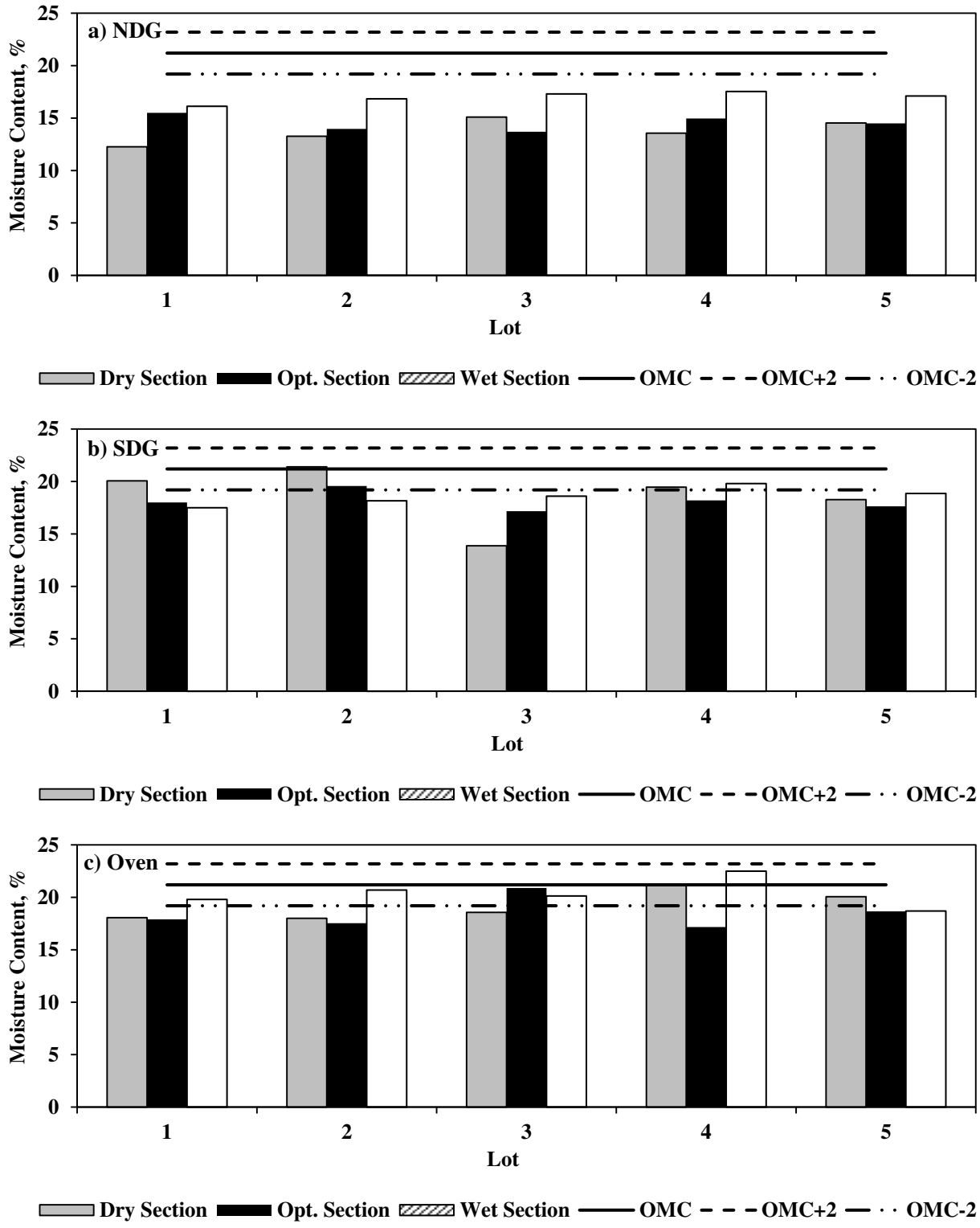

Figure I.4.2 – Spatial Variations of Moisture Contents Immediately after Compaction of Subgrade

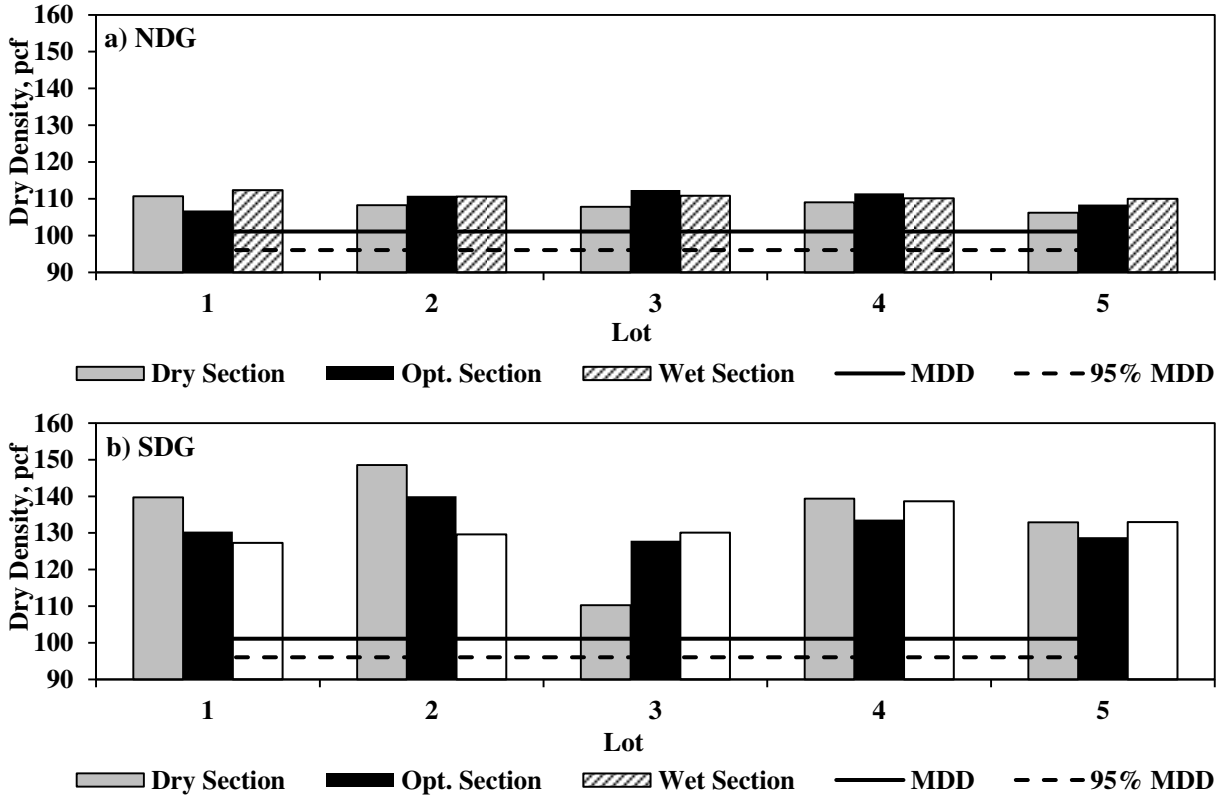

Figure I.4.3 – Spatial Variations of Dry Densities Immediately after Compaction of Subgrade

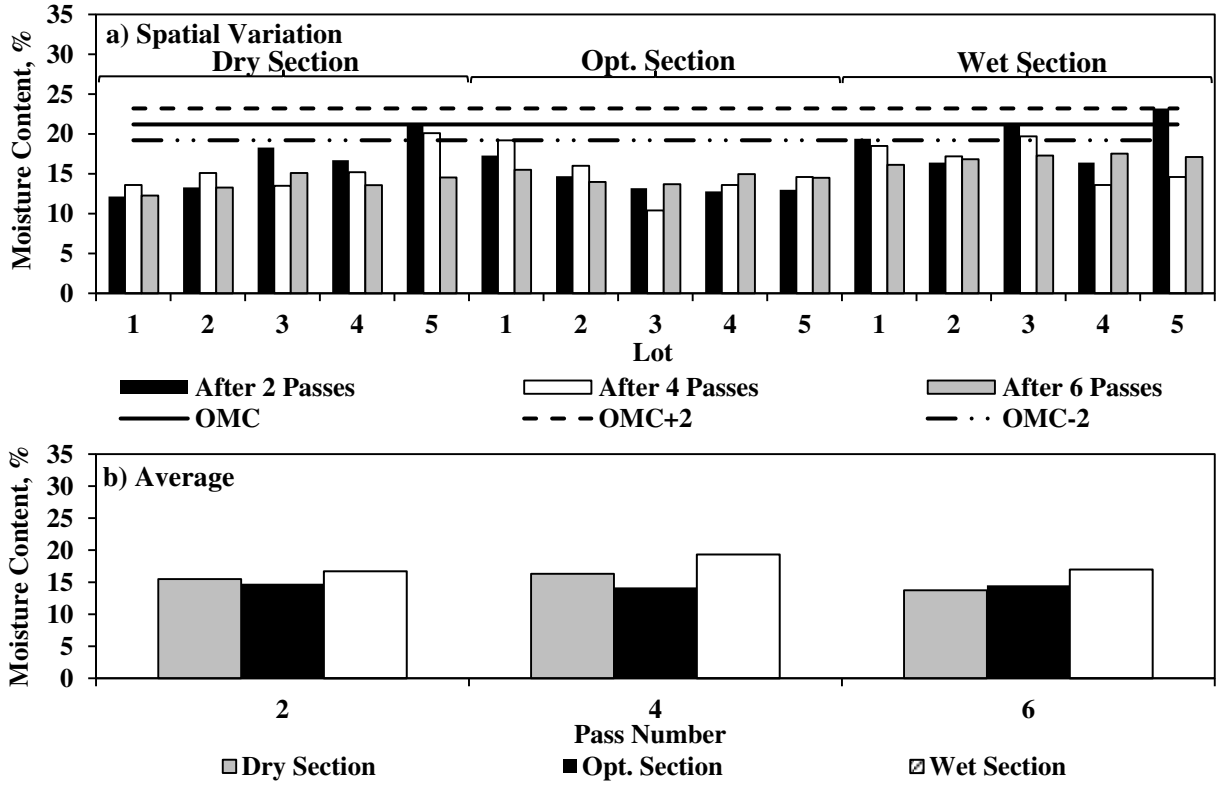

Figure I.4.4 –Variations of NDG Moisture Contents during Compaction of Subgrade Layer

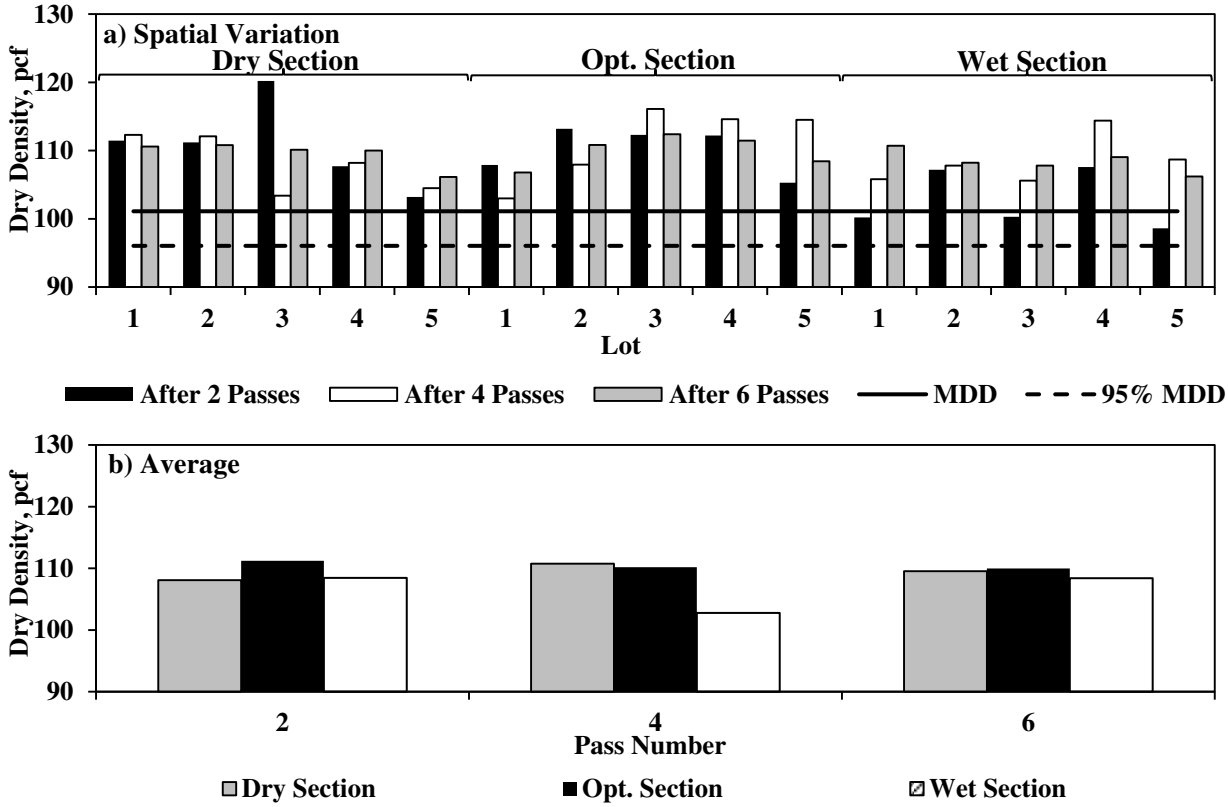

Figure I.4.5 –Variations of NDG Dry Density during Compaction of Subgrade Layer

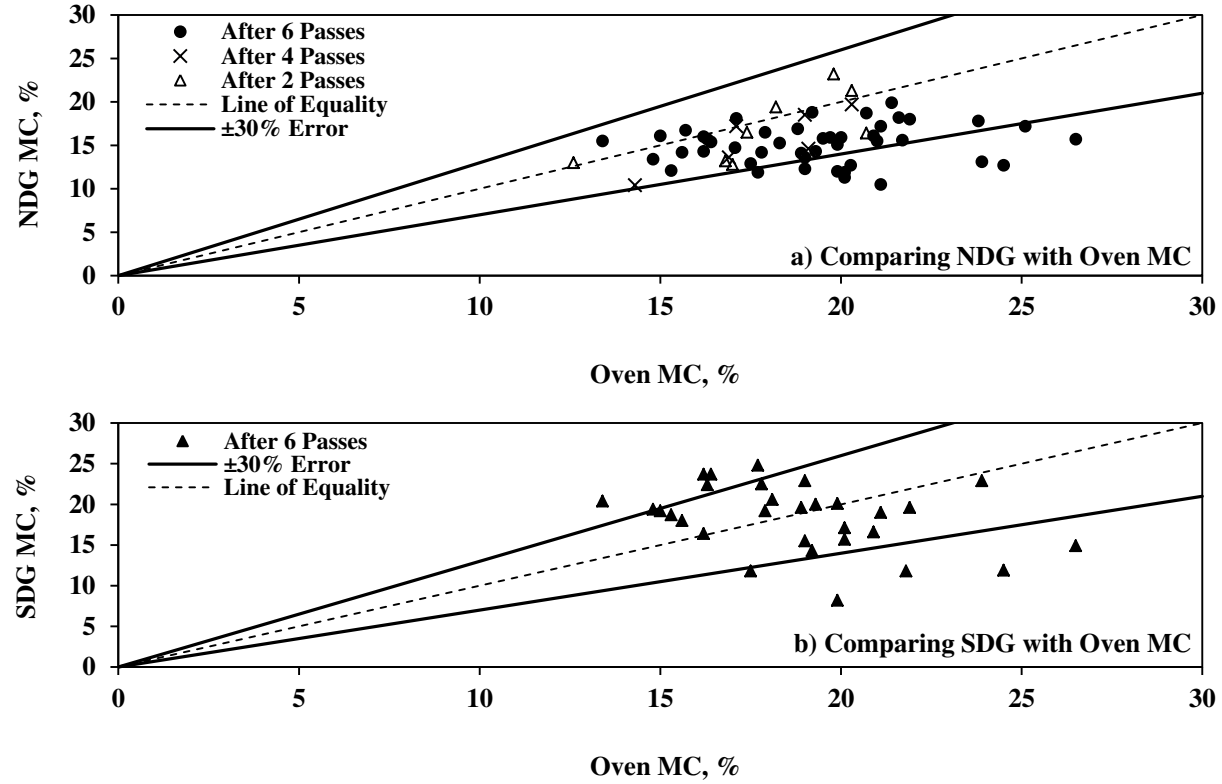

Figure I.4.6 – Comparisons of SDG and NDG Moisture Contents with Oven Moisture Contents for Subgrade Layer

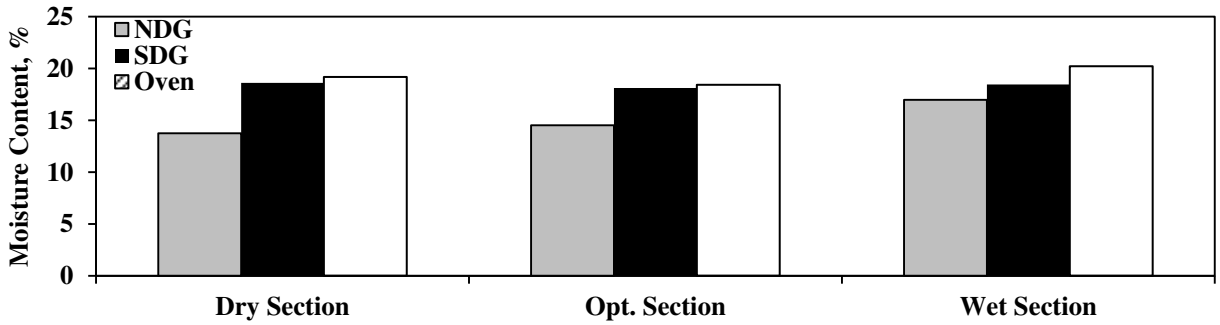

Figure I.4.7 – Average Moisture Contents after Compaction of Subgrade Layer from Different Methods

I.5 Evaluating Variability of Layer Properties with Modulus-Based Devices

Embankment Layer - Figure I.5.1 summarizes the results of modulus-based devices used on embankment layer. The PSPA and LWD devices depict the same general patterns of modulus variations throughout the test section. The average PSPA moduli of the embankment for the dry, optimum and wet subgrade sections are 28, 35 and 27 ksi, respectively. Such moduli for the LWD are 6 ksi, 7 ksi and 4 ksi. The embankment under the subgrade section placed at OMC is slightly stiffer than that of the dry or the wet section.

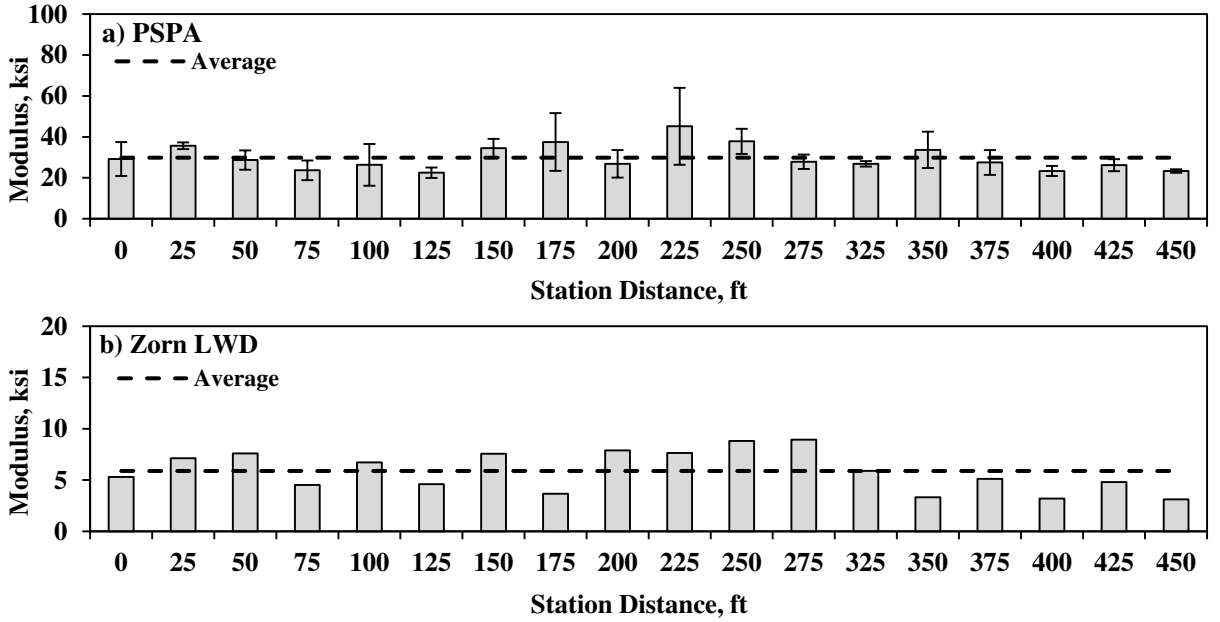

Figure I.5.1 – Spatial Variations of Measured Modulus of Embankment Layer before Placement of Subgrade

Subgrade Layer - The measured moduli on top of the subgrade layer immediately after compaction are shown in Figure I.5.2. The standard deviation of replicate tests at each test point is depicted as error bars in the figure. According to the PSPA measurements, the average moduli of the Dry, Optimum and Wet sections are 35 ksi, 27 ksi and 25 ksi, respectively. Based on Geogauge readings, the average moduli are 36 ksi, 45 ksi and 25 ksi, respectively. The average LWD moduli are 5 ksi, 4 ksi and 3 ksi, respectively. The average DCP moduli are 14 ksi, 12 ksi and 12 ksi for the Dry, Optimum and Wet sections,

respectively. The DCP shows a similar trend to the PSPA and LWD. The high average Geogauge modulus of the second section could be due to the high variability of the measurements.

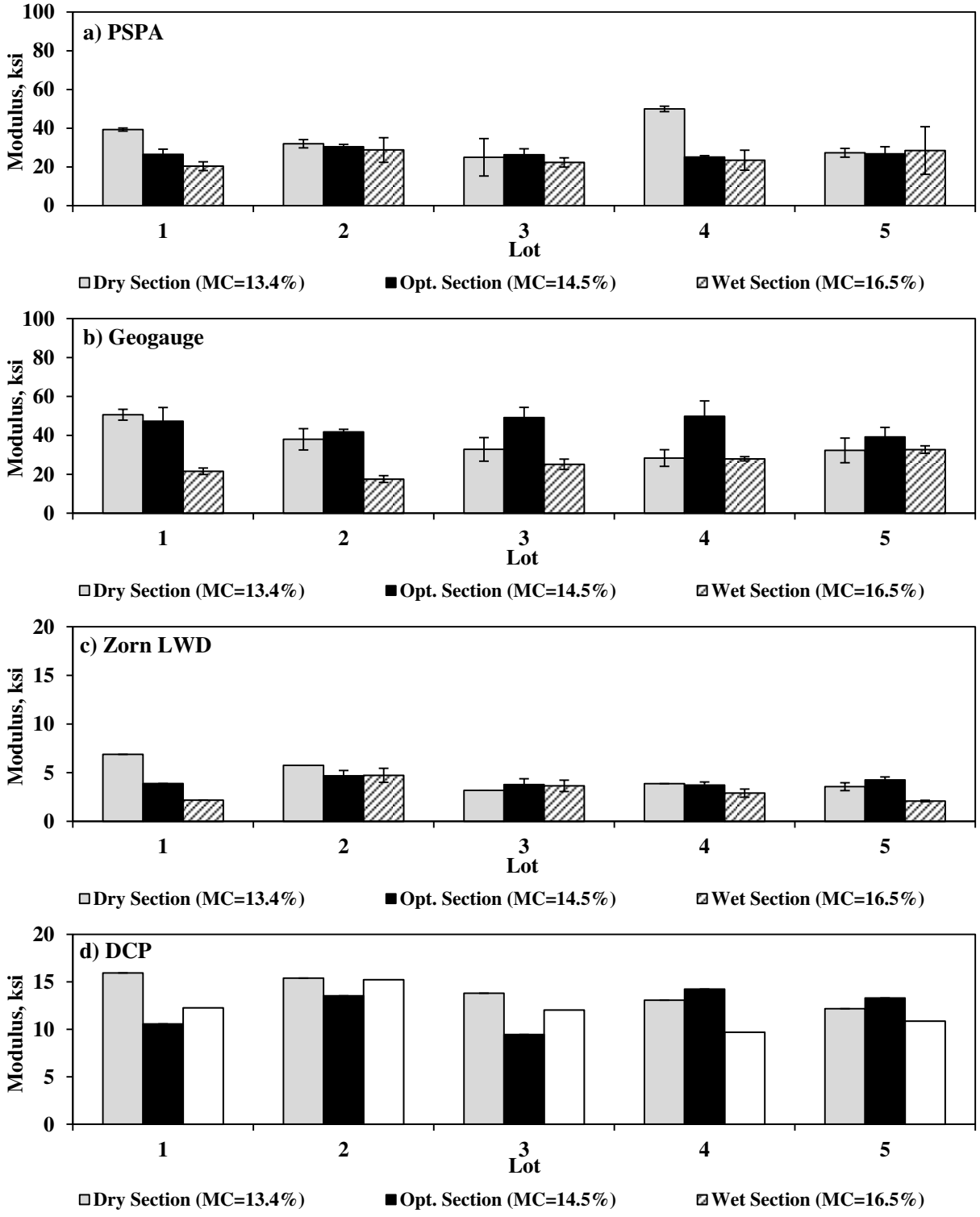

Figure I.5.2 – Variations of Measured Moduli of Subgrade Layer with Different Devices

Figures I.5.3 and I.5.4 depict the variations of the PSPA and LWD moduli after the second, fourth and sixth passes of the sheep foot roller. Some of the LWD data points from the second pass are missing due to device malfunction. The variations in the moduli after the second pass are small with both devices. Slight degradation or increase in modulus with the increase in the number of passes is observed.

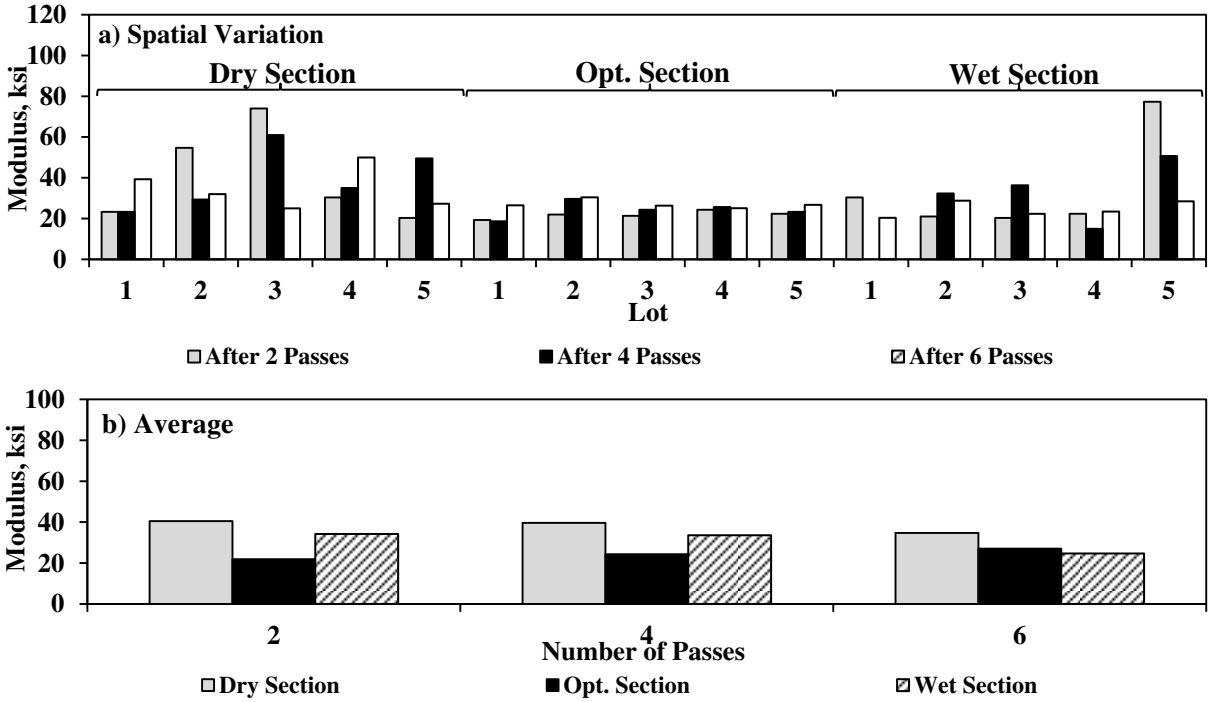

Figure I.5.3 – Measured PSPA Moduli between Passes of IC Roller during Compaction of Subgrade Layer

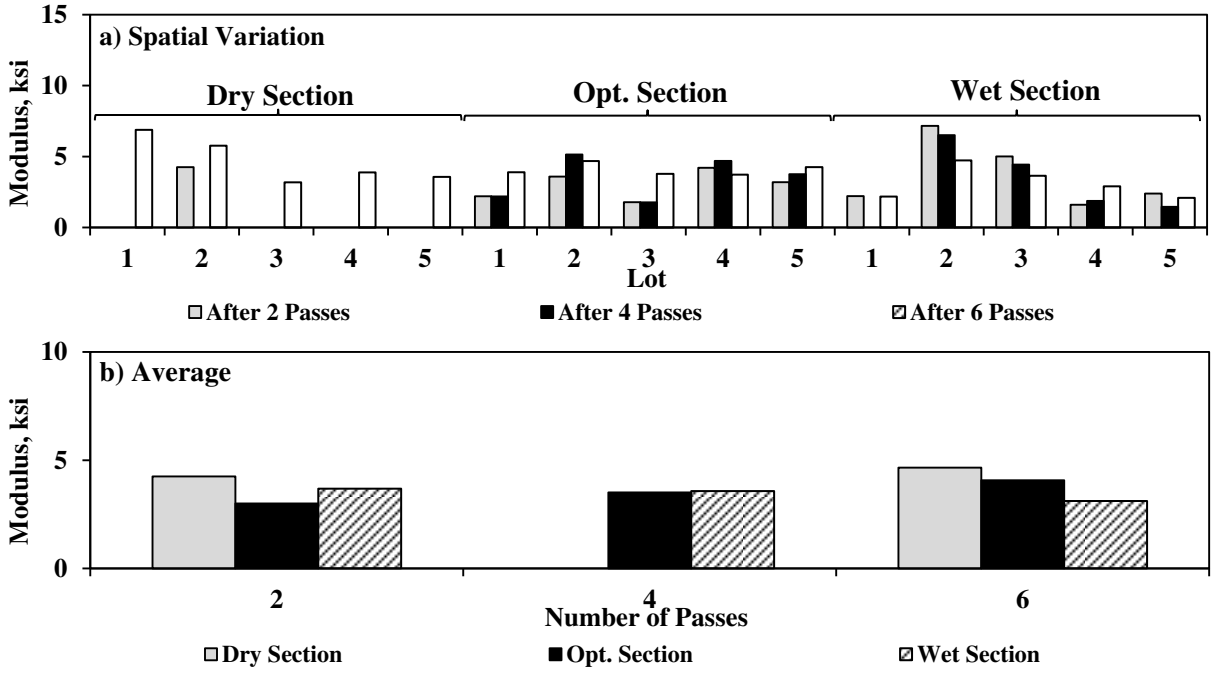

Figure I.5.4 – Measured LWD Moduli between Passes of IC Roller during Compaction of Subgrade Layer

I.6 Investigating Moisture-Modulus Relationships for Different Devices

Figure I.6.1 summarizes the correlations between measured moduli from different devices and the NDG moisture contents. Due to uncertainties associated with the NDG measurements, strong correlation could not be observed from any device. The same process was repeated with oven dry moisture contents in Figure I.6.2. The moisture-modulus correlations improved when oven dry moisture contents were used. Among all devices, the LWD and DCP moduli are better correlated with the oven moisture contents. Such correlations were further employed to estimate the modulus at optimum (M_{opt}).

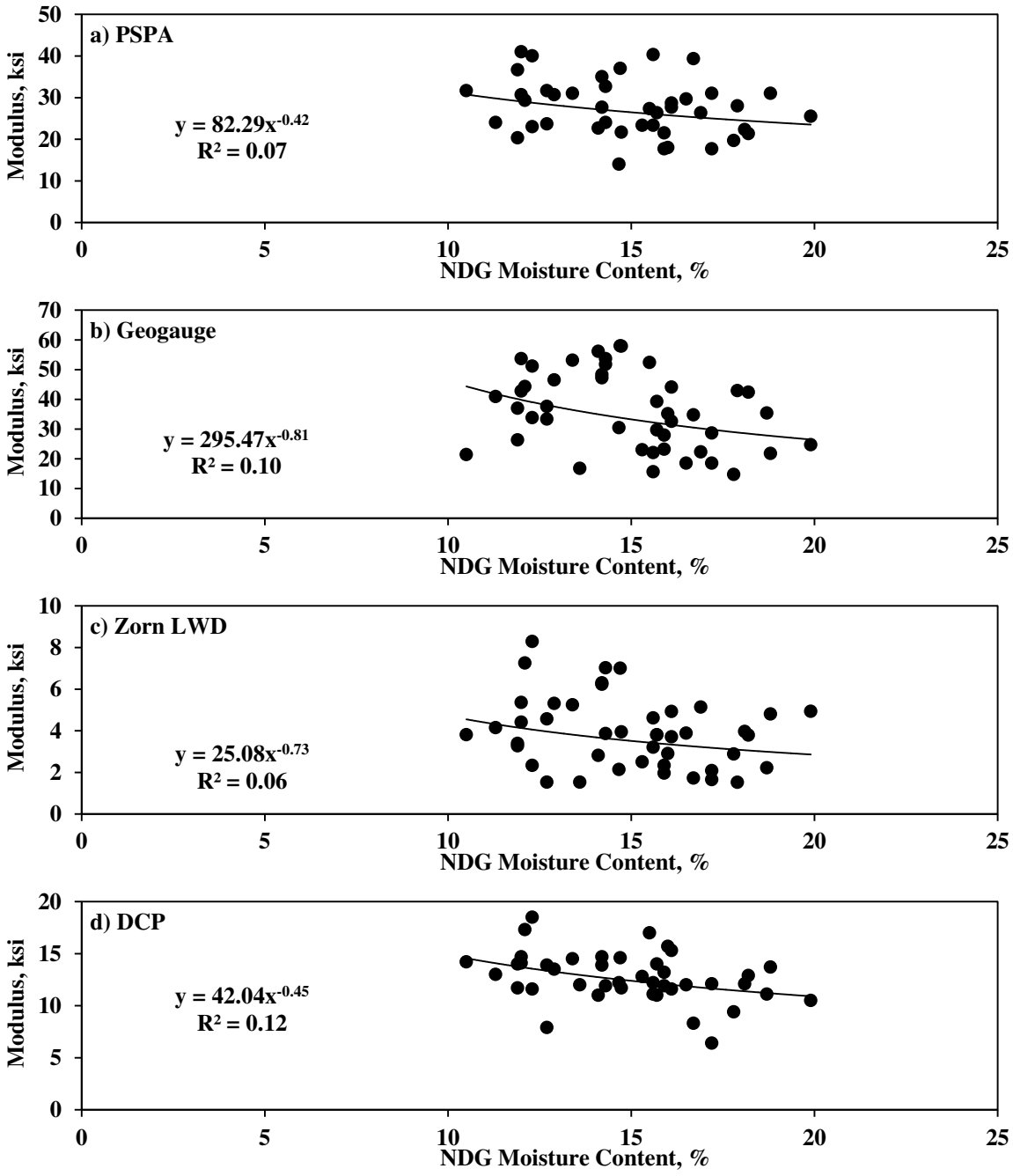

Figure I.6.1 – Moisture-Modulus Relationships with NDG Moisture Contents

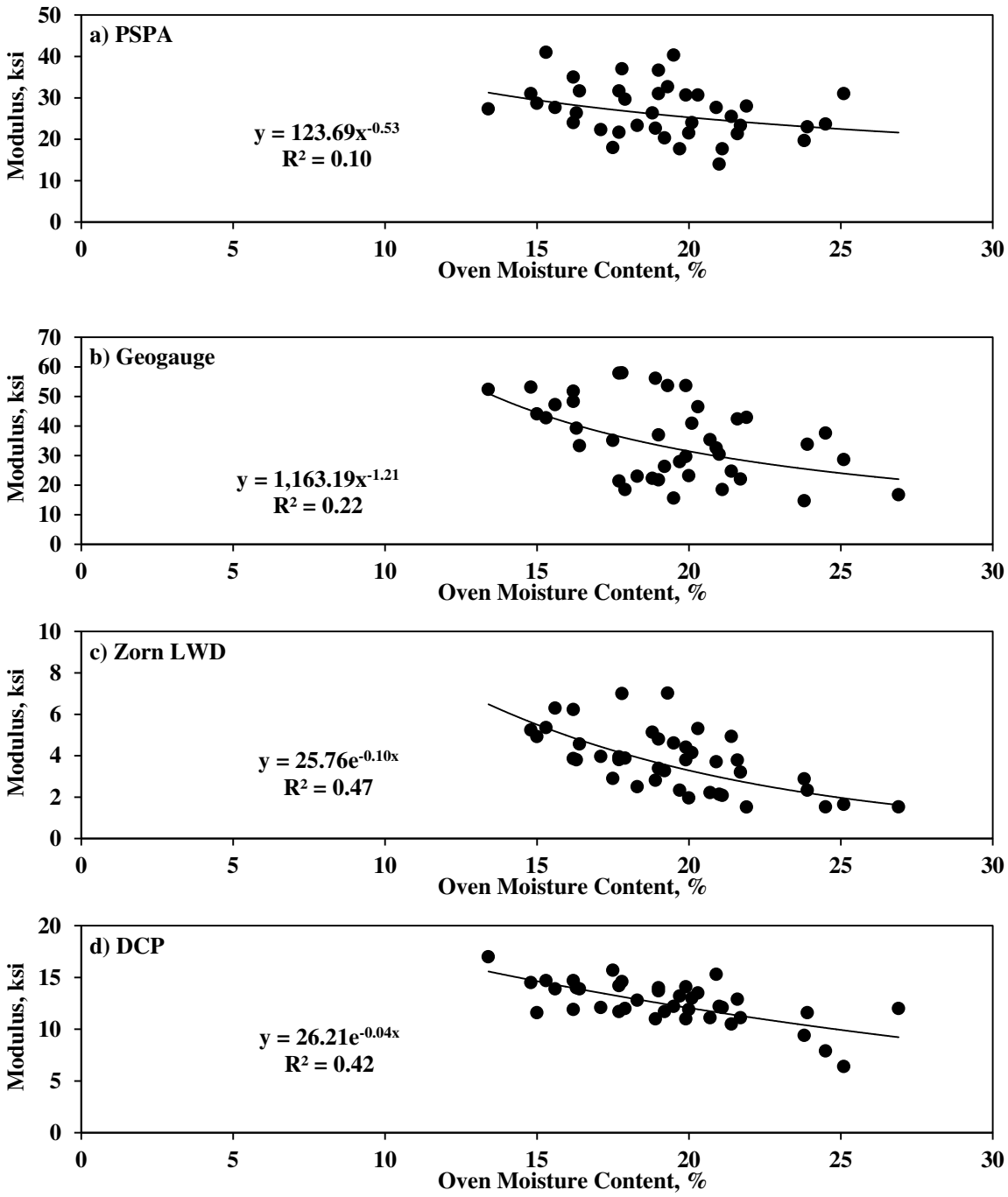

Figure I.6.2 – Moisture-Modulus Relationships with Oven Moisture Contents

Figure I.6.3 illustrates the normalized moduli (M/M_{opt}) compared with normalized oven moisture contents [(MC-OMC)/OMC]. The best-fit curves for such correlations are compared with the same relationships obtained from the laboratory MR and FFRC tests in Chapter 3. The field data from the PSPA, Geogauge and DCP are closer to the laboratory MR model and the Zorn LWD field data better match the laboratory FFRC models from Chapter 3.

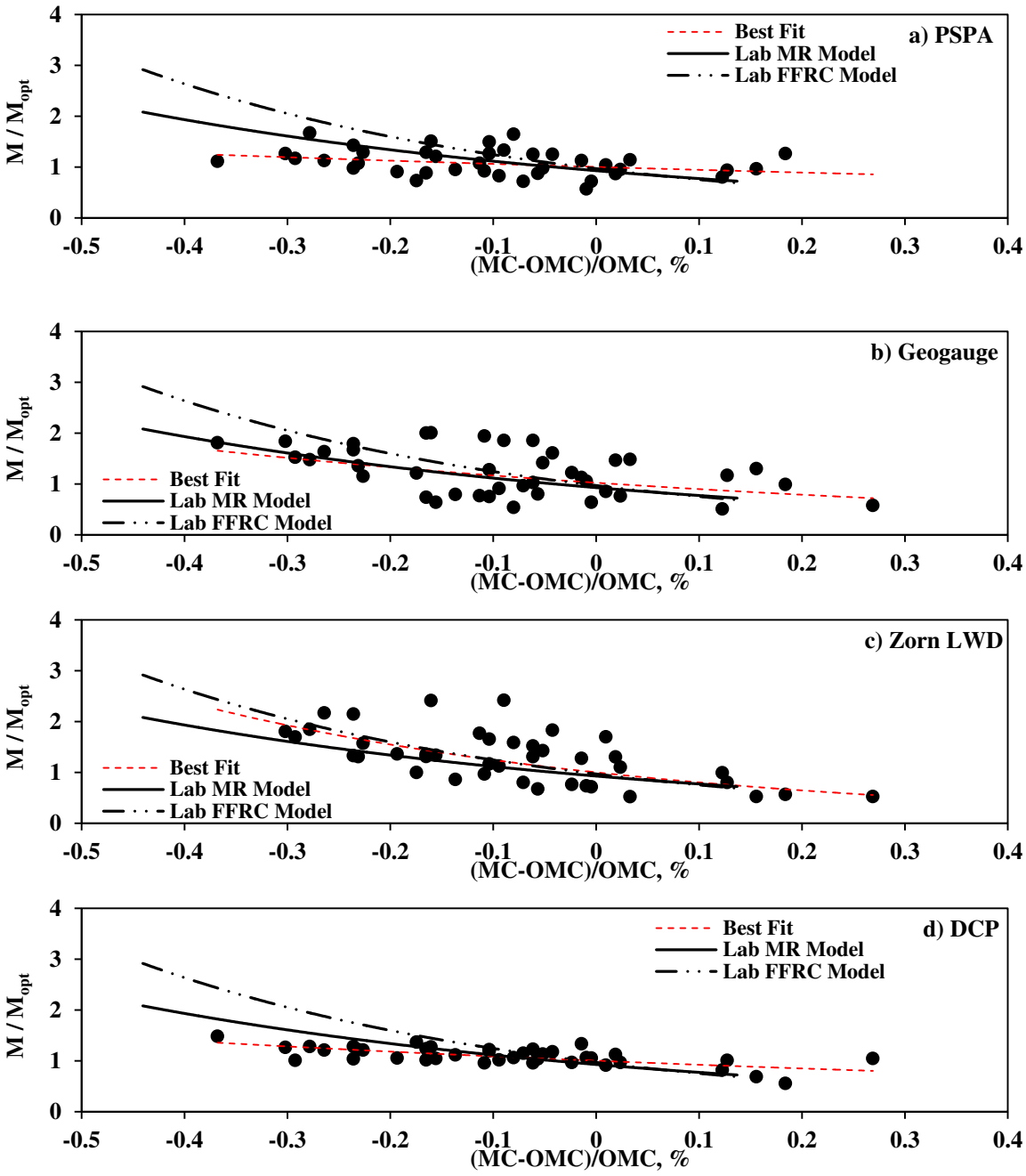

Figure I.6.3 – Correlation between Normalized Measured Modulus and Normalized Oven Moisture Contents

The same process was repeated for the degree of saturation calculated from the oven dry moisture contents and the NDG dry densities. Normalized moduli (M/M_{opt}) are compared with the normalized degree of saturation ($S\text{-}S_{opt}$) in Figure I.6.4. The best-fit curves from the field data are superimposed on the MEPDG and Cary and Zapata equations (as discussed in Chapter 4). The field data better match the Cary and Zapata model with *wPI*=0.

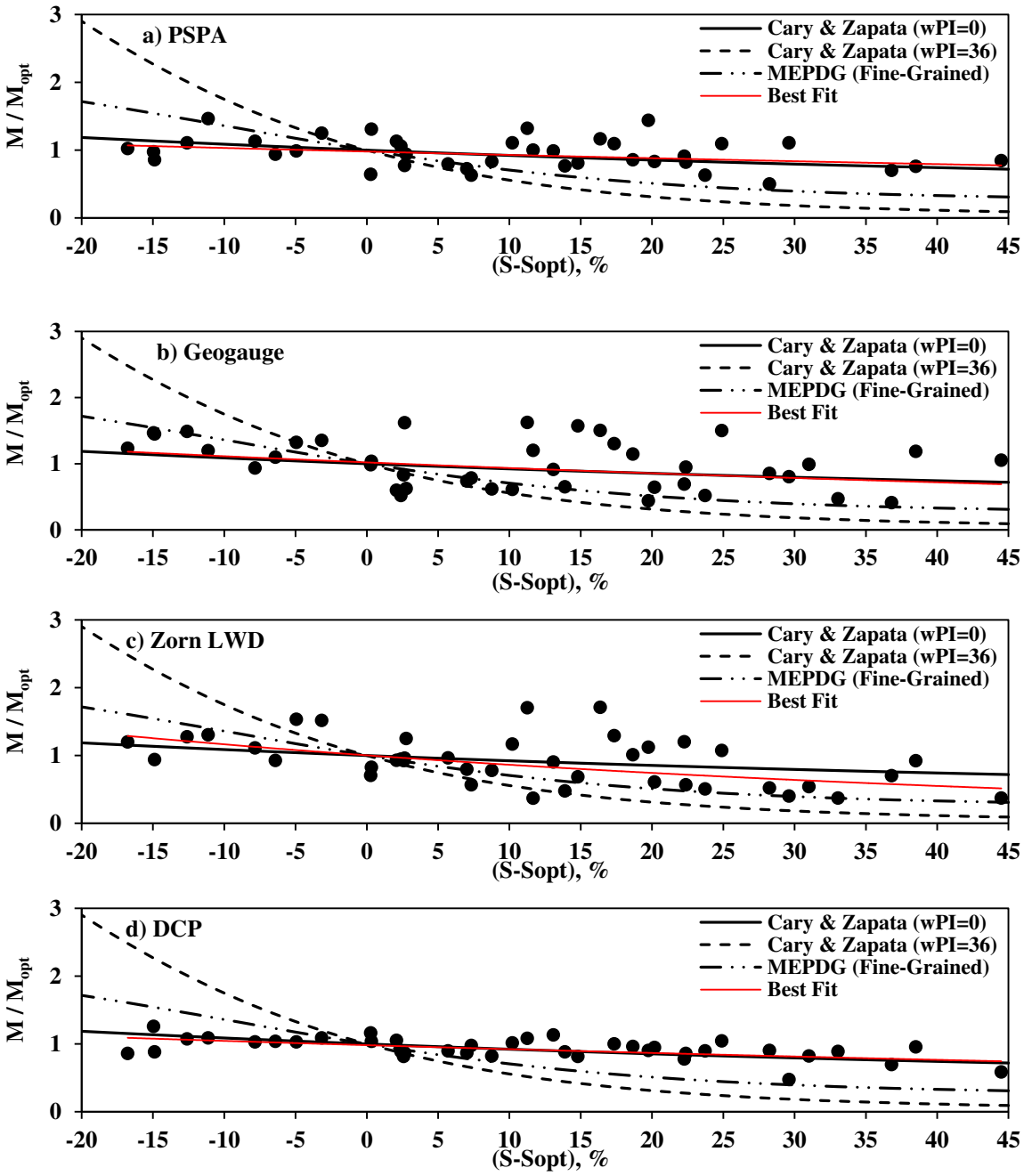

Figure I.6.4 – Correlations between Normalized Measured Modulus and Normalized Degree of Saturation (Calculated from Oven Moisture Content and NDG Dry Density)

I.7 Acceptance Scenarios for Compacted Subgrade Geomaterials

In addition to the modulus measurements during and immediately after the compaction of the subgrade layer, the compacted sections were also tested about 24 hrs after compaction. The target modulus of the compacted subgrade materials at OMC were calculated for each device. The estimated field moduli based on the field moisture contents were also estimated to compare with the field moduli immediately and 24 hrs after compaction. The results of such analyses for the PSPA, LWD and Geogauge are summarized in

Figures I.7.1 to I.7.3, respectively. The Geogauge moduli after 24 hrs for the dry and opt. sections were not collected due to construction time constraints.

Figure I.7.1 compares the average measured PSPA moduli (average of the three readings along line A, B and C considered as a lot) after compaction and about 24 hrs after compaction with the target moduli established from the lab-derived k' parameters at the OMC. The three sections fail the acceptance criterion of 80% of the target modulus at OMC. The estimated field moduli based on the compaction moisture contents are close to the measured field moduli for the wet section, but greater for the dry and optimum sections. The measured PSPA moduli after 24 hrs are about 20% greater than the ones immediately after compaction.

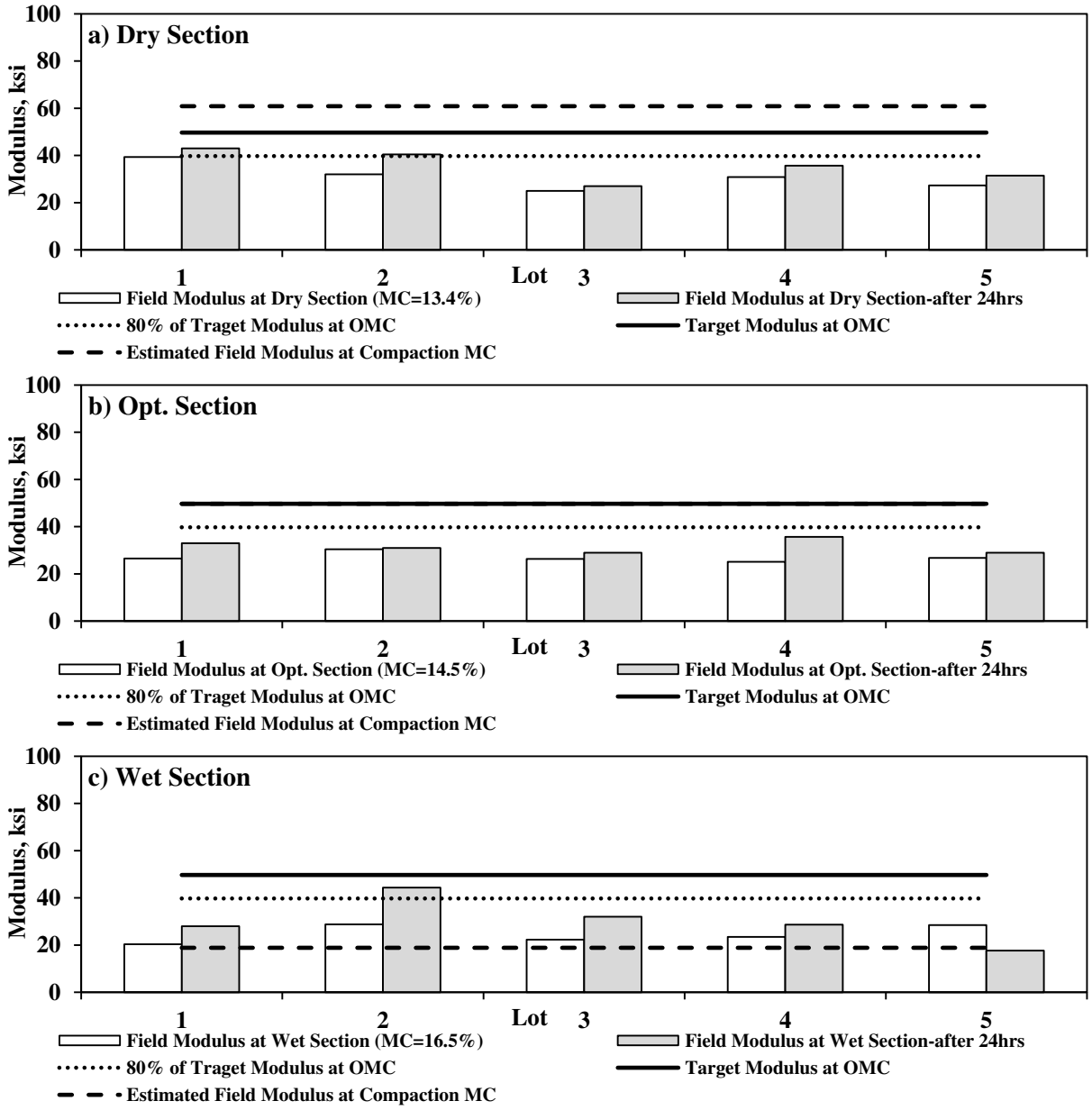

Figure I.7.1 – Acceptance Scenarios for PSPA Measurements

Figure I.7.2 summarizes the field results from the LWD. The dry and optimum sections pass the established acceptance criterion marginally while the wet section fails the criterion. Considering the measured moduli of embankment layer (see Figure I.5.1), the LWD and PSPA data can be considered complementary since the LWD measures the composite modulus of the subgrade and embankment while the PSPA measures the modulus of the subgrade layer only. The estimated field moduli match the measured LWD moduli at optimum and wet sections while overestimate the moduli of the dry section. The LWD moduli after 24 hrs are on average about 80% greater than the ones measured after compaction.

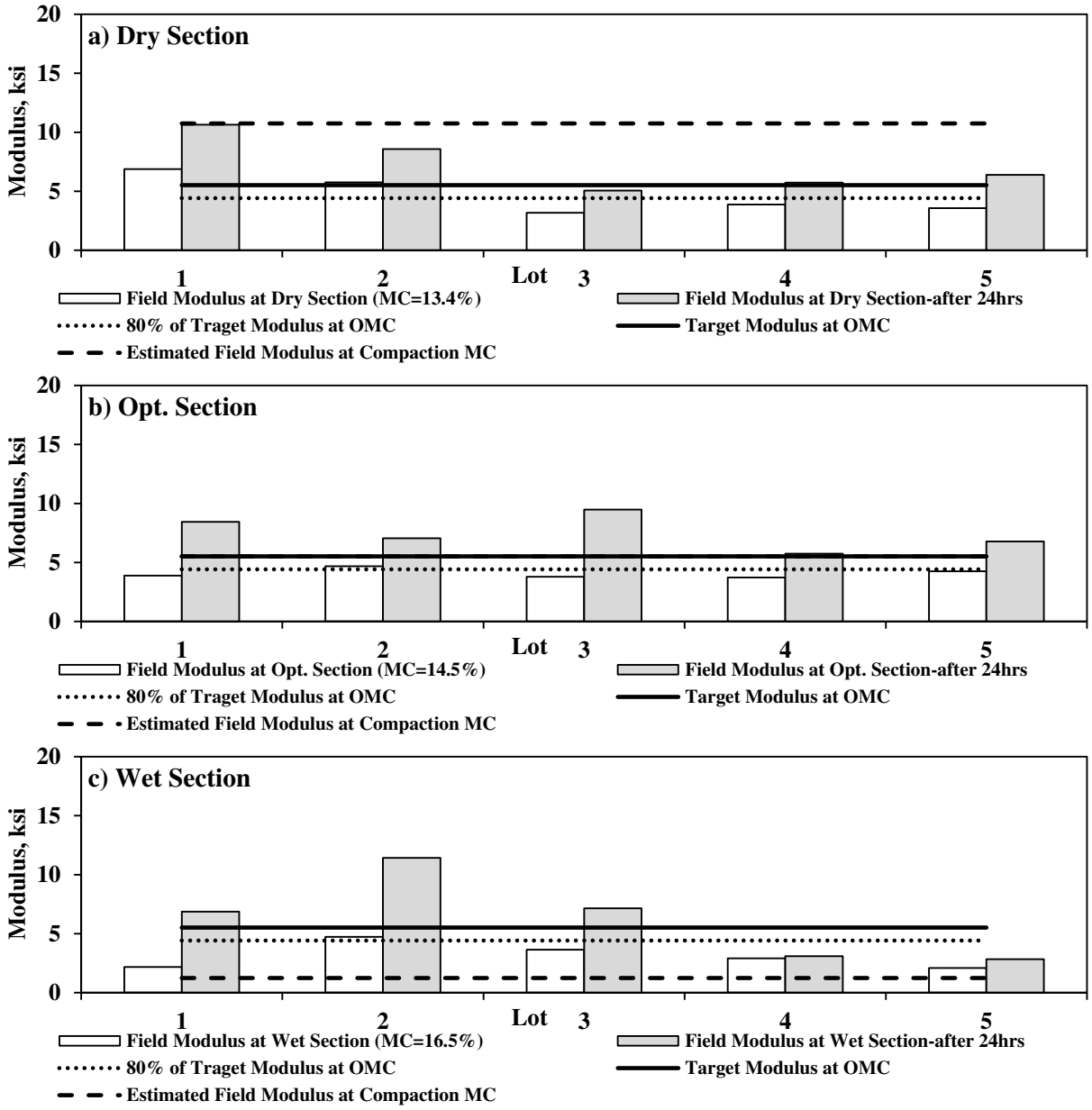

Figure I.7.2 – Acceptance Scenarios for LWD Measurements

Figure I.7.3 summarizes the field and target moduli from the Geogauge. The measured Geogauge moduli for all sections are greater than the target modulus. Such results might not be quite reliable due to the high variability associated with the measurements at this site. Due to device malfunction, the Geogauge

moduli after 24 hrs for the dry and optimum sections were not collected. The measured Geogauge moduli are about 20% greater after 24 hrs of compaction for the wet section.

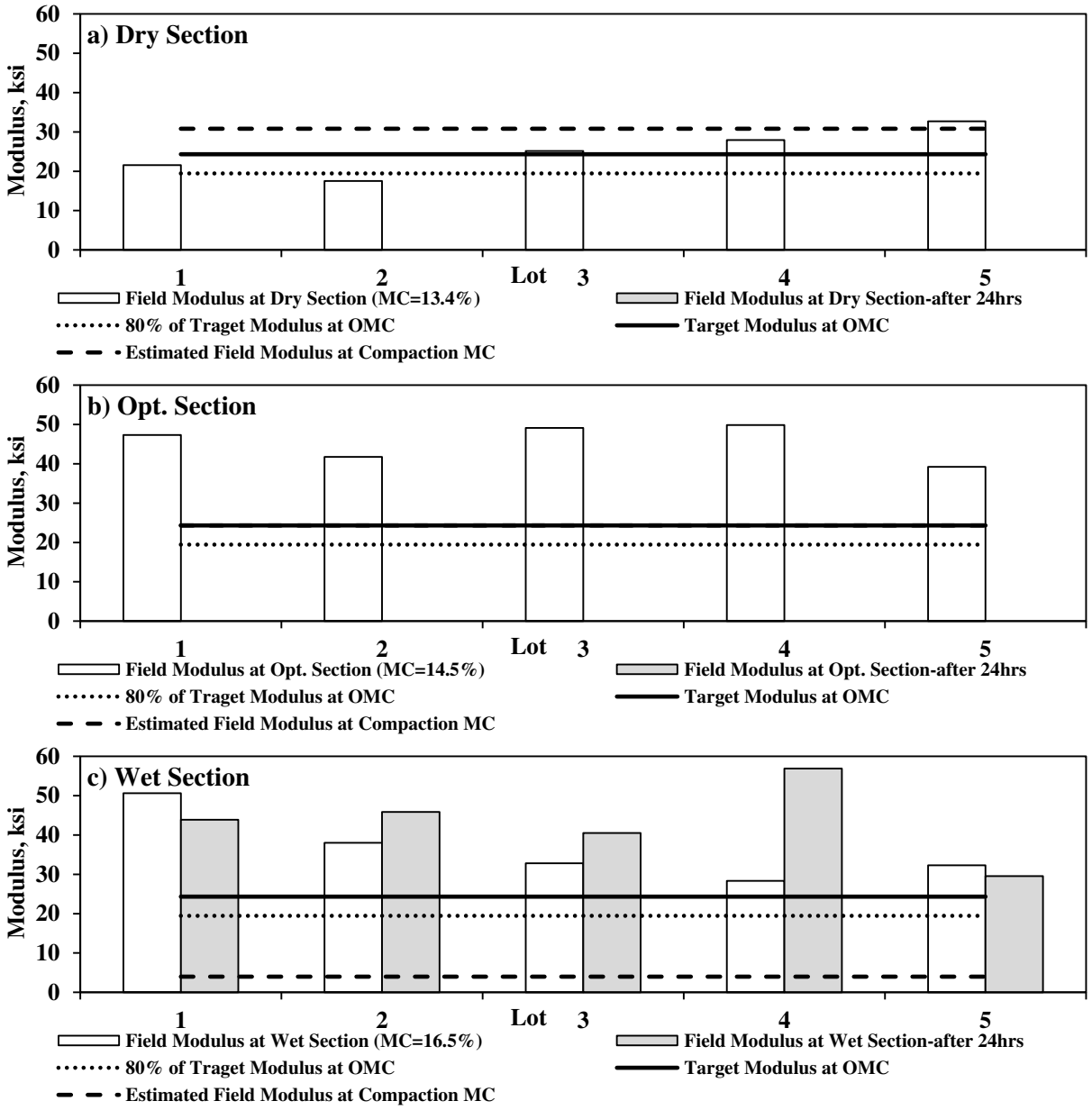

Figure I.7.3 – Acceptance Scenarios for Geogauge Measurements

I.8 Intelligent Compaction

In Site I.2, the roller drum and the soil interaction to compaction process were captured using the Machine Drive Power (MDP). The MDP technology relates the roller drum rolling resistance to determine the energy required to overcome the resistance to motion.

The new Caterpillar roller available at the site came with the factory installed MDP data kit. In addition to the existing MDP kit, a Trimble accelerometer kit collecting CMV was also installed on the same roller

on the second day of the field study. Due to the delay in installation of the Trimble kit, only the MDP measurements were recorded on the existing embankment on all the three test sections. Due to a malfunction, the MDP measurements from the 3rd pass on the dry and OMC sections were not recorded. Both the MDP and CMV data were recorded successfully for all passes of the wet section. IC measurements 16 hrs after compaction on the wet section were not carried out due to roller break down.

Figure I.8.1 presents the cumulative distributions of the MDP and/or CMV measurements during the compaction process of the subgrade sections. The MDP measurements for the dry section (Figure I.8.1a) increased with an increase in the number of roller passes despite the theoretical concept of the reduction in the MDP with an increase in the compactive effort. The CMV measurements for the OMC section (Figure I.8.1b) increased and the section became more uniform with the number of passes. As observed in the case of the dry section, the MDP distributions of the wet section (Figure I.8.1c) tend toward higher values with the increase in the number of roller passes. The CMV measurements carried out simultaneously with the MDP measurements for the wet section are depicted in Figure I.8.1d. The distributions of the CMV measurements tend toward higher values with an increase in the compactive effort.

To evaluate the influence of the subgrade lift placement on the IC measurements, the distributions of the roller measurements before and after the placement of the lift for the dry and wet sections are compared in Figure I.8.2. Since the embankment and the subgrade were constructed with similar soils, the roller measurements from the before and after placement of the lift vary marginally.

The influence of testing time can be visualized in Figure I.8.3. As indicated above, such data are only available for the dry section. The MDP measurements after 16 hrs are slightly greater than those just after the completion of compaction.

Figures I.8.4 and I.8.5 present the relationships between the dry density from the NDG and the CMV or MDP measurements for all sections tested. The two parameters are not strongly correlated.

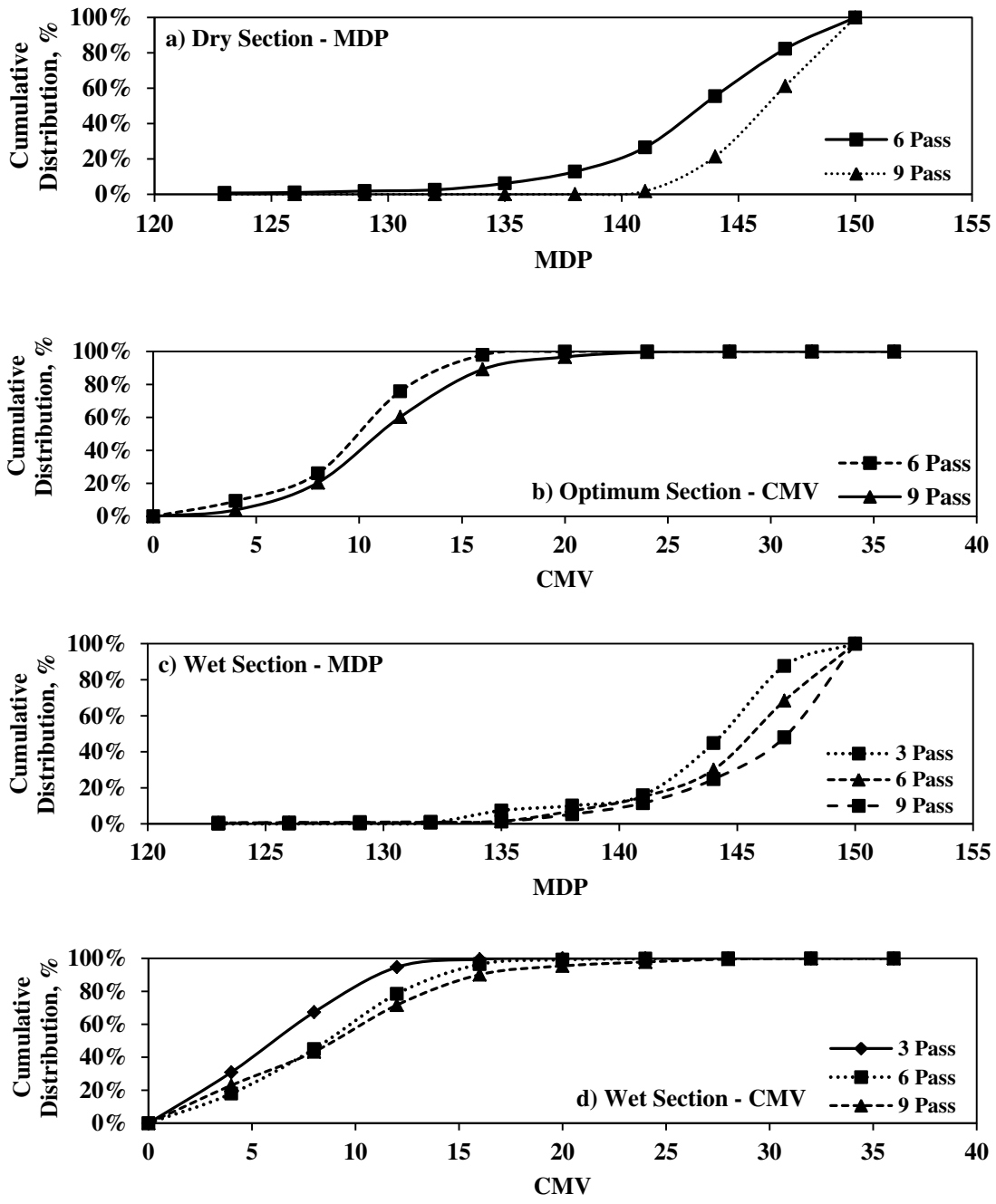

Figure I.8.1 - Distributions of the MDP and the CMV with Passes for Different Sections

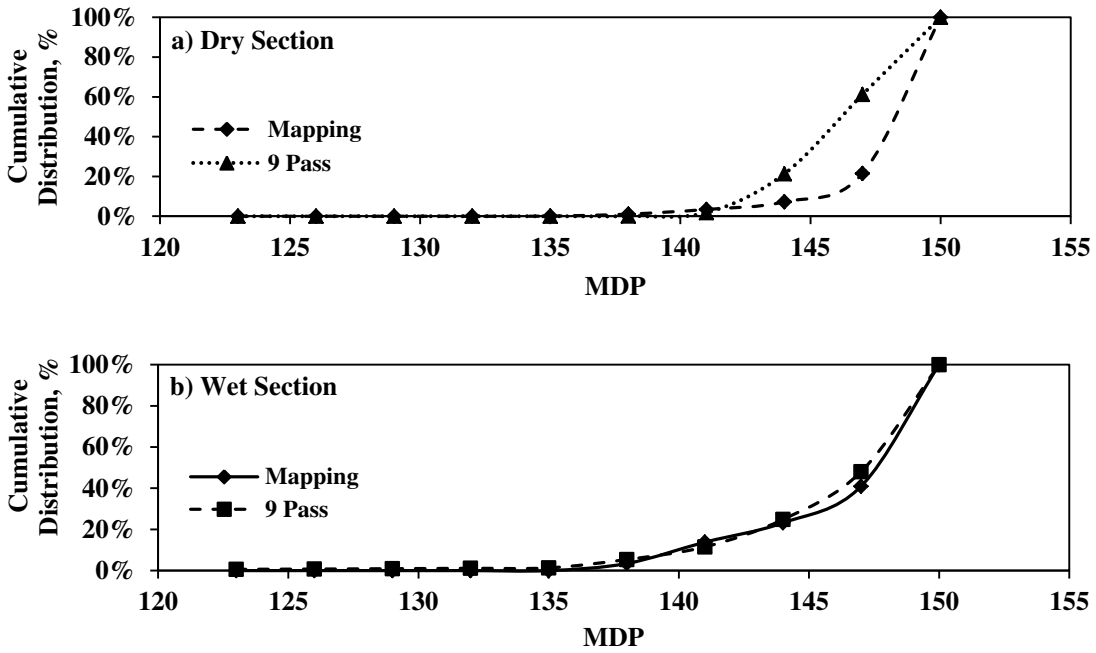

Figure I.8.2 - Influence of the Subgrade Lift Placement for different Test Sections

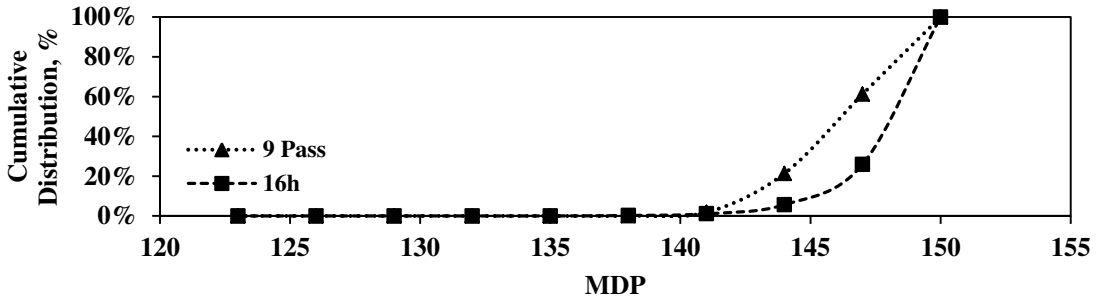

Figure I.8.3 - Influence of the Time of Testing on the Roller Measurement Values for Dry Section

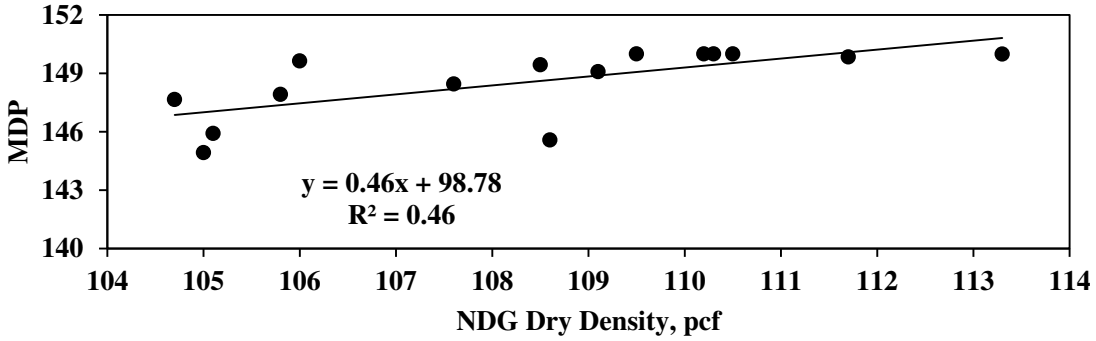

Figure I.8.4 - Correlation between the NDG Density and the MDP for Dry Section

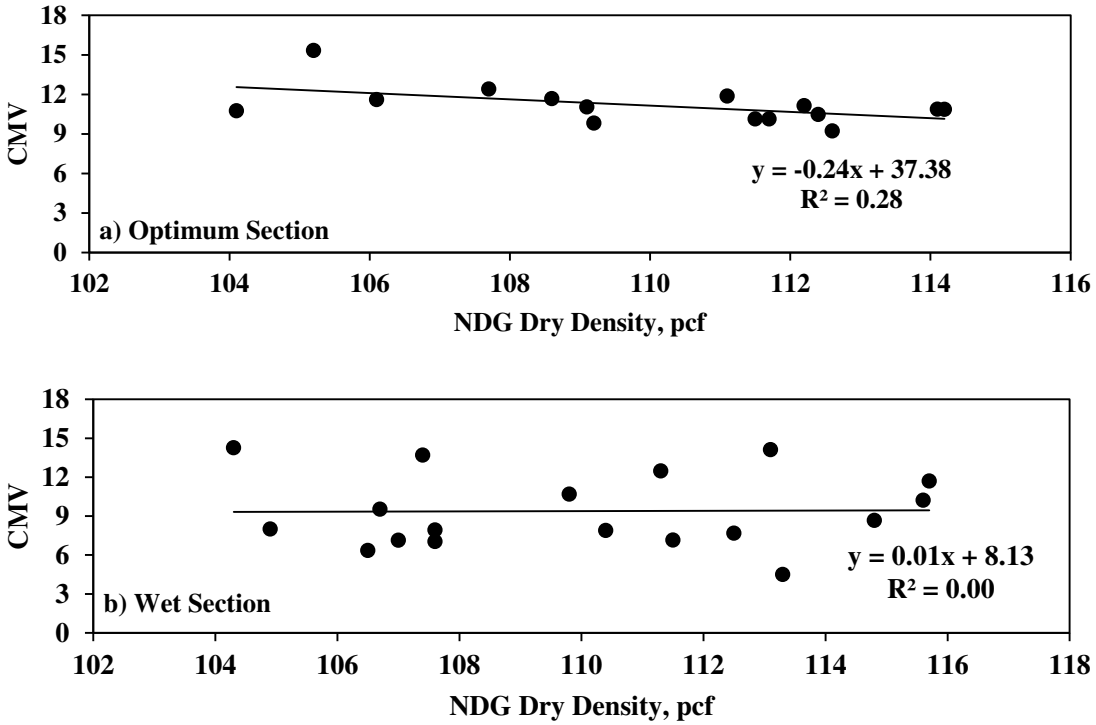

Figure I.8.5 - Correlation between the NDG Density and the CMV for OMC and Wet Sections

Appendix J

OBSERVATIONS FROM IMPLEMENTATION OF SPECIFICATION

Site I.3

J.1 Introduction

This field evaluation was carried out on several sections of a construction project for County of Somerset in conjunction with the New Jersey Department of Transportation (NJDOT). Figure J.1.1 illustrates the location of the construction site and testing sections. The project involved improvements to the US Route 22 corridor in Bridgewater Township, between Interstate 287 on the western end and Thompson Avenue on the eastern end. Figure J.1.2 illustrates the schematic of testing spots on the selected sections for the base, subbase and subgrade layers conducted during the first week of October 2013. The thickness of the base layer was 8 in. and the subbase layer was 6 in.

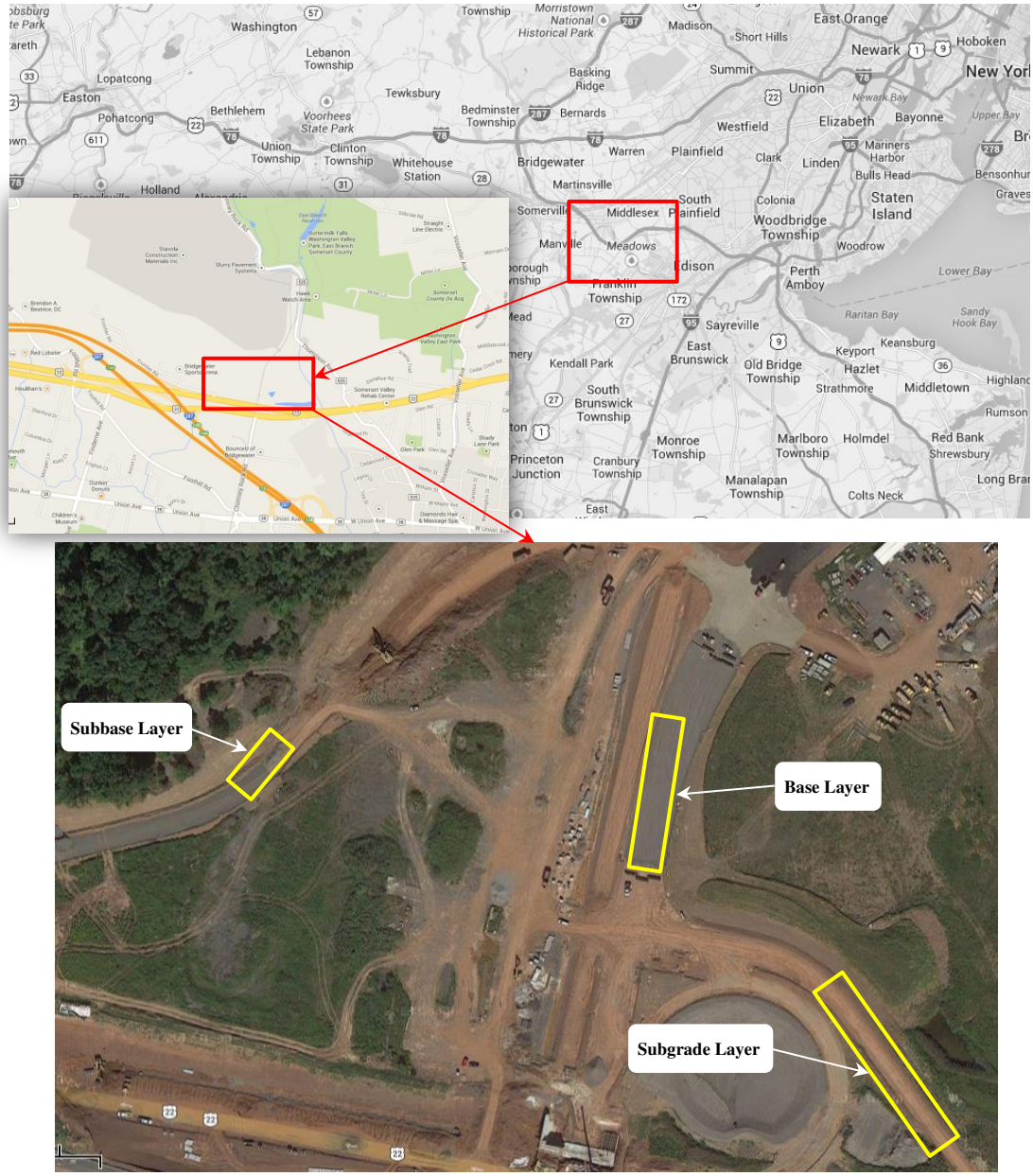

Figure J.1.1 – Location of Field Evaluation Site on US-22 Route in Bound Brook, NJ

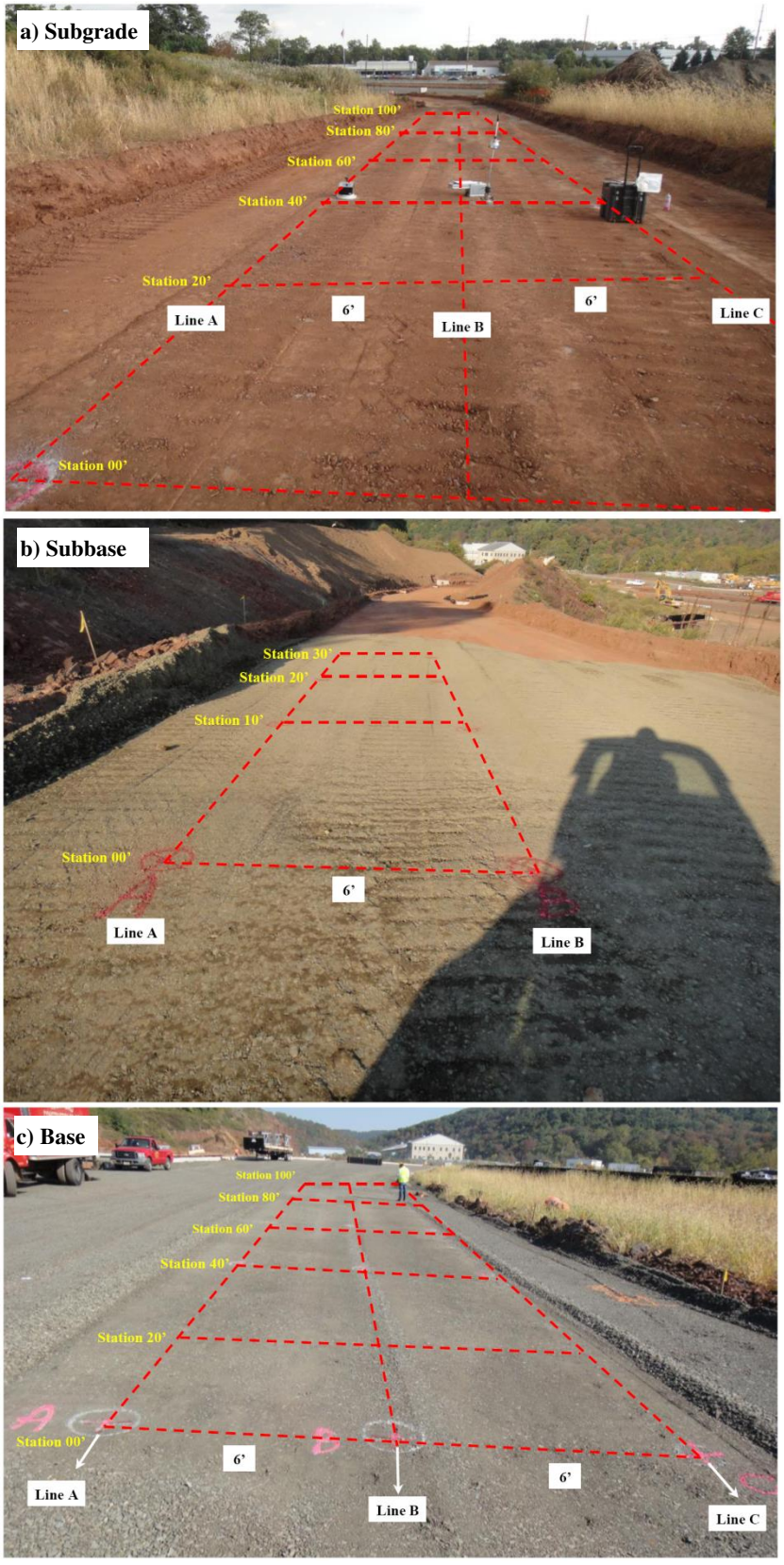

Figure J.1.2 – Location of Testing Sections

J.2 Laboratory Results

The index properties of the subgrade, subbase and base materials are summarized in Table J.2.1, and their gradation curves are presented in Figure J.2.1. The subgrade was classified as low-plasticity clay as per Unified Soil Classification System (USCS). The subbase and base were categorized as well-graded gravel. The optimum moisture contents and maximum dry unit weights obtained as per standard Proctor tests (AASHTO T99) for the subgrade and as per modified Proctor tests (AASHTO T180) for the subbase and base are also reported in Table J.2.1.

Table J.2.1 - Index Properties of Dublin Geomaterials

Soil Type	Gradation %				USCS Class.	Atterberg Limits			Moisture/Density	
	Gravel	Coarse Sand	Fine Sand	Fines		LL	PL	PI	OMC,* %	MDUW,** pcf
Subgrade	12	20	13	55	CL	32	18	14	12.2	127.7
Subbase	63	26	10	0.7	GW	Non-Plastic			4.8	147.5
Base	59	32	7	0.9	GW	Non-Plastic			4.6	147.3

*OMC = Optimum Moisture Content, **MDUW = Maximum Dry Unit Weight

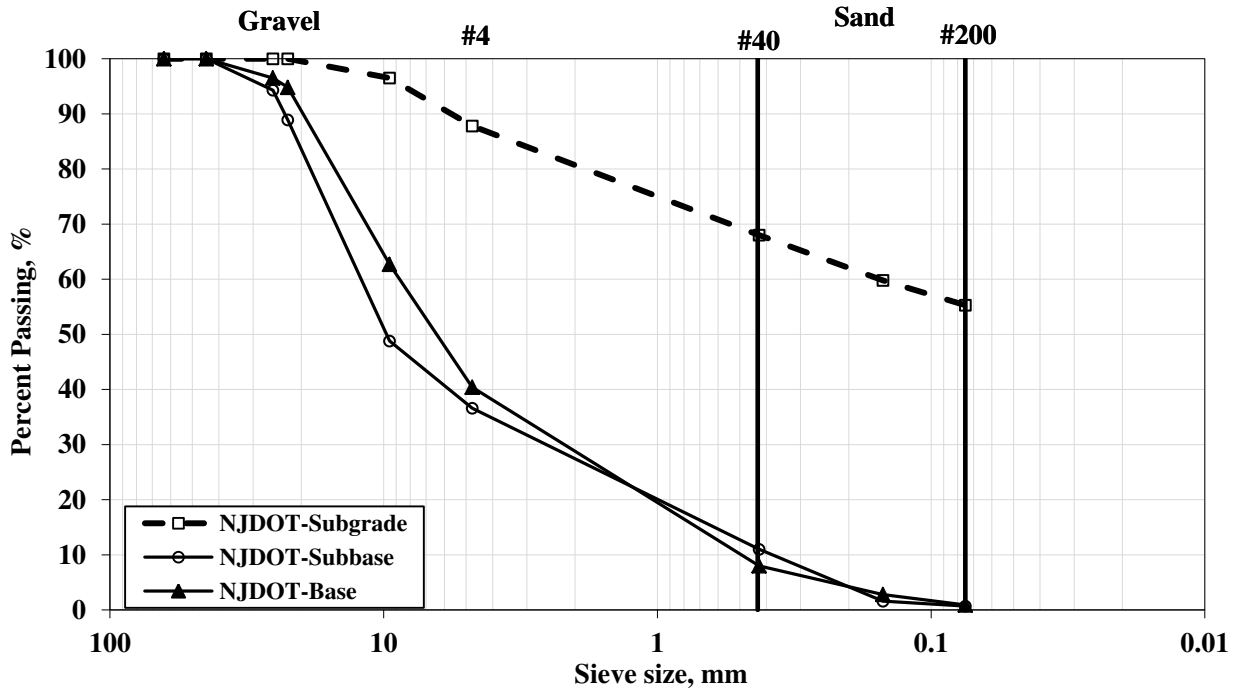

Figure J.2.1 – Gradation Curves of NJDOT Geomaterials

The resilient modulus (MR) and FFRC tests were performed on laboratory specimens prepared at the OMC, dry of OMC and wet of OMC as summarized in Table J.2.2. Figure J.2.2 illustrates the variations of the FFRC moduli and representative MR values with moisture content.

Table J.2.2 – Laboratory Results of MR and FFRC Tests of NJDOT Geomaterials (Subgrades, Subbase and Base)

Type	Target Moisture Content	Actual Moisture Content, %	Dry Density, pcf	FFRC Modulus, ksi	Nonlinear Parameters			Representative MR, ksi*
					k'_1	k'_2	k'_3	
Subgrade	OMC-2	10.1	123.2	66	1257	0.39	-1.73	17.1
	OMC-1	11.3	123.1	43	326	1.14	-3.00	5.5
	OMC	12.6	125.2	24	437	1.12	-3.00	7.3
	OMC+1	13.9	123.0	3	39	1.71	-0.05	1.6
	OMC+2	Too Wet to Test						
Subbase	OMC-2	2.9	142.1	34	732	0.77	-0.05	25.2
	OMC-1	3.9	144.4	48	1144	0.63	-0.05	33.7
	OMC	4.8	149.7	55	883	0.74	-0.05	29.2
	OMC+1	5.9	145.6	17	628	0.58	-0.05	17.5
	OMC+2	6.9	145.0	4	646	0.26	-0.05	12.5
Base	OMC-2	2.6	140.5	67	1152	0.58	-0.05	32.0
	OMC-1	3.6	146.4	82	1405	0.49	-0.05	35.3
	OMC	4.6	147	35	982	0.71	-0.05	31.6
	OMC+1	5.6	143.8	20	928	0.66	-0.05	28.3
	OMC+2	6.6	141.5	11	644	0.67	-0.05	19.8

* from Eq. 3.2.1 based on τ_{oct} and θ values of 7.5 psi and 31 psi for base and 3 psi and 12.4 psi for subgrades as recommended by NCHRP Project 1-28A.

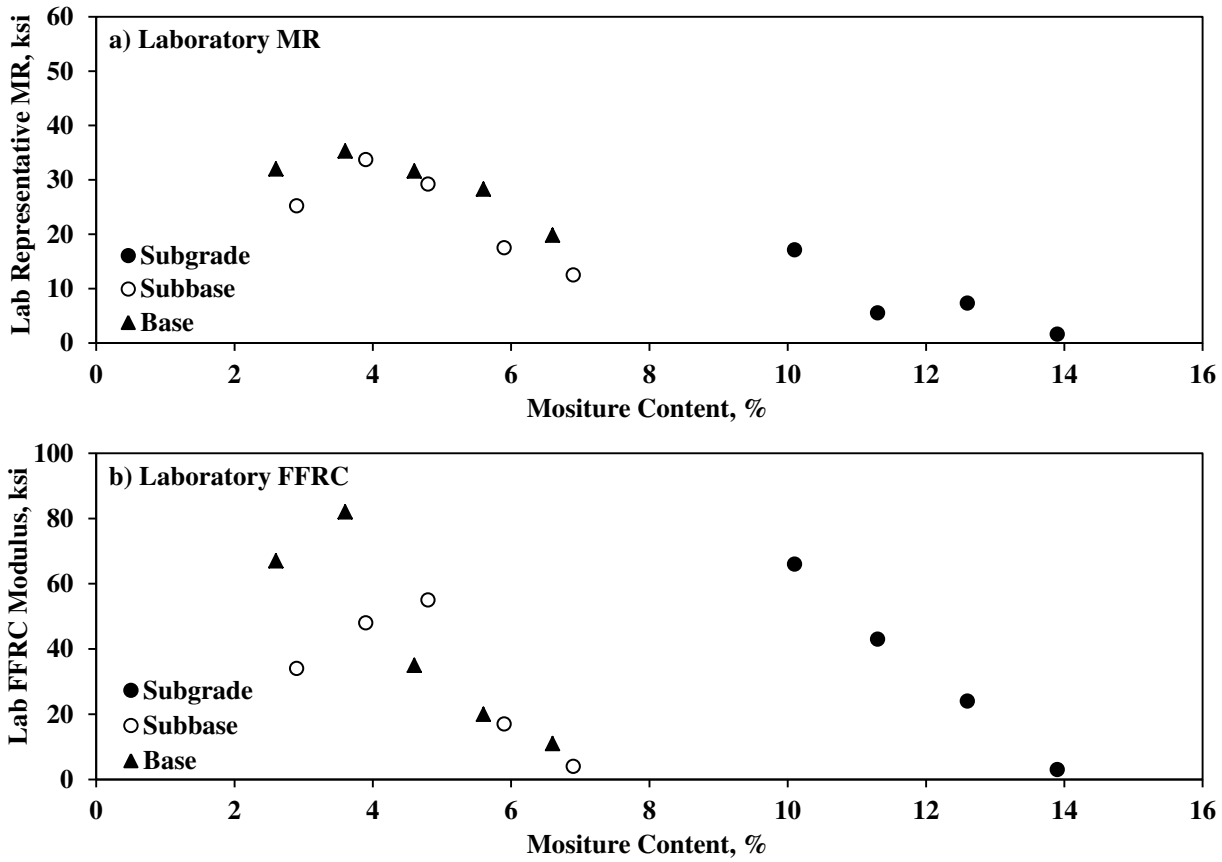

Figure J.2.2 – Variations of Laboratory MR and FFRC Moduli with Moisture Content

J.3 Field Testing Program

As illustrated in Figure J.3.1, field-testing was carried out along 100 ft-long sections of subgrade and base layers and along a 30 ft-long section on subbase layer. The following tests were performed on the compacted layer along lines A, B and C:

- Soil Density Gauge (SDG)
- Zorn Light Weight Deflectometer (LWD) as per ASTM E2835
- Portable Seismic Property Analyzer (PSPA)
- Dynamic Cone Penetrometer (DCP) as per ASTM D6951
- Nuclear Density Gauge (NDG)

In addition, soil samples were extracted from the compacted layers at some points to estimate their oven-dried moisture contents.

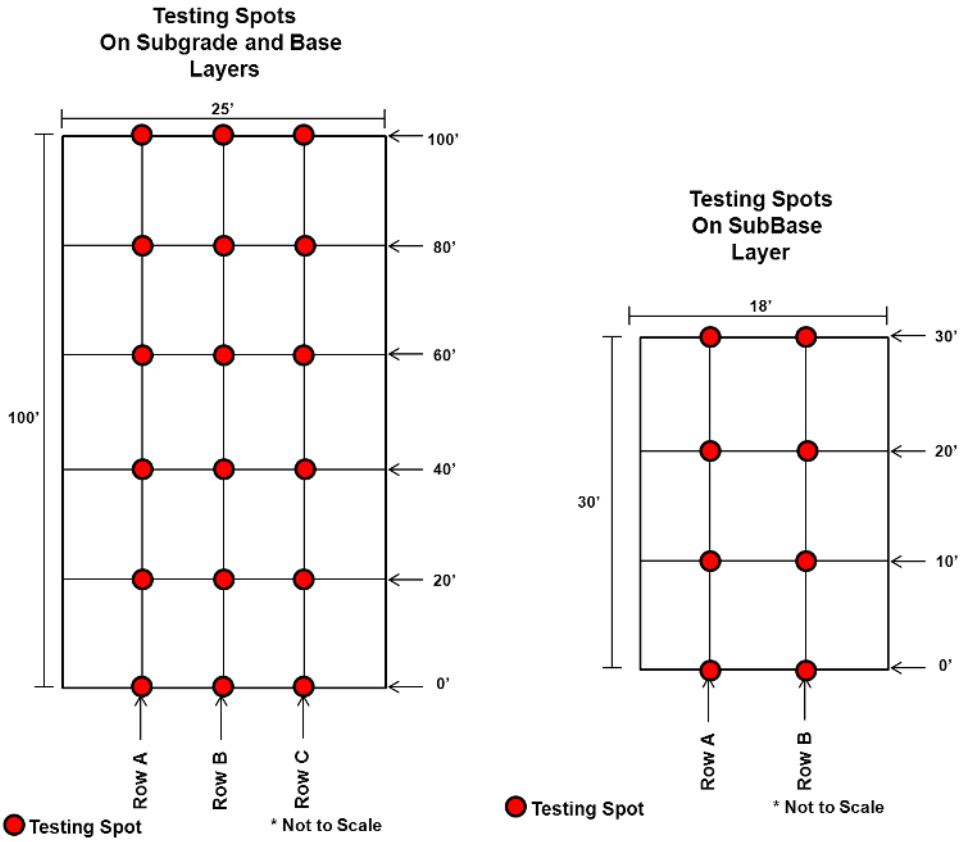

Figure J.3.1 – Schematic of Testing Spots in NJDOT

J.4 Evaluation of Moisture-Density Devices

All materials (base, subbase and subgrade) were transported from the quarry to the site without adding any water. The existing moisture contents of the quarry materials were deemed adequate for the compaction process.

Subgrade Layer: The moisture contents at the testing spots were measured with the SDG and NDG. Figure J.4.1 illustrates the measured moisture content of the compacted subgrade. Several of the NDG data were not collected due to time constraints between construction phases. The average moisture content measured with the NDG was 6.7% and with the SDG was 9.7%.

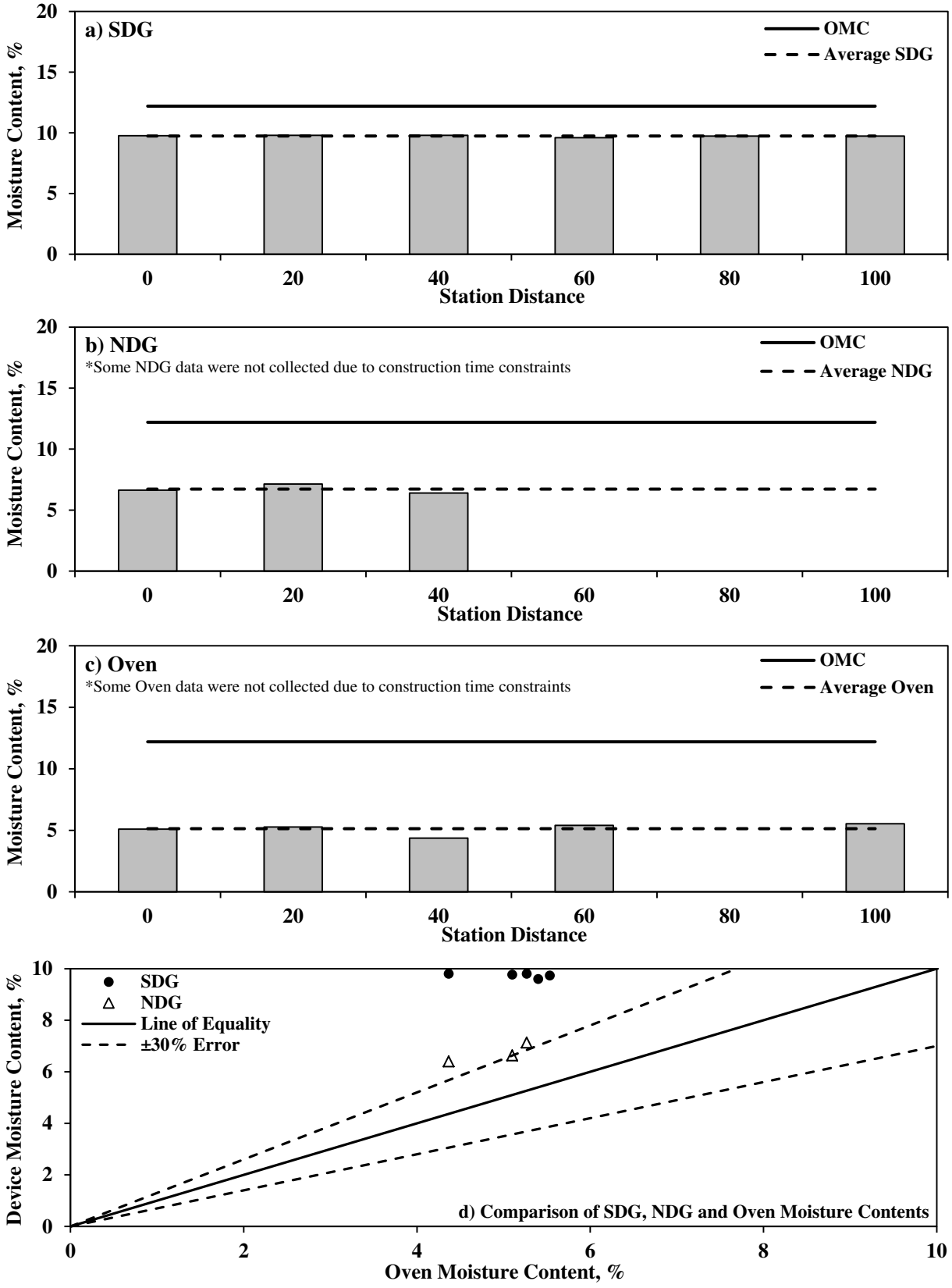

Figure J.4.1 – Variation of Moisture Contents for NJDOT Subgrade

Figure J.4.1c depicts the oven-dry moisture contents of the subgrade layer from soil samples extracted from the SDG/NDG test locations. The average oven-dry moisture content was 5.1%. As compared to the laboratory OMC of 12.2%, the compacted material was already dry of optimum by 6.8%. The NDG results are closer to the oven moisture contents as compared to the SDG results (see Figure J.4.1d).

Figure J.4.2 summarizes the SDG and NDG density readings on the subgrade layer. The average SDG dry density of 202.0 pcf is far from a realistic value and shows the need for calibration of the results. The average NDG dry density was 126.4 pcf. Based on the NDG results, the compacted layer marginally passed the acceptance limit of 95% MDD.

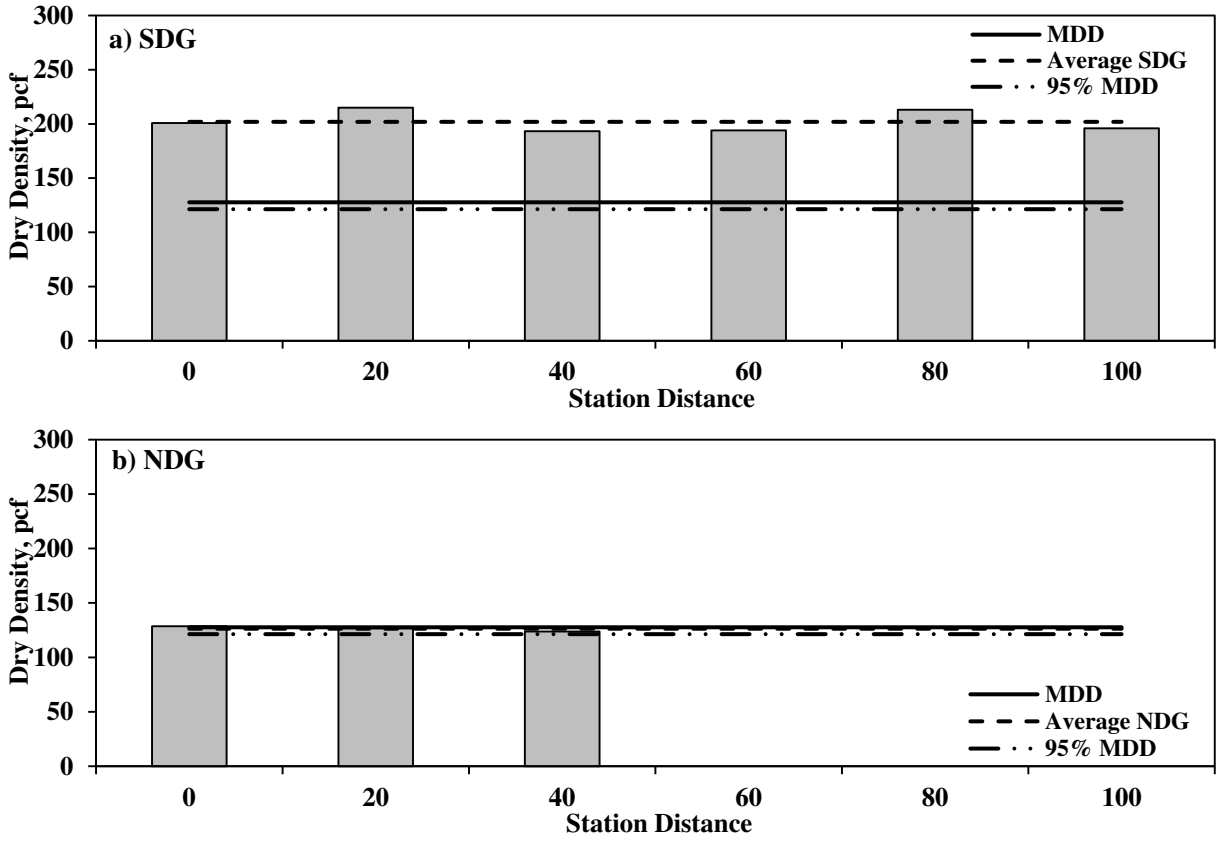

Figure J.4.2 – Variation of Dry Density for NJDOT Subgrade Geomaterial

Subbase Layer: As reflected in Figure J.4.3, the average SDG moisture content was 9.7%. The average NDG moisture content was 4.2% that was close to the laboratory OMC of 4.8% as reflected in Table J.2.1. As reflected in Figure J.4.3c, the average oven-dry moisture content from specimens extracted from the compacted subbase was 4.9%. As such, the section was placed and compacted at OMC.

Figure J.4.4 summarizes the density measurements with the SDG and NDG on the subbase layer. The average dry density from the SDG was 191.2 pcf and with the NDG was 136.7 pcf. Compared to the laboratory maximum dry density of 147.5 pcf, the compacted subbase layer marginally passes the acceptance limit of 95%MDD.

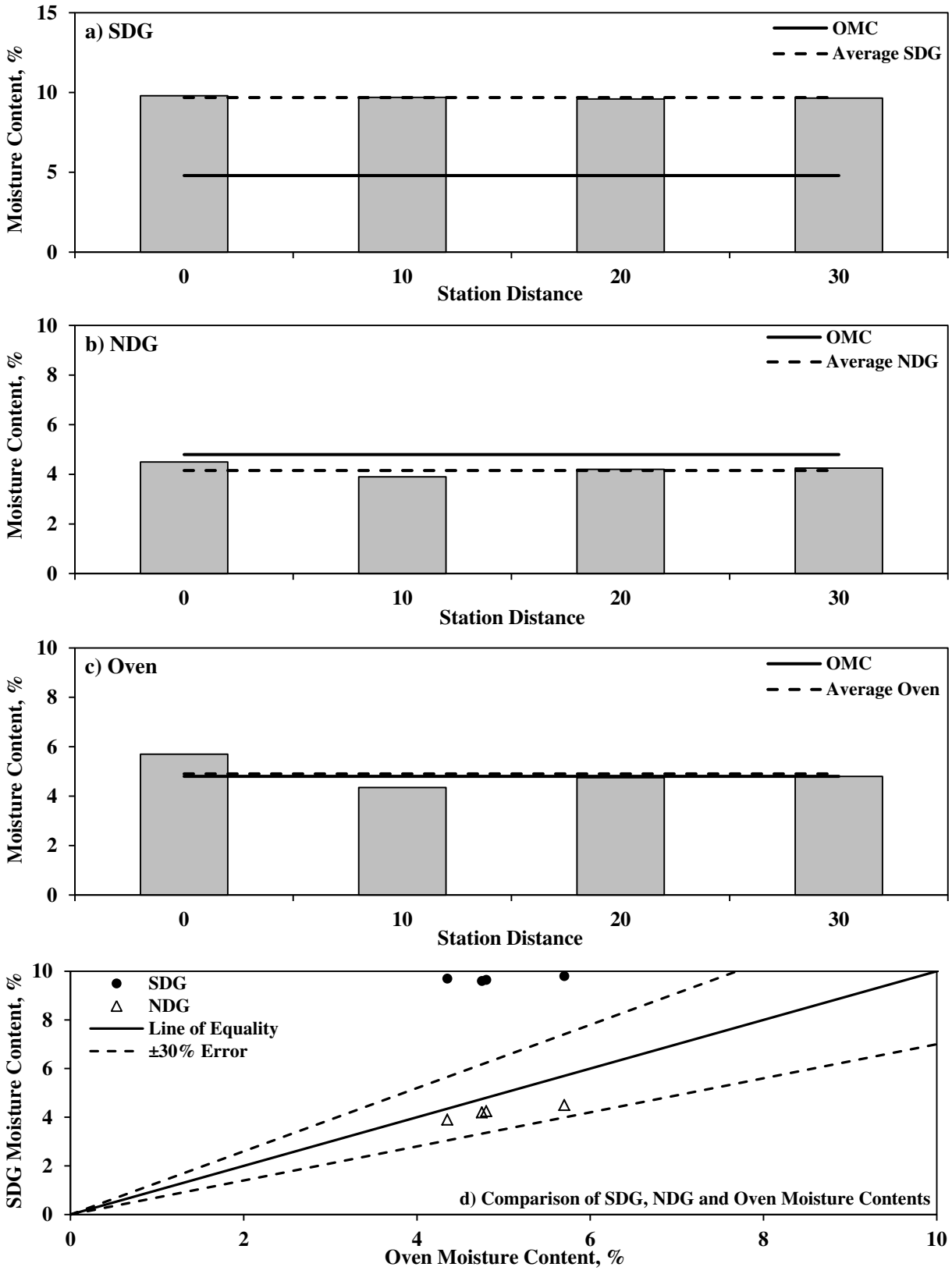

Figure J.4.3 – Variation of Moisture Content for NJDOT Subbase Geomaterial

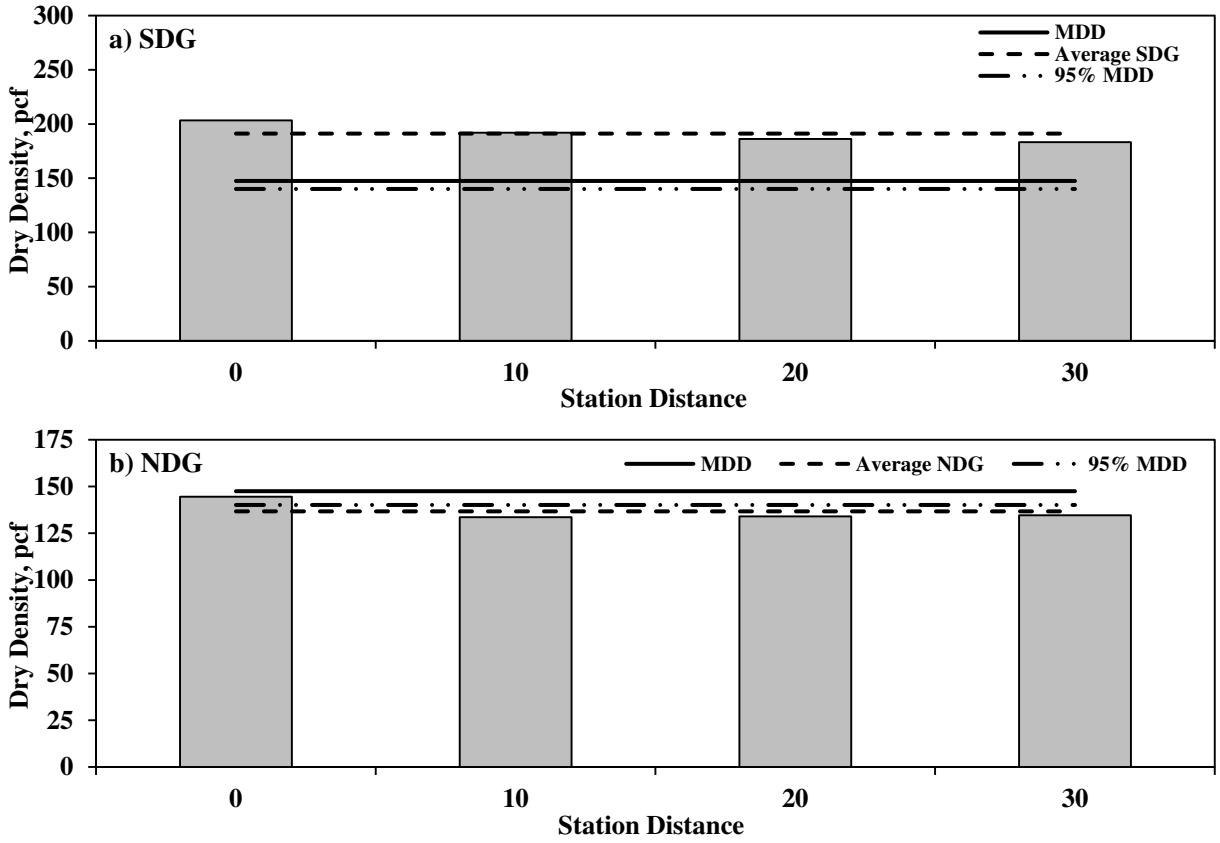

Figure J.4.4 – Variation of Moisture Content for NJDOT Subbase Geomaterial

Base Layer: Figure J.4.5a and J.4.5b summarizes the NDG and SDG moisture contents after compaction of the base layer. The average SDG and NDG moisture contents were 9.9% and 4.3%, respectively. The average of oven-dry moisture contents for the base layer was 3.5%, which was 1.1% dry of laboratory OMC (see Figure J.4.5c).

Figure J.4.5d compares the oven-dry, SDG and NDG moisture contents. The SDG mostly overestimated the moisture content with more than 30% error while the NDG results are generally within the 30% error limits.

Figure J.4.6 depicts the estimated dry densities of the testing spots on base layer. According to the SDG readings, the average dry density of the compacted base layer is 183.9 pcf. SDG data should be calibrated to reflect a reasonable value for dry density. The laboratory maximum dry density of the base materials was 147.3 pcf. The average NDG density was 126.1 pcf. Therefore, the compacted base layer is not passing the specification limit for density (95% of MDD).

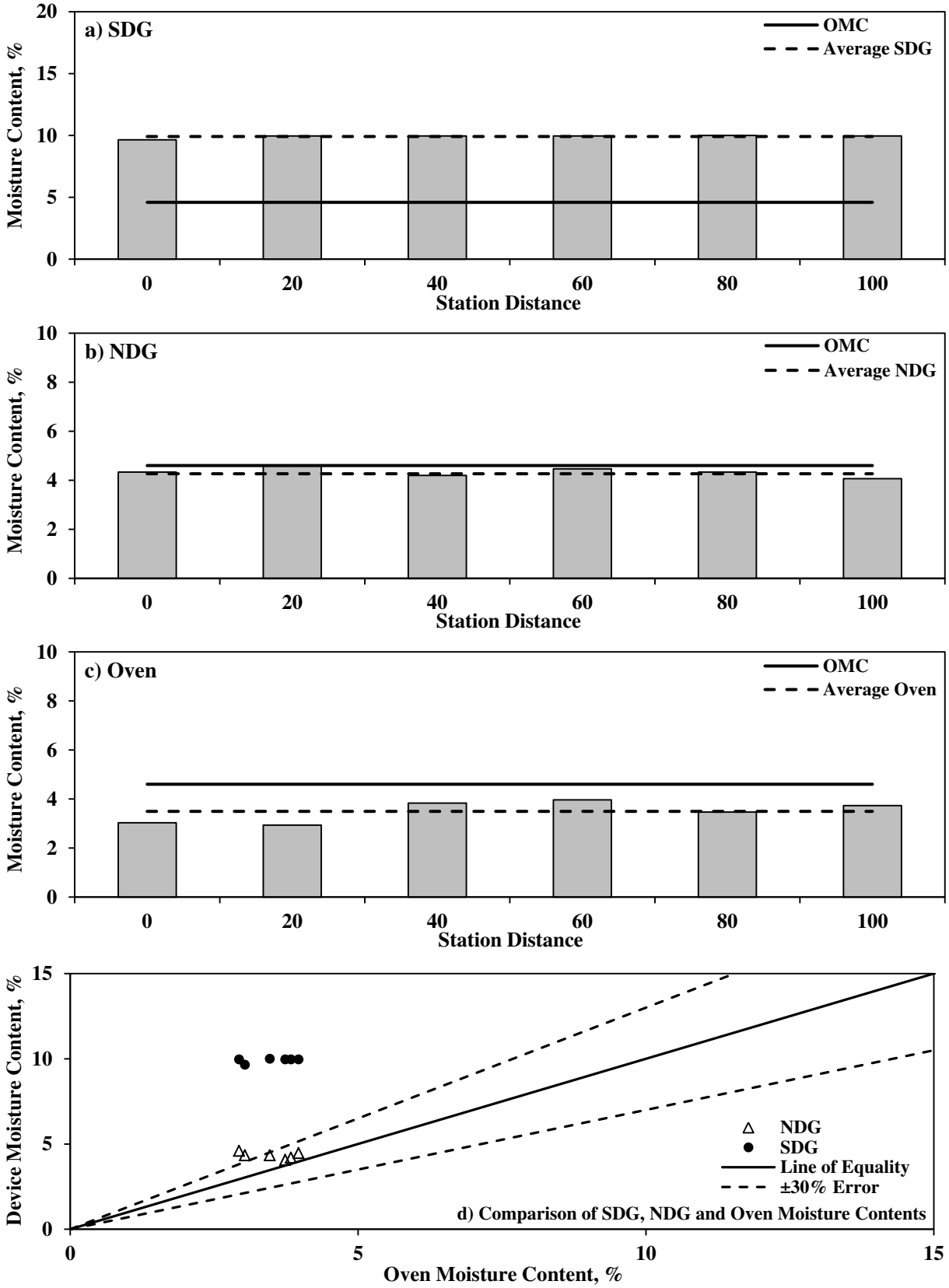

Figure J.4.5 – Variation of Moisture Content for NJDOT Base Geomaterial

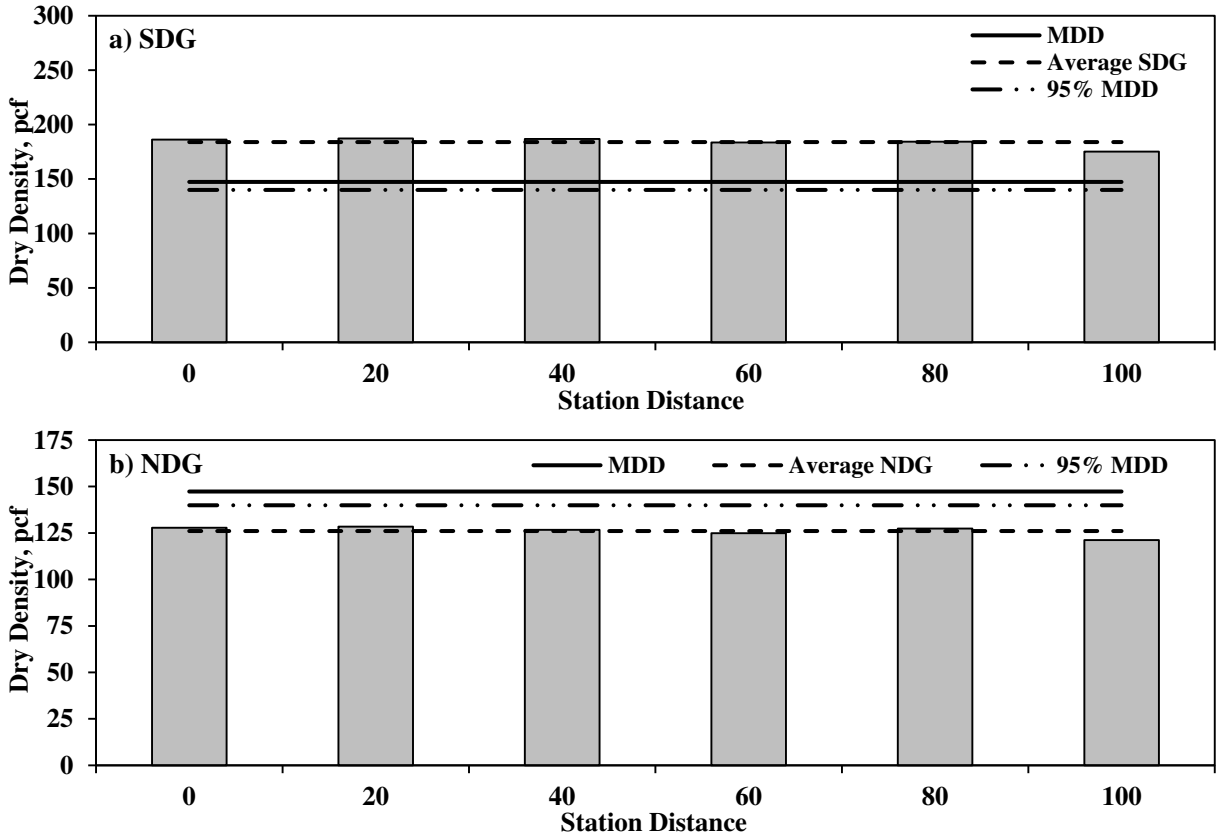

Figure J.4.6 – Variation of Dry Density for NJDOT Base Geomaterial

J.5 Evaluation of Modulus-Based Devices

Subgrade Layer: Figure J.5.1 contains the results of the measurements with the PSPA, Zorn LWD and DCP immediately after the compaction of the subgrade layer. The average (average of measurements along line A, B and C) PSPA modulus was 52.2 ksi while those of the LWD and DCP were 15.6 ksi and 14.6 ksi, respectively. The spatial standard deviations of modulus measurements along the section for PSPA, LWD and DCP were 6.7 ksi, 1.1 ksi and 3.1 ksi, respectively. The PSPA and LWD measurements were repeated three times at each testing spot to investigate the in-place variability of these two devices. The standard deviations are depicted as error bars for each testing spot in Figure J.5.1. The average standard deviations of in-place modulus measurements of the PSPA and LWD were 7.8 ksi and 1.2 ksi, respectively.

Subbase Layer: Figure J.5.2 summarizes the modulus measurements after compaction of the subbase layer. The average PSPA, LWD and DCP moduli was 104.8 ksi, 9.6 ksi and 14.5 ksi, respectively. The spatial standard deviations were 28.4 ksi and 1.8 ksi for the PSPA and LWD tests, while the average standard deviations of the in-place repetitions were 12.8 ksi and 0.7 ksi, respectively. The spatial standard deviation for the DCP was 0.9 ksi.

Base Layer: Figure J.5.3 illustrates the measured moduli with the PSPA, LWD and DCP after compaction of the base layer. The average PSPA modulus was 75.7 ksi as compared to the average LWD modulus of 9.7 ksi and average DCP modulus of 12.6 ksi. The spatial standard deviations of 4.0 ksi for PSPA, 1.1 ksi for LWD and 0.6 ksi for DCP modulus show less spatial variation of the measured moduli of base layer as compared to the subgrade and subbase layer. The in-place standard deviations of PSPA and LWD were 6.2 ksi and 0.7 ksi, respectively.

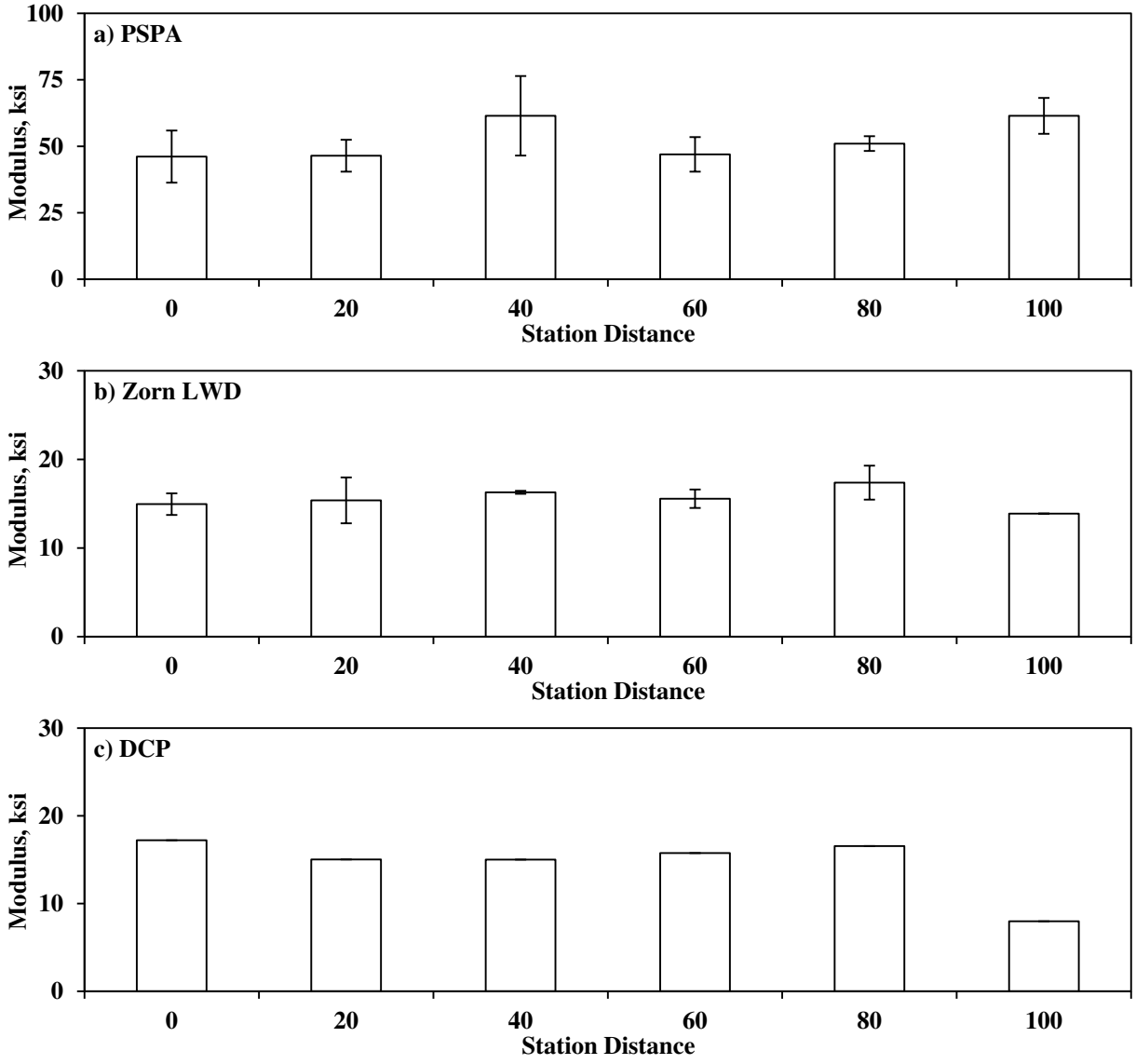

Figure J.5.1 – Variations of Subgrade Modulus immediately after Compaction

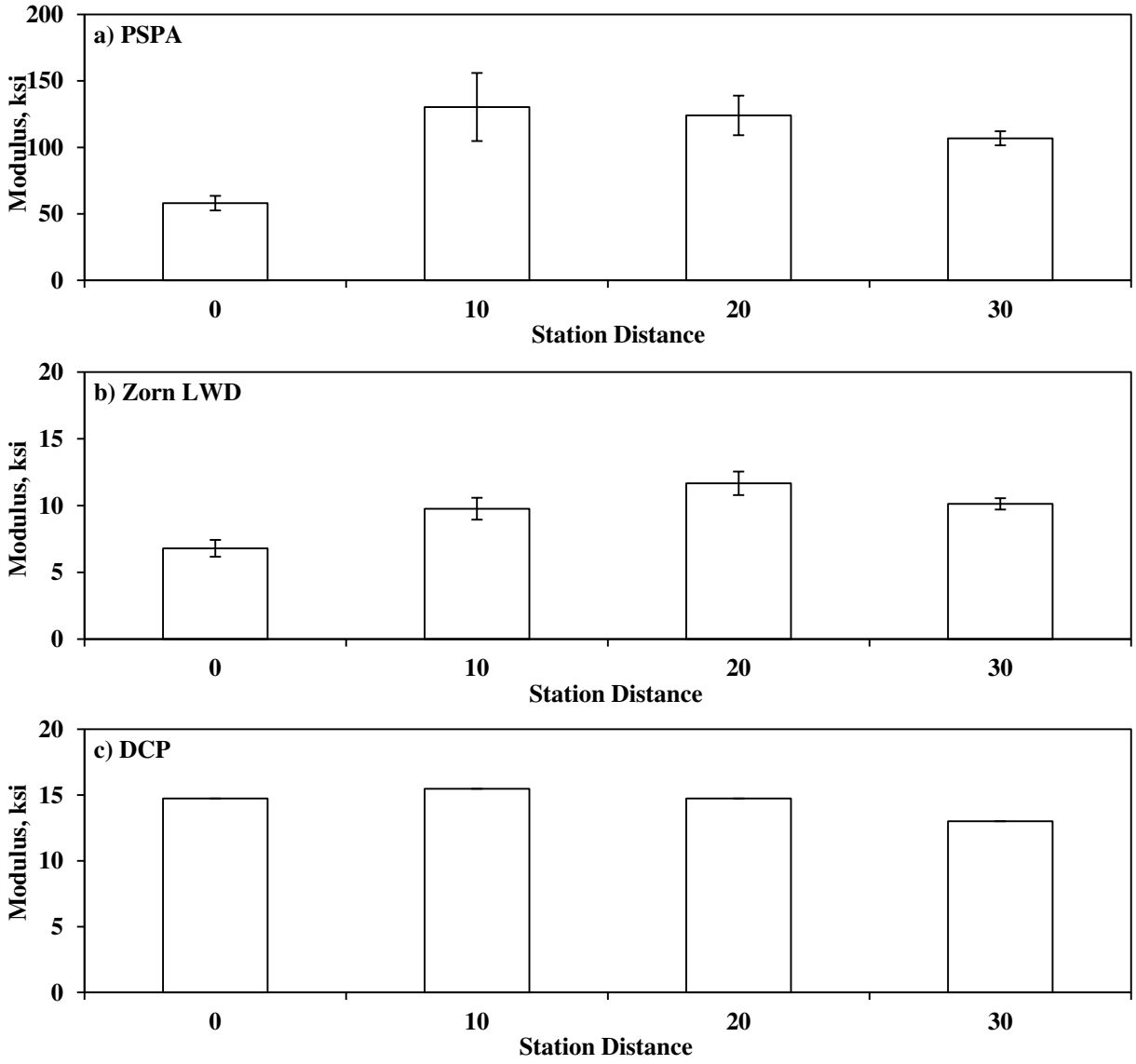

Figure J.5.2 – Variations of Subbase Modulus immediately after Compaction

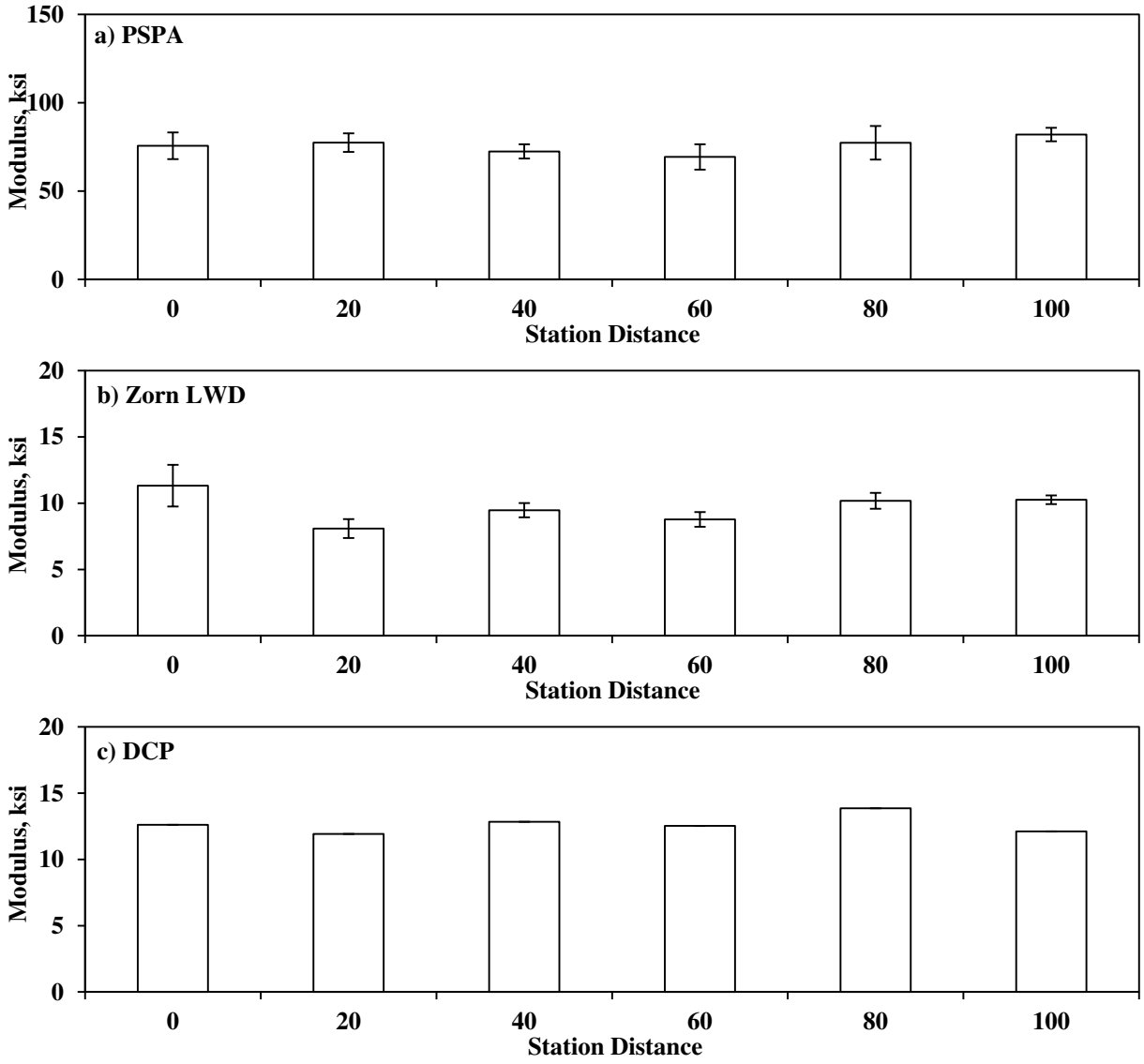

Figure J.5.3 – Variations of Base Modulus Immediately after Compaction

J.6 Variability of Modulus-Based Devices

The in-place and between testing spots standard deviations of modulus measurements were summarized in Section J.5. The variations of the in-place coefficients of variation (COVs) among three test repetitions with measured moduli for subgrade, subbase and base layers are depicted in Figures J.6.1 through J.6.3, respectively. A distinct pattern between the COV values and measured moduli is not observed. The COV of the PSPA modulus measurements are somehow higher for subgrade layer as compared to the base and subbase layers.

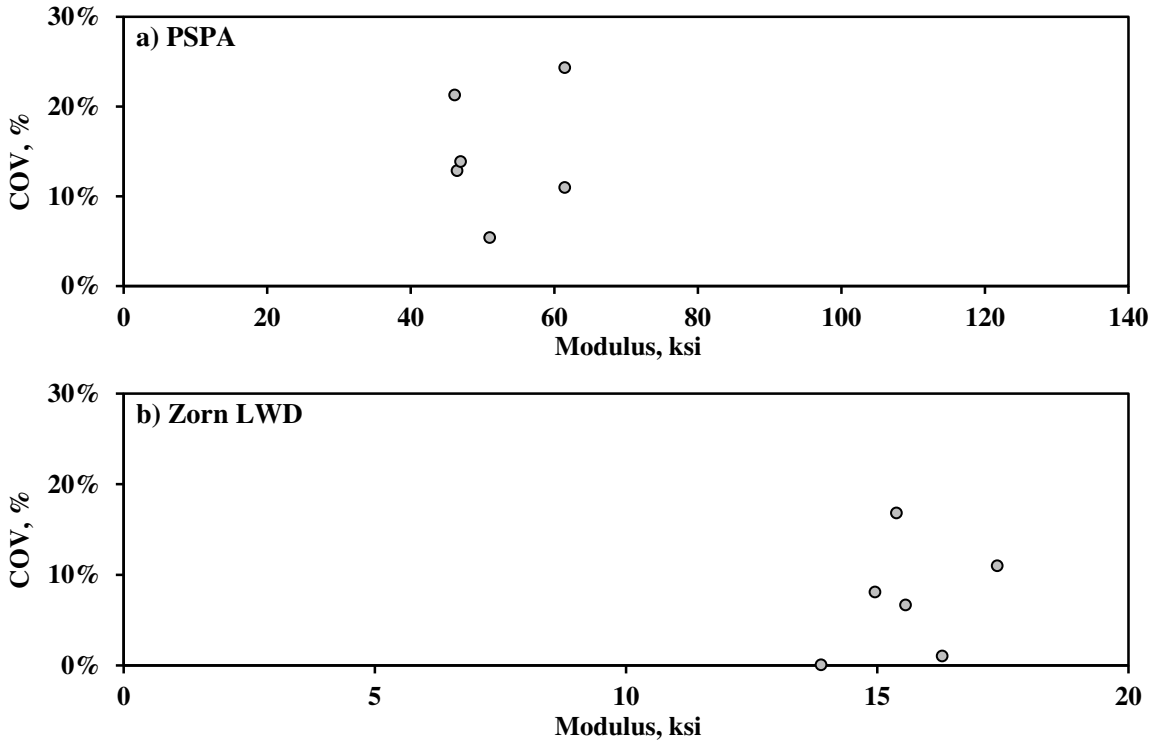

Figure J.6.1 – Coefficients of Variation (COV) of Repeated Measured Moduli at each Testing Spot (Subgrade Layer)

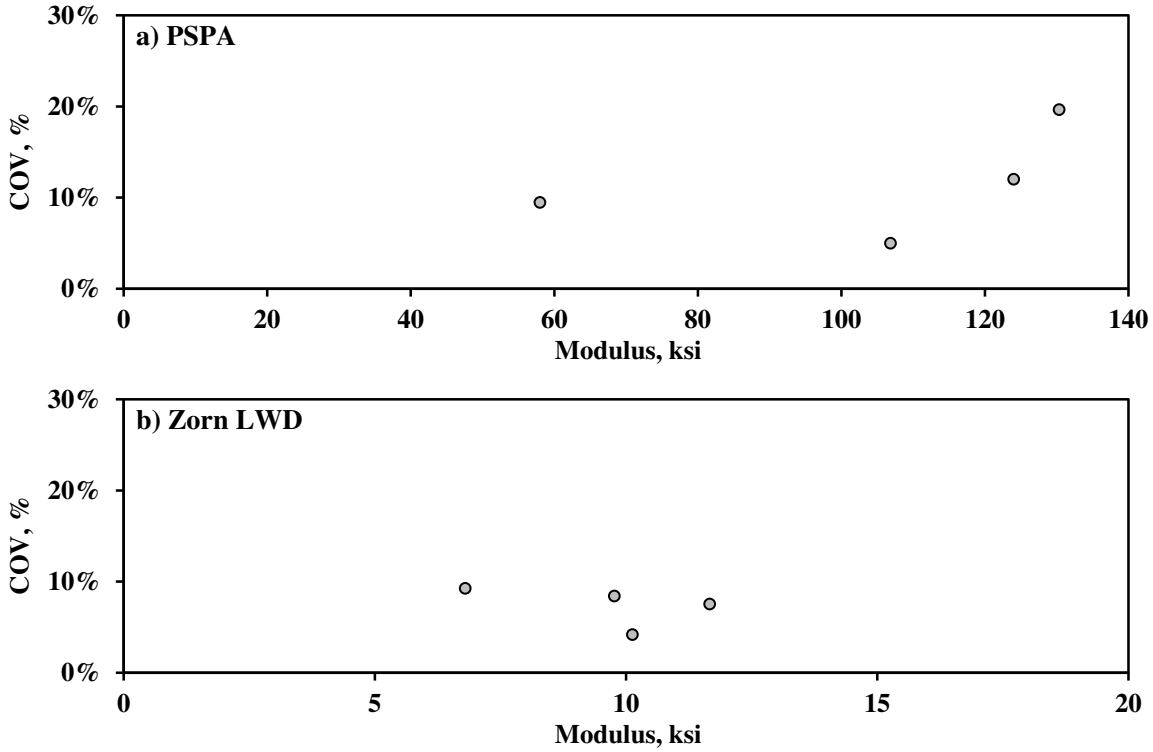

Figure J.6.2 – Coefficients of Variation (COV) of Repeated Measured Moduli at each Testing Spot (Subbase Layer)

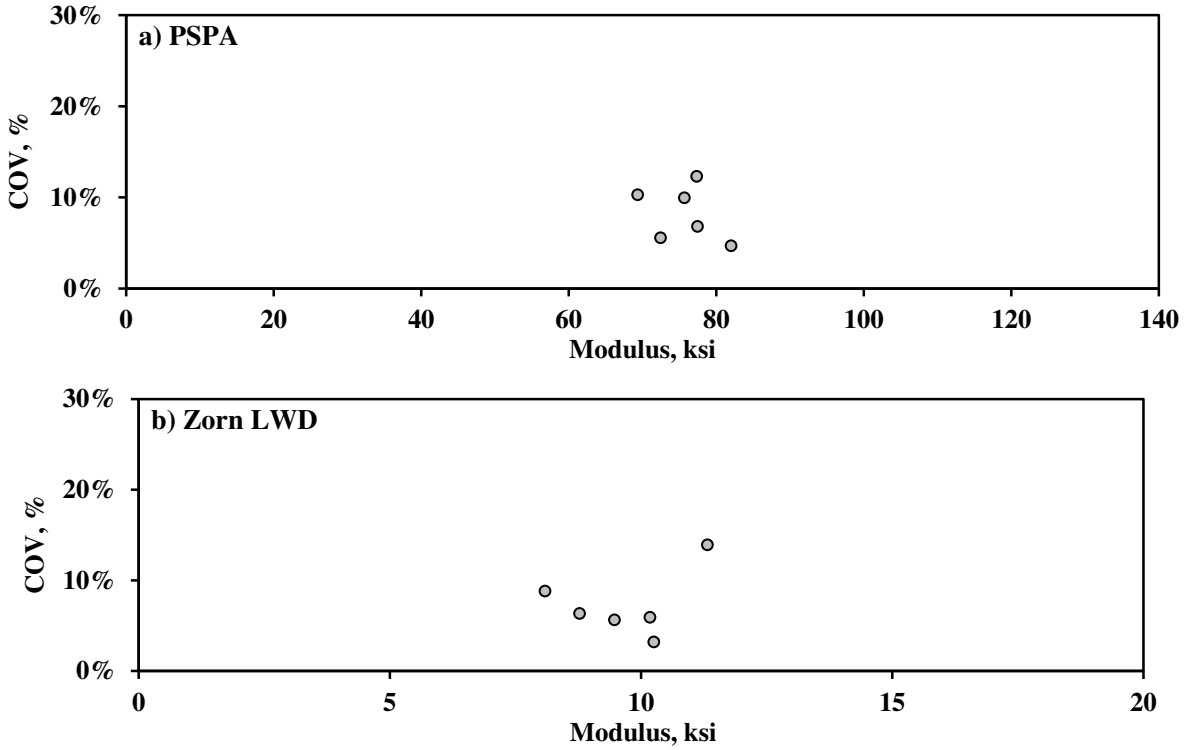

Figure J.6.3 – Coefficients of Variation (COV) of Repeated Measured Moduli at each Testing Spot (Base Layer)

J.7 Moisture-Modulus Relationships

The relationships between the field moduli from different devices and their corresponding oven dry moisture contents are summarized in Figures J.7.1 through J.7.3 for subgrade, subbase and base layers, respectively. Due to uncertainties associated with the NDG and SDG results, the oven-dry moisture contents were selected to correlate the measured moduli with in-situ moisture contents. The variations in the moisture contents for all three layers lie around narrow ranges. As expected, the moduli from all devices decrease with the increase in moisture content. The PSPA and LWD show better correlations between measured moduli and oven-dry moisture contents. As compared to the results from the subgrade layer, the moisture-modulus relationships for the base and subbase layers are better correlated.

J.8 Acceptance Scenarios for Modulus-Based Devices

Subgrade: The target modulus of the subgrade was established for the LWD as discussed in Chapter 6. Laboratory-measured resilient modulus parameters (k'_1, k'_2 and k'_3) at OMC and MDD were used as input to these equations. The target moduli for the LWD and PSPA are indicated in Figure J.8.1. Based on the PSPA results, the measured field moduli pass the acceptance limit of 80% of target modulus (See Figure J.8.1a). The LWD field moduli pass the specified acceptance limit of 80% of target modulus by a wide margin; perhaps because of the stiff existing embankment layer just underneath the subgrade layer (see Figure J.8.1b).

Comparing the moduli after 24 hrs with the ones immediately after compaction of subgrade layer, on average the PSPA moduli increased by about 30% and the LWD moduli decreased by about 10%. The reason for the decrease in the modulus of the LWD cannot be explained.

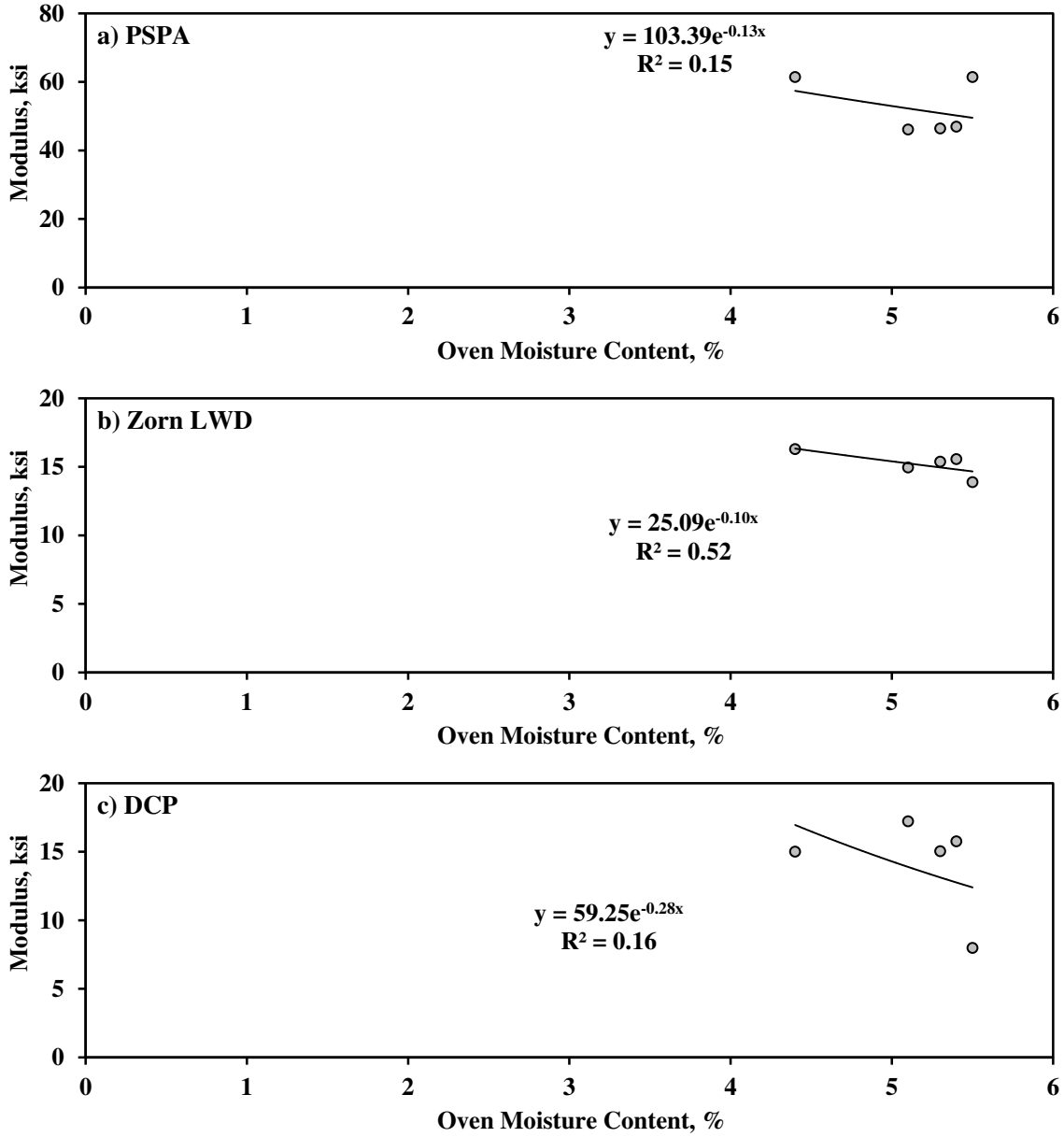

Figure J.7.1 – Moisture-Modulus Correlation after Compaction of Subgrade Layer

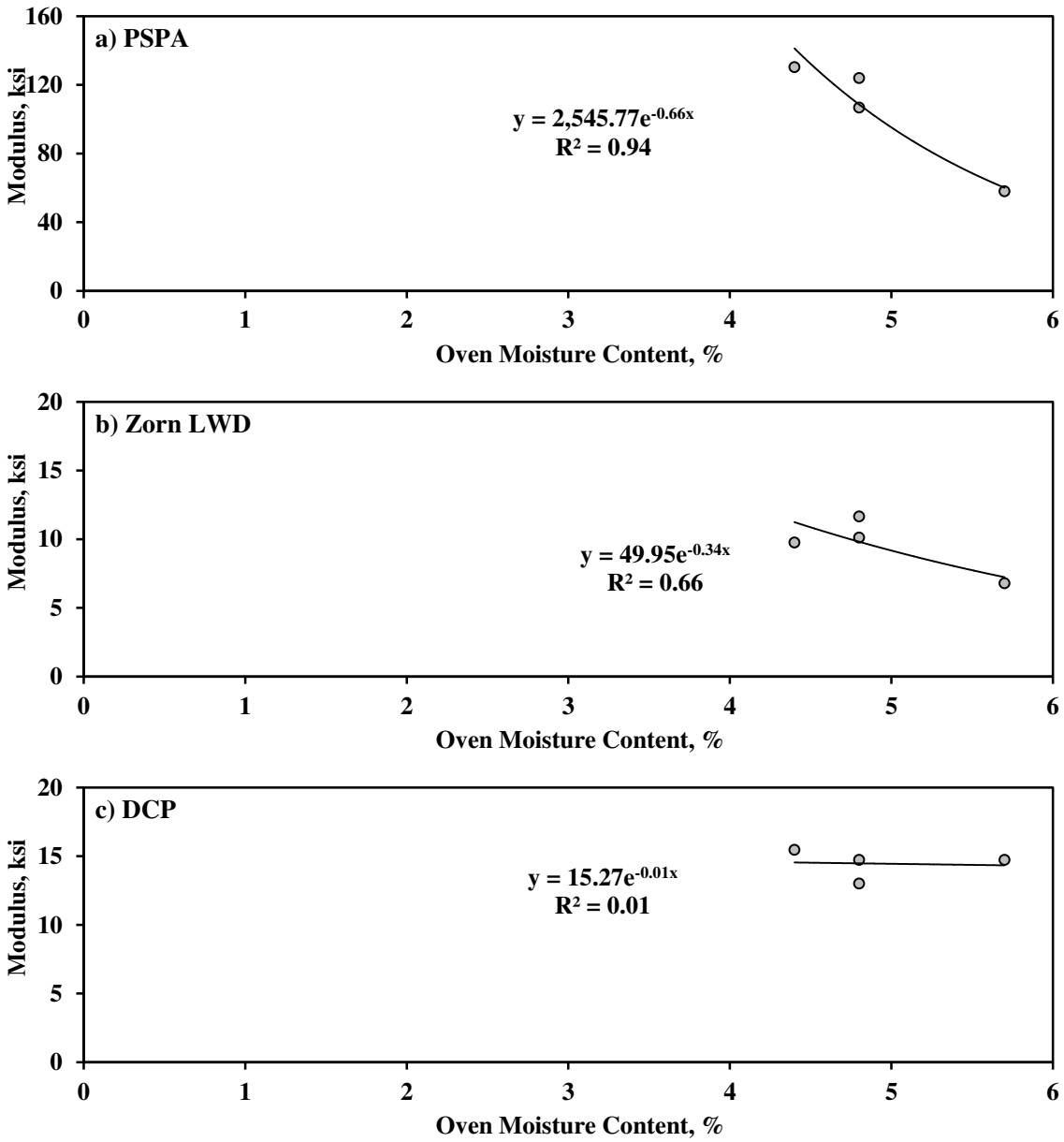

Figure J.7.2 – Moisture-Modulus Correlation after Compaction of Subbase Layer

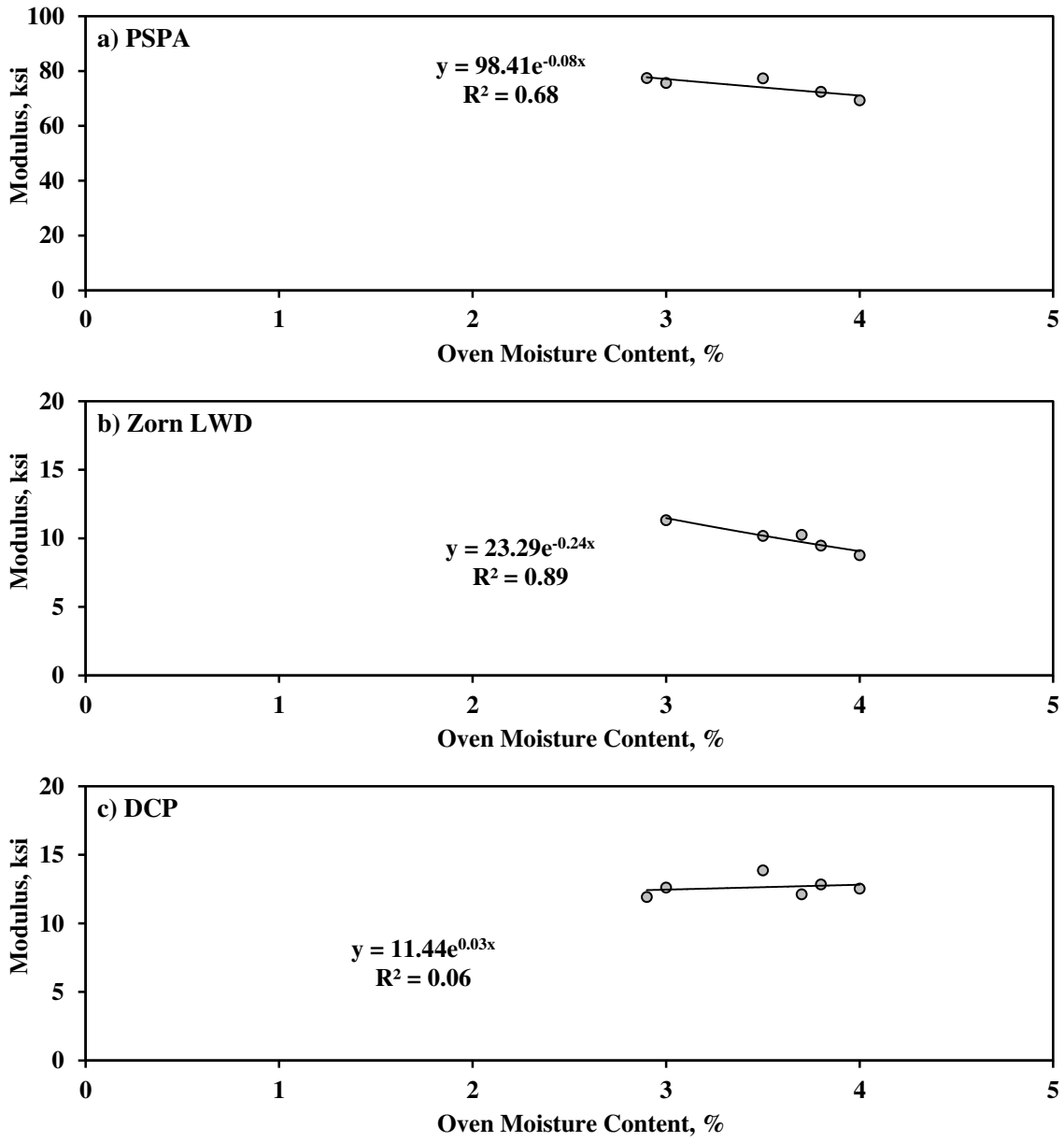

Figure J.7.3 – Moisture-Modulus Correlation after Compaction of Base Layer

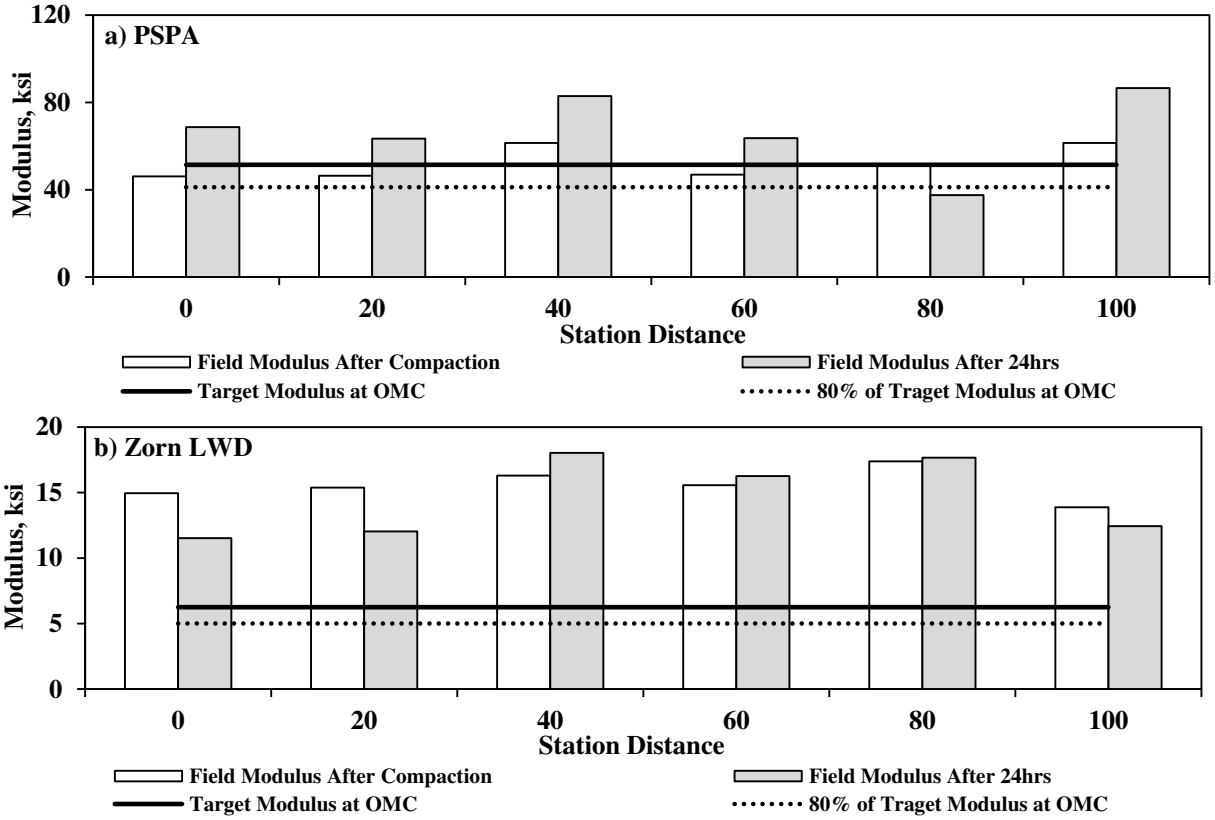

Figure J.8.1 – Comparison of Field and Target Moduli for Subgrade Layer

Subbase Layer: The target moduli for the LWD and PSPA for the subbase layer are summarized in Figure J.8.2. Based on the PSPA results the compacted section passes the acceptance criteria. According to the LWD results, the selected test section fails. This could be associated with the depth of influence of the LWD as compared to the PSPA (which estimates the low-strain modulus of the layer). The average PSPA and LWD moduli after 24 hrs relative to those at the time of compaction increased by 20% and 10%, respectively.

Base Layer: Figure J.8.3 compares the PSPA and LWD field moduli with the established target moduli. According to the LWD, none of the sections passes the acceptance criteria. Meanwhile, the PSPA moduli pass the acceptance limit of the established target modulus. This could be due to differences in the intrinsic nature of the PSPA and LWD modulus as discussed earlier. The PSPA moduli increased by 40% 24 hrs after the time of compaction while the LWD moduli increased by 20%.

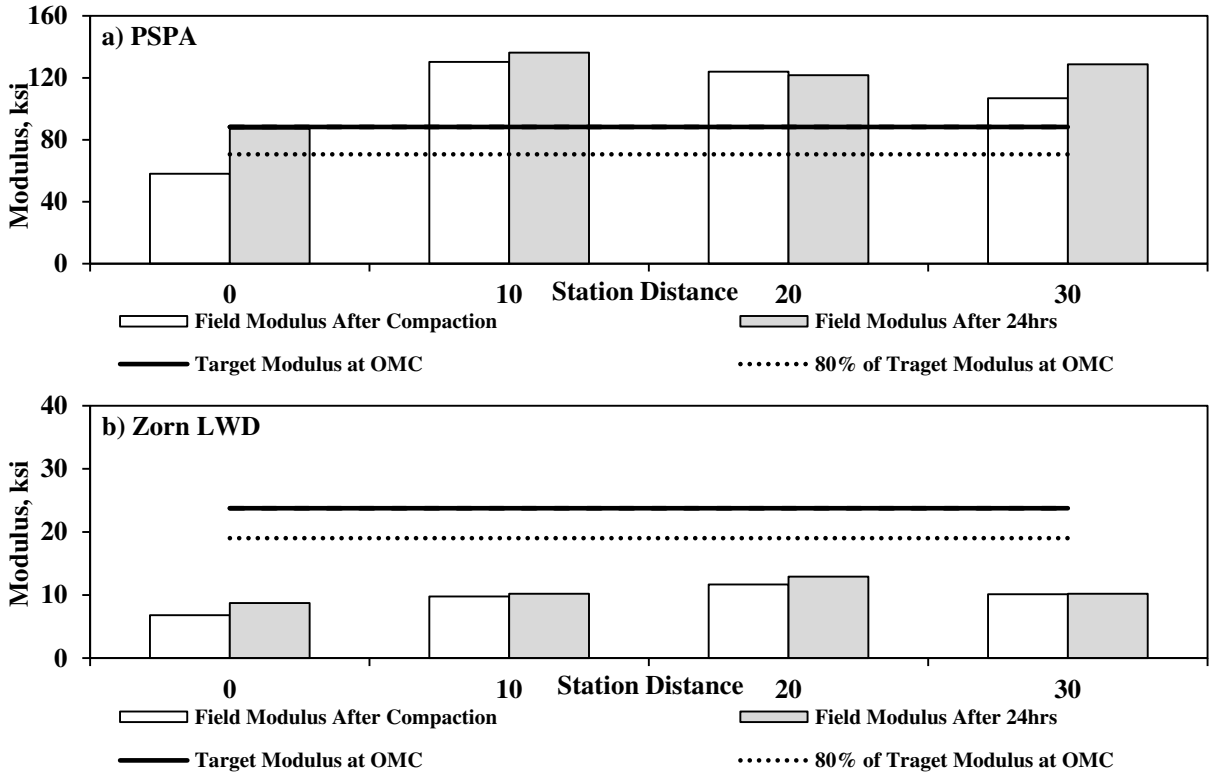

Figure J.8.2 – Comparison of Field and Target Moduli for Subbase Layer

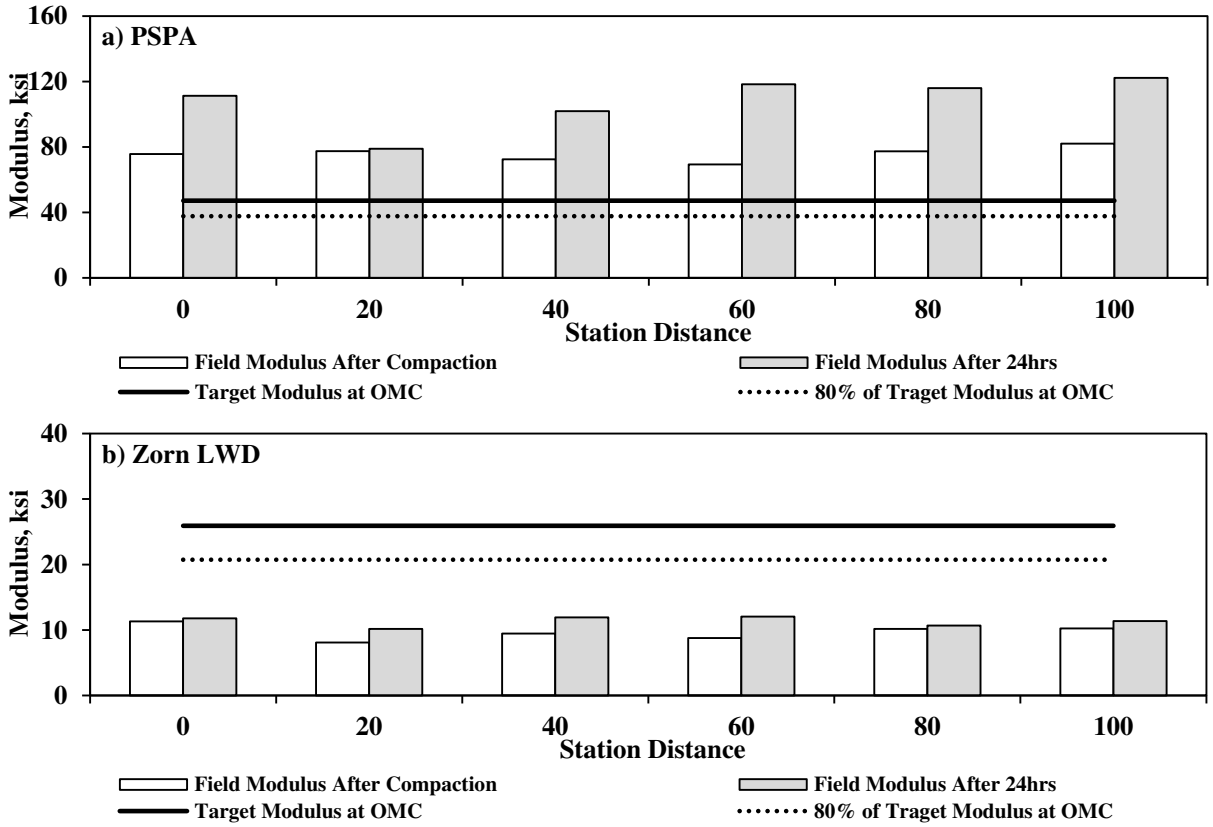

Figure J.8.3 – Comparison of Field and Target Moduli for Base Layer

Appendix K

OBSERVATIONS FROM IMPLEMENTATION OF SPECIFICATION

Site II.1

K.1 Introduction

The evaluation was carried out at the National Airport Pavement Testing Facility (NAPTF) of the U.S. Federal Aviation Administration (FAA) located at the William J. Hughes Technical Center near Atlantic City, New Jersey as reflected in Figure K.1.1. Figure K.1.2 illustrates the schematic of test spots on the selected section along the testing facility. Subgrade layer was placed at 8 in. lifts. A 6-in.-thick subbase layer was prepared and placed after compaction of subgrade materials. The thickness of compacted base layer was 8 in.

Figure K.1.3 depicts the testing configuration and cross sections of the selected test section of the facility. Two 30 ft×300 ft sections, one called the low-strength subgrade flexible pavement (LFP) on the north side and the other the low-strength subgrade flexible pavement with conventional base (LFC) on the south side, were tested. The subbase (designated as P-154) layer had a uniform thickness of 20 in. on the south side and varied from 29 in. to 41 in. on the north side. Figure K.1.4 depicts the testing spots on compacted subgrade layer on the north side. The testing of subgrade layer was completed during the week of August 12, 2103. The subbase layer was prepared and tested by the NAPTF during November, 2013. The construction and testing of the base layer took place in May 2014.

Figure K.1.1 – Location of Field Evaluation Site in National Airport Pavement Testing Facility

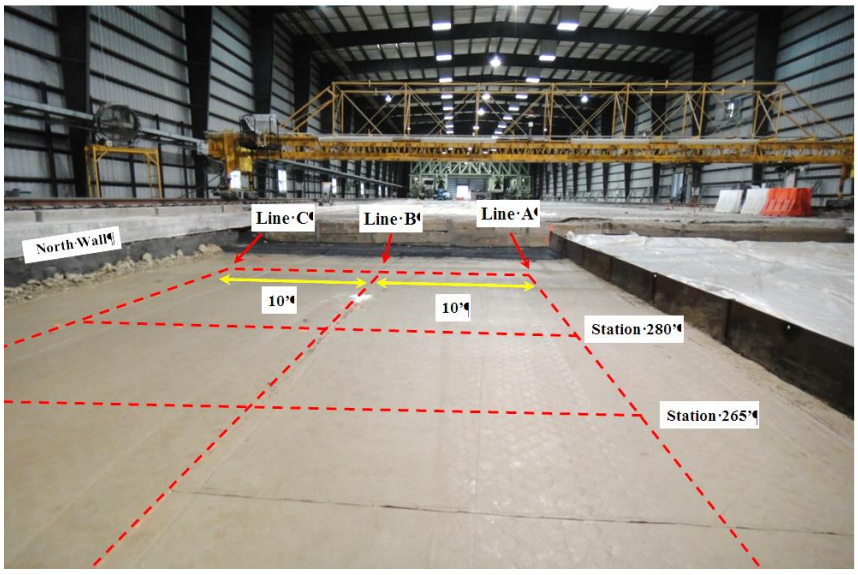

Figure K.1.2 – Illustration of Prepared Test Section in FAA

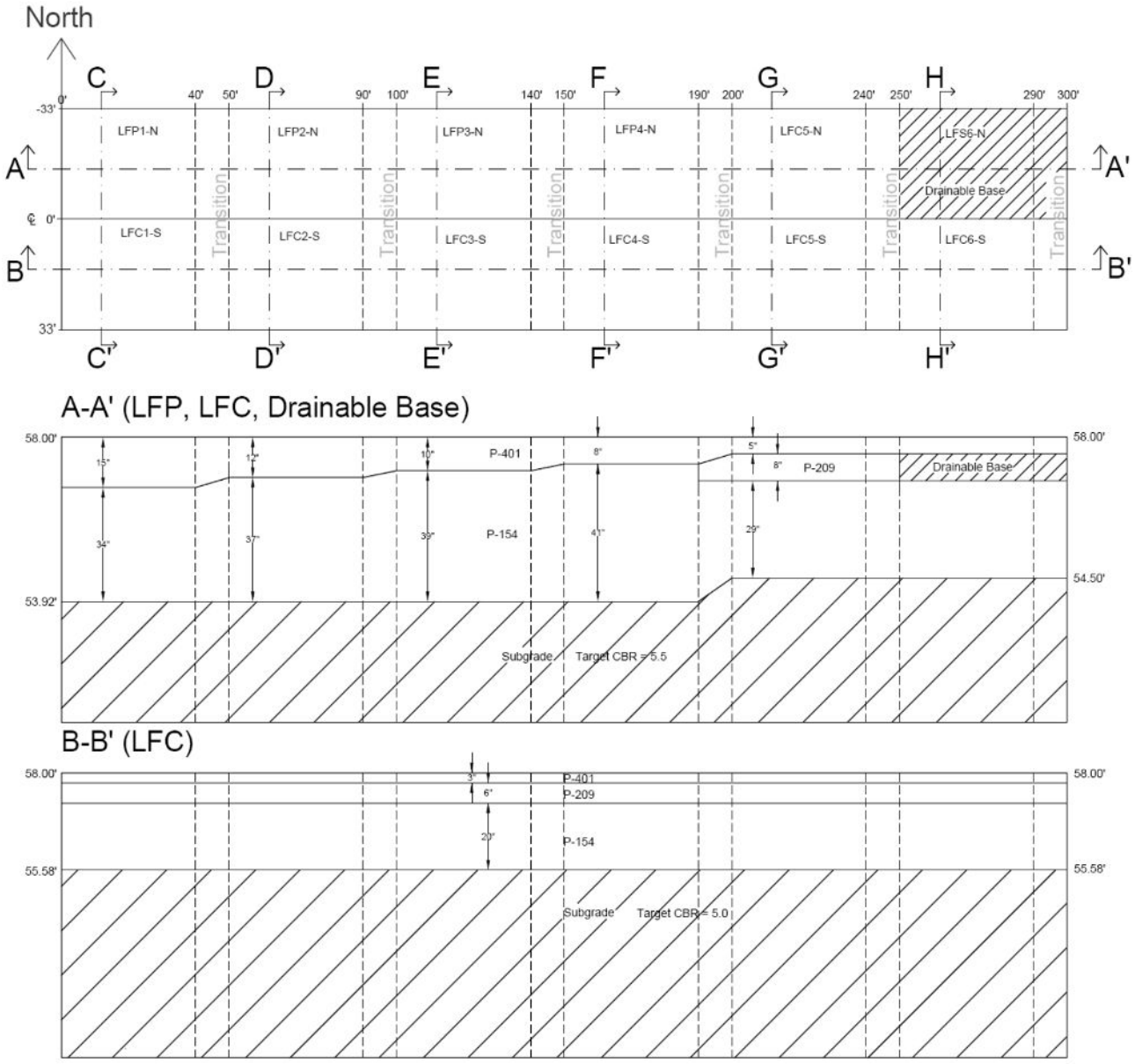

* LFP: Low-Strength Subgrade Flexible Pavement
* LFC: Low-Strength Subgrade Flexible Pavement with Conventional Base
* P-154: Coarse-grained subbase materials
* P-209: Flexible base materials

Figure K.1.3 – Schematic of Selected Test Sections in FAA

K.2 Laboratory Results

The index properties of the subgrade, subbase and base materials are summarized in Table K.2.1, and their gradation curves are presented in Figure K.2.1. The subgrade was classified as low-plasticity clay as per Unified Soil Classification System (USCS). The subbase was categorized as poorly-graded sand and the base material as well-graded gravel. The optimum moisture contents and maximum dry unit weights obtained as per standard Proctor tests (AASHTO T99) for the subgrades and as per modified Proctor tests (AASHTO T180) for the subbase and base are also reported in Table K.2.1.

Table K.2.1 - Index Properties of Dublin Geomaterials

Soil Type	Gradation %				USCS Class.	Specific Gravity	Atterberg Limits			Moisture/Density	
	Gravel	Coarse Sand	Fine Sand	Fines			LL	PL	PI	OMC,* %	MDUW,** pcf
Subgrade	5.2	3.7	2.4	88.7	CL	2.65	48	15	33	24.0	97.9
Subbase	0.3	79	18	2.6	SP	2.65	0	0	0	8.9	132.0
Base	50	35	13	2	GW	2.65	0	0	0	5.4	152.0

*OMC = Optimum Moisture Content, **MDUW = Maximum Dry Unit Weight

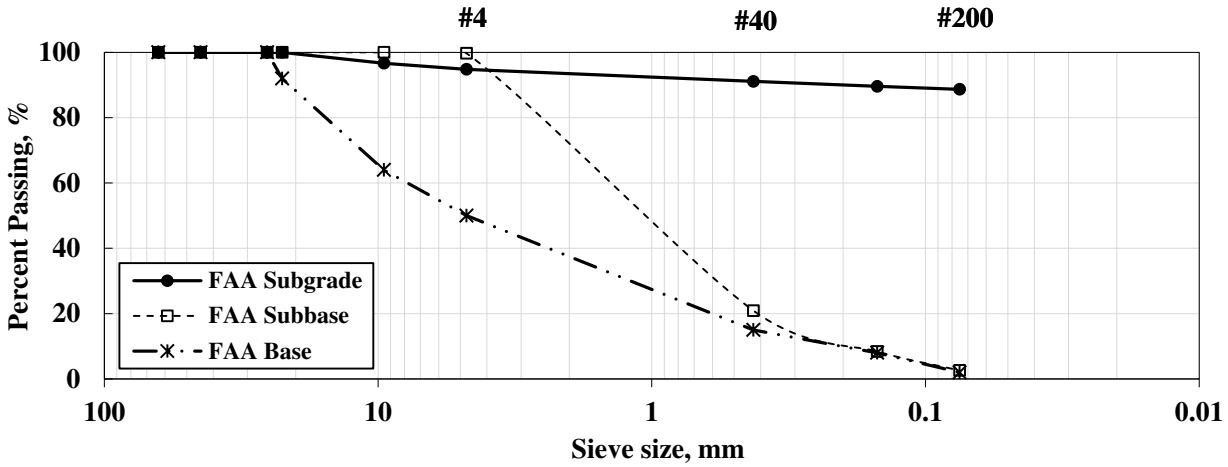

Figure K.2.1 – Gradation Curves of FAA Geomaterials

The resilient modulus (MR) and FFRC tests were performed on laboratory specimens prepared from the materials at the OMC, dry of OMC and wet of OMC as summarized in Table K.2.2. Figure K.2.2 illustrates the variations of the FFRC moduli and representative MR values with moisture content. Laboratory specimens made from the subbase materials were not stable enough to perform modulus tests.

K.3 Field Testing Program

As illustrated in Figure K.3.1, field-testing was carried out along a 300 ft section. The subgrade layer at the site had been prepared and covered before the research team arrived. The subbase (P-154) and base (P-209) materials were placed and compacted a few months after the preparation of subgrade layer due to some operational and weather issues. The following tests were performed on the compacted layers along lines A, B and C:

- Soil Density Gauge (SDG)
- Zorn Light Weight Deflectometer (LWD) as per ASTM E2835
- Dynatest LWD as per ASTM 2583
- Portable Seismic Property Analyzer (PSPA)
- Dynamic Cone Penetrometer (DCP)

Only the Dynatest LWD, DCP and PSPA tests were performed on the compacted subbase layer. No DCP tests were carried out on the base layer. Limited number of sand cone test on subbase and drive cylinder test on subgrade layer was performed to measure the dry density and moisture content of the compacted layer. The NDG tests were performed on the compacted base layer.

Table K.2.2 – Laboratory Results of MR and FFRC Tests of FAA Geomaterials

Type	Target Moisture Content	Actual Moisture Content, %	Dry Density, pcf	FFRC Modulus, ksi	Nonlinear Parameters			Representative MR, ksi*
					k'_1	k'_2	k'_3	
Subgrade (Dupont Clay)	OMC-2	20.1	95.0	35	1335	0.07	-1.02	17.0
	OMC-1	22.5	97.4	29	1296	0.05	-1.81	14.1
	OMC	24.3	98.5	25	1217	0.12	-2.85	11.3
	OMC+1	25.9	96.7	22	614	0.16	-3.00	5.7
	OMC+2	28.7	92.3	6	86	0.61	-3.00	1.1
Subbase (P-154)	OMC-2	Data from subbase materials were not available since the cylindrical laboratory samples were instable to perform the resilient modulus test						
	OMC-1							
	OMC							
	OMC+1							
	OMC+2							
Base (P-209)	OMC-2	3.5	146.4	80.2	1271	0.46	-0.05	30.8
	OMC-1	4.3	147.7	53.9	940	0.58	-0.05	26.1
	OMC	5.4	152.8	49.9	811	0.78	-0.10	27.5
	OMC+1	6.2	149.0	34.1	820	0.52	-0.05	21.2
	OMC+2	6.6	148.4	33.3	498	0.68	-0.05	15.5

* from Eq. 3.2.1 based on τ_{oct} and θ values of 7.5 psi and 31 psi for base and 3 psi and 12.4 psi for subgrades as recommended by NCHRP Project 1-28A.

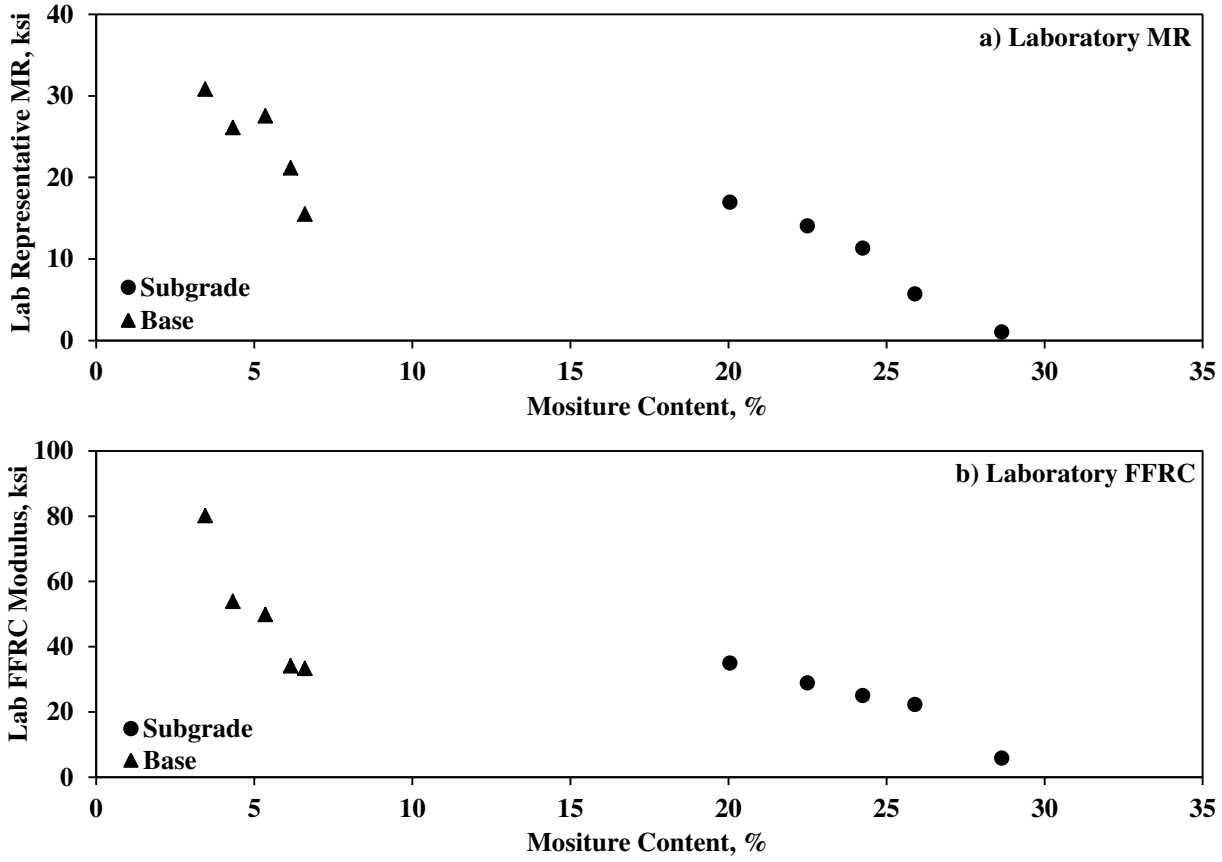

Figure K.2.2 – Variations of Laboratory MR and FFRC Moduli with Moisture Content

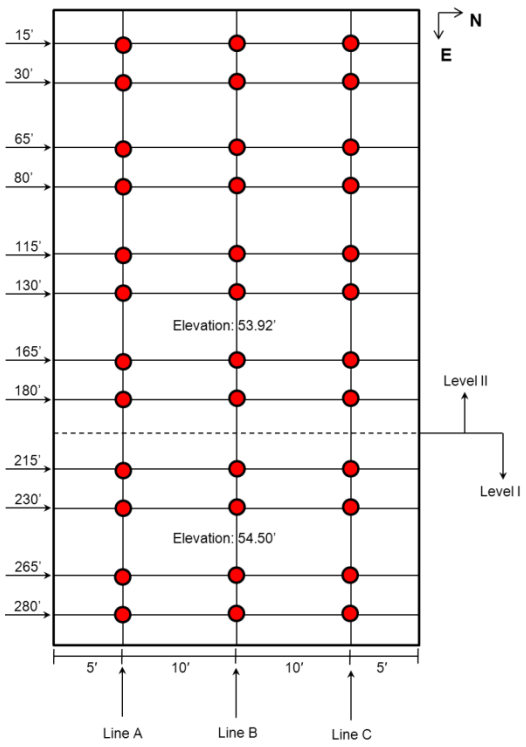

Figure K.3.1 – Schematic of North Side Testing Spots in FAA

K.4 Evaluation of Moisture-Density Devices

Subgrade Layer: The entire section (especially between stations 215' to 15') was placed and compacted at wet of OMC. The SDG was utilized on top of the compacted subgrade layer to estimate the moisture content and dry density of the compacted layer (see Figure K.4.1). The average SDG moisture content was 22.3%, which was close to the laboratory OMC (24.0% as reflected in Table K.2.1). Several soil samples were extracted along the compacted subgrade section to determine the oven-dry moisture contents. As reflected in Figure K.4.1b, the average oven-dry moisture contents were 28.4%, which was 4.4% greater than the laboratory OMC. Figure K.4.1c compares the oven-dry and SDG moisture contents. The SDG mostly underestimated the moisture content with a maximum of 30% error.

Figure K.4.2 depicts the estimated dry densities of the testing spots on subgrade layer. According to the SDG readings, the average dry density of the compacted subgrade layer was 160.1 pcf, much greater than the laboratory MDD of 97.9 pcf.

Subbase/Base Layer: The results of a few sand cone tests on the subbase layer are summarized in Figure K.4.3. The average moisture content of the subbase layer was 5.4% less than its corresponding laboratory OMC. The results of density tests show that the average subbase dry density is 7.6 pcf greater than the laboratory MDD and the section passed the density criteria for quality control purposes.

Figure K.4.4 illustrates the moisture contents and dry densities estimated by the NDG device after the compaction of the base layer. The average dry density and moisture content of the base layer was 135.6 pcf and 3.1%, respectively. It seems that the last three stations of the base layer (station 230 to 280) are less compacted.

K.5 Evaluation of Modulus-Based Devices

Subgrade Layer: Figure K.5.1 contains the results of the measurements with the PSPA, Zorn and Dynatest LWDs and DCP after the compaction of the subgrade layer. The average field moduli were 20.7 ksi, 4.5 ksi, 6.0 ksi and 1.8 ksi for the PSPA, Zorn LWD, Dynatest LWD and DCP, respectively. The

standard deviation of the replicate tests at each station is shown as error bar in this figure (except for DCP that no replicate tests were performed). The average standard deviation of replicate tests for the PSPA is 0.8 ksi. Such values for the Zorn and Dynatest LWD are 0.3 ksi and 0.2 ksi, respectively. At Station 215, the PSPA and the two LWDs exhibit higher moduli as compared to the other test stations.

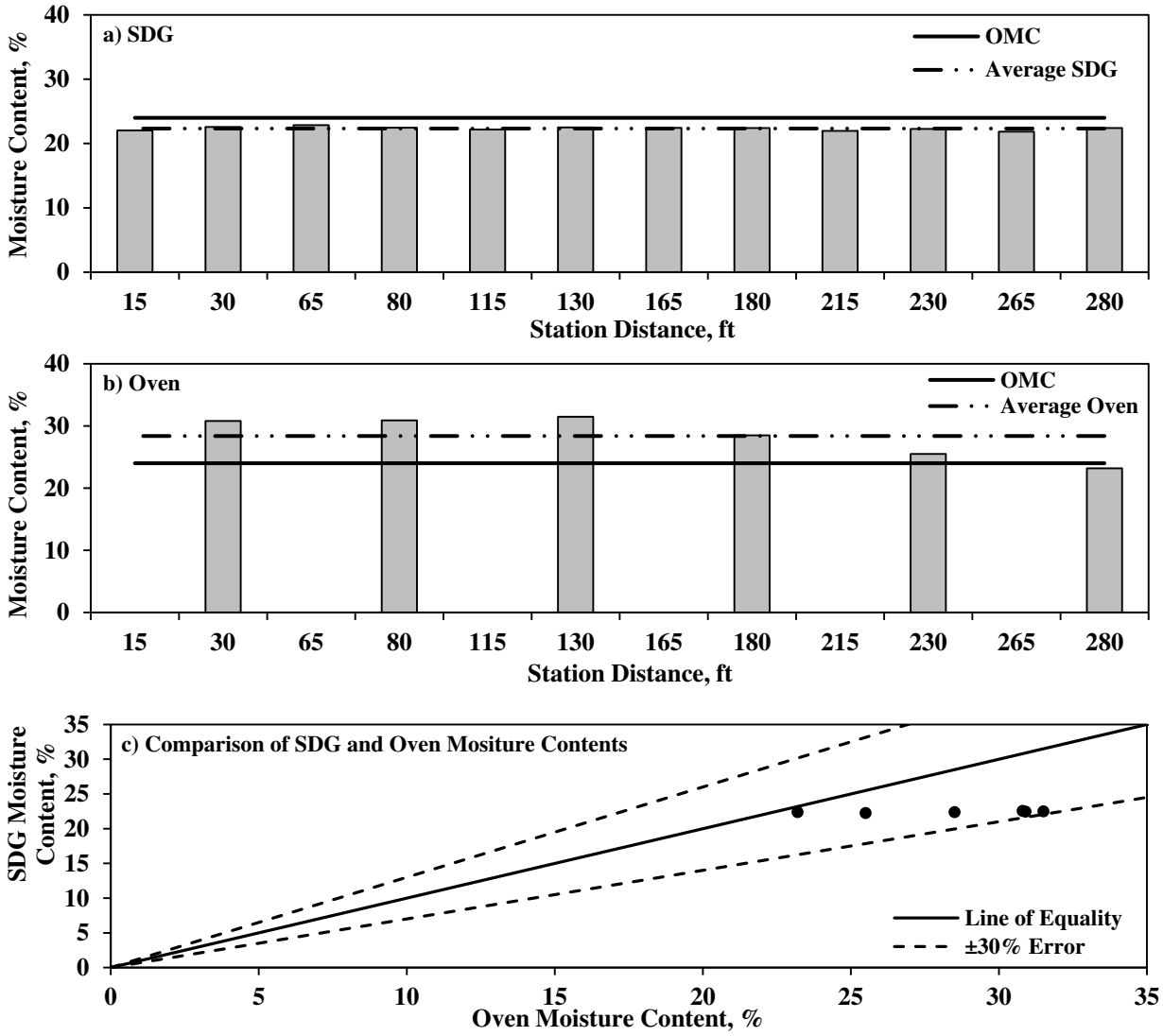

Figure K.4.1 –Variations of SDG and Oven Dry Moisture Contents of the Subgrade Layer

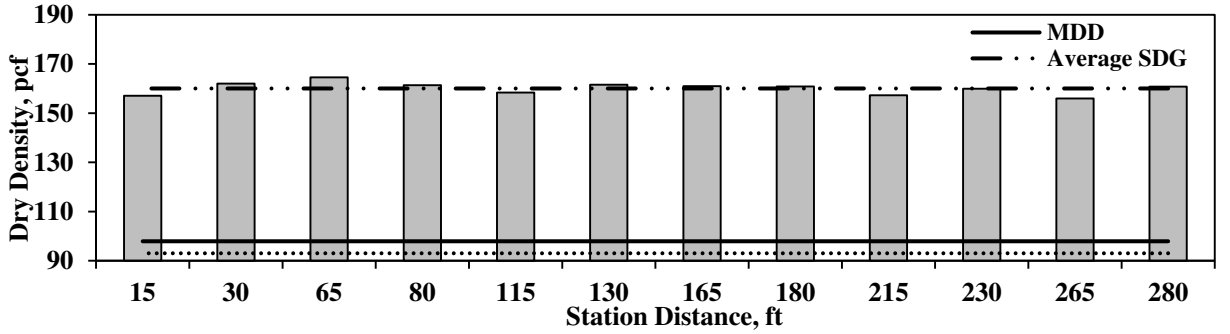

Figure K.4.2 – Spatial Variations of SDG Dry Densities of Subgrade Layer

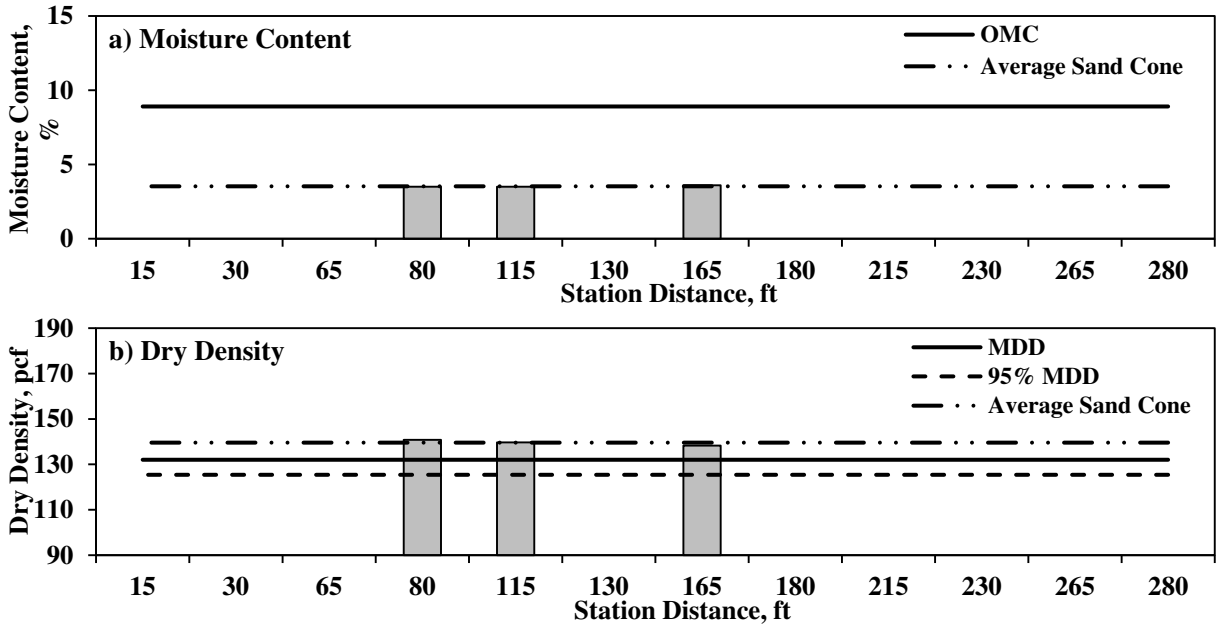

Figure K.4.3 – Spatial Variations of Moisture Content and Dry Densities of Subbase Layer from Sand Cone Tests

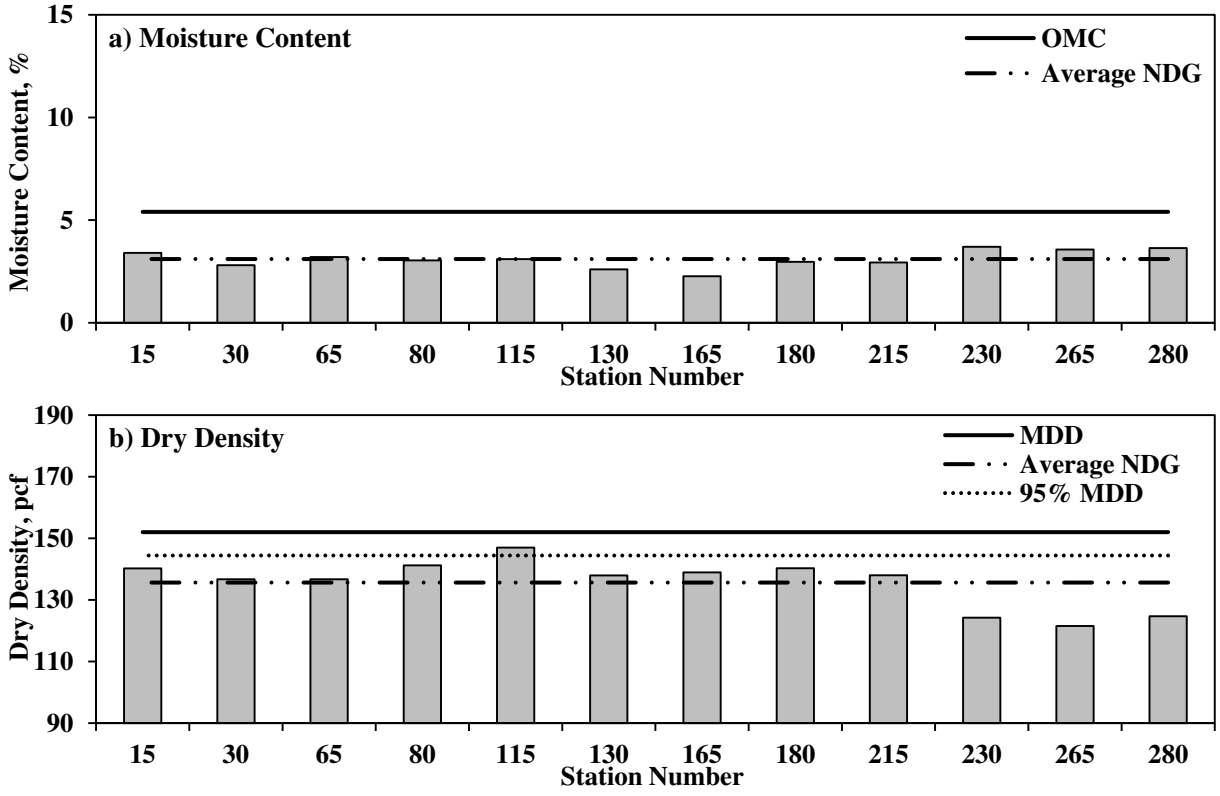

Figure K.4.4 – Spatial Variations of Moisture Content and Dry Densities of Base Layer from NDG Tests

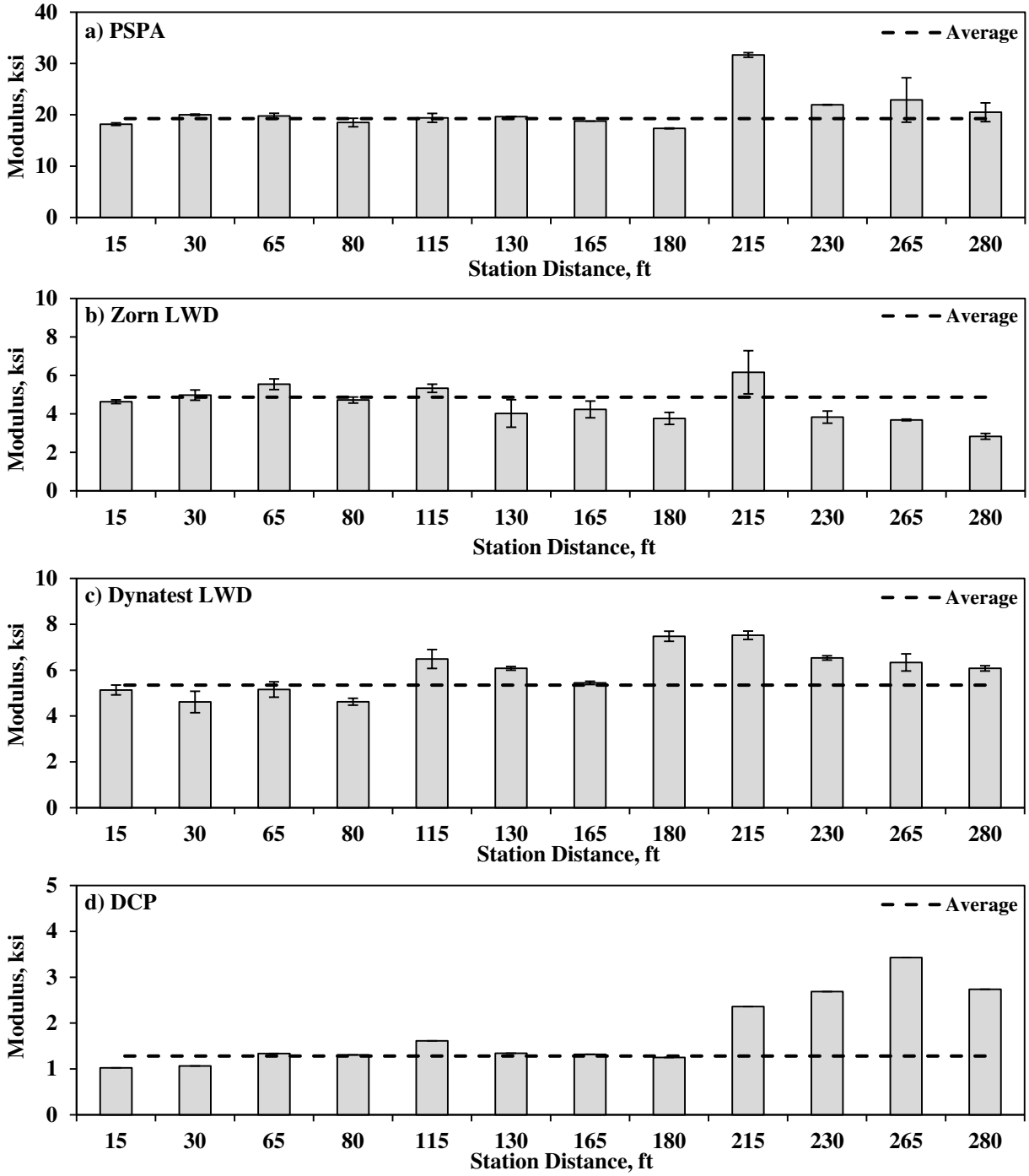

Figure K.5.1 – Spatial Variations of Measured Moduli of Subgrade Layer

Subbase Layer: Figure K.5.2 summarizes the spatial variation of modulus after compaction of subbase layer. Only the PSPA, Dynatest LWD and DCP were used on subbase layer. The average PSPA modulus was 92 ksi with the average standard deviation of 12ksi for replicate tests at the same station. Such values were 13.3 ksi and 0.5 ksi for the LWD. The average DCP modulus was 14.2 ksi. The standard deviations of the PSPA measurements on subbase materials are greater than those on the subgrade layer.

Base Layer: Figure K.5.3 illustrates the spatial distribution of measured moduli after the compaction *of* the base layer. The average moduli of PSPA and Dynatest LWD were 120 ksi and 19 ksi, respectively.

The PSPA device exhibited a standard deviation of 6 ksi while such value for the Dynatest LWD was 1 ksi. As mentioned earlier, the DCP tests were not performed on the base layer.

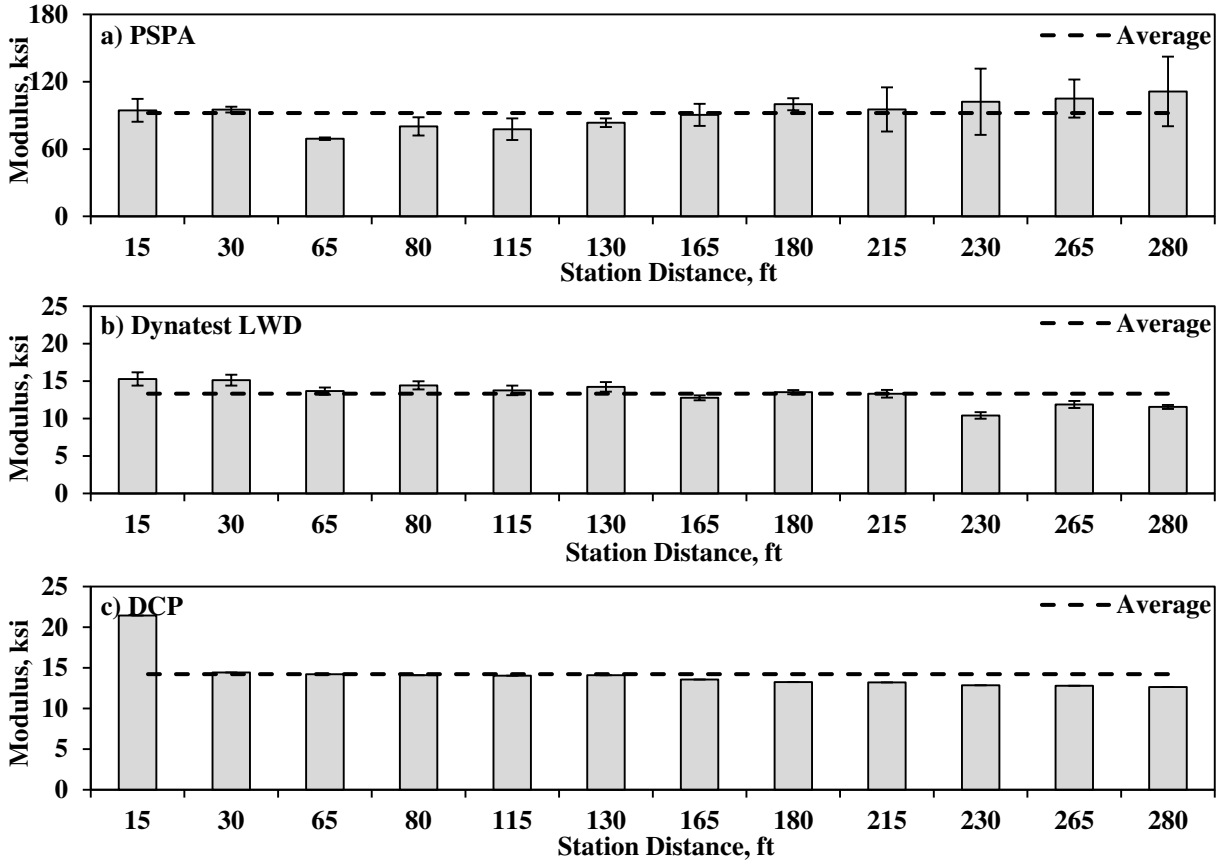

Figure K.5.2 – Spatial Variations of Measured Moduli of Subbase Layer

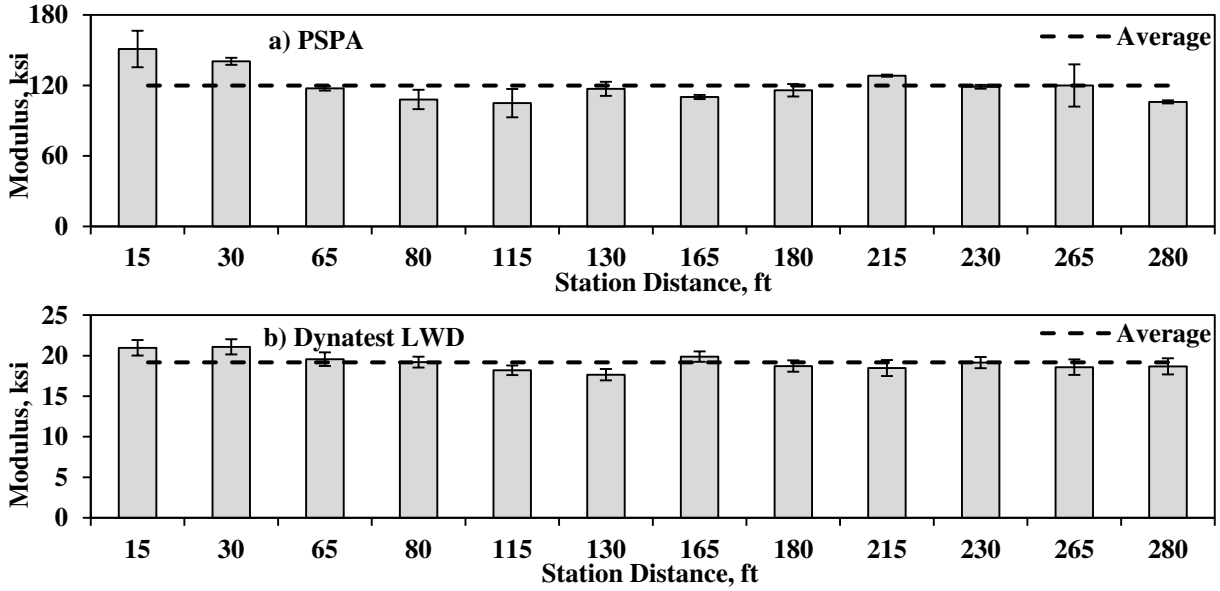

Figure K.5.3 – Spatial Variations of Measured Moduli of Base Layer

K.6 Variability of Modulus-Based Devices

Subgrade Layer: In order to investigate the variability of modulus-based devices for in-situ modulus estimation, the coefficient of variation (COV) of the replicate tests at each test spot was calculated. The distributions of the COVs with measured field moduli for the PSPA, Zorn LWD and Dynatest LWD are summarized in Figure K.6.1. The maximum COVs for the PSPA, Zorn LWD and Dynatest LWD were 23%, 18% and 10%, respectively.

Subbase Layer: The distributions of the COVs with measured field moduli for the PSPA and Dynatest LWD on the subbase layer are summarized in Figure K.6.2. The maximum COVs for the PSPA and Dynatest LWD were 29% and 6%, respectively.

Base Layer: Figure K.6.3 summarizes the variability of the PSPA and Dynatest LWD while estimating the modulus of the compacted base layer. The maximum COV of the PSPA was 15% with an average of 5%. Such values for the Dynatest LWD were 5% and 4%, respectively.

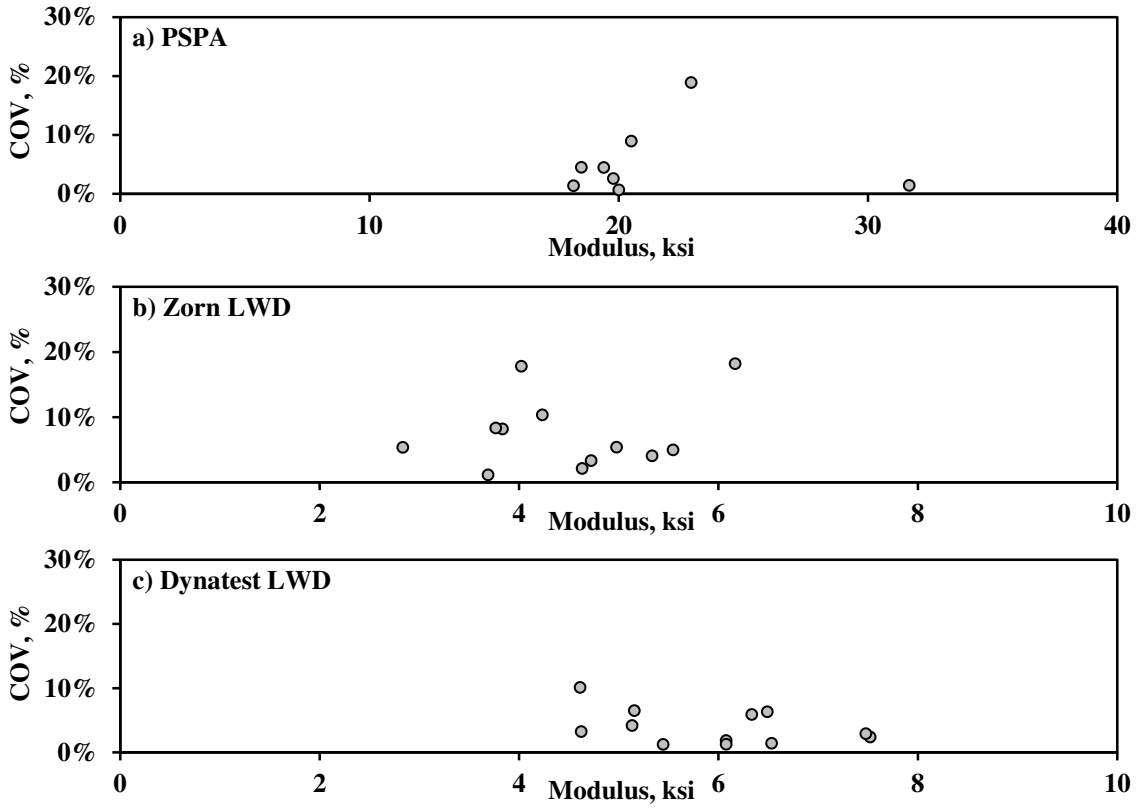

Figure K.6.1 – Variations in Coefficient of Variation (COV) of Modulus-based Devices with Average Measured Modulus of Subgrade Layer

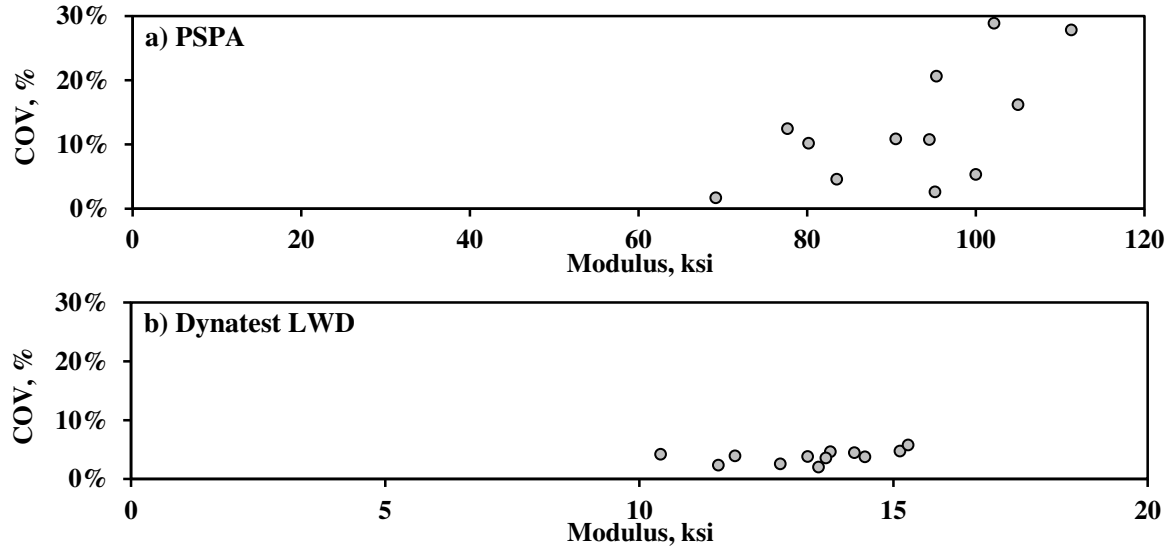

Figure K.6.2 – Variations in Coefficient of Variation (COV) of Modulus-based Devices with Average Measured Modulus of Subbase Layer

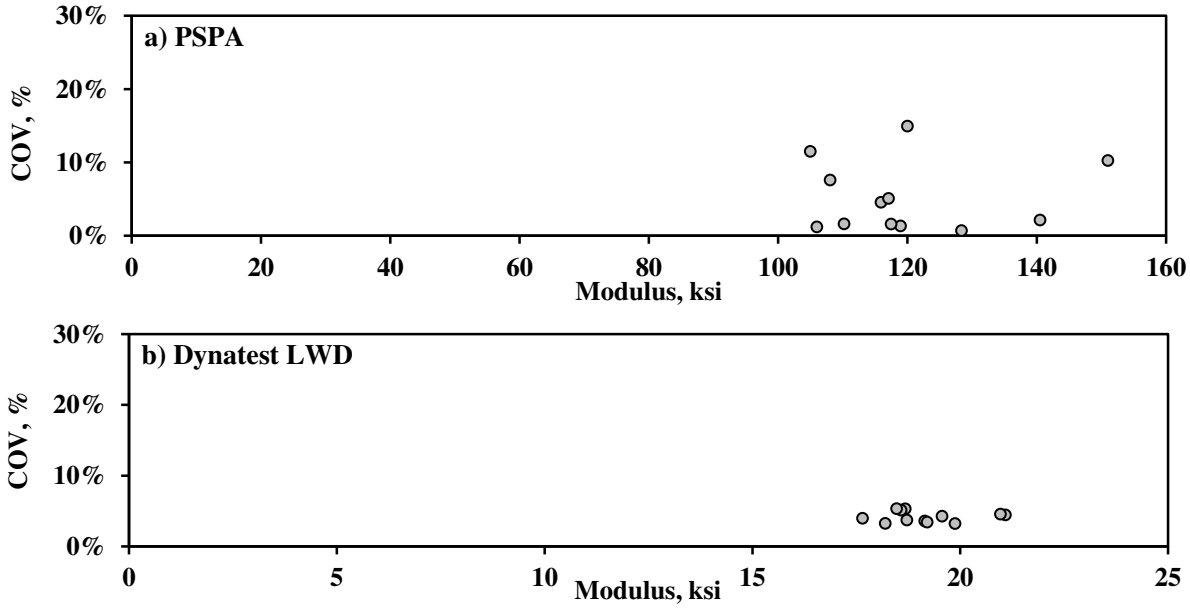

Figure K.6.3 – Variations in Coefficient of Variation (COV) of Modulus-based Devices with Average Measured Modulus of Base Layer

K.7 Moisture-Modulus Relationships

Subgrade Layer: The relationships between the field moduli from different devices and their corresponding oven dry moisture contents are summarized in Figure K.7.1. Since soils samples for the oven-dry moisture tests were extracted at six stations, there are only few data points in Figure K.7.1. The moduli from all devices decrease with the increase in moisture content except for the Zorn LWD. Only the DCP results illustrate a reasonable correlation with corresponding moisture contents.

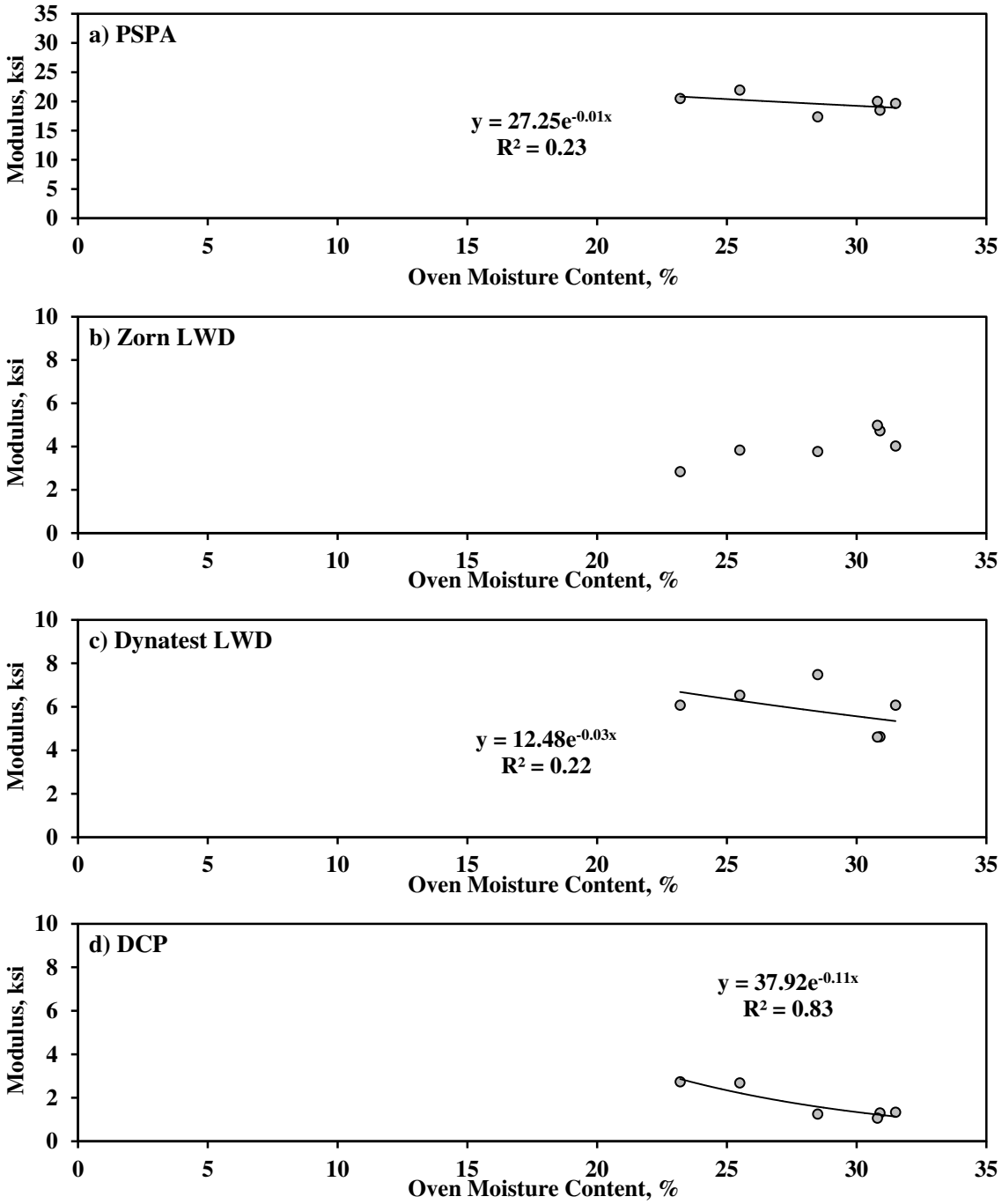

Figure K.7.1 – Relationship between Measured Moduli and Oven-Dry Moisture Contents after Compaction of Subgrade Layer

Subbase Layer: Since the moisture contents were estimated at only at two test sections after compaction of subbase layer, not enough data were available to investigate the moisture-modulus correlations.

Base Layer: The modulus-moisture correlations for the compacted base layer are summarized in Figure K.7.2. A strong correlation is not observed with either device.

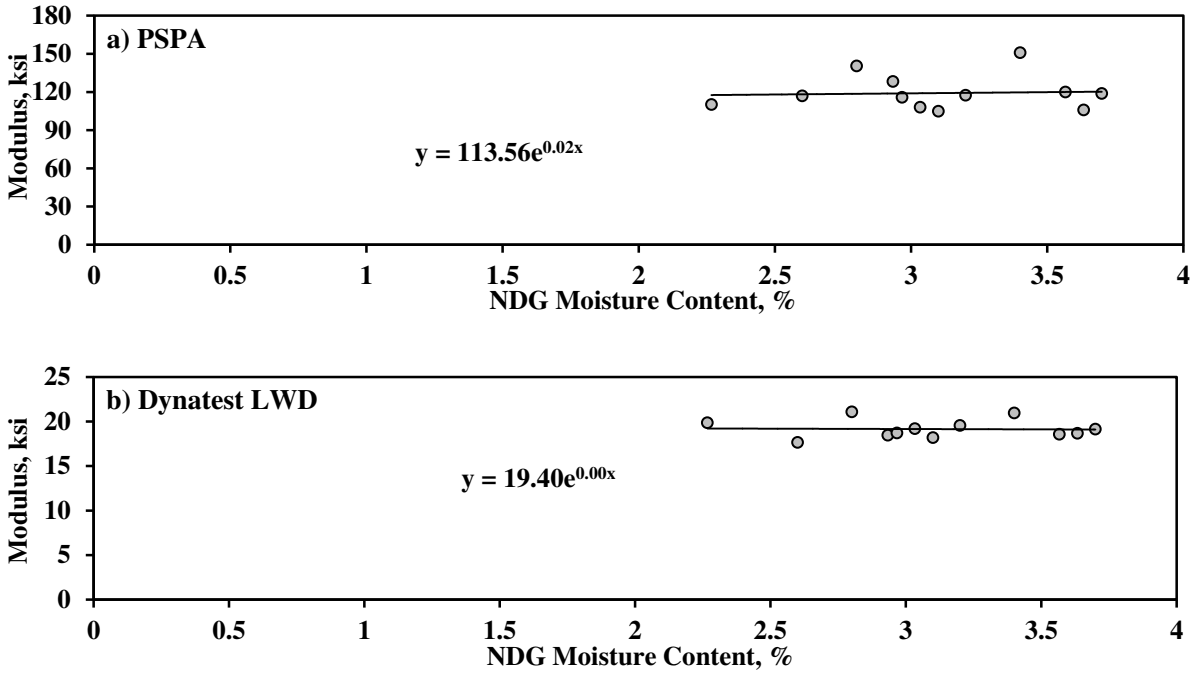

Figure K.7.2 – Relationship between Measured Moduli and NDG Moisture Contents after Compaction of Base Layer

K.8 Acceptance Scenarios for Compacted Geomaterials

Subgrade Layer: The target moduli of the compacted materials at laboratory OMC were calculated for each device. The estimated field moduli based on the field moisture contents were also estimated to compare with the measured field moduli immediately after compaction. The results of such analyses for the PSPA, Zorn LWD and Dynatest LWD are summarized in Figure K.8.1.

For the PSPA measurements, all field moduli are less than the acceptance limit of 80% of target modulus. However, the estimated field modulus based on compaction moisture content of the compacted materials is fairly close to the average measured field modulus. As indicated in Figure K.8.1b, the measured Zorn LWD moduli are for many points less than acceptance limit. In this case, the estimated field modulus based on field moisture content (after compaction) is relatively low as compared to the measured moduli. Figure K.8.1c compares the Dynatest LWD moduli with the established target modulus. The measured field moduli for most points are less than the target modulus. Same as for the Zorn LWD results, the estimated field modulus based on compaction moisture content is lower than the measured moduli.

Subbase Layer: Due to instability of cylindrical laboratory specimens, resilient modulus tests were not feasible to perform for subbase materials. Therefore, the establishment of target moduli and estimation of field moduli, based on laboratory k' parameters, were not possible.

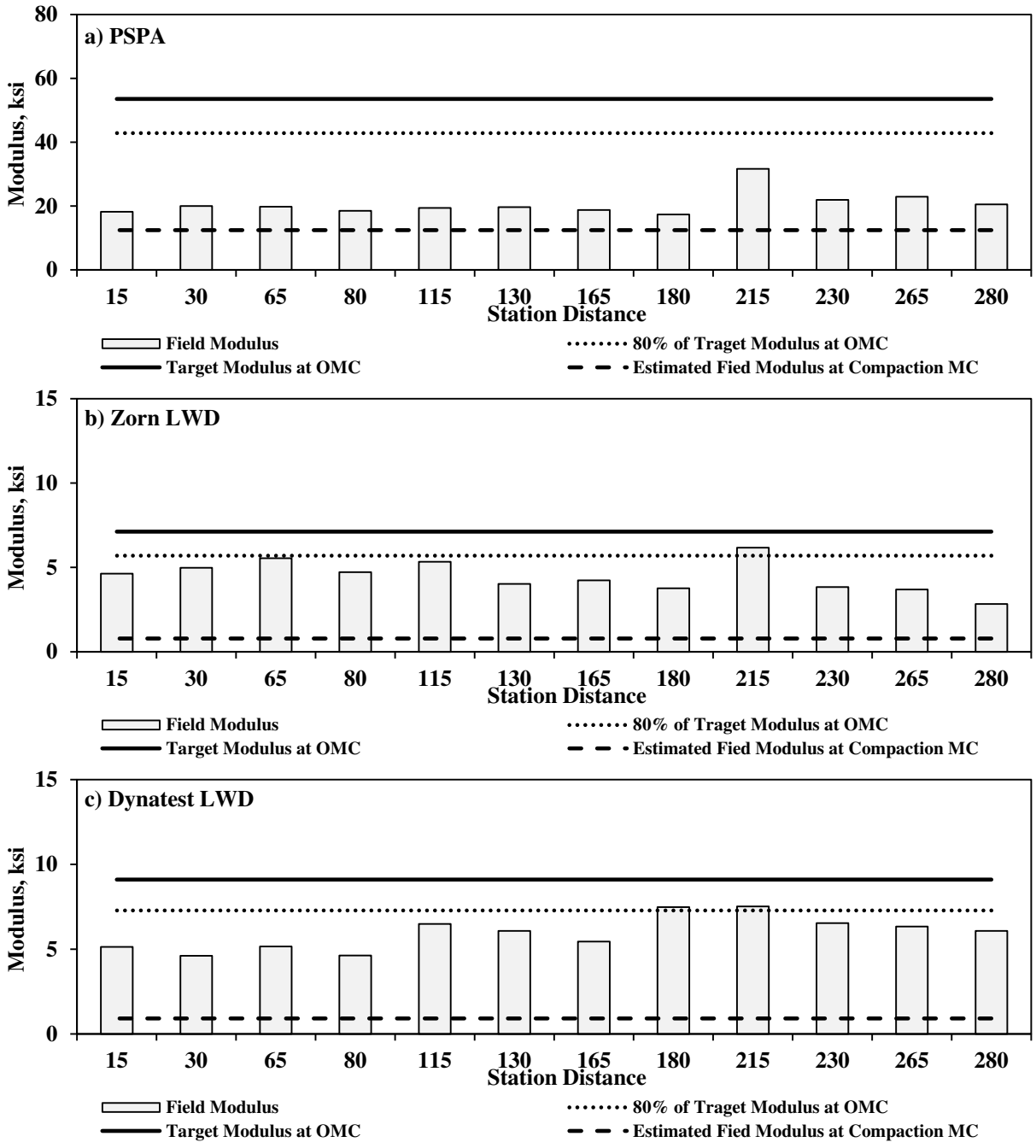

Figure K.8.1 – Acceptance Scenarios for Modulus-Based Devices (Subgrade Layer)

Base Layer: Figure K.8.2 summarizes the modulus-based acceptance scenarios based on the PSPA and Dynatest LWD results. As discussed earlier, the target moduli were established based on laboratory parameters at OMC. Based on the PSPA readings, all test stations on the base layer pass the established modulus-based criteria (80% of target modulus at OMC). However, referring to Figure K.4.4, the average moisture content at compaction was 3.1% (about 2.3% dry of OMC). The estimated field modulus based on the moisture content at the time of compaction is also included in Figure K.8.2a. This modulus is close to the measured field moduli.

Similarly, the results of the Dynatest LWD field moduli are compared to the established target modulus at OMC in Figure K.8.2b. All sections pass the established target modulus. In this case, the estimated field modulus at compaction moisture content is greater than the measured LWD data because of the influence of the layers below the base.

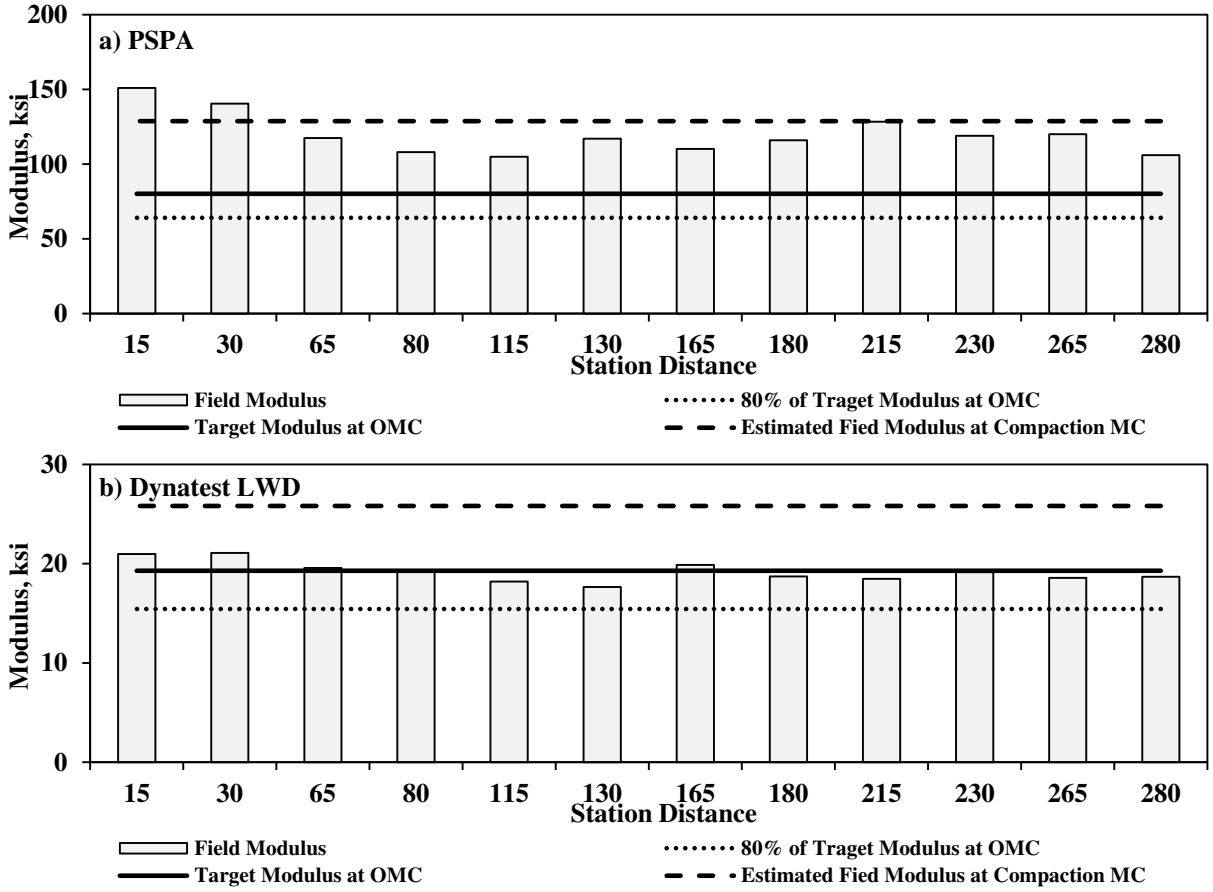

Figure K.8.2 – Acceptance Scenarios for Modulus-Based Devices (Base Layer)

Appendix L

OBSERVATIONS FROM IMPLEMENTATION OF SPECIFICATION

Site II.2

L.1 Introduction

The field evaluation was carried out at a section of US-50 located at the west urban area boundary of North Vernon, Indiana as reflected in Figure L.1.1. Figure L.1.2 illustrates the schematic of testing spots on the selected section. A 14-in.-thick lime-modified subgrade layer was placed and compacted. Figure L.1.3 depicts the testing spots on compacted subgrade layer. The testing of subgrade layer was initiated during the week of August 16, 2103. Due to heavy rain after the second day of work, the testing of the subbase layer was conducted during the week of August 23, 2013.

L.2 Laboratory Results

The index properties of the subgrade and subbase materials are summarized in Table L.2.1, and their gradation curves are presented in Figure L.2.1. The subgrade and subbase were classified as low-plasticity clay and well-graded gravel, respectively, as per Unified Soil Classification System (USCS). The optimum moisture contents and maximum dry unit weights obtained as per standard Proctor tests (AASHTO T99) for the subgrade and as per modified Proctor tests (AASHTO T180) for the subbase materials are also reported in Table L.2.1.

Table L.2.1 - Index Properties of InDOT Geomaterials

Soil Type	Gradation %				USCS Class.	Specific Gravity	Atterberg Limits			Moisture/Density	
	Gravel	Coarse Sand	Fine Sand	Fines			LL	PL	PI	OMC,* %	MDUW,** pcf
Subgrade	5	8	22	65	CL	2.73	27	11	16	16.4	111.9
Subbase	56	34	10	1.0	GW	2.65	0	0	0	5.8	143.8

*OMC = Optimum Moisture Content, **MDUW = Maximum Dry Unit Weight

The resilient modulus (MR) and FFRC tests were performed on laboratory specimens prepared at the OMC for the subgrade and five moisture contents for subbase as summarized in Table L.2.2. Figure L.2.2 illustrates the variations of the FFRC moduli and representative MR values with moisture content for the subbase layer.

L.3 Field Testing Program

As illustrated in Figure L.3.1, field testing was carried out along a 100 ft section. The subgrade layer at the site had been prepared shortly before the research team arrived at the site. The following tests were performed on the subgrade layer along lines A, B and C:

- Zorn Light Weight Deflectometer (LWD) as per ASTM E2835
- Portable Seismic Property Analyzer (PSPA)
- Dynamic Cone Penetrometer (DCP)

The testing spots on the subgrade layer were mapped to the compacted subbase layer. The SDG and LWD tests were then performed on the subbase layer. The results from the moisture and modulus devices on the compacted sections are summarized in the following sections.

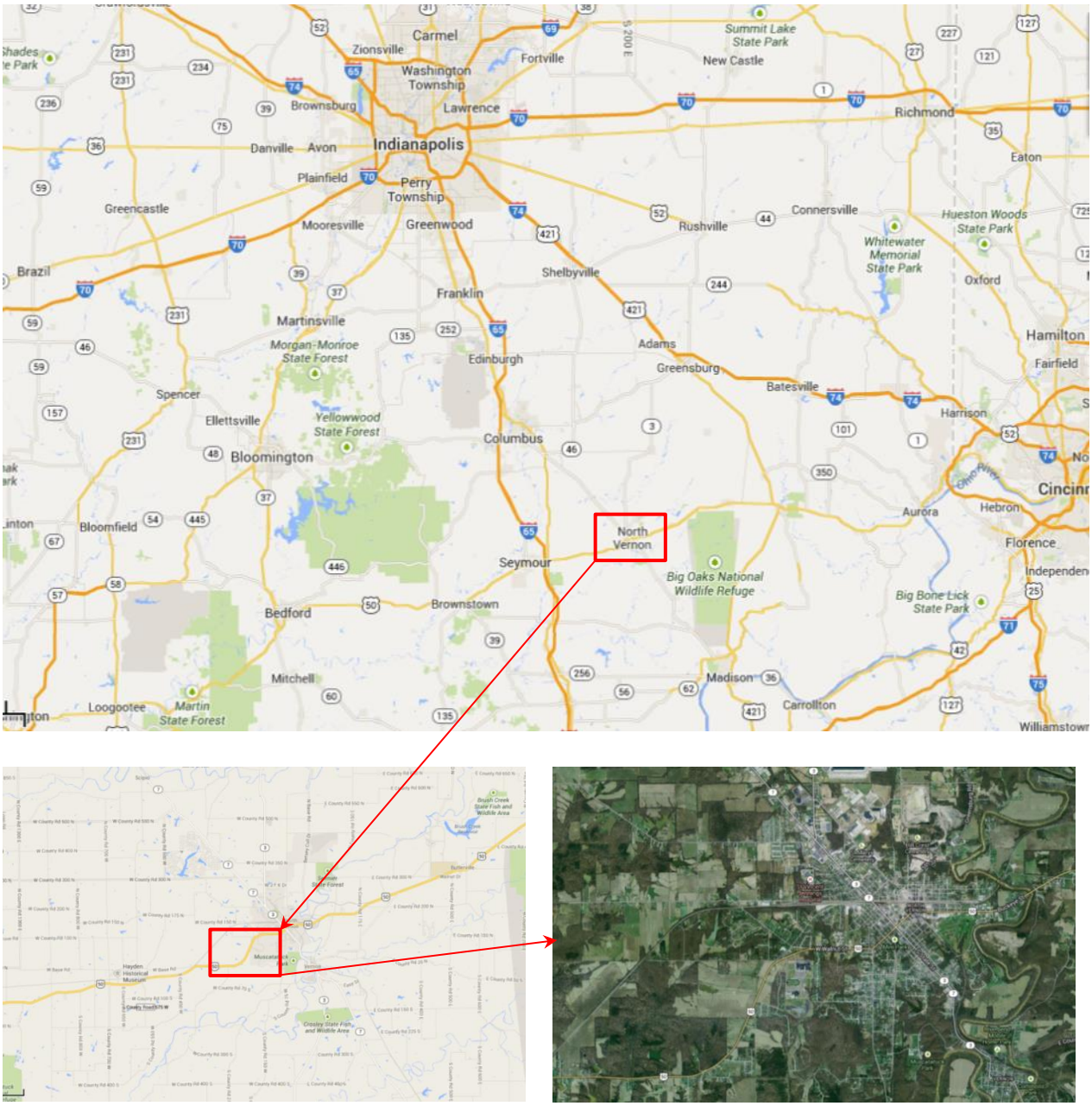

Figure L.1.1 – Location of Field Evaluation Site on US-50 Route in North Vernon, Indiana

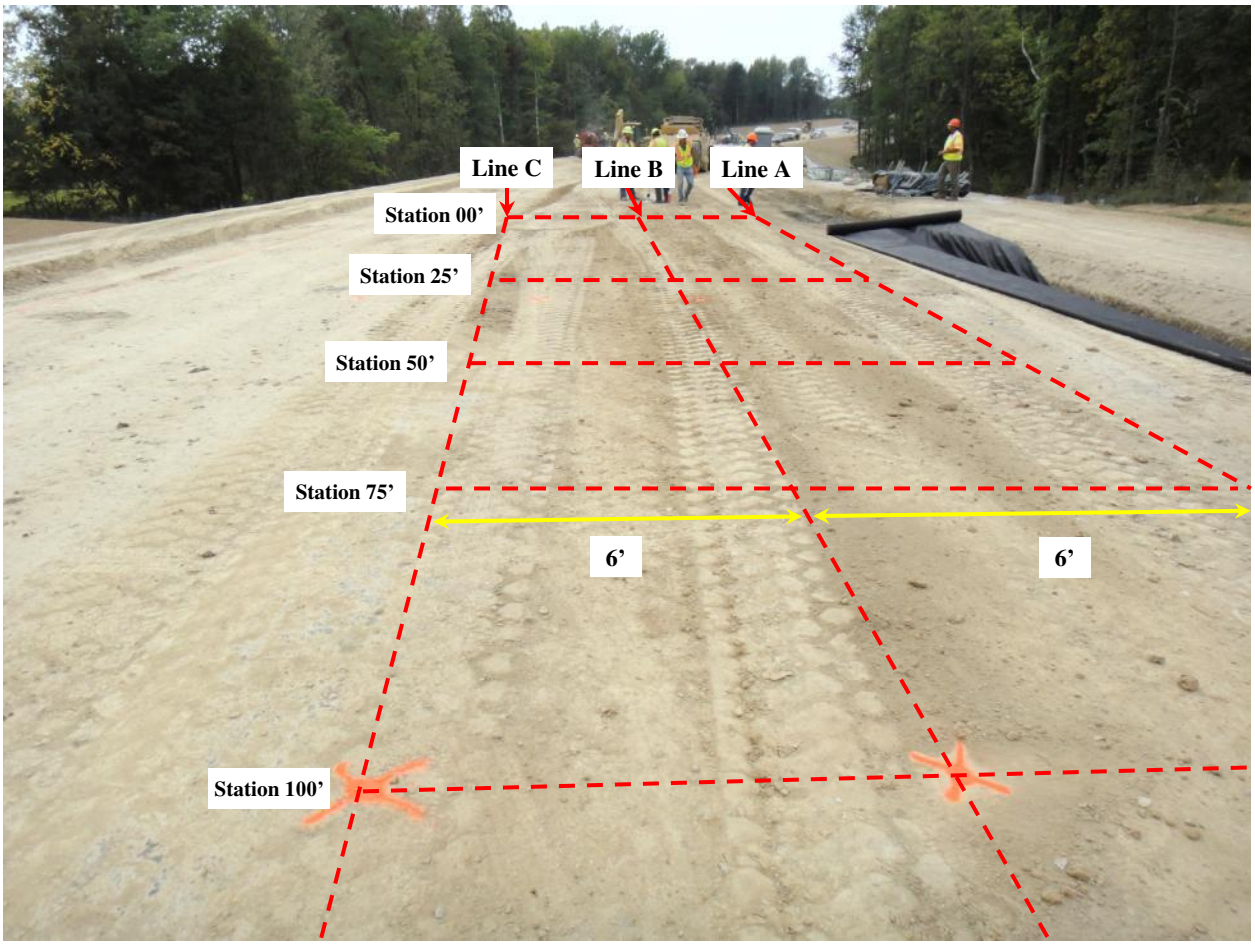

Figure L.1.2 – Location of Testing Spots on Selected Test Section in North Vernon, Indiana

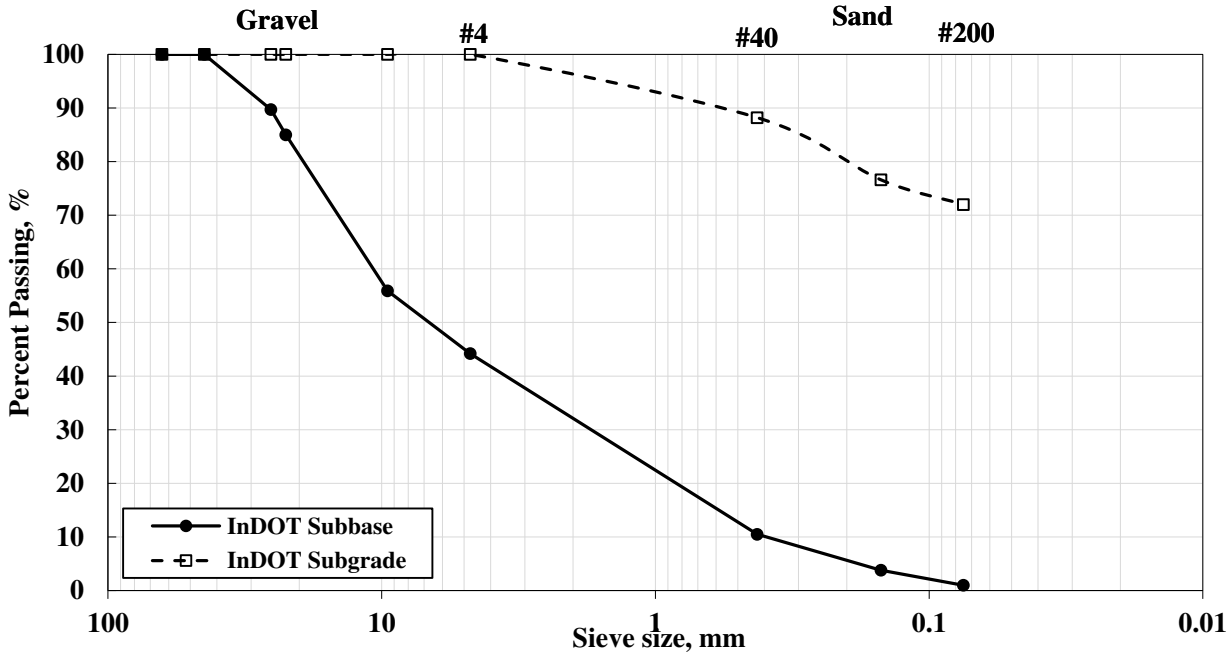

Figure L.2.1 – Gradation Curve of InDOT Geomaterials

Table L.2.2 – Laboratory Results of MR and FFRC Tests of InDOT Geomaterials (Subgrade and Subbase)

Type	Target Moisture Content	Actual Moisture Content, %	Dry Density, pcf	FFRC Modulus, ksi	Nonlinear Parameters			Representative MR, ksi*
					k'_1	k'_2	k'_3	
Subgrade	**OMC****	16.5	108.0	37.5	667	0.65	-1.67	10.7
Subbase	**OMC-2**	3.6	138.5	34.8	940	0.69	-0.05	29.6
	OMC-1	4.8	142.9	40.6	819	0.77	-0.06	28.0
	OMC	5.8	148.3	24.3	665	0.52	-0.05	17.1
	OMC+1	6.9	145.0	20.2	576	0.58	-0.05	16.0
	OMC+2	7.9	142.8	21.1	572	0.59	-0.05	16.0

* from Eq. 3.2.1 based on τ_{oct} and θ values of 7.5 psi and 31 psi for base and 3 psi and 12.4 psi for subgrades as recommended by NCHRP Project 1-28A. **subgrade material was tested only at Optimum Moisture Content

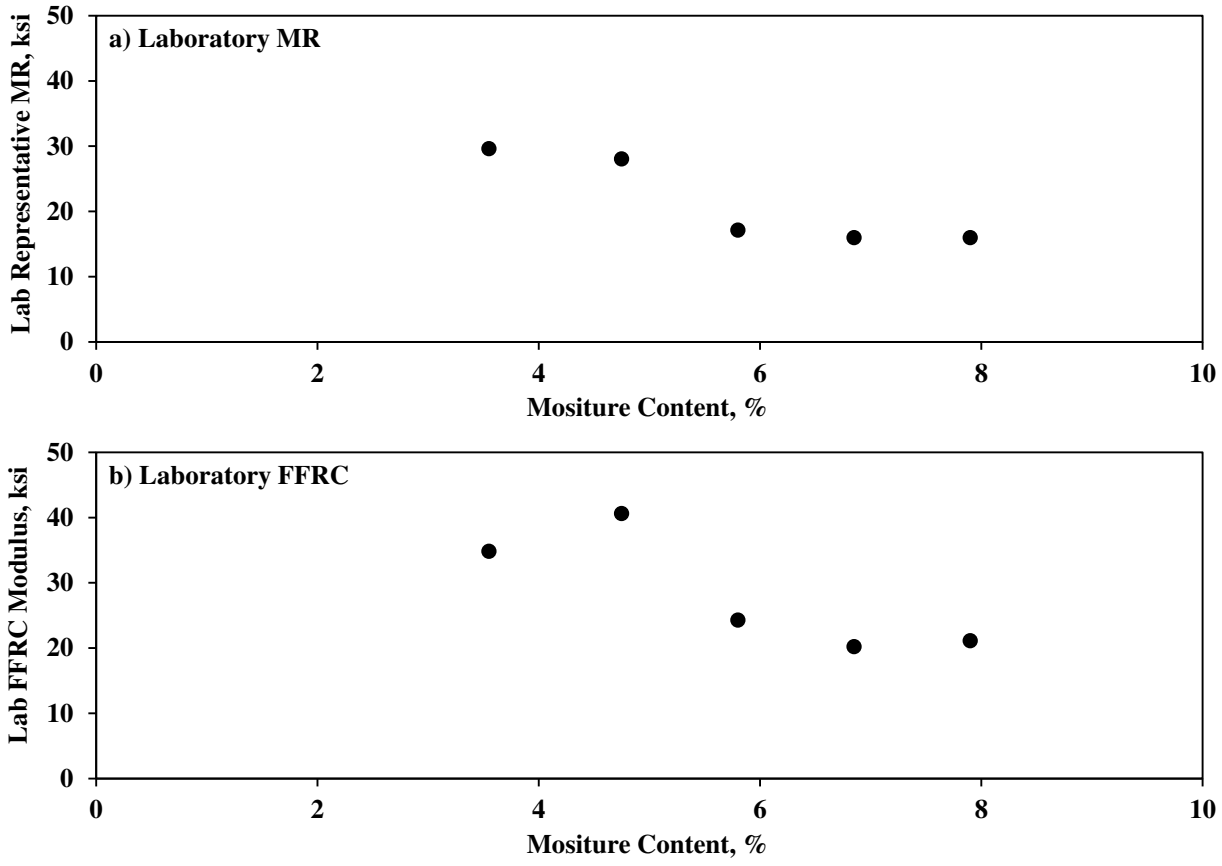

Figure L.2.2 – Variations of Laboratory MR and FFRC Moduli with Moisture Content for Subbase

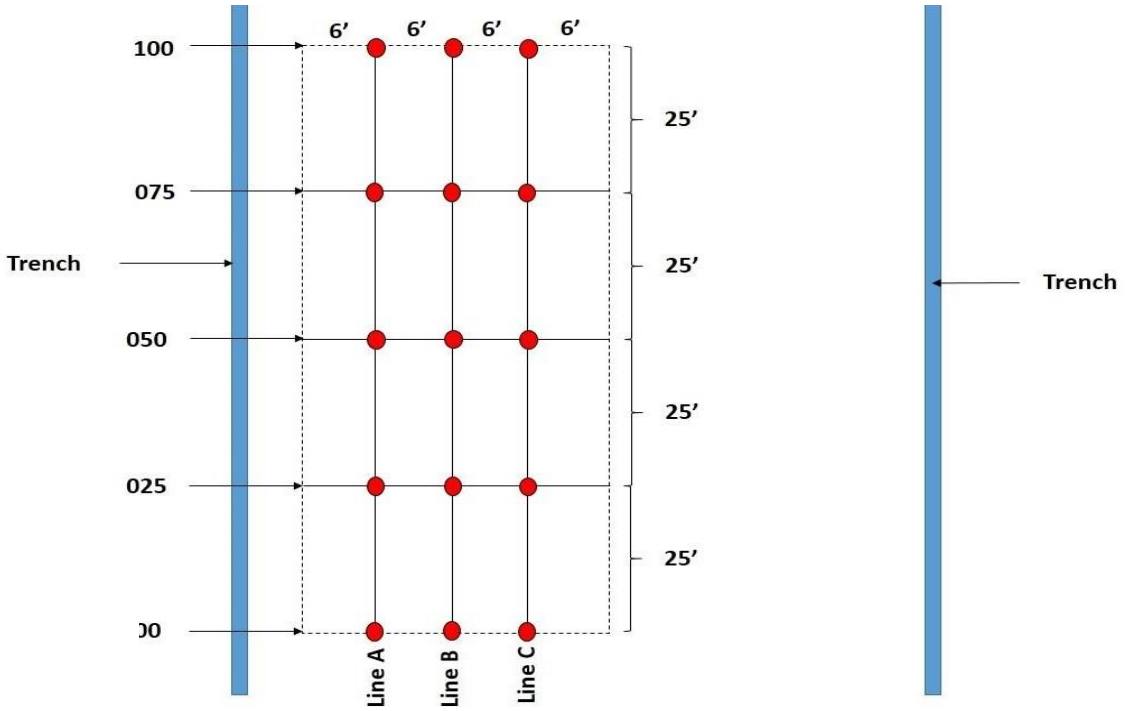

Figure L.3.1 – Schematic of Testing Spots for InDOT Site

L.4 Evaluation of Moisture-Density Devices

Due to sudden rain during the testing of the subgrade section, no moisture and density data were available for the subgrade section. Since InDOT does not utilize NDG anymore, the SDG device was utilized on top of the compacted subbase layer (see Figure L.4.1). The average SDG moisture content was 10.5%, which was about 5% greater than the laboratory optimum moisture content. Considering the previous field and laboratory results of SDG, the device is not sensitive to moisture changes in materials and needs rigorous calibration. As illustrated in Figure L.4.1b, the average dry density from the SDG measurements was 100.2 pcf which is again not close to the laboratory maximum dry density of the materials (which was 143.8 pcf).

L.5 Evaluation of Modulus-Based Devices

Subgrade Layer: ***The*** Zorn LWD, PSPA and DCP were tested on top of the compacted subgrade layer along Lines A, B and C shortly after the placement of the subgrade layer. Figure L.5.1 summarizes the measured field moduli from the three devices. The average PSPA modulus is 54.2 ksi while the average LWD modulus was 13.8 ksi. The standard deviation of replicate tests at each station is shown as error bar in the figures. The average standard deviation of PSPA measurements was 5.5 ksi and that value for Zorn LWD measurements was 0.4 ksi.

Figures L.5.1c and L.5.1d show the DCP modulus for 6-in. and 12-in. penetration, respectively. The DCP modulus of the top 6-in. layer was 29.5 ksi while the average DCP modulus for the 12-in. penetration (the composite modulus of the layer) was 14.9 ksi.

Subbase Layer: Only the Zorn LWD was tested on top of compacted subbase layer. The average LWD modulus was 14.0 ksi. Comparing the average LWD modulus on top of the subgrade layer (which was 13.8 ksi), the small difference could be due to the depth of influence of the LWD device. The average standard deviation of the LWD replicate tests was 0.5 ksi.

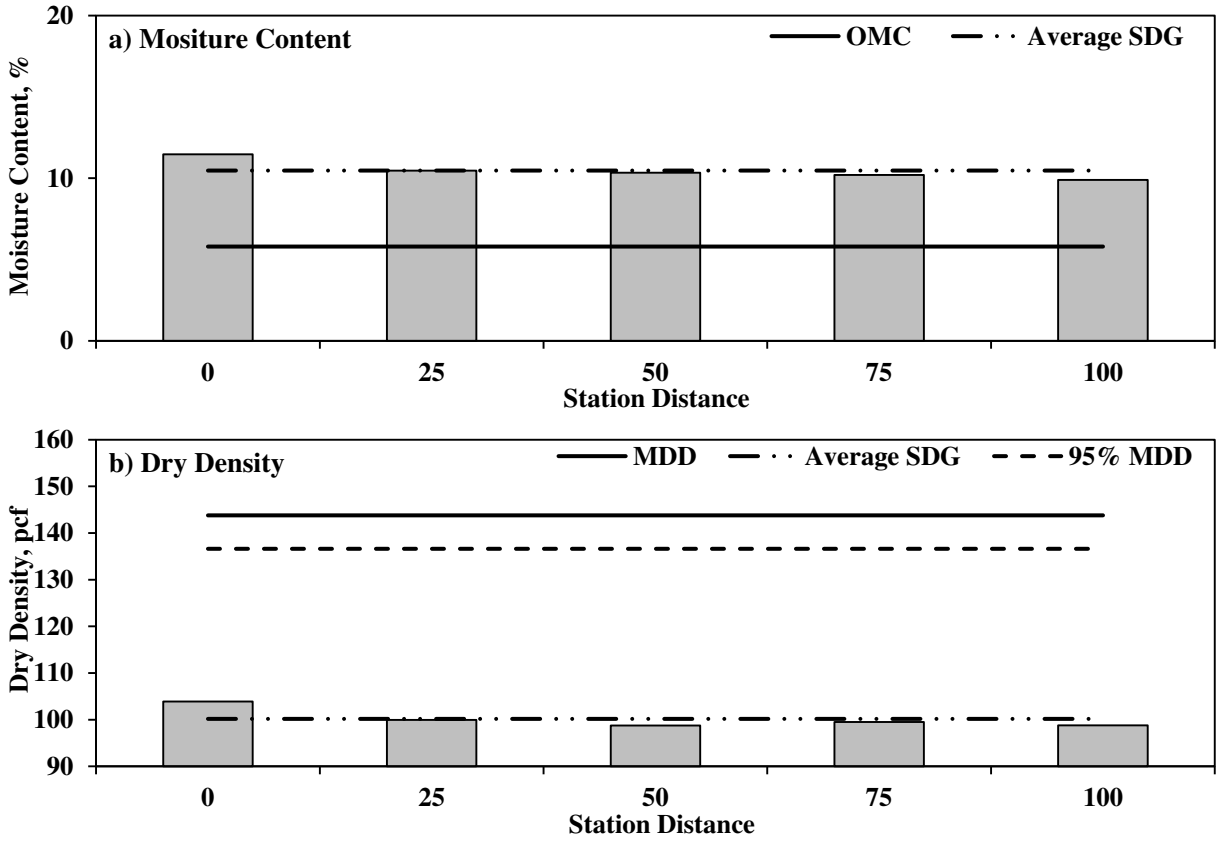

Figure L.4.1 –Variations of SDG Moisture Content and Dry density of the Subbase Layer

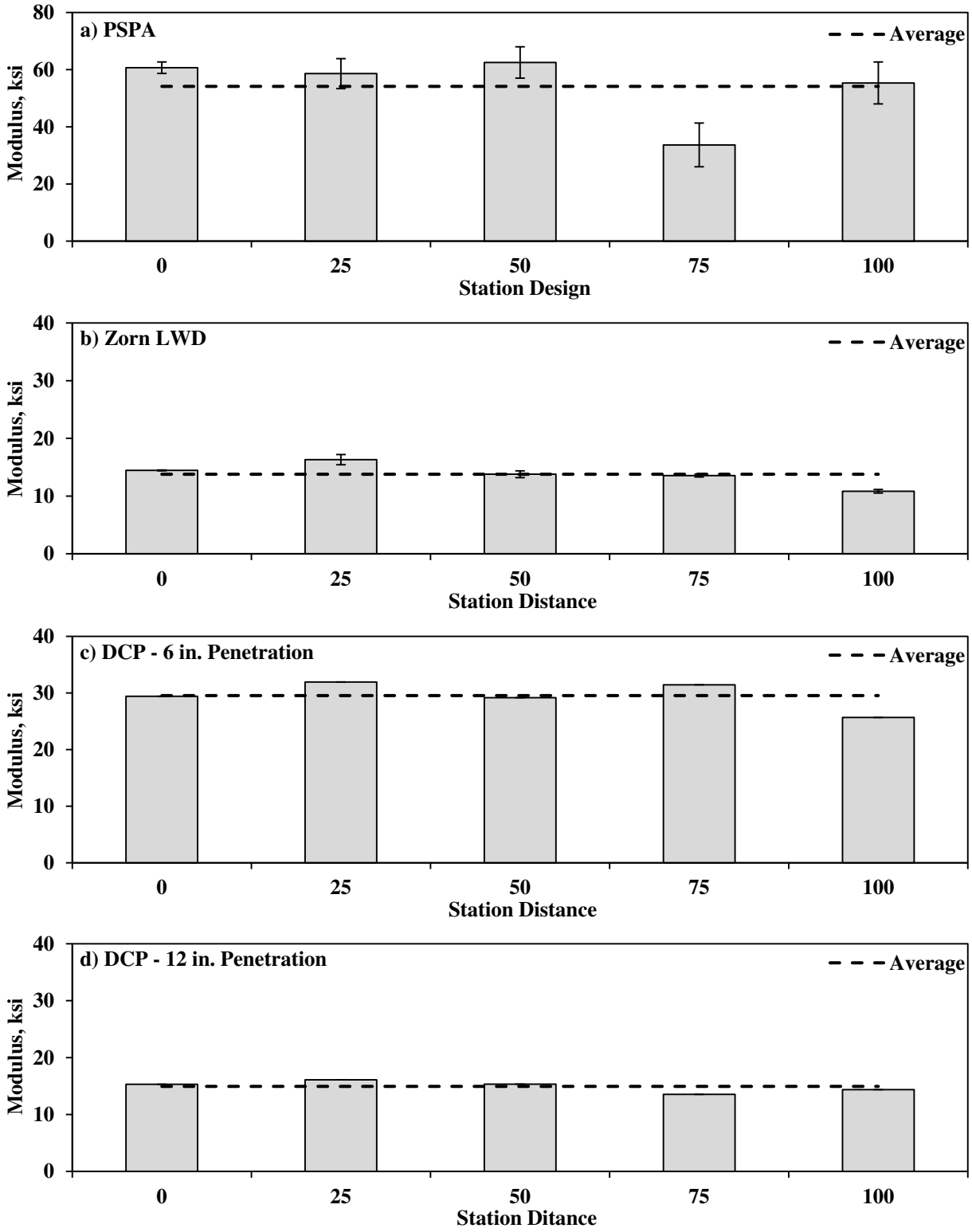

Figure L.5.1 – Spatial Variation of Modulus Measurements after Compaction of Subgrade Layer

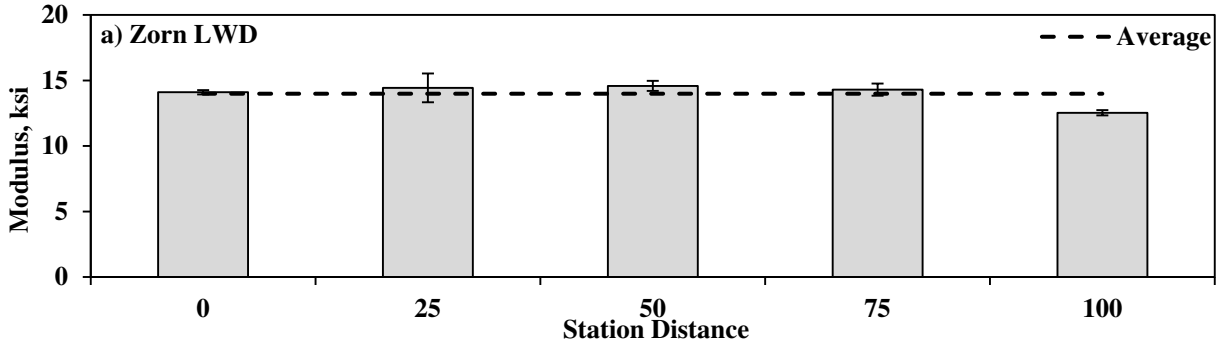

Figure L.5.2 – Spatial Variation of Modulus Measurements after Compaction of Subbase Layer

L.6 Variability of Modulus-Based Devices

Subgrade Layer: In order to investigate the variability of modulus-based devices for in-situ modulus estimation, the coefficient of variation (COV) of the replicate tests at each test spot was calculated. The distributions of the COVs with measured field moduli for the PSPA and LWD are summarized in Figure L.6.1. The maximum COVs for the PSPA and Zorn LWD were 23% and 5% respectively.

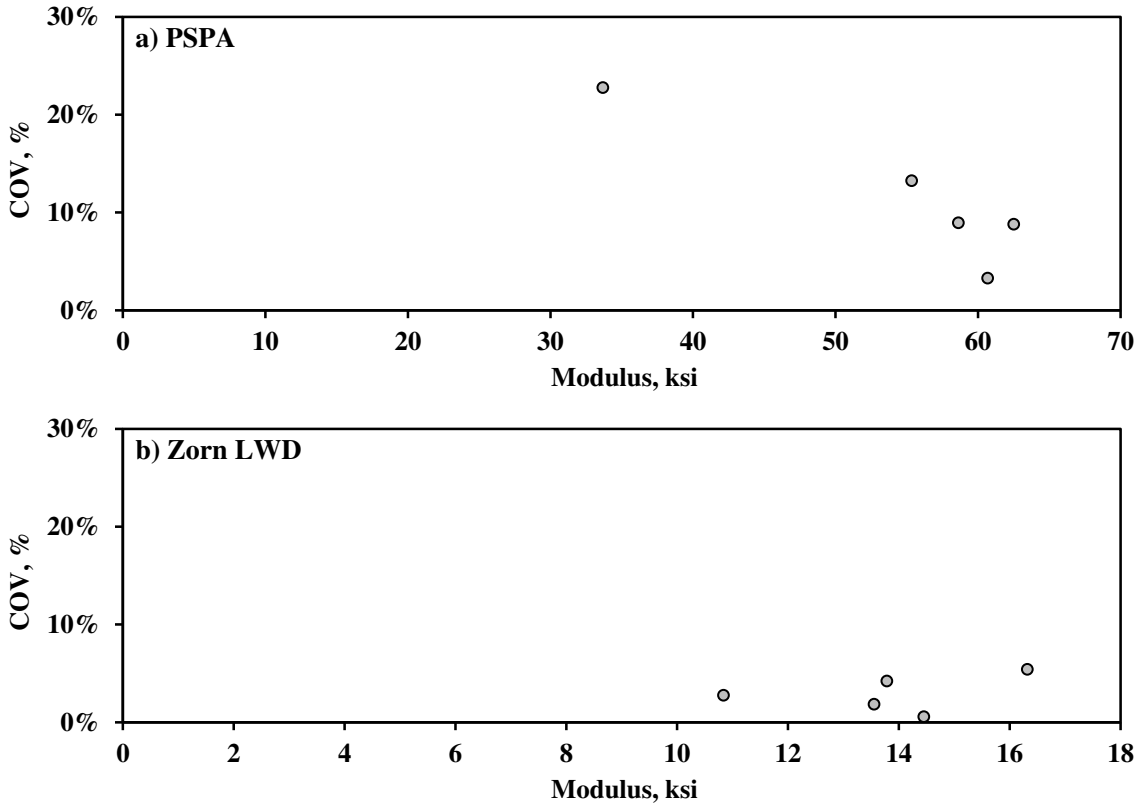

Figure L.6.1 – Variability of Modulus Measurements after Compaction of Subgrade Layer

Subbase Layer: The variability of modulus measurements for the subbase layer is summarized in Figure L.6.2. The maximum COV of the LWD measurements was 8%.

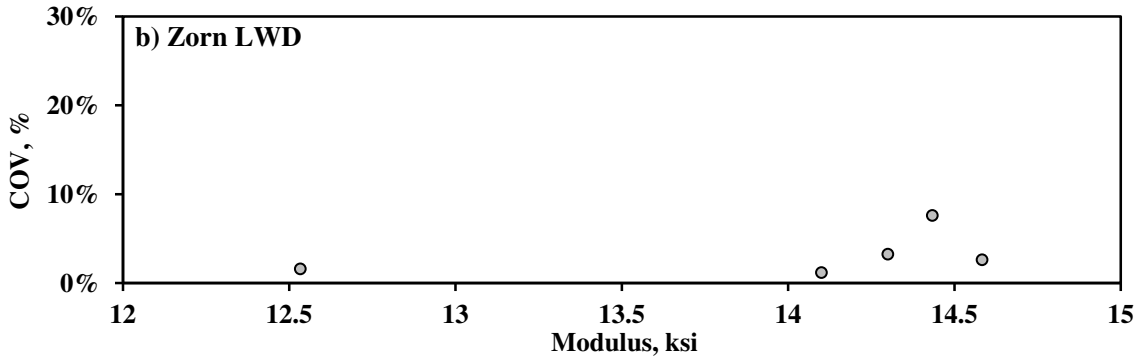

Figure L.6.2 – Variability of Modulus Measurements after Compaction of Subbase Layer

L.7 Moisture-Modulus Relationships

The moisture data was collected using the SDG after compaction of subbase layer. Due to uncertainties associated with the SDG results, such results could not be used to establish moisture-modulus correlations. As discussed before, the SDG results are not sensitive enough to the changes of moisture content at compacted layer.

L.8 Acceptance Scenarios for Compacted Geomaterials

Subgrade Layer: The target moduli at the laboratory OMC for the PSPA and Zorn LWD are summarized in Figure L.8.1. Based on the PSPA measurements, about 80% of the points marginally achieve the acceptance limit for target modulus. Based on the LWD measurements, all test points pass the acceptance criterion.

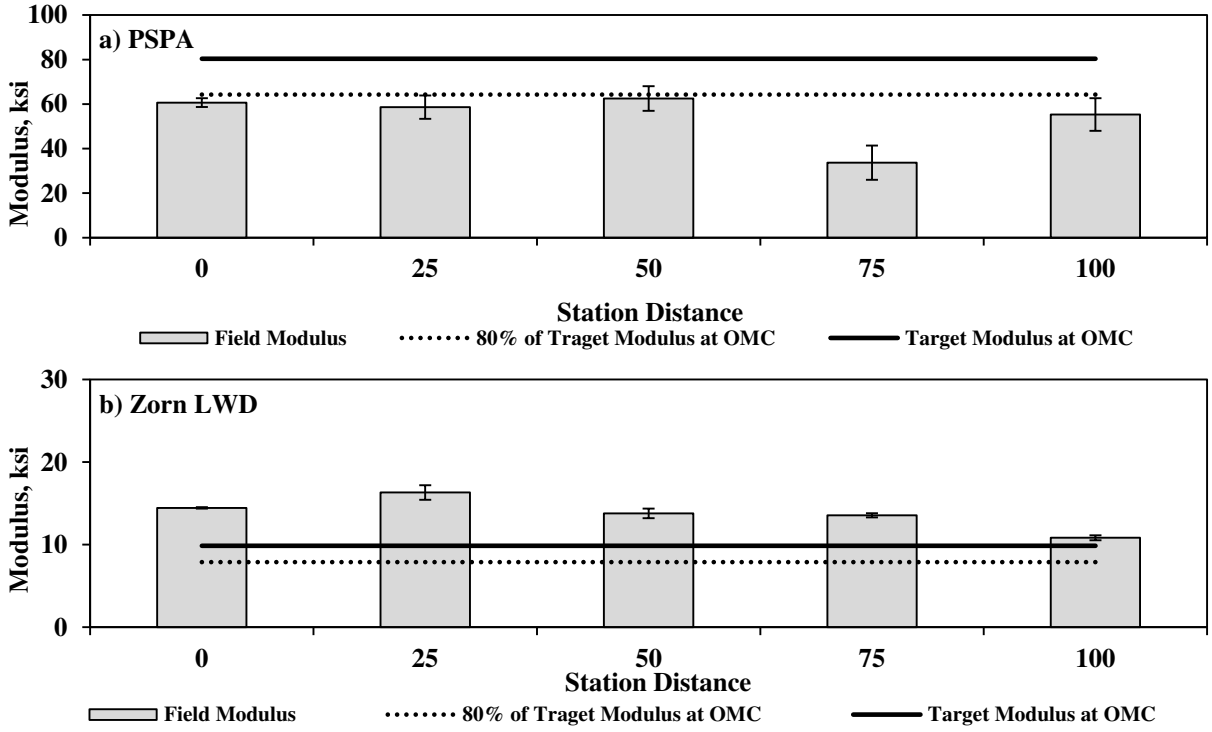

Figure L.8.1 – Acceptance Scenarios for Compacted Subgrade Layer

Subbase Layer: Figure L.8.2 summarizes the measured field moduli compared to the established target moduli of the subbase layer. All test stations passed the acceptance criteria established based on the laboratory-derived MR parameters at OMC.

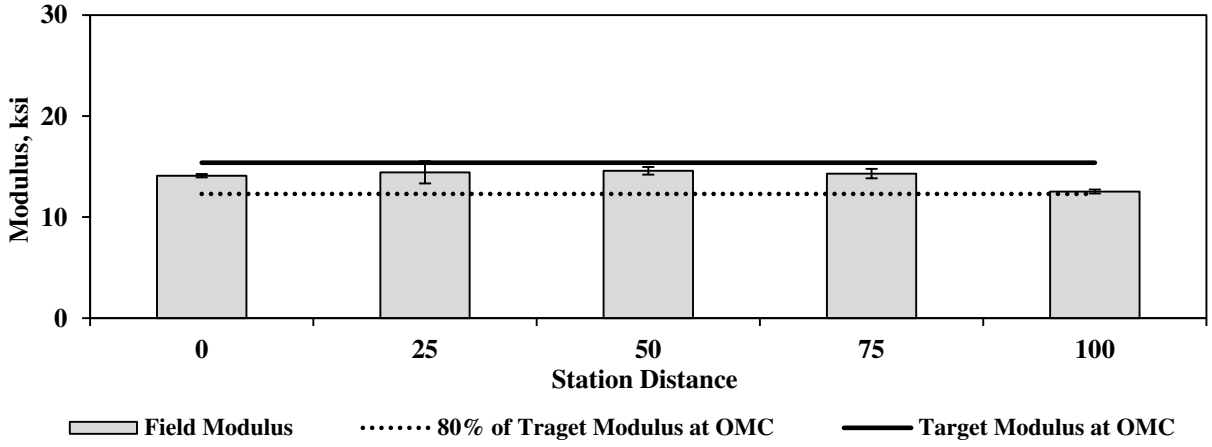

Figure L.8.2 – Acceptance Scenarios for Compacted Subbase Layer (Zorn LWD)